*A la memoria de **YENISET GONZÁLEZ GÉ (YENI)**, aliento de Fuerza,*

Coraje y Amor

Donde quiera que esté…

….. No es el fin, muchacha no es el fin….!!!!

Dedico además esta obra a los que siempre me acompañan, caminan en silencio a mi lado, me protegen de todo mal y permiten que todo sea posible….
Con toda mi alma… GRACIAS!!!

Agradecimientos

Esta obra no hubiera sido posible sin la invaluable contribución de personas que desde el principio creyeron en este proyecto. Ahora, es el turno de agradecer a quienes se alentaron a confiar en mis ideas.

Agradezco en primer lugar a mi familia, principalmente a mi hermana Elisabeth así como a mis padres Elisa y Pepe por su esmerada educación y soporte emocional, que hicieron de mí ese hombre en constante búsqueda del bien y la superación humana en todo sentido. No puedo dejar de agradecer particularmente a mi padre José Crespo Gallardo por ser un modelo de hombre de ingenio, creatividad y talento innato cuyos valores ha sabido donar a mi formación, lo cual constituye sin lugar a dudas el principio más valioso para la creación científica y que hacen de la ciencia un arte, valores que no pueden ser enseñados en universidad alguna. En toda intención creativa de esta obra está el ejemplo que me ha legado mi padre.

A mi entrañable amigo Juan Paiba por toda la ayuda brindada y tantos kilómetros recorridos para contribuir pacientemente a mi formación como profesional desde el mismo inicio de mi carrera.

De igual modo, quisiera agradecer a mis tutores: prof. Dr Jan Yperman (Universidad de Hasselt), prof. Dr Robert Carleer (Universidad de Hasselt), prof.Dr Ángel L Brito Sauvanell (Universidad de Oriente) y Ángel Sánchez Roca (Universidad de Oriente) por su confianza y por darme la posibilidad de doctorarme bajo su supervisión.

Un profundo agradecimiento al profesor y primer maestro del ron cubano de la corporación Cuba Ron S.A. Héroe del trabajo de la república de Cuba: Ing. José P. Navarro Campa por todo el apoyo brindado en materia científica y como experto del ron cubano, cuyos consejos resultaron vitales para dar forma a este trabajo. Agradezco además, toda la confianza y amistad compartida durante todo el proceso de concepción y ejecución de esta investigación. Muchas gracias maestro, un honor contar con su estima y poder tomar de usted el ejemplo a seguir como profesional revolucionario.

Un agradecimiento especial a los trabajadores y directivos de la corporación Cuba Ron S.A. por todo el apoyo brindado para llevar a cabo este proyecto. En especial al estimado amigo Ing. Freddy Fong Casas por todo el esfuerzo, tenacidad, creatividad e intelecto que aportó a este trabajo. A la directora de la Ronera Santiago de Cuba, Ing. Liliana Mengana Orozco por todo el soporte logístico sin el cual no se hubieran podido concretar las tareas tecnológicas planificadas en el proyecto. Del mismo modo, se agradece a los especialistas: Ing. Noemí del Toro, Ing. Yudeisi Tardo, Ing. Vladimir Leyva y MRC Julio Ayán por su apoyo incondicional.

Agradezco al gobierno de la bellísima localidad de Baracoa y a los trabajadores de la planta de carbón activado, especialmente a su director: Ing. Alexis Delgado Ortiz por su esmerada atención, esfuerzo, profesionalidad y disciplina tecnológica en la regeneración del carbón activado a escala industrial.

Agradezco a los profesores de la facultad de ingeniería química de la Universidad de Oriente por todo el conocimiento y educación brindados en estos largos años de formación profesional, pues todo el cúmulo de sabiduría por ellos entregada, resultó ser una efectiva herramienta para enfrentar los mayores retos científico-técnicos en el desarrollo de este trabajo. Quisiera agradecer además a la MSc. Thayset Mariño Peacok por su siempre dispuesta colaboración en el proyecto y su constante búsqueda del perfeccionamiento científico.

Mi eterno agradecimiento al proyecto VLIR-UOS (Flemish Interuniversity Council for University Development Cooperation) entre la Universidad de Oriente (Cuba) y la Universidad de Hasselt (Bélgica) por garantizar la infraestructura necesaria en pos del desarrollo y culminación exitosa de esta investigación. A los profesores, especialistas, colegas y amigos de la Universidad de Hasselt: Peter Adriaensens, Kenny Vanrepplen, Jens Maggen, Sara Vanderheyden, Jan Czech, Gunter Reekmans, Guy Reggers, Elsy e Ivo del grupo de química analítica y aplicada (TANC) así como a las investigadoras Vera Meynen, K. Leyssens (Universidad de Amberes) y Grazina Gryglewicz (Universidad de Wroclaw) por su apoyo en todo lo concerniente a la planificación, ejecución e interpretación de los análisis de laboratorio que resultaron trascendentales como evidencia científica.

Al especialista mecánico Johan Soogen (Universidad de Hasselt) por llevar a cabo la construcción del toma-muestras sin el cual no se hubieran podido realizar la recolección de los carbones a distintas profundidades del filtro industrial.

Del mismo modo, al prof. Dr Hipólito Carvajal Fals de la Universidad de Oriente por todas las ideas brindadas la cuales permitieron mejorar y ampliar el espectro científico de esta obra.

Agradezco a mí querida tía y ser humano excepcional: Martina Leijnen, por alentarme en momentos de flaqueza y hacer crecer en mí la esperanza de que todo es posible con esfuerzo y amor.

A mi querida muchacha, motivo de alegría y amor en mi vida: Claudia Fernández Gómez por ese candor con el que hace que cada día sea especial. Gracias mi aceituna!

Quisiera agradecer además, a todos mis amigos del Hospital Oncológico de Santiago de Cuba por estar a mi lado los momentos más oscuros que acompañaron el proceso creativo de esta obra. En especial a la enfermera: Aracelis Vejerano, especialista en Rx: Jesús Verdecia y al Dr. Manuel Velazco. ¡Muchas gracias amigos!

A todos aquellos que de una forma u otra hicieron posible este trabajo que hoy se presenta:

¡MUCHAS GRACIAS!!!

Table of Contents

List of Symbols

A: Area (m^2)

a : Adsorbent surface area (m^2/g)

A*: Equilibrium absorbance (UA)

AC: Activated carbon

A_R : Cross sectional area (m^2)

ASTM: American Standard Test Methods

BET: Brunauer-Emmett-Teller method

BP: Band-pass signal processing filter

C: Constant related to the energy of monolayer adsorption

c_0 : Initial concentration (g/L)

C_0 : Cost of the original operational process using imported GAC ($/year)

C_1, C_2 and C_3 : Constants related to the boundary layer thickness

$C_{e,i}$: Equilibrium concentration of the colored compound (g/L)

C_{eq} : Equivalent color concentration (g/L)

c_i : Adsorbate concentration in equilibrium (g/L)

C_m : Cost of the operational process using mixed GAC ($/year)

C_{ti} : Bulk concentration of colored compound "*i*" at any time (g/L)

C_v : Cost for buying imported GAC ($/year)

DFT: Density Functional Theory

DR: Dubinin-Radushkevich method

DSST: Derivative SS in function of temperature (Vs/°C)

DTG: Differential thermogravimetric profile (%/°C)

E: Adsorption potential (J)

E_0 :Characteristic adsorption energy (J)

e_B : Contactor efficiency

EBCT : Empty bed contact time (h)

EMP: Envelope maximal peak amplitude (V)

ES: GAC extracted solution

F_A : Ascending force

FCR: Fractional contribution ratio

FIR : Finite impulse response

g : Acceleration of gravity (m/s^2)

GAC: Granular activated carbon

GAI: General Adsorption Isotherm equation

h : Bed height (m)

HAP: Hazardous air pollutant

k: Number of experimentally counted bubbles

k_1, k_2..... k_i : Rate constants

k_{des} : Desorption rate constant

K_F : Freundlich's equilibrium constant

K_i : Langmuir's equilibrium constant

L: Avogadro constant

L_0 : Pore width (nm)

LSD: Lower significant difference statistic method

LUB: Length of unused bed (m)

m: mass (g)

M(t): Transversal magnetization function

m_0^i : Normalized magnetization of water in pores of type "i"

MOE: Mixed order rate equation

MPnO: Modified pseudo-n order rate equation

MTZ: Mass transfer zone

MW: Molar weight

n : Amount adsorbed (mol)

NLDFT: Non-Local Density Functional Theory

n_m : Monolayer capacity (mol)

NMR : Nuclear magnetic resonance

Np: Number of particles of GAC

OES: Oak extracted solution

P : Total pressure (Pa)

P_0 :Total purchase cost of the virgin GAC to fill the rum filters ($/m^3)

p : Equilibrium pressure (Pa)

p^0 : Saturation vapor pressure (Pa)

PAC: Powdered activated carbon

P_{ext} : External static pressure of the liquid (Pa)

PFO: Pseudo-first order rate equation

PM_{10} : Particulate matter with a diameter of 10 microns or less

P_m: Total purchase cost of the GAC mixture to fill the rum filters ($/m^3$)

PSO: Pseudo-second order rate equation

P_r : Total purchase cost of the regenerated GAC ($/m^3$)

q_0 : Maximum amount adsorbed on the GAC that can be desorbed (g/g GAC)

q_{des} : Amount of desorbed substance per unit adsorbent mass (g/g GAC)

Qe : Volumetric flow of exhausted GAC (m^3/year)

$q_{e,i}$: Equilibrium amount of the colored compound desorbed (g/g GAC)

Qm : Volumetric flow of mixed GAC (m^3/year)

QSDFT: Quenched-solid-density functional theory

q_t : Amount of product desorbed at time "t" (g/g GAC)

q_t : Substance amount still adsorbed at time "t" (g/g GAC)

$q_{t,i}$: Desorbed amount of colored compound "*i*" at any time (g/g GAC)

Qv' : Volumetric flow of virgin GAC (m^3/year)

r : Bubble radius (mm)

RAC: Regenerated GAC

SAC: Saved GAC

S_{BET} : BET apparent surface area of the adsorbent (m^2/g)

SEM : Scanning Electron Microscopy

S_i/V_i : Surface area-to-volume ratio of a pore "i"

SS: Integral area under the envelope curve "sound surface" (V·s)

S_w : Weight for a single GAC grain (g/GAC grain)

T: Temperature (°C)

t: Time (s)

$T_{2,bulk}$: Transverse bulk relaxation time of water (s)

$T_{2,i}$: Transverse relaxation time (μs)

Tcr: Critical temperature (°C)

TD-(GC/MS): Thermal Desorption – Gas Chromatography /Mass Spectrometry

TGA: Thermogravimetric analysis

t_m : Time-of-exploitation of a volume V_0 of mixed GAC (years)

t_r: Effective contact time (h)

t_v , t_s , t_r Time-of-exploitation of a volume V_0 of virgin, saved and regenerated GAC (years)

V: Bubble volume (cm^3)

V.C.: Variability coefficient (%)

V_0 : Volume of carbon to fill a rum filter (contactor) (m^3)

VAC: Virgin GAC

V_{DR}: Micropore volume (cm^3/g)

V_e : Volume of exhausted GAC (m^3)

V_f : Apparent volume of a flattened bubble (cm^3)

V_i : Volume of a bubble (cm^3)

V_L : Volume of GAC loss during regeneration (m^3)

V_{mes}: Mesopore volume (cm^3/g)

V_r : Volume of regenerated GAC (m^3)

V_R : Bed volume (m^3)

V_s : Volume of spherical sector (cm^3)

$V_{T\ "imm"}$: Immersion total volume of released bubbles per gram of GAC (cm^3/g)

V_T: Total volume of pores (cm^3/g)

V_{Tb} : Total volume of air bubbles released per GAC sample (cm^3)

V_V : Volume of virgin GAC (m^3)

w : Pore width (nm)

W : Volume of adsorbate filling micropores (cm^3)

W_0: Total micropore volume (cm^3)

wt : Weight (g)

wt % : Percent in terms of weight

$x_{2,i}$: Fractional contribution of each pore size type to the total porosity

Xi : Solid-liquid relation (grams of GAC per volume of ammonia solution)

x_r,x_s : Volumetric fraction of regenerated and saved GAC

Y_{max}; X_{max} : Maximal desorption rate coordinates

β_i : Fractional time -of-exploitation in terms of t_v of a material "i"

ΔH_R: Reaction enthalpy (J/mol)

ε_B : Bed porosity (%)

θ : Fractional coverage

λ : Wavelength (nm)

ρ : Liquid density (kg/m^3)

ρ_i : Surface relaxivity ($m/\mu s$)

σ_m : Molecular cross-sectional area (nm^2)

τ_i : Capacity of time-of-exploitation for a "i" GAC ($year/m^3$)

$\sigma(x)$: Standard deviation

Research objectives and outline

Activated Carbon (AC) adsorption is the most common technique for removing various pollutants in gas and liquid phase. AC (the most used industrial adsorbent) has been broadly and successfully applied in diverse industries such as: Water Treatment, Chemical, Food, Medical, Metallurgy or Electronic because of its extended specific surface area, well-developed porous structure and surface activated function.

AC is generally produced by heating various carbonaceous materials (precursors) like coal, coconut shells, wood, bones etc. to temperatures of about 1000 °C in a controlled soft oxidant media. The world demand for activated carbon is forecast to expand 5.2 percent per year (2012) with an estimate of 2.3 million metric tons for activated carbon production in 2017.

AC can be used powdered (PAC) or granular (GAC) (0.2-5 mm).The use of PAC has some disadvantages: huge dust production, difficulty for its filtration and regeneration, thus being an environmental problem. In contrast, GAC can overcome these technological inconveniences keeping the same adsorption potential. GAC produces almost no dust, its transportation and management is easier than PAC and it can be reused for many times considering its regeneration. The operations using GAC are simple, which make it possible for continuous and automatic production processes. These advantages enhance the expansion of GAC manufacturing and its wide use in many fields and moreover, the necessity to regenerate and reuse of the exhausted GAC. It can not only economize the natural resources, reduce the secondary pollution, but also bring along considerable economic profit.

In Cuba among other uses, the GAC is applied in high quality rum production. Rum is a fairly tasteless and neutral spirit, traditionally (but not exclusively) produced in the Caribbean and Central America countries. According to the statement No 110/2008 of the European Union Council, rum is defined as: ‘the spirit beverage derived from the fermentation and distillation of sugar molasses, the black treacle-like substance which remains after sugar crystallization which is distilled below 96% (in volume fraction of ethanol) and the product of the distillation must perceptively have the specific organoleptic characteristics of the rum.

Rum is organoleptically characterized by the content of many volatile compounds, also known as congeners, such as higher alcohols, esters, carboxylic acids, carbonyl compounds, phenols, and furan derivatives, among others, which contribute to the peculiar flavor of the spirit.

The distilled product (as primary rum) known in Cuba as "Aguardiente", is a colorless liquid which is aged in barrels of white oak wood during a timed period in order to transform and improve its sensorial characteristics. The ageing process (maturation) results in changes of the aguardiente: a light amber color appears; taste softens and a pleasant aroma is produced. During this stage; these sensorial changes are obtained by complex chemical reactions due to the interaction between the aguardiente and the wood where the ageing time plays an important role. Once the aged aguardiente is obtained, it undergoes further processing such as percolation through carbon (GAC) contactors "filters", blending and usually aged several times using specially selected oak barrels in conditioned cellars, which give to the Cuban rum its characteristic aroma and bouquet.

With respect to international Cuban rum trade, 35.1 million liters were exported to Europe, America and Asia in 2012 with a sustained growing of 2% since 2008. According to that demand and the quality of the product, the leader brand of exportable Cuban rum is regarded among the 25 best global brands and occupies the fifth place among the global brands of rum. Clearly, the establishment of standard parameters to maintain the quality of the spirit is essential to meet the needs of national and foreign markets and to be also competitive. To reach the desirable organoleptic features in Cuban rum, the operation of percolation "filtration" of aged aguardiente using GAC is essential. This operation is meticulously monitored by the rum taste experts (rum masters).

GAC is used to remove/balance some organic compounds that affect the sensorial quality and organoleptic features in the final product. Fixed bed of GAC is placed in cylindrical contactors where the aged aguardiente is applied at the top of the filter, flows downward through the carbon bed, and is withdrawn as "filtered aged aguardiente" at the bottom of the column. When GAC becomes exhausted in the rum production it is landfilled and replaced by fresh GAC.

As an estimate, 10-12 tons per year of exhausted GAC from rum production is landfilled.

Therefore the same amount of expensive fresh GAC for replacing is imported. The landfilled GAC (WAC) creates a solid waste problem which grows proportionally to the spirit production rate. For this reason a regeneration process should be applied and the effectiveness of regenerated GAC must be guaranteed.

At present, specialized rum taste experts determine when GAC needs to be replaced based on the sensorial judgment of the filtered aged aguardiente and not on the exhausted level of the GAC. The GAC quality control is done at industrial scale and is performed empirically. The GAC used is always provided by the same supplier, selected by the rum taste experts and only based on the sensorial characteristics of the filtered product. The surface group functionality and its relationship with the effectiveness to achieve the desirable taste and Cuban rum aroma have not yet been studied. The practical evidence gathered for years has been the main (only) criteria to accept the used kind of GAC. When the filtered aged aguardiente quality reaches minimum organoleptic standards, the GAC is completely removed from the filter. The algorithm of the current GAC management in Cuban rum factories is presented in Fig. I.

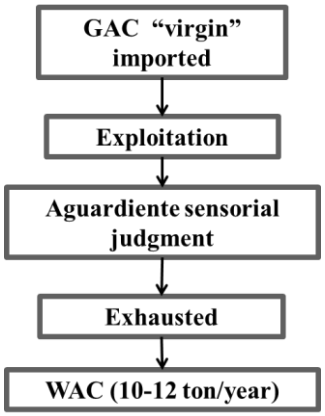

Fig. I: Algorithm of the GAC management at present in Cuban rum factories

Although effective, effluent sensorial judgment cannot offer quantitative information about the real exhaustion degree of the GAC in the filter. As the filtration takes place in a fixed bed system, a further characterization of the GAC in industrial rum contactors gives the possibility to save a part of the GAC.

It can be reused in the rum production process if its less exhaustion degree is quantified.

In order to determine the exhaustion level of GAC a proper and fast analytical technique based on determination of specific surface area and porosity has to be applied.

However, the technological facilities of rum producers are limited. Additional this quality parameter needs to be checked on a very regular base during the whole rum production process. Furthermore, it is found that for detecting the exhaustion degree in exhausted GAC in rum production, the widely applied BET analysis could not be performed. Consequently, an alternative, economic, fast and reliable method to measure the exhaustion level of GAC in rum production and the regeneration degree reached is more than welcome.

While GAC demand in rum production is arising, the future of exhausted GAC is consistently becoming a concern. Under such circumstances, reuse by regeneration of the exhausted GAC could give some advantages by stabilizing adsorbents and recovering resource by reutilization.

The most common technique practiced in regeneration is a thermal treatment in which adsorbed substances are desorbed by volatilization followed by oxidation at high temperature. Thermal regeneration effectively restores the activity of carbons loaded with organic adsorbates. It can be divided into four process stages: drying at temperatures of up to 200 °C to remove the associated water; evaporation of volatile adsorbates and decomposition of unstable adsorbates to form volatile fragments at temperatures of 200-500°C, pyrolysis of non-volatile adsorbates and adsorbent fragments to form carbonaceous char on the activated carbon surface at temperatures of about 500-700°C and oxidation of the char using steam and carbon dioxide at temperatures above 700°C.These processes are mainly performed in rotary kilns, fluidized-bed furnaces and multiple-hearth furnaces. Therefore, thermal process is an attractive alternative to regenerate the exhausted GAC in rum production.

Based on the aspects discussed above, a new proposal of GAC management in Cuban rum production can be formulated. The idea is to combine the traditional sensorial judgment, novel quantitative analytical techniques for characterizing GAC (adequate for rum manufacturer’s facilities) and a proper regeneration strategy in order to improve the efficiency of GAC management in rum industry.

Fig. II displays the algorithm of the new proposal of GAC management in rum production.

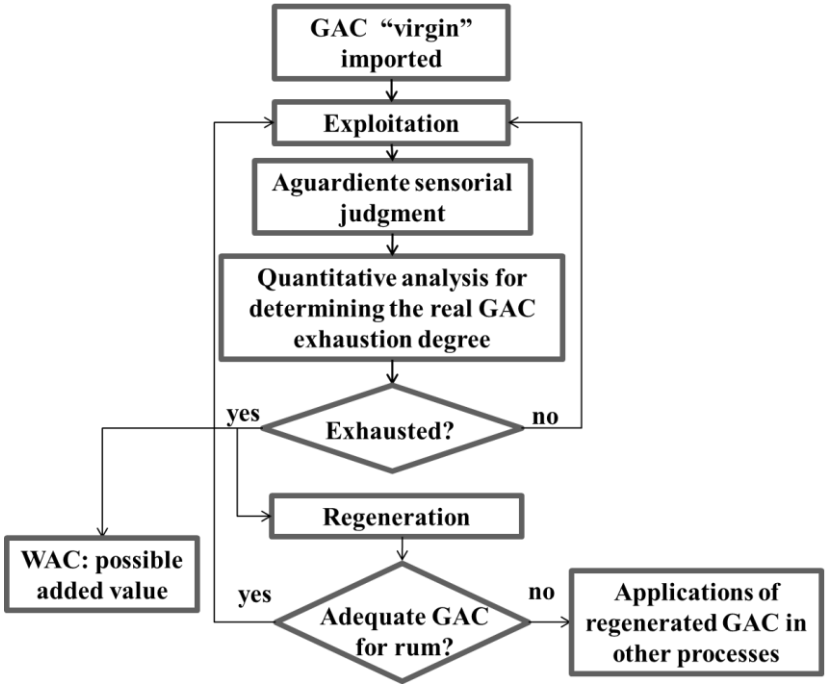

Fig. II: Algorithm of the new proposal of GAC management in Cuban rum factories

The GAC virgin is imported and placed in the fixed-bed contactors, after the exploitation period the rum masters declared the rum filter out of service based on the sensorial judgment of the filtered Aguardiente. Then, the GAC in the contactor's bed is analyzed using quantitative methods in order to determine its exhaustion level. If the GAC were partially exhausted (near to the filter's bottom) the GAC is reused again to refill a new GAC filter but without applying regeneration. In contrast, if the exhaustion were confirmed, the GAC is sent to the regeneration process. Being adequate for rum production, the regenerated GAC can be sent back to the rum process. After a limited number of cycles, the regenerated GAC will not be suitable for rum production any more. However, potential application of the regenerated GAC in other industries can be found and also for the produced WAC.

According to the presented scenario for the rum production process in Cuba, We are facing as **scientific issue**: the necessity to establish a new strategy of management for the GAC used in the Cuban rum production process, the new proposal must include not only an effective method of regeneration of the exhausted GAC, but also to provide suitable quantitative methods to determine the GAC porous characteristics in order to guarantee an efficient, clean and sustainable exploitation of this material in the rum industry.

Based on the previous arguments, the **hypothesis** to be considered in this research is: The thermal regeneration of the exhausted GAC could efficiently restore the adsorptive properties of this material to be reused in the rum production. In addition, novel and suitable quantitative methods could be implemented to determine the porous characteristics of the GAC before and after the regeneration process. If these changes were jointly applied, it could substantially improve the current GAC management in the Cuban rum industry.

In this work, the **main objective** is to present a new and improved proposal of GAC management in rum production based on the thermal regeneration of the exhausted GAC complemented with novel, robust, accurate and suitable quantitative methods to determining its porous characteristics.

The study has been addressed to answer three **specific sub-questions**:

(I) When is a GAC exhausted in rum production?

(II) Could thermal regeneration successfully applied for the exhausted GAC in rum production?

(III) Is it possible to improve the management of GAC in rum production at the current conditions by introducing the regeneration process and new, innovative, robust and more suitable analytical methods to characterize the GAC?

Derived from these specific sub-questions the following **specific objectives** are formulated:

1- To develop novel quantitative methods to determine porous characteristics of granular activated carbons used in rum production. The proposed methods have to be trustable, fast and robust techniques being also suitable for the rum producer facilities.

2- To determine the proper conditions for the thermal regeneration of the exhausted GAC in order to restore its porous characteristics to be efficiently reused in the rum production process.

3-To perform the thermal regeneration at industrial scale of exhausted GAC used in rum production in order to assess important aspects such as: sensorial judgment of the filtered aged aguardiente using the regenerated GAC, efficiency and economic viability of the regeneration process.

The **scientific novelty and uniqueness** in this research, viewed in a general way, it is the proposal of a new strategy of GAC management in the rum industry. However, this general scientific novelty has as basis very distinctive and specific scientific novelties which are implicit in the research body giving it uniqueness and transcending the rum production process. These specific scientific novelties are based on three new quantitative methods to determining the porous characteristics of granular activated carbons and the assessment of its exhaustion degree.

In **Chapter 1**, an introduction about the adsorption theory and the activated carbon features as adsorbent are presented, including important aspects such as: activated carbon production, properties and methods of characterization, exploitation and regeneration. Additionally, the technology of activated carbon and its management in the Cuban rum industry is discussed.

Chapter 2 describes the materials under investigation and an overview of the different methodologies applied. The latter not only comprises a description of the analytical methods performed, sampling procedures and the data processing tools used but also, the description of the set up to performing novel methods for characterizing activated carbon in the rum production are presented.

Chapter 3 focusses on the development of novel methods to determining the characteristics of the activated carbons used in the rum production process. The obtained results applying these methods are correlated and compared with other well-stablished conventional analytical techniques in order to demonstrate its efficacy, feasibility, robustness and accuracy.

In **Chapter 4**, the thermal regeneration of the exhausted activated carbon used in Cuban rum production resembling industrial plants is discussed. The effect of the regeneration parameters (temperature and residence time) over the porous characteristics of the regenerated activated carbon is studied by applying the acoustic emission and gas sorption methods in order to assess the carbon porosity and apparent surface area after regeneration. Furthermore, the results of a sensorial judgment performed on filtered aged aguardiente at industrial scale using regenerated activated carbon is presented in this chapter as the organoleptic ultimate test. In addition, an economic overview of the regeneration process is debated.

In **Supplementary materials**, complementary information is provided in order to strengthen and clarify theoretical and practical aspects discussed in the manuscript body.

Chapter 1-Introduction

1.1-Adsorption

In general, adsorption is defined as the enrichment of molecules, atoms or ions in the vicinity of an interface. In the case of gas/solid systems, adsorption takes place in the vicinity of the solid surface and outside the solid structure. The material in the adsorbed state is known as the adsorbate, while the adsorptive is the same component in the fluid phase. The adsorption space is the space occupied by the adsorbate [1-6].Adsorption is a phase transfer process that is widely used in practice to remove substances from fluid phases (gases or liquids)[2,5]. Adsorption occurs whenever a solid surface is exposed to a gas or liquid [3].The accumulation of concentration at a surface is essentially an attraction of adsorbate molecules (a gaseous or liquid component) to an adsorbent surface (a porous solid). Adsorption can occur between two phases (gas–solid, or liquid–solid interfaces) being the solid adsorbing phase. A hypothetical interfacial layer exists between the solid and fluid phases. This layer consists of two regions: that part of the fluid (gas or liquid) residing in the force field of the solid surface and the surface layer of the activated carbon. Adsorptive surface reactions occur as a result of the active forces within the phase or surface boundaries [3-7] .These forces result in characteristic boundary energies. The surface tension developed at the surface of the fluid phase results from the attractive forces between the molecules of the fluid. Interaction between adsorbate and adsorbent consists of molecular forces embracing permanent dipole, induced dipole and quadrupole electrostatic effects, known as Van der Waals forces. The preferential concentration of molecules in the proximity of a surface arises because the surface forces of an adsorbent solid are unsaturated. Both short range (repulsive) and longer range (attractive) forces between adsorbate and adsorbent become balanced when adsorption occurs. Adsorption is nearly always an exothermic process and takes place with the evolution of heat The magnitude of the heat of adsorption is considerable, and its knowledge is important both for practical as well as theoretical purposes [4,8]. It is sometimes difficult or impossible to distinguish between adsorption and absorption: it is then convenient to use the wider term sorption which embraces both phenomena, and to use the derived terms sorbent, sorbate and

sorptive [6].Adsorption is considered to be an important phenomenon in most natural physical, biological, and chemical processes[1].

1.1.1-Desorption

The counterpart of adsorption is called desorption. Desorption denotes the process in which the amount of adsorbed material decreases. The terms adsorption and desorption often are used adjectivally to indicate the measurement direction from which experimentally determined adsorption values have been approached. If the adsorption and desorption curves do not coincide, then the process is said to exhibit adsorption hysteresis [1-9] (discussed later).

1.1.2-Monolayer and multilayer adsorption

When an adsorbate begins to form on a nascent surface, it is possible for each molecule to adsorb directly onto the surface. More precisely, each molecule occupies a position of closest approach to the adsorbent. In this state, the adsorbate is said to form a monolayer. If adsorption persists in excess of monolayer adsorption, we may visualize additional layers of adsorbate forming on top of the initial monolayer, each new layer being more remote from the substrate than the preceding layer. Adsorption that progresses beyond monolayer adsorption is called multilayer adsorption. For a given state of multilayer adsorption, there may be more pore space available than is occupied by the adsorbate. Fluid capillary condensation onto pores often contributes to the occurrence of adsorption hysteresis [1-9].

1.1.3-Monolayer Capacity

The amount of adsorbate needed to cover the surface of the adsorbent with a monolayer of molecules is called the monolayer capacity and is denoted here by the symbol n_m.The total surface coverage then can be described with respect to a monolayer of adsorbate. For both monolayer and multilayer adsorption, the surface coverage (θ) is defined as the ratio of the amount of adsorbed substance to the monolayer capacity [3-9].

1.1.4-Types of Adsorption

Physisorption

The adsorption induced by Van der Waals forces is generally termed physical adsorption or physisorption, in which intermolecular attractions take place between favorable energy sites. Physisorption is independent of the electronic properties of the adsorbate and adsorbent molecules. Exchange of electrons does not occur in physisorption. The adsorbate is attached to the surface by relatively weak Van der Waals forces. In physisorption, multiple layers may be formed which have heats of adsorption decreasing as a function of the layer thickness. Physical adsorption is predominant at temperatures below 150°C, and is characterized by relatively low adsorption energy at most a few kcal mol^{-1}. As a rule, it is a reversible process (desorption) that occurs at a lower temperature close to the critical temperature of an adsorbed substance. Therefore, physically adsorbed molecule is free to move within the interface. Gas adsorption measurements by physisorption are widely used for the determination of the surface area and pore size distribution. [1,3-5].

Chemisorption

In chemical adsorption, or chemisorption, the adsorbate undergoes chemical interaction with the adsorbent. Table 1.1 gives a comparison of physical and chemical adsorption.

Chemisorption involves an exchange of electrons between specific surface sites and solute molecules, a chemical bond being formed. Chemically adsorbed adsorbates are not free to move on the surface or within the interface. Chemical adsorption is characterized by a high adsorption energy (tens of kcal/mol), since the adsorbate forms strong localized bonds at active centers on the adsorbent. Chemical adsorption is more predominant at high temperatures compared to physisorption, because chemical reactions proceed more rapidly at higher temperatures. Generally, only a single molecular layer can be chemically adsorbed. These two forms of adsorption interact together in adsorption [1,4-6].

Table1.1: Comparison of physical and chemical adsorption

	Physisorption	**Chemisorption**
Coverage	Mono or multilayer	Monolayer
Nature of adsorption	Non-dissociative and reversible	Often dissociative, may be irreversible
Specify to adsorption sites	Non-specific	Very specific
Temperature range	Near or below the condensation point of the gas	Unlimited
Temperature dependence of uptake (with increasing T)	Decreases	Mostly increases
Adsorption enthalpy	5-40 $kJmol^{-1}$	40-800 $kJ\ mol^{-1}$
Kinetics of adsorption	Fast	Very variable, often slow
Desorption	Easy by reduced pressure or increased temperature	Difficult-high temperature is required to break bonds.
Desorbed species	Adsorbate unchanged	Adsorbate may change

- Adapted from [4]

1.2-Factors influencing adsorption

1.2.1-Surface area of adsorbent

The extent of adsorption is generally considered to be proportional to the specific surface area. Specific surface area is that proportion of the total surface area which is available for adsorption. The more finely divided and more porous adsorbents would be expected to yield more adsorption per unit weight of adsorbent. The surface can be characterized either as external when it involves bulges or cavities with width greater than depth or internal when it involves pores and cavities that have depth greater than width [4,5]. The term surface area of a porous solid is (nothing more and nothing less) a convenient way to indicate adsorption capacity [10].

1.2.2-Physical and chemical characteristics of the adsorbate

In general, the adsorbability of a compound increases with increasing molecular weight and increasing number of functional groups such as double bonds or halogens. In the case ofliquid phase, the degree of solubility of the solute is also of primary concern for adsorption. There is an inverse relationship between the extent of adsorption of a particular solute and its solubility in the solvent from which the adsorption occurs [4,5,11]. High solubility means that the solute–solvent bonds are stronger than the attractive forces between the solute and the adsorbent. Polarity of the adsorbate is another important factor. A polar solute is preferably adsorbed by a polar adsorbent, whereas a nonpolar solute is more easily adsorbed by a nonpolar adsorbent. Consequently, any change that increases solubility may be associated with reduced adsorbability [4,5].

1.2.3-pH

In the case of liquid phase, the adsorption is rather complex: organic molecules can form negative ions or neutral molecules at high pH values, positive ions or neutral molecule at low pH values, and a mixture at intermediate pH values. Adsorption behavior depends on the acid-base nature of the organic molecule, thus its pK_a or pK_b but also on the pH_{pzc} of the AC itself. Adsorption depends also on the predominant character of the molecule towards the characteristics of the AC [4,5].

1.2.4-Temperature

The extent of adsorption should increase with decreasing temperature because the adsorption reactions are exothermic. However; for the liquid phase, increased temperature also increases the rate of diffusion of the solute through the liquid to the adsorption sites, which eventually leads to an increased adsorption [3-5]. An important difference in the adsorption of solutes versus gases is found in the role of temperature. An increase in temperature increases the tendency of a gas to escape from the interface and thus diminishes adsorption. However, in adsorption from the liquid, the influence of temperature on solvent affinities is more dominant [4,5].

1.2.5- Adsorbent porosity

The adsorption performance is dependent on the condition of internal surface accessibility. A very important and decisive property of adsorbent materials is the pore structure [4,11].The total number of pores and their shape and size determine the adsorption capacity and even the rate of adsorption. The significance of pores in adsorption processes largely depends on their sizes. Most of the solid adsorbents possess a complex structure that consists of pores of different sizes and shapes [4,5].

It is difficult to obtain accurate information on the shape of the pores. Several different methods used to determine the shapes of the pores have indicated ink-bottle shape, capillaries open at both ends or with one end closed, regular slit-shaped, V-shaped. This classification is based on their width (w), which represents the distance between the walls of a slit-shaped pore or the radius of a cylindrical pore. The pores are divided into three groups: the micropores, the mesopores (transitional pores), and the macropores [6-16].

Micropores

Micropores have molecular dimensions, the effective width being less than 2 nm. The adsorption in these pores occurs through volume filling, and no capillary condensation takes place. Micropores are dominantly used for storage of adsorbed molecules. The potentials exerted by the confinement of small pores are so great that molecules inside those pores are not free from the attractive adsorption forces exerted by both walls of the pore [7].The adsorption energy in these pores is much larger compared to larger mesopores or to the nonporous surface [6-16].Micropores are usually modeled as slit pores although this is a gross idealization of real pores, which are known to be finite, contain functional groups, defects, and do not have perfectly flat surface. Although there are attempts to relax some of the above restrictions, the ideal model of perfectly flat slit pore of infinite extent is still the most popular model used in almost all characterization methods. The complexity and the extreme computation time of more structured models are such that the ideal model ofslit pore is still the obvious choice for pore characterization [17].As a rule, the internal surface area increases with increasing micropore volume. In principle, the higher the micropores volume, the larger is the amount of adsorbate that can be adsorbed.

However, it has to be considered that in the case of very fine pores and large adsorbate molecules, there may be a limitation of the extent of adsorption by size exclusion. Such size exclusion can be found, for instance, in the case of the adsorption of high-molecular-weight natural organic matter onto microporous adsorbents [17].

Mesopores

Also called transitional pores, mesopores have effective width in the 2 to 50 nm range; these pores are characterized by capillary condensation of the adsorbent with the formation of a meniscus of the liquefied adsorbate[6-16].Mesoporosity is often described as being cone-shaped and forming part of the surface of activated carbon[10].

Macropores

Macropores have effective width larger than 50 nm, and frequently in the 500 to 2000 nm range. They act as transport channels for the adsorbate into the micro and mesopores. Macropores are not filled by capillary condensation [6-16].These limits, which were suggested by the analysis of nitrogen (77 K) adsorption-desorption isotherms (discussed later) are therefore to some extent arbitrary [6].

Pore types and chemical surface characteristics

Modelling of porosity is a serious challenge and must relate to an understanding of what changes are possible within a solid phase [10].With a simplified reference to Fig. 1.1, it is possible to classify pores according to how accessible they are to an external fluid. In this context, one category (closed pores) consists of pores that are inaccessible to an external fluid and totally isolated from their neighbors, as in region (a). Closed pores influence macroscopic properties such as bulk density, elasticity, mechanical strength, and thermal conductivity, but they are inactive in processes such as fluid flow and adsorption of gases. On the other hand, pores that have a navigable channel of communication with the external surface of the body (like b, c, d, e, and f) are described as open pores. Open pores are further classified into "through pores" and "blind pores." Through pores have an open channel that begins at one location on the surface, extends into the particle, and re-emerges on the surface at a different location (like the pore channels c-e-c and c-e-d) [4,10].

Blind pores (also called dead-end or saccate pores) are open to the surface only at one end (like b and f). A special distinction is made for blind pores like those in region of "g" of Fig. 1.1. While these small surface irregularities are technically blind pores, it is often more useful and convenient to consider them separately as part of a distinct attribute, called surface roughness.

A simple convention often used is to assume that surface irregularities are counted as pores only if they are deeper than they are wide. Pores may be classified further according to their shape. Common shape terms include cylindrical (open c or blind f), ink-bottle (b), funnel (d), and slit shapes.

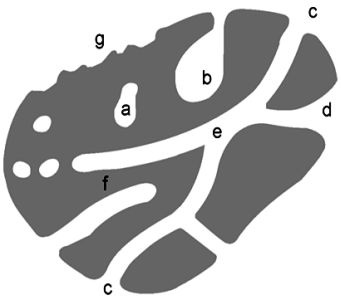

Fig.1.1: Cross section of a porous solid (adapted from [9])

The adsorption performance is dependent on chemical surface characteristics of the adsorbent. Heterogeneity of the activated carbon surface significantly contributes to adsorption capacity [4,5].

1.3-Adsorbent classification

Adsorbents are of natural origin or the result of an industrial production and/or activation process. Typical natural adsorbents are clay minerals, natural zeolites, oxides, or biopolymers. Engineered adsorbents can be classified into carbonaceous adsorbents (activated carbons), polymeric adsorbents, oxidic adsorbents, and zeolite molecular sieves [2,9]. In general, engineered adsorbents exhibit the highest adsorption capacities. They are produced under strict quality control and show nearly constant properties. In most cases, the adsorption behavior towards a broad variety of adsorbates is well known, and recommendations for application can be derived from scientific studies and producers' information.

On the other hand, engineered adsorbents are often very expensive [2,3,9]. Since the adsorption process is a surface process, the surface area of the adsorbent is of great importance for the extent of adsorption and therefore a key quality parameter [2,4,5]. In general, natural adsorbents have much smaller surface areas than highly porous engineered adsorbents. The largest surface areas can be found for activated carbons and special polymeric adsorbents. A precondition for high surface area is high porosity of the material, which enables a large internal surface constituted by the pore walls. The internal surface of engineered adsorbents is much larger than their external particle surface. As a rule, the larger the pore system and the finer the pores, the higher is the internal surface [2-4]. On the other hand, a certain fraction of larger pores is necessary to enable fast adsorbate transport to the adsorption sites. Therefore, pore-size distribution is a further important quality aspect. Besides the texture, the surface chemistry may also be of interest, in particular for chemisorption processes [2,4].

1.4 -Physisorption isotherms

There is no doubt that the most efficient experimental approach to obtain the above information about adsorption is to use the adsorption method itself [10]. The property which is most commonly studied initially is the equilibrium isotherm(s) for the chemical system to be separated or purified. The relation, at constant temperature, between the amount adsorbed and the equilibrium pressure of the gas is known as the physisorption isotherm. The physisorption isotherm results from the controlled physical adsorption of a gas or vapor into an adsorbent. This process of physical adsorption is the way in which the adsorptive (gas or vapor) enters into the porosity. In the case of physisorption of gases, the "retention" of these gas adsorbate molecules on the surface is the result of enhanced Van der Waals forces (dispersion forces) within the porosity [10].The way the pressure is plotted depends on whether the adsorption is carried out at a temperature under or above the critical temperature of the adsorptive. At an adsorption temperature below the critical point, one usually adopts the relative pressure p/p^0, where p is the equilibrium pressure and p^0 the saturation vapor pressure at the adsorption temperature [6].

1.4.1-Classification of physisorption isotherms

In the 1985 IUPAC recommendations physisorption isotherms were grouped into six types [6-16].

However, over the past 30 years various new characteristic types of isotherms have been identified and shown to be closely related to particular pore structures. Therefore, a new refining of the original IUPAC classifications of physisorption isotherms and associated hysteresis loops was considered [6]. The proposed updated classification of physisorption isotherms is shown in Fig. 1.2.

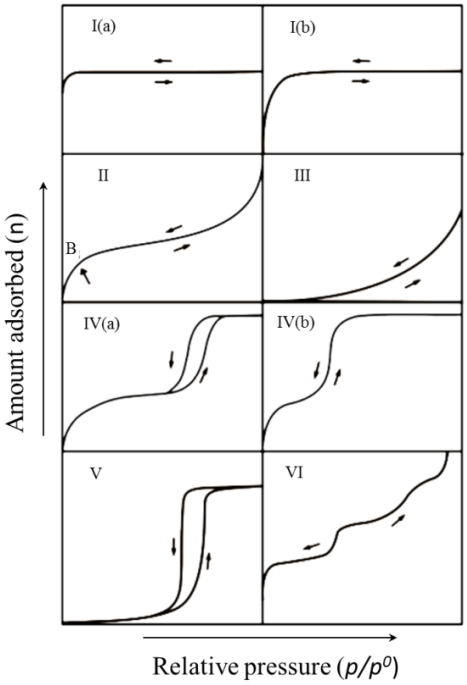

Fig.1.2: Classification of physisorption isotherms [6]

Reversible **Type I isotherms** are given by microporous solids having relatively small external surfaces (e.g., some activated carbons, molecular sieve zeolites and certain porous oxides). A Type I isotherm is concave to the p/p^0 axis and the amount adsorbed approaches a limiting value. This limiting uptake is governed by the accessible micropore volume rather than by the internal surface area [6,9]. A steep uptake at very low p/p^0 is due to enhanced adsorbent-adsorptive interactions in narrow micropores (micropores of molecular dimensions), resulting in micropore filling at very low p/p^0.

For nitrogen and argon adsorption at 77 K and 87 K, Type I(a) isotherms are given by microporous materials having mainly narrow micropores (of width < ≈1 nm); **Type I(b)** isotherms are found with materials having pore size distributions over a broader range including wider micropores and possibly narrow mesopores (<≈ 2.5 nm).

Reversible **Type II isotherms** are given by the physisorption of most gases on nonporous or macroporous adsorbents. The shape is the result of unrestricted monolayer-multilayer adsorption up to high p/p^0. If the knee is sharp, Point B – the beginning of the middle almost linear section – usually corresponds to the completion of monolayer coverage. A more gradual curvature (i.e., a less distinctive Point B) is an indication of a significant amount of overlap of monolayer coverage and the onset of multilayer adsorption [6-16].The thickness of the adsorbed multilayer generally appears to increase without limit when $p/p^0 = 1$.

In the case of a **Type III isotherm**, there is no Point B and therefore no identifiable monolayer formation; the adsorbent-adsorbate interactions are now relatively weak and the adsorbed molecules are clustered around the most favorable sites on the surface of a nonporous or macroporous solid. In contrast to a Type II isotherm, the amount adsorbed remains finite at the saturation pressure (i.e., at $p/p^0 = 1$). **Type IV isotherms** are given by mesoporous adsorbents (e.g., many oxide gels, industrial adsorbents and mesoporous molecular sieves). The adsorption behavior in mesopores is determined by the adsorbent-adsorptive interactions and also by the interactions between the molecules in the condensed state.

In this case, the initial monolayer-multilayer adsorption on the mesopore walls, which takes the same path as the corresponding part of a Type II isotherm, is followed by pore condensation. Pore condensation is the phenomenon whereby a gas condenses to a liquid-like phase in a pore at a pressure p less than the saturation pressure $p^0$of the bulk liquid [16,17]. A typical feature of Type IV isotherms is a final saturation plateau, of variable length (sometimes reduced to a mere inflexion point).

In the case of a **Type IVa isotherm**, capillary condensation is accompanied by hysteresis. This occurs when the pore width exceeds a certain critical width, which is dependent on the adsorption system and temperature (e.g., for

nitrogen and argon adsorption in cylindrical pores at 77 K and 87 K, respectively, hysteresis starts to occur for pores wider than ≈4 nm) [14, 16, 15]. With adsorbents having mesopores of smaller width, completely reversible Type IV b isotherms are observed. In principle, **Type IV b** isotherms are also given by conical and cylindrical mesopores that are closed at the tapered end. In the low p/p^0 range, the **Type V isotherm** shape is very similar to that of Type III and this can be attributed to relatively weak adsorbent–adsorbate interactions. At higher p/p^0, molecular clustering is followed by pore filling. For instance, Type V isotherms are observed for water adsorption on hydrophobic microporous and mesoporous adsorbents. The reversible stepwise **Type VI isotherm** is representative of layer-by-layer adsorption on a highly uniform nonporous surface. The step-height now represents the capacity for each adsorbed layer, while the sharpness of the step is dependent on the system and the temperature. Amongst the best examples of Type VI isotherms are those obtained with argon or krypton at low temperature on graphitized carbon blacks.

1.4.2-Adsorption hysteresis

Reproducible, permanent hysteresis loops, which are located in the multilayer range of physisorption isotherms, are generally associated with capillary condensation. This form of hysteresis can be attributed to adsorption metastability and/or network effects. In an open-ended pore (e.g., of cylindrical geometry), delayed condensation is the result of metastability of the adsorbed multilayer. It follows that in an assembly of such pores the adsorption branch of the hysteresis loop is not in thermodynamic equilibrium. Since evaporation does not involve nucleation, the desorption stage is equivalent to a reversible liquid–vapor transition. Therefore, if the pores are filled with liquid-like condensate, thermodynamic equilibration is established on the desorption branch [13–17]. In more complex pore structures, the desorption path is often dependent on network effects and various forms of pore blocking. These phenomena occur if wide pores have access to the external surface only through narrow necks (e.g., ink-bottle pore shape). The wide pores are filled as before and remain filled during desorption until the narrow necks empty at lower vapor pressures. In a pore network, the desorption vapor pressures are dependent on the size and spatial distribution of the necks.

If the neck diameters are not too small, the network may empty at a relative pressure corresponding to a characteristic percolation threshold. Then, useful information concerning the neck size can be obtained from the desorption branch of the isotherm.

Theoretical and experimental studies have revealed [13-17] that if the neck diameter is smaller than a critical size (estimated to be ca. 5–6 nm for nitrogen at 77 K), the mechanism of desorption from the larger pores involves cavitation (i.e., the spontaneous nucleation and growth of gas bubbles in the metastable condensed fluid).

Types of hysteresis loops

Many different shapes of hysteresis loops have been reported (Fig.1.3), but the main types are shown in Fig. 3. Types H1, H2 (a), H3 and H4 were identified in the original IUPAC classification of 1985, which is now extended in the light of more recent findings.

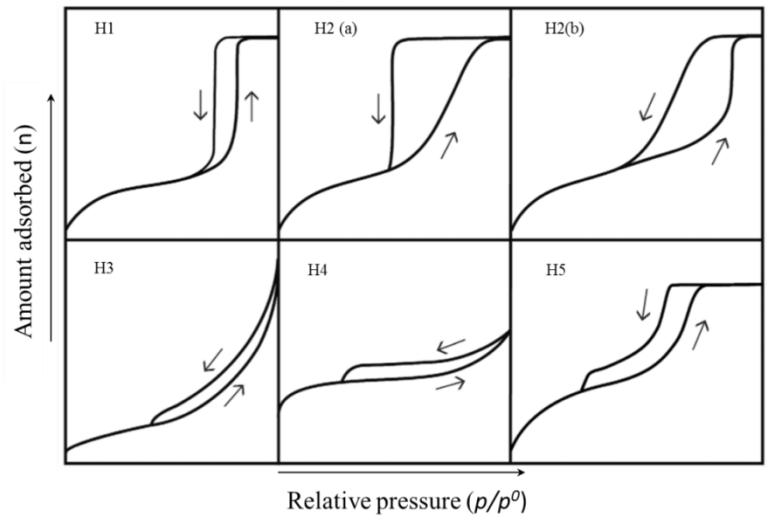

Fig.1.3: Different shapes of hysteresis loops according to IUPAC

Each of these six characteristic types is fairly closely related to particular features of the pore structure and underlying adsorption mechanism.

The **Type H1** loop is found in materials which exhibit a narrow range of uniform mesopores, as for instance in templated silica, some controlled pore glasses and ordered mesoporous carbons.

Usually, network effects are minimal and the steep, narrow loop is a clear sign of delayed condensation on the adsorption branch. However, Type H1 hysteresis has also been found in networks of ink-bottle pores where the width of the neck size distribution is similar to the width of the pore/cavity size distribution [6,15,16].

Hysteresis loops of **Type H2** are given by more complex pore structures in which network effects are important. The very steep desorption branch, which is a characteristic feature of **H2 (a)** loops, can be attributed either to pore-blocking/percolation in a narrow range of pore necks or to cavitation-induced evaporation. H2 (a) loops are for instance given by many silica gels, some porous glasses as well as some ordered mesoporous materials. The Type H2 (b) loop is also associated with pore blocking, but the size distribution of neck widths is now much larger. Examples of this type of hysteresis loops have been observed with meso-cellular silica foams and certain mesoporous ordered silicas after hydrothermal treatment [6,15,16].

There are two distinctive features of the **Type H3 loop**: (1) the adsorption branch resembles a Type II isotherm (2) the lower limit of the desorption branch is normally located at the cavitation-induced p/p^0. Loops of this type are given by non-rigid aggregates of plate-like particles (e.g., certain clays) but also if the pore network consists of macropores which are not completely filled with pore condensate [6,16,17].

The **Type H4 loop** is somewhat similar, but the adsorption branch is now a composite of Types I and II, the more pronounced uptake at low p/p^0 being associated with the filling of micropores. H4 loops are often found with aggregated crystals of zeolites, some mesoporous zeolites, and micro-mesoporous carbons.

Although the **Type H5 loop** is unusual, it has a distinctive form associated with certain pore structures containing both open and partially blocked mesopores. As already indicated, the common feature of H3, H4 and H5 loops is the sharp step-down of the desorption branch. Generally, this is located in a narrow range of $p/p^0$for the particular adsorptive and temperature (e.g., at $p/p^0 \approx$ 0.4 – 0.5 for nitrogen at temperatures of 77 K)[6,17].

1.5-Equations to describe adsorption isotherms

The more important equations to describe adsorption isotherms are the **Langmuir**, the **Freundlich**, the **Brunauer-Emmett-Teller** (**BET**), and the **Dubinin-Radushkevich** (**DR**) equations. Although the Langmuir and Freundlich isotherms are equally important for physisorption, both equations are also used for chemisorption.

1.5.1-Brunauer-Emmett-Teller (BET) method

The BET equation and DR equations are most important for analysis of the physical adsorption of gases and vapors on porous carbons [18-29].

The **Brunauer–Emmett–Teller method** continues to be the most widely used procedure for evaluating the surface area of porous and finely-divided materials, in spite of the weakness of its theoretical foundations [6,18,21,22,25]. Two stages are involved in the application of the BET method. First, it is necessary to transform a physisorption isotherm into the 'BET plot' and from it derive a value of the BET monolayer capacity, n_m. In the second stage, the BET-area, a(BET), is calculated from n_m.

It is customary to apply the BET equation in the linear form:

$$\frac{(p/p^0)}{n\cdot(1-p/p^0)} = \frac{1}{n_m\cdot C} + \frac{C-1}{n_m\cdot C}\cdot(p/p^0) \qquad (1.1)$$

Where, n is the specific amount adsorbed at the relative pressure p/p^0 and n_m is the specific monolayer capacity. According to the BET theory, the parameter C is exponentially related to the energy of monolayer adsorption. Thus, if the value of C is at least ≈ 80 the knee of the isotherm is sharp and Point B is fairly well defined [6,18,25]. It was this characteristic point which was first identified by Brunauer and Emmett as the stage of monolayer completion and the beginning of multilayer adsorption. If C is low ($< \approx 50$) Point B cannot be identified as a single point on the isotherm. There is then an appreciable overlap of monolayer and multilayer adsorption and the precise interpretation of n_m is questionable. When $C < 2$, the isotherm is either Type III or Type V and the BET method is not applicable. A high value of C (say, $> \approx 150$) is generally associated with either adsorption on high-energy surface sites or the filling of narrow micropores [6,21,25].

The second stage in the application of the BET method is the calculation of the BET-area from the monolayer capacity. This requires a knowledge of the average area, σ_m (molecular cross-sectional area), occupied by the adsorbate molecule in the complete monolayer, thus

$$S_{BET} = n_m \cdot L \cdot \sigma_m / m \qquad (1.2)$$

Where L is the Avogadro constant, m is mass of adsorbent and S_{BET} is the BET specific area of the adsorbent (of mass m).

The calculated value of the BET area is dependent on (1) the adsorptive and operational temperature and (2) the procedure used to locate the pressure range in applying the BET equation [6,18,21,22,25].

Nitrogen (at its boiling temperature, 77 K) was traditionally the adsorptive generally used to obtain S_{BET}, with $\sigma_m(N_2)$ assumed to be 0.162 nm^2 (based on the assumption of a closed-packed monolayer). This is partly due to the fact that liquid nitrogen was readily available and also because nitrogen isotherms on many adsorbents were found to exhibit a well-defined Point B. However, it is now recognized that due to its quadrupole moment, the orientation of a nitrogen molecule is dependent on the surface chemistry of the adsorbent. This may lead to uncertainty in the value of $\sigma_m(N_2)$ – possibly ≈20% for some surfaces [6].

Argon may seem to be an alternative adsorptive for surface area determination. Argon does not have a quadrupole moment and is less reactive than the diatomic nitrogen molecule. There are, however, several reasons why argon at 77 K is considered to be less reliable than nitrogen. At 77 K, argon is ca. 6.5 K below the bulk triple point temperature and hence the bulk reference state is in doubt. Furthermore, there is evidence that at 77 K, the structure of the argon monolayer is highly dependent on the surface chemistry of the adsorbent [6].An alternative is argon adsorption at 87 K, i.e., at liquid argon temperature. Here, the problems encountered with argon at 77 K are not present. At 87 K, a cross-sectional area, σ_m(Ar), of 0.142 nm^2 is usually assumed. Because of the absence of a quadrupole moment and the higher temperature, σ_m(Ar) is less sensitive to differences in the structure of the adsorbent surface [6]. Furthermore, argon adsorption at 87 K offers advantages in particular for micropore analysis (see later). Measurements at 87 K can be performed by using either liquid argon (instead of liquid nitrogen).

The BET method can be applied to many Type II and Type IV isotherms, but extreme caution is needed in the presence of micropores (i.e., with Type I isotherms and combinations of Types I and II or Types I and IV isotherms). It may be impossible to separate the processes of monolayer multilayer adsorption and micropore filling. With microporous adsorbents, the linear range of the BET plot may be very difficult to locate [6,18,21,22,25].

It must be re-emphasized that this procedure should not be expected to confirm the validity of the BET monolayer capacity.

Thus, the BET-area derived from a Type I isotherm must not be treated as a realistic probe accessible surface area. It represents an apparent surface area, which may be regarded as a useful adsorbent "fingerprint" [6,8,2,22,25].

Physisorption filling of micropores always occurs at low relative pressures. The range of low pressure is dependent on the shape and dimensions of the micropores, the size of the adsorptive molecules and their interactions with the adsorbent and with each other. Adsorption in narrow micropores (i.e., the "ultramicropores" of width no more than two or three molecular diameters depending on pore geometry) involves some overlap of the adsorption forces and takes place at very low relative pressures. This process has been termed 'primary micropore filling', whereas wider micropores are filled by a secondary process over a wider range of higher relative pressure (e.g., $p/p^0 \approx 0.01–0.15$ for argon and nitrogen adsorption at 87 K and 77 K). Enhancement of the adsorbent-adsorbate interaction energy is now reduced and cooperative adsorbate–adsorbate interactions in the confined space become more important for the micropore filling process [6,2,4].

1.5.2-Dubinin-Radushkevich (DR) method

The method was originally developed to investigate the microporosity of activated carbons, can be used for any microporous material. Adsorption isotherms of pure gases on microporous sorbents can be described by means of Polanyi's potential theory (basis of the DR equation). Each gas-sorbent system is characterized by an adsorption potential E (in $Jmol^{-1}$) which is influenced in particular by the chemical properties of the adsorbent. The volume of adsorbate filling micropores W (in cm^3g^{-1}) at a given relative pressure p/p^0 as a part of the

total micropore volume W_0 (in cm^3g^{-1}) is a function of the adsorption potential E [19,23-26]:

$$W = f(E) \quad (1.3)$$

According to Dubinin, the adsorption potential equals the work required to bring an adsorbed molecule into the gas phase. For T<Tcr (critical temperature), Polanyi's potential yields

$$E = -RTln\left((p/p^0)\right) \quad (1.4)$$

For the characteristic function, the empirical relation can be expressed as:

$$\frac{W}{W_0} = exp\left[-\left(\left(\frac{RT}{\beta E_0}\right)\cdot ln\left(\frac{p}{p^0}\right)\right)^2\right] \quad (1.5)$$

The characteristic adsorption energy E_0 (in $Jmol^{-1}$) characterizes the pore distribution, while the affinity coefficient β unites all the curves for each gas on the same adsorbent to one characteristic curve. The DR isotherm then can be written in logarithmic form to give a straight line [1,6,19,23-26]:

$$\log_{10} W = \log_{10} W_0 - D\left[\left(\log_{10}\left(\frac{p^0}{p}\right)\right)^2\right] \quad (1.6)$$

$$D = \frac{1}{\log_{10}(e)}\cdot\left(\frac{RT}{\beta E_0}\right)^2 \quad (1.7)$$

To evaluate the data, the region of relative pressure $10^{-4}<(p/p^0)< 0.1$ is usually preferred.

The data are registered in a diagram $\log_{10}W$ versus $\left(\log_{10}\left(\frac{p^0}{p}\right)\right)^2$.The slope of the regression line gives the parameter D. The total micropore volume W_0 can be calculated from the ordinate intercept [1,2,6,19,23-26].

The DR model has its roots in the structure of porosities and their distributions of structure (and hence of adsorption potential). The DR equation is not based on a model of the adsorption process. It is a derivative of the mathematics of Rayleigh, Gaussian or Lorenztian distributions.

Micropore size analysis

Two important methods have been developed to describe the sorption and phase behavior of inhomogeneous fluids confined to porous materials: computer simulation and Density Functional Theory (DFT).

DFT is a computational method that treats the intrinsic free energy of a system as a functional of the particle distribution function (Evans 1992). These methods can be used to calculate equilibrium density profiles of a fluid adsorbed on surfaces and in pores from which the adsorption/desorption isotherms, heats of adsorption, and other thermodynamic quantities can be derived. Although the local DFT provides qualitatively reasonable description of adsorption in the pores, it is quantitatively inaccurate especially in the range of small pores. A significant improvement in accuracy was obtained with the Non-Local Density Functional Theory (NLDFT) which was first used for the pore size analysis of microporous carbons in 1993 by Lastoskie et al. (Lastoskie 1993). Since then, the NLDFT has been applied frequently to the pore size analysis of microporous and mesoporous materials [15-17,25,26]. They describe the distribution of adsorbed molecules in pores on a molecular level and thus provide detailed information about the local fluid structure near the adsorbent surface. The fluid–solid interaction potential is dependent on the pore model. Different pore shape models (e.g., slit, cylinder and spherical geometries and hybrid shapes) have been developed for various material classes such as carbons, silicas, zeolites. It follows that pore size characterization methods based on the NLDFT approach are applicable to the whole range of micropores and mesopores. [25,26].

NLDFT based methods for pore size/volume analysis of nanoporous materials are now available for many adsorption systems [7,14,16,25,26]. They are included in commercial software and are also featured in international standards (such as ISO 15901-3). These methods allow to calculate for a particular adsorptive/adsorbent pair a series of theoretical isotherms, N(p/p^0,W), in pores of different widths for a given pore shape. The series of theoretical isotherms is called the kernel, which can be regarded as a theoretical reference for a given class of adsorbent/adsorptive system. The calculation of the pore size distribution function f(W) is based on a solution of the General Adsorption Isotherm (GAI) equation, which correlates the experimental adsorption isotherm $N(p/p^0)$ with the kernel of the theoretical adsorption or desorption isotherms $N(p/p^0,W)$. For this purpose, the GAI equation is expressed in the form:

$$N(p/p^0) = \int_{W_{\min}}^{W_{\max}} N(p/p^0, W)\, f(W)\, dW \qquad (1.8)$$

$N(p/p^0)$ = experimental adsorption isotherm data

W = pore width (in nm)

$N(p/p^0, W)$= isotherm on a single pore of width W

$f(W)$ = pore size distribution function

Although the solution of the GAI equation with respect to the pore size distribution function $f(W)$ is strictly an ill-posed numerical problem, it is now generally accepted that meaningful and stable solutions can be obtained by using regularization algorithms [6,7,14,16,25,26].

Several approaches have been suggested to account for the heterogeneity of most adsorbents, which, if not properly taken into account, can lead to appreciable inaccuracy in the pore size analysis. Such methods include the development of complex 3D structural models of disordered porous solids by advanced molecular simulation techniques, but these are still too complex to be implemented for routine pore size analysis. The drawbacks of the conventional NLDFT model which assumes a smooth and homogenous adsorbent surface have been addressed by the introduction of two-dimensional DFT approaches [6,7,12].

Quenched Solid Density Functional Theory (QSDFT) is another approach to quantitatively allow for the effects of surface heterogeneity in a practical way [6, 8,25,26]. It has been demonstrated that taking into account surface heterogeneity significantly improves the reliability of the pore size analysis of heterogeneous nanoporous carbons.

1.5.3-Langmuir equation

Most important assumptions of Langmuir equations are:

(a) The adsorbed entities (atoms or molecules or ions) are attached to the surface at definite localized sites.

(b) Each site accommodates one and only one adsorbed entity.

(c) The energy state of each adsorbed entity is the same at all sites on the surface independent of the presence or absence of other absorbed entities at neighboring sites.

Thus, the Langmuir model (also called localized model) assumes that the surface is perfectly smooth and homogenous and that the lateral interactions between the adsorbed entities are negligible [27,28].

In reality, none of the above assumptions apply to heterogeneous adsorbents, even approximately, so it comes as a surprise that the Langmuir equation can be used to linearize adsorption isotherms. In fact, assumptions (a) and (b) probably compensate for each other, as adsorbate-adsorbate interactions increase with increasing coverage at the same time as enthalpies of adsorption decrease with increasing coverage.

Nevertheless, the Langmuir equation (eq.1.9) still retains an important position in physisorption [1,2,5,27,28].

$$\frac{(p/p^0)}{n} = \frac{1}{n_m \cdot b} + \frac{(p/p^0)}{n_m} \tag{1.9}$$

Where p= equilibrium vapor pressure, p^0= saturation vapor pressure (both in Pa), n= amount adsorbed and n_m= monolayer capacity (both in mol g^{-1})

In contrast, Langmuir and Freundlich are the two most common models for chemisorption from a solution. The Langmuir model is more fundamental, has conceptual endpoints as it asymptotically approaches a maximum solid-phase concentration at the very high liquid-phase concentration range, and has a linear equilibrium relationship at the very low–concentration ranges.

In that case, Langmuir is also presented in terms of the adsorbate concentration in equilibrium c_i in the fluid phase as [8,28,29]:

$$n = \frac{n_m \cdot K_i \cdot c_i}{1 + K_i \cdot c_i} \tag{1.10}$$

K_i is the equilibrium constant. These parameters are often determined by plotting $1/n$ versus $1/c_i$.

1.5.4-Freundlich equation

The Freundlich model can be derived theoretically from the Langmuir model assuming a distribution of adsorption site energies.

$$n = K_F \cdot {c_i}^m \tag{1.11}$$

Where K_F is the Freundlich equilibrium constant, m is positive and generally not an integer. The isotherm corresponds approximately to an exponential distribution of heats of adsorption. Although it lacks the required linear behavior in the Henry's law region, it can often be used to correlate data on heterogeneous adsorbents over wide ranges of concentration [28,29].

1.6-Fundamental aspects to take into account for adsorbent characterization

The growing importance of adsorption (e.g. in separation technology, industrial catalysis and pollution control) has resulted in the appearance of various new procedures over the past few years for the interpretation of adsorption data particularly for micropores and mesopores size analysis[3,6].
However, some aspects must be considered in the characterization of an adsorbent in order to properly interpret the obtained results to get more significant, accurate and useful information about the possible performance of the adsorbent for a dedicated application.

1.6.1-Specific surface area

As was previously defined, the "specific surface area" is defined as the area of solid surface per unit mass of material. In practice, what is actually determined is the accessible (or detectable/apparent) area of solid surface per unit mass of material.
This distinction is important because the value determined in a measurement is dependent on the method, the experimental conditions employed, and the size of the probe (e. g., the molecular size of the adsorbate or the wavelength of a radiation probe) [28,29].
More significantly, the specific surface area is usually deduced from measured quantities that must be interpreted using simplified models of the measurement process. Consequently, the recorded value depends inherently on the validity of the assumptions used in the model.

1.6.2-Pore size

"Pore size," like specific surface area, it is not amenable to a precise definition. The problems already mentioned for the specific surface area are complicated further by the fact that the pore shape is usually highly irregular and variable, leading to a variety of definitions of "the size." Moreover, pore systems usually consist of interconnected networks. As a result, the detected pore volume may depend on the sequence in which pores are encountered by the probe substance.

Consequently, quantitative descriptions of pore structure usually are based on model systems. The limiting feature of a pore, for most applications, is the size of the smallest dimension of the assumed pore shape. In the absence of greater precision, the smallest dimension is referred to as the width of the pore, i.e., the width of a slit-shaped pore and the diameter of a cylindrical pore. To avoid a misleading change in scale when comparing cylindrical and slit-shaped pores, the convention is to use the diameter of a cylindrical pore, rather than its radius, as its "pore width" [6].

1.6.3-Pore analysis instruments

Apart of the methods based on physisorption, several methods have been developed for determining the surface area and the pore size distribution in porous systems [7,13]. The operations of these different methods generally are based on different physical principles. It should be expected, therefore, that they effectively represent probes of different sizes and, hence, that the pore size ranges in which they are most reliable are necessarily different.

Figure 1.4 compares the ranges of validity of a selection of methods commonly used for pore characterization. In despite of all the proposed methods, the complexity of the porous texture of materials is such that even on theoretical grounds the concepts which can be used to describe the texture usually entail the introduction of simplifying assumptions.

No experimental method provides the absolute value of parameters such as porosity, surface area, pore size, and surface roughness. Each gives a characteristic value that depends on the principles involved and the nature of the probe used (atom or molecule, radiation wavelength...). One cannot speak of the surface area of an adsorbent but, instead, further specifications must be provided, being more appropriated to use terms such as: "BET-nitrogen surface area", "equivalent/apparent BET-nitrogen surface area", "modified HJ-calorimetric surface area", "cumulative water thermoporometry surface area", etc.[2,5,7].The method chosen must indeed assess a parameter related as directly as possible to phenomena involved in the application of the porous material. In this respect, it may often be advisable to select a method involving physical phenomena similar or close to those involved during the practical application [1,5,7].

Rather than to "check the validity" of distinct methods, certified reference porous materials are needed to establish how these methods differ and, of course, to calibrate any individual equipment or technique.

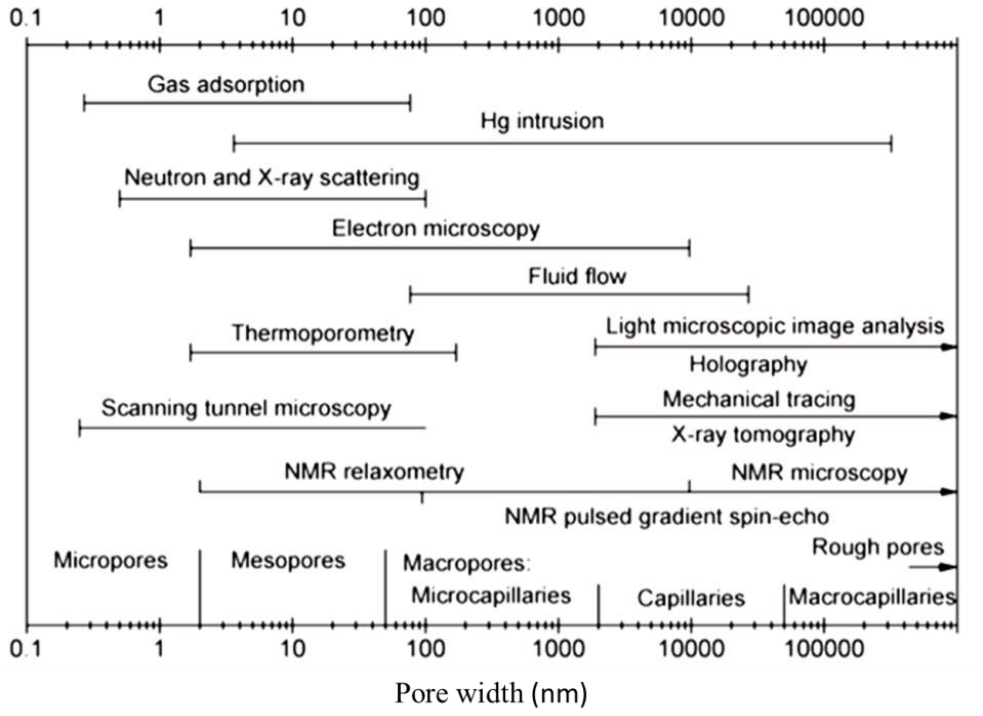

Fig.1.4: Measuring ranges of methods for pore size determination (adapted from [7]).

As a consequence, one must not look for a "perfect agreement" between parameters provided by different methods. Such an agreement, when it occurs, is not necessarily a proof of the validity of the derived quantities. Instead, one must be aware of the specific, limited, and complementary significance of the information delivered by each method of characterization of a porous solid [7].

1.6.4-Choice of the adsorptive probe for pore size distribution assessment

The gases used are bound by physisorption at the solid surface, in particular N_2 at 77 K, Ar at 77 K or 87 K, or CO_2 at 195 K. It should be noted that these gas molecules have different sizes and the measurement temperatures are different.

Consequently, they are not expected to yield the same values[3,7,8].For many years, nitrogen adsorption at 77 K has been generally accepted as the standard method for both micropore and mesopore size analysis, but for several reasons it is now becoming evident that nitrogen is not an entirely satisfactory adsorptive for assessing the micropore size distribution.The rate of diffusion is slow in this ultra-low pressure range, which makes it difficult to measure equilibrated adsorption isotherms. Additional problems are associated with pre-adsorbed N_2 molecules, which can block the entrances of narrow micropores, and specific interactions with surface functional groups so that the pore filling pressure is not clearly correlated with the pore size/structure.

It follows that in order to measure an adsorption isotherm accurately careful consideration should be given to the choice of the adsorptive and the operational temperature.

In contrast to nitrogen, argon does not exhibit specific interactions with surface functional groups. However, the interpretation of argon isotherms at liquid nitrogen temperature is not straightforward. At 87 K, this problem is avoided since argon fills narrow micropores at significantly higher relative pressures in comparison with nitrogen at 77 K [6, 25,26]. This leads to accelerated equilibration and permits the measurement of high resolution adsorption isotherms. Hence, argon adsorption at 87 K allows a much more straightforward correlation to be obtained between the pore filling pressure and the confinement effect (depending on pore width and shape).

Because of kinetic restrictions at cryogenic temperatures (87 K, 77 K) argon and nitrogen adsorption is of limited value for the characterization of very narrow micropores. One way of addressing this problem is to use CO_2 (kinetic dimension 0.33 nm) as the adsorptive at 273 K. At 273 K, the saturation vapor pressure of CO_2. is very high (~ 3.5 MPa) and hence the pressures required for micropore size analysis are in the moderate range (~ 0.1 to–100) kPa. Because of these relatively high temperatures and pressures, diffusion is much faster and pores as small as 0.4 nm can be accessed. On the other hand, the easily measurable maximum relative pressure for measurements with CO_2 at 273 K is $p/p^0 \approx 3 \times 10^{-2}$ (corresponding to ambient pressure) and hence only pores < 1 nm can be explored.

Adsorption of CO_2 at 273 K has become an accepted method for studying carbonaceous materials with very narrow micropores and has been described in various textbooks and reviews [6,8,25,26]. However, CO_2 cannot be recommended for the pore size analysis of microporous solids with polar surface groups.

1.6.5-General procedures for sampling and sample preparation

Sampling

The goal of sampling is to collect a small amount of powder from the bulk quantity such that this smaller fraction is representative of the characteristics of the entire bulk. That requires the inspection of the bulk (thereby greatly reducing the amount of time and effort spent in sampling) [30,31].

Outgassing

Prior to the measurement of an adsorption isotherm, all the physisorbed species should be removed from the surface of the adsorbent. This may be achieved by outgassing, a procedure involving exposure of the surface to a high vacuum at elevated temperatures, or by flushing the adsorbent with an inert gas, typically with helium or nitrogen.

To obtain reproducible isotherms, it is necessary to control the outgassing conditions such as temperature level, outgassing time, change in pressure over the adsorbent, and the residual pressure.

Some samples require careful attention when heat is applied due to the possibility of thermal degradation. Outgassing is usually carried out at a high temperature and under ultrahigh vacuum conditions for several hours, as well as flushing with certain gases, this practice may lead to changes in the surface composition, e.g. through decomposition of hydroxides or carbonates, formation of surface defects, or irreversible changes of the structure.

The maximum temperature at which the sample is not affected may be determined by thermogravimetric analysis or by trial experiments using different degassing conditions of time and temperature [3,5,6,7,25,26].

1.7- Activated Carbon

Activated carbon is the most widely used adsorbent material [1]. Their adsorbent properties are essentially attributed to their large surface area, microporous structure, high adsorption capacity, a high degree of surface reactivity and a favorable pore size which makes the internal surface accessible and enhances the adsorption rate [8,9].

World demand for activated carbon is forecast to expand 5.2 percent per year through 2012 to 1.15 million metric tons. In another estimate activated carbon production is expected to reach 2.3 million metric tons by 2017. Consumption of activated carbons for industrial use has now become an indicator of development and environmental management efficiency.

The per capita consumption of active carbons per year is 0.5 kg in Japan, 0.4 kg in the U.S., 0.2 kg in Europe and 0.03 kg in the rest of the world [8,9].There are several hundred commercial activated carbons available, with different sizes of porosity with specific applications [10].

1.7.1-Characteristics of the activated carbon as adsorbent

The elemental composition of a typical active carbon is found to be around 88% C, 0.5% H, 0.5% N, less than 1% of S, and 6 to 7% O [8].The most widely used activated carbons have a surface area of about 800 to 1500 m^2/g and a total pore volume in the order of 0.20 to 0.80 cm^3/g[8].Generally micropores have a total pore volume of 0.15 to 0.70 cm^3/g. Their specific surface area constitutes about 95% of the total surface area of the active carbon. Thus, adsorption on active carbons takes place in micropores and only small amounts in mesopores. It is suggested that for some active carbons, the microporous structure can be subdivided into two overlapping microporous structures involving specific micropores (ultramicropores) [6] with effective pore width smaller than 0.6 to 0.7 nm and the super micropores showing width of 0.7 to 1.6 nm. Mesopores volume usually varies between 0.1 and 0.2 cm^3/g. The surface area of these pores does not exceed 5% of the total surface area of the carbon. However, by using special methods, it is possible to prepare activated carbons that have an enhanced mesoporosity, the volume of mesopores attaining a volume of 0.2 to 0.65 cm^3/g and their surface area reaching as high as 200 m^2/g.

Macropores are not of considerable importance to the process of adsorption in active carbons because their contribution to the surface area of the adsorbate is very small and does not exceed 0.5 m^2/g. Thus, the porous structure of active carbons is polydisperse comprising pores of different sizes and shapes which are included in the general categories: micro, meso, and macropores [2,8,25,26]. Each of these groups of pores plays a specific role in the adsorption process. The micropores constitute a large surface area and micropores volume and therefore determine to a considerable extent the adsorption capacity of a given active carbon, provided that the molecular dimensions of the adsorbate are not too large to enter the micropores. The macropores enable adsorbate molecules to pass rapidly to smaller pores situated deeper within the particles of active carbons being primarily relevant for the mass transfer into the interior of the adsorbent particles [2,3,7,25,26]. Thus, the pattern of porous structure in active carbons constitutes macropores opening up directly to the external surface, the transitional pores branching off from the macropores, and the micropores in turn branching off from the transitional pores. The pore size distribution in a given carbon depends on the type of the raw material and the method and conditions under which the carbon has been prepared. Although the adsorption capacity of active carbons is determined by their physical or porous structure, it is strongly influenced by the chemical structure of their surface too. In addition, active carbons are generally associated with oxygen and hydrogen, which are present in the form of specific functional surface groups. These surface groups are bonded at the edges of the aromatic sheets. Because these edges constitute the main adsorption surface, these surface groups profoundly influence the adsorption behavior of active carbons. Besides, active sites in the form of edges, dislocations and discontinuities determine the chemical reactions (chemisorption) and the catalytic properties of active carbon [8].

1.7.2-Activated carbon manufacturing

Active carbons are mainly and almost exclusively prepared by the pyrolysis of carbonaceous raw material at temperatures near to 1000°C. The preparation involves two main steps: carbonization and activation. In gas activation, usually hard woods, coconut shells, fruit stones and coal are used as raw materials. The carbonization is conducted at temperatures below 800°C in an inert atmosphere.

The carbonized material already has certain porosity but their adsorption capacity, measured as a micropore volume or surface area, is too low for commercial applications. In the activation, the carbonized material is brought in contact with an activation gas (usually steam or carbon dioxide) at elevated temperatures (800°C–1000°C) [1-13,32-75]. During the activation, the activation gas reacts with the solid carbon to form gaseous products. In this manner, closed pores are opened and existing pores are enlarged. Thus, all carbonaceous materials can be converted into active carbons, although the properties of the final product will be different, depending upon the nature of the raw material used, the nature of the activating agent, and the conditions of the activation process. During carbonization most of the non-carbon elements such as oxygen, hydrogen, nitrogen, and sulphur are eliminated as volatile gaseous products by the pyrolytic decomposition of the source raw material [1,2,8]. The residual elementary carbon atoms group themselves into stacks of aromatic sheets cross-linked in a random manner. The mutual arrangement of these aromatic sheets is irregular and therefore leaves free interstices between the sheets, which may become filled with the tarry matter or the products of decomposition or at least blocked partially by disorganized carbon. These interstices give rise to pores that make active carbons excellent adsorbents. The char produced after carbonization does not have a high adsorption capacity because of its less developed pore structure. This pore structure is further enhanced during the activation process when the spaces between the aromatic sheets are cleared of various carbonaceous compounds and disorganized carbon. The activation process converts the carbonized char into a form that contains the largest possible number of randomly distributed pores of various shapes and sizes, giving rise to a product with an extended and extremely high surface area. The activation process enhances the volume and enlarges the width of the pores. The structure of the pores and their pore size distribution are largely determined by the nature of the raw material.

The main reaction equations for the chemical processes during gas activation together with the related reaction enthalpies are given below. A positive sign of the reaction enthalpy indicates an endothermic process, whereas a negative sign indicates an exothermic process [2,3,9,10].

The reactions cause a mass loss of the solid material (burn-off). The pore volumes, expressed per unit weight of activated carbon, increase continuously with burn-off, a similar behavior for the development of surface area. Since the development of the pore system and the surface area are correlated with the burn-off, an optimum for the extent of the activation has to be found. This optimum depends on the material and is often in the range of 40% to 50% burn-off.

$C_{(s)} + H_2O_{(g)} \leftrightarrow CO_{(g)} + H_{2(g)}$	$\Delta H_R = 131$ kJ mol^{-1}	(I)
$C_{(s)} + CO_{2(g)} \leftrightarrow 2CO_{(g)}$	$\Delta H_R = 172$ kJ mol^{-1}	(II)
$2C_{(s)} + O_{2(g)} \leftrightarrow 2CO_{(g)}$	$\Delta H_R = -111$ kJ mol^{-1}	(III)
$CO_{(g)} + 0.5O_{2(g)} \leftrightarrow CO_{2(g)}$	$\Delta H_R = -285$ kJ mol^{-1}	(IV)
$CO_{(g)} + 3H_{2\,(g)} \leftrightarrow CH_{4(g)} + H_2O_{(g)}$	$\Delta H_R = -210$ kJ mol^{-1}	(V)
$CO_{(g)} + H_2O_{\,(g)} \leftrightarrow CO_{2(g)} + H_{2\,(g)}$	$\Delta H_R = -41$ kJ mol^{-1}	(VI)
$H_{2\,(g)} + 0.5O_{2(g)} \leftrightarrow H_2O_{(g)}$	$\Delta H_R = -242$ kJ mol^{-1}	(VII)

Higher burn-off degrees lead to a decrease of net surface area because no more new pores are opened, but existing pore walls are burned away and leading to the formation of macroporosity. Therefore, activated carbon production is dominated by the compromise between porosity development and yield of the process. Gas activation processes can also be used for a further activation of chemically activated carbons [2,8,10,32]. In the gas activation process, different reactor types can be applied. Rotatory kiln and multiple hearth furnaces are the most commonly used reactors [2,32].

Fig.1.5 shows a typical rotatory kiln for AC manufacturing (for more info, see also Fig.S1 in supplementary materials.) Those furnaces differ in constructions requiring expertise in quality control of the product.

Dominantly, activated carbons are used in gas- and liquid-phase applications where quite different types of porosity are needed to optimize procedures. Although not excessively expensive, say 1-10 USD per kg, the importance of regeneration is acknowledged (discussed later).

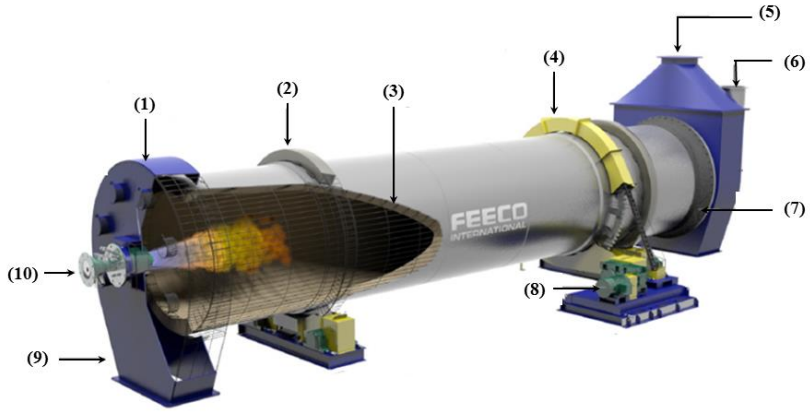

(1)Discharge breeching; (2) Riding ring; (3) Refractory lining; (4) Gear/sprocket guard; (5) Counter current exhaust system; (6) Inlet chute; (7) Leaf seal; (8) Drive motor; (9) Discharge chute; (10) Burner.

Fig.1.5: Typical rotatory kiln for activated carbon production.

1.7.3- Industrial applications of activated carbon.

Activated carbon is applied in many industrial scenarios, but especially in the environmental field. Aside from environmental pollution control, activated carbon is mainly used in industry in various liquid and gas phase adsorptions. Gas phase applications include recovery of organic solvents, removal of sulfur-containing toxic components from exhaust gases and recovery of sulfur, biogas purification, use in gas masks, among others [10]. However, adsorption from the liquid phase (mainly water) is more common than from the gas phase. Among liquid phase applications one can list food processing, preparation of alcoholic beverages, color removal of oils and fats, product purification in sugar refining, purification of chemicals (acids, amines, glycerin, glycol, etc.), enzyme purification, decaffeination of coffee, gold recovery, refining of liquid fuels, purification in electroplating operations, purification in the clothing, textile, personal care, cosmetics, and pharmaceutical industries, and applications in the chemical and petrochemical industries. They are also used in medical and veterinary applications, soil improvement, removal of pesticide residues, and nuclear and vacuum technologies. Activated carbons are applied in two different forms, as granular activated carbon (**GAC**) with particle sizes in the range of 0.2 to 5 mm and powdered activated carbon (**PAC**) with particle sizes < 40 μm.

A summary of some physical properties of PAC and GAC are presented in Table 1.2. Basically, in the case of adsorption from a liquid phase, the activated carbon is used for removal of taste, color, and odor. In general, liquid phase applications require activated carbons with a larger pore size in comparison with those used for adsorption from a gas phase [2,5,8-10,32].

Table 1.2: Physical characteristics of typical activated carbons for industrial use

		Apparent density (kg/m^3)		**Average particle diameter (mm)**	
Porosity (cm^3/g)	**Surface area (m^2/g)**	**GAC**	**PAC**	**GAC**	**PAC**
0.2-0.8	800-1500	300-650	200-750	0.2-5.0	0.01-0.04

The different particle sizes are related to different application techniques. More technological details are discussed in the following chapters.

1.7.4- Adsorption from a liquid phase using powdered activated carbon

The industrial use of PAC for adsorption in liquid phase can be carried out by two methods: contact batch and continuous layer filtration methods. There is a third method, which is a combination of both methods.

The contact batch method (more applied) is a batch process where a given amount of PAC is added to the liquid placed in a stirred tank (mixed-batch contactor) [1,2,4,5,8-11,32].The resulting suspension is kept at constant temperature for a time period, which is sufficient long to attain adsorption equilibrium. The suspension is then pumped into filter presses to remove the carbon.

1.7.5- Adsorption from a liquid phase using granular activated carbon

Fixed-bed contactor system by packing granular activated carbon is generally used to conduct adsorption separation and purification in liquid phase. The GAC adsorber consists of a lined steel column or a steel or concrete rectangular tank in which the carbon is placed to form a 'filter' bed. The liquid is applied at the top of the carbon column, flows downward through the carbon bed, and is withdrawn at the bottom of the column. As the liquid flows through the column, the pollutants are adsorbed [1,2,4,5].

The carbon is held in place with a drain system at the bottom of the contactor. Often, a small layer (5 to 10 cm) of sand (1 to 2 mm in diameter) is located between the activated carbon and the bottom. This helps to remove carbon fines. Fixed-bed carbon adsorbers may be operated under pressure or gravity flow [8-11,32].

1.8- Principle of adsorption from a liquid phase

The literature relevant to adsorption from liquid phase is extensive and confusing [9,10]. A dominant reason for this, is that many of these studies are not comprehensive enough, meaning that an individual study must look, without exception, at all of the variables which influence extents of such adsorptions. The same variables apply, more or less equally, to adsorptions of both inorganic and organic solutes [4,10].

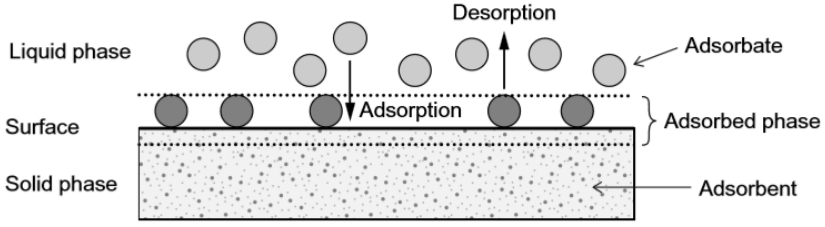

Fig.1.6: Adsorption process in liquid phase (adapted from [2])

Basically, for the adsorption in liquid phase (Fig.1.6), the adsorbent provides the surface for adsorption where the adsorbed species will be retained in an adsorbed phase. By changing the properties of the liquid phase (e.g. concentration, temperature, pH) adsorbed species can be desorbed from the surface and transferred back into the liquid phase.

1.8.1- Adsorption kinetics from a liquid phase

In an adsorption system, equilibrium is established between the adsorbent and the adsorbate in the bulk phase. The definition of adsorption kinetics is the rate of approach to equilibrium. Adsorption equilibrium does not appear instantaneously because the rate of adsorption is usually limited by the following mass transport mechanisms and depends both on the properties of the adsorbent and the adsorbate [1,5].

Due to solute concentration gradients between solution and solid, molecules diffuse and tend to accumulate as a surface layer until the balance of surface forces is reached. The adsorption mechanism, corresponding to solute transfer from solution to solid and to interactions between solute and surface, is described by several steps that are presented in Figure 1.7.

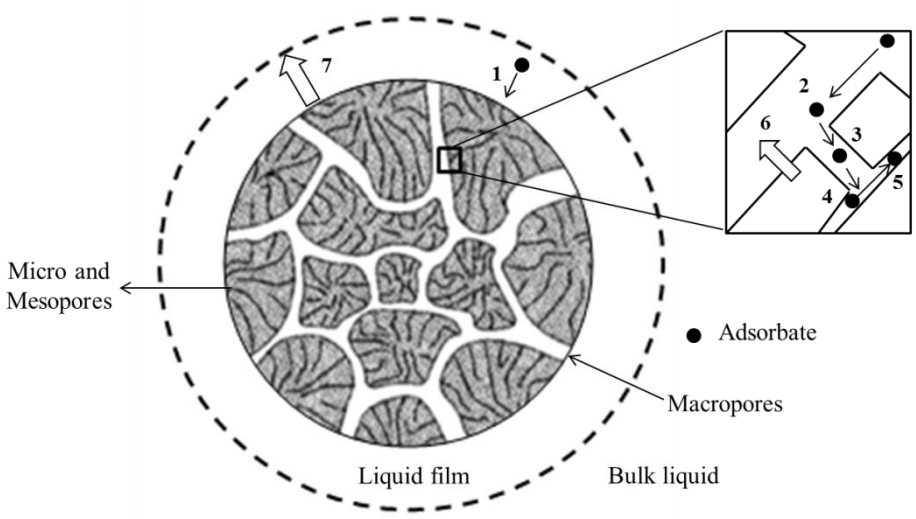

Fig.1.7: External and internal (intraparticle) transport of an adsorbate in an AC grain.

1. **Bulk diffusion.** Adsorbates must first be transported from the bulk solution to the boundary layer of the liquid (liquid film) surrounding the activated carbon particle. External diffusion in adsorption may be an additional resistance to the mass transfer to the carbon surface associated with the transport of adsorbate from the bulk of solution across the stationary layer of liquid. Mass transport through this layer occurs by molecular diffusion for which the driving force is the concentration difference. The rate of this diffusion depends on the hydrodynamic properties of the system [1,2,4].

2. **External mass transfer.** The mass transfer occurs through the high-concentration liquid film around the adsorbent. The film thickness is a function of the turbulence in the system.

3. **Diffusion in the porous volume.** Intraparticle diffusion involves the transfer of adsorbate from the surface of a particle to sites within the particle.

It is independent of hydrodynamic conditions in a system, but depends on the size and pore structure of the particle [1,5]. Intraparticle diffusion may occur by pore diffusion, which is the molecular diffusion of solutes in fluid-filled pores. The diffusion coefficient evolution is a function of the pore width. The diffusivity is close to that found in a liquid for macropores while the values are smaller for micropores, depending on the size ratio between adsorbate and pore size.

4. **Adsorption.** After the transport of the adsorbate to an available site, an adsorption bond is formed. In the case of physical adsorption, the actual physical attachment of adsorbate onto adsorbent is regarded as taking place very rapidly. Therefore, the slowest step among the preceding diffusion steps, called the rate-limiting step, will control the overall rate at which the adsorbate is removed from solution. However, if adsorption is accompanied by a chemical reaction that changes the nature of the molecule, the chemical reaction may be slower than the diffusion step and may thereby control the rate of removal [5] .The adsorbate interacts very quickly with the solid surface and produces an exothermic reaction. The reaction energy depends on the adsorbate molecular properties and adsorbent structure.

5. **Slow surface diffusion.** After adsorption, the molecules diffuse on the adsorbent surface. In this case, the diffusivity is very low: about 10,000 times lower than the pore diffusion coefficient. This transfer usually limits the global kinetics of adsorption.

6. **Thermal conduction inside the porous material.** Due to the adsorption reaction, heat is conducted through the solid to the solution.

7. **Thermal conduction through the aqueous solution.** The energy produced during adsorption reaction is transferred to the bulk liquid.

Based on the mechanisms involved in adsorption kinetics, a dominant aim of liquid phase adsorption studies is to maximize adsorption of the adsorbates, from solutions as efficiently as possible using activated carbons of known characteristics. The variables within an liquid phase adsorption system controlling extents of adsorption include [8,10]:

1. Volume of ultramicropores, < 0.7nm (including the pore-size distributions).
2. Volume of supermicropores, 0.7-2.0 nm (including the pore-size distributions).
3. Volume in mesopores, 2-5nm, (including the pore-size distributions).

4. The parameter "surface area" which is a crude parameter and fails to quantify, adequately, the capacity of the all-important micropores and their size distributions.
5. The amphoteric nature of the carbon surface.
6. The controlled formation of surface oxygen complexes from known sources.
7. The effects of surface oxygen complexes upon pore volumes and pore size distributions
8. The characteristics of surface oxygen complexes.
9. The pH of the solution
10. Ionic strength (natural and industrial water, often, is a mixture of solutes)
11. Temperature.

1.8.2-Influence of porosity on adsorption from solution

The porosity has two main effects on an adsorption process. The first one is a selectivity effect. If the liquid in equilibrium with the porous system is a mixture of molecules whose size is in the same range as pore size, a molecular sieving effect may occur. This effect can be refined enough to separate molecules which are chemically very similar as well in size. The second one is an affinity effect. Although adsorption from a liquid phase is a displacement phenomenon, the enhancement of adsorption potential in a pore, whose width is of molecular size order, is still important [5,8]. By using the same reasoning as that used for the enhancement of adsorption potential of one molecule in a pore, it is expected that the enthalpy of displacement of solvent by adsorbate in a pore will be strongly increased as compared with that on an open surface. The consequence is that the affinity of a molecule for a porous solid, as seen for example from the initial slope of adsorption isotherms, will be strongly increased if the pore size and the adsorbate molecular size are of the same order. It is appropriate to discuss these effects in terms of the size of the adsorbate molecules. For small molecules (less than 1 nm), the effect of porosity will be clearer in the microporous range. Microporosity has a strong effect on the adsorption of small molecules. Nevertheless, depending on the molecule nature, the microporous character is not sufficient to get the best efficiency: pollutants are more or less hydrophobic and the chemical functions at the surface of the carbon play an important role in the adsorption affinity [4,5,8-11].

1.9- Fixed-bed versus contact batch system

Both technical options exhibit advantages as well as disadvantages. PAC is easy to dose (typically as suspension) and is therefore ideally suited for temporary application. Due to the small particle size, the adsorption rate is very fast. Displacement processes due to competitive adsorption are less pronounced in comparison to fixed-bed adsorption. A concentration increase over the initial concentration is therefore not observed.

Disadvantages of the PAC application in slurry reactors consist of the particle discharge from the reactor that requires an additional separation step; thus, an extra cost and time consuming, the remaining residual (equilibrium) concentration of pollutant, and the missing regenerability of PAC which has to be burned or deposited after use [8-11,17,32]. Fixed-bed contactors are simple and relatively inexpensive to fabricate. Secondly, minimal attrition of adsorbent occurs when it remains fixed in position, although it should be noted that attrition in fixed bed processes which are subject to frequent changes of pressure and flow direction still remains a practical industrial problem. In contrast, they assure low outlet concentrations (zero in ideal case) until breakthrough. Particle discharge does not need to be suspected. A major advantage of GAC is that they can be regenerated and repeatedly applied for reuse when their adsorption capacity is exhausted. The slower adsorption kinetics and possible concentration overshoots due to displacement processes (discussed later) are the main disadvantages of GAC application in fixed-bed "filters" [17].

An important difference between batch reactors and fixed-bed contactors consists in the different exploitation of the adsorption capacity for the same adsorbate concentration. In batch reactors a residual concentration of pollutant remains in the liquid, and is lower than the initial concentration, while the adsorption capacity that can be utilized in the batch process is the adsorbent loading in equilibrium with the residual concentration. In the case of fixed-bed adsorption, the adsorbate solution is fed continuously to the contactor, and the adsorbent loading is in equilibrium with the inlet concentration. That permits a more efficient exploitation of the absorbent [8-11,17,32].

1.9.1- Fixed-bed technology

As discussed, vessels and columns which hold the adsorbent in a fixed position provides distinct advantages over their batch counterparts in which the adsorbent is allowed to move [8-11,17,32].

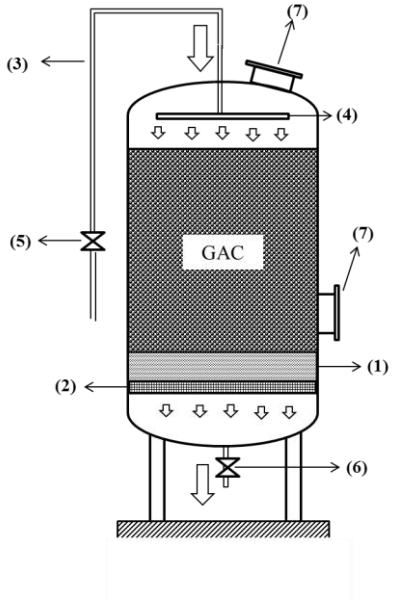

(1) Sand layer, (2) Screen, (3) Inlet tube (influent), (4) Liquid distribution header, (5) Feeding valve, (6) Outlet valve (effluent), (7) Manhole with cover.

Parameter	symbol	unit	typical values
Bed height	h	m	2 - 4
Cross sectional area	A_R	m^2	5 -30
Empty bed contact time	EBCT	min	5 - 30
Effective contact time	t_r	min	2 - 10
Bed volume	V_R	m^3	10 - 50
Bed porosity	ε_B	-	0.35-0.45

Fig.1.8: Basic model of a fixed-bed contactor and its typical operating conditions.

Such advantages enhance the use of this system in several industrial scenarios where adsorption in liquid phase takes place. Fig. 1.8 presents a basic design of a typical fixed-bed contactor and its operational conditions.

Adsorption process in a fixed bed of adsorbent is, in virtually all practical cases, an unsteady state rate controlled process. This means that conditions at any particular point within the fixed bed vary with time [8,10,17,32]. Adsorption therefore occurs only in a particular region of the bed, known as the mass transfer zone (MTZ), which moves through the bed with time.

The progress of the MTZ through a fixed bed for a single adsorbate in a diluent and the correspondent breakthrough curve are shown schematically in Fig.1.9.

According to this, fixed-bed adsorption process is time- and distance-dependent, in which each adsorbent particle in the bed accumulates adsorbate from the percolating solution as long as the state of equilibrium is reached. This equilibration process proceeds successively, layer by layer, from the column inlet to the column outlet.

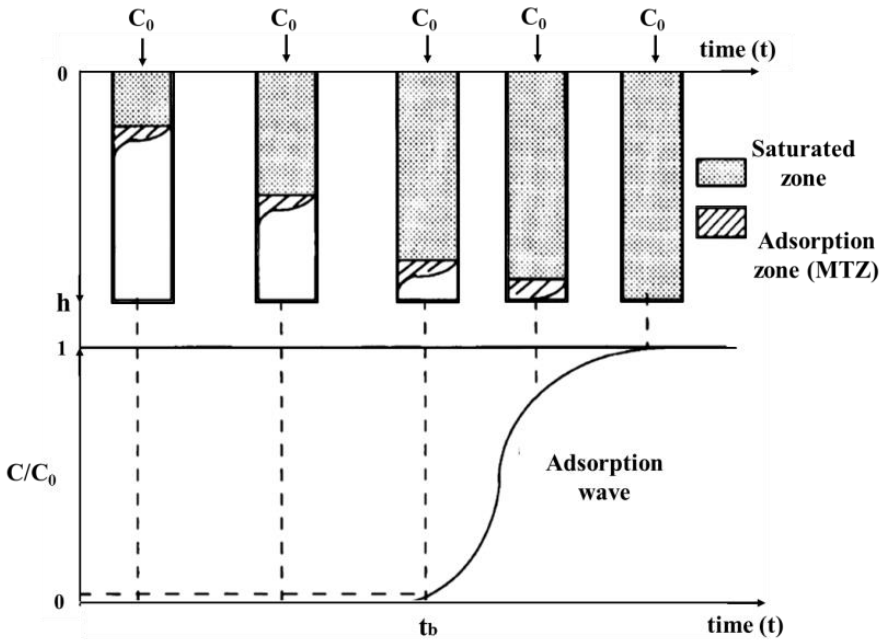

Fig.1.9: Movement of the MTZ through the bed (top) and the correspondent schematic breakthrough curve (inferior).

However, due to the slow adsorption kinetics, there is no sharp boundary between loaded and unloaded adsorbent layers. Usually, MTZ is a broad region characterized by typical concentration and loading profiles [8-11].

In practice, it is difficult to follow the progress of the MTZ inside a column packed with adsorbent because it is difficult to make meaningful measurements of parameters other than temperature. By following the progress of the exothermic which accompanies the adsorption process it is possible to gain an indication of the position of the MTZ.A detector could be placed within the adsorbent bed but there is then the risk that uncertainties about the shape of the MTZ and the possibility of channeling could lead to breakthrough earlier than anticipated.

In despite of such difficulties, valuable information to the design process can be gleaned from the time to breakthrough and from the shape of the breakthrough curve [8-11,17,32].

During the adsorption process, the MTZ travels through the adsorber with a velocity that is much slower than the liquid velocity.

The stronger the adsorption of the adsorbate, the greater is the difference between the MTZ velocity and the liquid velocity. As long as the MTZ has not reached the adsorber outlet, the outlet concentration is C = 0. The adsorbate occurs in the contactor outlet for the first time when the MTZ reaches the end of the contactor [8-11,17,32].

According to Fig. 1.9, this time is referred to as breakthrough time, "tb". After the breakthrough time, the concentration in the adsorber outlet increases due to the progress of adsorption in the MTZ and the related decrease of the remaining adsorbent capacity.

If the entire MTZ has left the adsorber, the outlet concentration equals $C=C_0$ (the thermodynamic equilibrium). At this point, all adsorbent particles in the fixed bed are saturated to the equilibrium loading, and no more adsorbate uptake takes place. MTZ depends on the flow velocity and, as mentioned previously, on the strength of adsorption. For a given flow velocity holds that the better adsorbable the adsorbate is, the later the breakthrough occurs [8-10,17].

1.9.2- Length of unused bed (LUB) model

The LUB model is a scale-up model that uses the length of the unused bed at the breakthrough point as parameter to characterize the breakthrough behavior. The location of the MTZ in a fixed-bed contactor at the breakthrough point is shown in Fig.1.10.

If the adsorption process is stopped at the breakthrough point, a fraction of the adsorbent capacity remains unused. This fraction is proportional to the distance between the location of the stoichiometric front (h_{st}) and the contactor height, (h). Accordingly, the length of the unused bed is given by

$$LUB = h - h_{st} \tag{1.12}$$

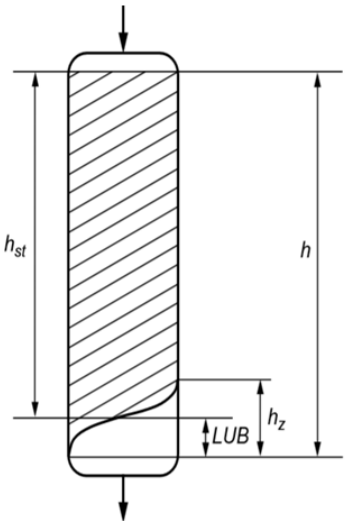

Fig. 1.10: Characteristic parameters of the LUB model (adapted from [2])

The LUB is related to the adsorption rate. The slower the mass transfer processes are, the longer is the LUB. Thus, the contactor efficiency "e_B" can be calculated as [8-11,17,32]:

$$e_B = \frac{LUB}{h} \tag{1.13}$$

1.9.3-Multiple contactors systems

The fixed-bed adsorption process in a single contactor is a semi-continuous process. Until the breakthrough, the solution can be continuously treated, but if the breakthrough occurs, the process has to be stopped and the adsorbent has to be replaced or regenerated [2,4,8-11,17, 32-75]. Multiple contactors systems can reduce the capacity loss, which results from the need to stop the process at the first adsorbate breakthrough. In principle, there are two different ways to connect single fixed-bed contactors to a multiple contactors system: (1) series connection and (2) parallel connection [2,4,8-11,17]. The principle of series connection is demonstrated in Fig. 1.11.

In this example, the total adsorbent mass is divided between four contactors. Only three contactors are in operation, whereas one is out of operation in order to replace or regenerate the adsorbent.

In the given scheme, the time, t_1, shows a point of time where contactor 1 is out of operation and the MTZ is located between contactors 3 and 4. Since the MTZ has already left contactor 2, the adsorbent in this contactor is fully saturated to the equilibrium.

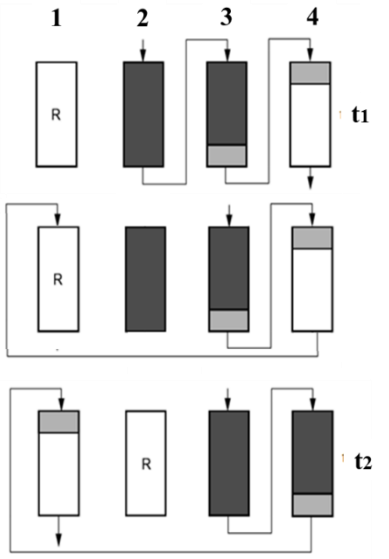

Fig. 1.11: Fixed –bed contactors in series connection. (R) contactor out of operation for GAC replacement or regeneration; dark gray: adsorbent loaded to equilibrium (exhausted); light gray: MTZ; white: adsorbent free of adsorbate (adapted from [2]).

Therefore, contactor 2 will be the next to go out of operation [2,5,8-11,32]. Time t2 represents a later time. In the meantime, the refilled contactor 1 has been put in stream again. The MTZ has traveled forward and is now located between contactors 4 and 1. The adsorbent in contactor 3 is fully saturated. Next, contactor 3 will be put out of operation, and so on. In an ideal case, all contactors can be operated until the equilibrium loading is reached for the entire adsorbent bed (maximum utilization of the adsorbent capacity). However, if the MTZ is very long and the number of contactors is limited, or if there is more than one MTZ as in mixture adsorbate systems, this maximum utilization might not be completely reached. Nevertheless, the adsorbent capacity is significantly better exploited than in a single contactor.

On the other hand, the cross-sectional area available for liquid flow through is that of a single contactor, independent of the number of contactors in operation. For a given linear liquid velocity, this cross-sectional area limits the volumetric flow rate [2,8-11,17,32].

In multiple contactor systems with parallel connection (Fig.1.12), the total solution stream to be treated is split into sub-streams, which are fed to a number of parallel operating contactors. The different contactors are put in operation at different start times.

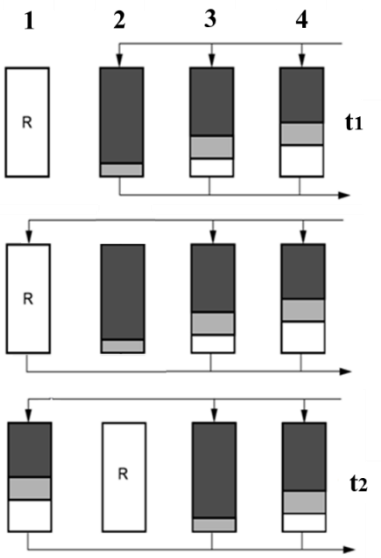

Fig. 1.12: Fixed –bed contactors in parallel connection. (R) contactor out of operation for GAC replacement or regeneration; dark gray: adsorbent loaded to equilibrium (exhausted); light gray: MTZ; white: adsorbent free of adsorbate (adapted from [2]).

Consequently, at a given time, the traveled distances of the MTZs are different in the different contactors, and therefore the breakthrough times are also different. The effluents of the different contactors with different concentrations are blended to give a total effluent stream [2,8-11,17,32]. Due to the different contactors lifetimes, the mixing of the effluents leads to low concentrations in the total effluent stream even if the effluent concentration of the contactor that was first started is relatively high [2,4,8-11,17,32].

If the blended effluent concentration becomes too high, the first loaded contactor is put out of operation for adsorbent replacement or regeneration and another contactor with fresh or regenerated adsorbent is put in operation. The scheme in Figure 1.12 shows the location of the MTZs and the degrees of saturation at two different times.

The time-shifted operation and the blending of the effluents allow operating all contactors in the system longer than in the case of a single-contactor system [2,8-11,17].Therefore, the adsorbent capacity for a parallel connection is also better exploited than in a single contactor. Although the effluent concentration in this type of multiple contactor systems is not zero, the concentration can be minimized and the treatment goal can be met by choosing an appropriate number of contactors and an optimum operating time regime. The main advantage of the parallel connection is that the total cross sectional area increases with increasing number of contactors. This type of multi contactor system is therefore very flexible and can be adapted to different requirements regarding the liquid volume to be treated [2,17].

Despite the apparent simplicity of fixed beds they are difficult to design accurately because the progress of the MTZ introduces "time" as variable into the design equations.

To solve the problem rigorously it is necessary, in most practical applications, to solve sets of partial differential equations which describe the mass and heat transfer phenomena. Several short-cut design techniques exist but they can vary considerably in their accuracy.

The uncertainties which arise, and the simplifications which are often required, inevitably introduce conservatism into the bed sizing calculations. In turn, this leads to equipment sizes and adsorbent inventories being larger than the minimum requirements [10].

1.9.4-Factors affecting GAC performance in adsorption from solutions

(1) The specific surface area and the pore volume are the most important characteristics. The adsorption capacities of a solute are directly proportional to them, additionally, pore diameters which range from less than 10 nm to over 10 μm, control the accessibility of molecules as a function of their size.

(2) The solute molecular structure (hydrocarbons, aromatic, double or triple bonds) and the presence of certain substituent groups (hydroxyl, carbonyl, amino, sulfonic, halogen or nitro groups) are important factors affecting the adsorption velocities and adsorption capacities.

Solute properties or characteristics, such as solubility and molar volume, can be correlated to adsorption parameters [2-9].

(3) In a multicomponent solution, the species compete for available adsorption sites, and this leads to a reduction in the amount adsorbed for a given adsorbate;

(3) The solvent competes with adsorption sites on the adsorbent but also attracts the adsorbate.

(4) The pH is extremely important when the adsorbate gives dissociated or ionized species.

(5) Rising temperature decreases the adsorption capacities (exothermic reaction) but the adsorption velocities increase due to the evolution of diffusion coefficients.

(6) Ionic strength affects the adsorption. It has been shown that the presence of NaCl in the solution enhances the adsorption of organics [10].

Mentioned factors influence the breakthrough pattern shape and hence performance of GAC. The spreading of the breakthrough pattern also occurs because of

(7) Dispersion in the fixed bed caused by mixing of the fluid as it passes around the GAC.

(8) External and internal mass transfer kinetics which can be affected by the properties of the adsorbent (e.g., the particle diameter) and the properties of the adsorbate (e.g., the diffusion coefficient) [32].The external surface area has a strong influence on the rate of the mass transfer during adsorption. The external mass transfer is the mass transfer through the hydrodynamic boundary layer around the adsorbent particle (Fig.7). Given that the boundary layer is very thin, the area available for mass transfer in the mass transfer equation can be approximated by the external adsorbent surface area [2,4,8].

1.9.5- Adsorption from solutions in multi-adsorbate system

So far, only single-adsorbate adsorption was considered. In the case of a multi-adsorbate system, individual MTZs for all components occur, which travel with different velocities through the adsorbent bed. As a result, displacement processes take place leading to quite different breakthrough behavior in comparison to single-adsorbate adsorption [2,8].

Figure 1.13 shows the breakthrough behavior of a two-component system. As a typical result of competition and displacement, a concentration overshoot can be observed for the weaker adsorbable component 1.Since the traveling velocity of the MTZ depends on the adsorption strength, the MTZ of the weaker adsorbable component 1 travels faster through the adsorber. It always reaches the layers of fresh adsorbent as the first component and is therefore adsorbed in these layers as a single adsorbate.

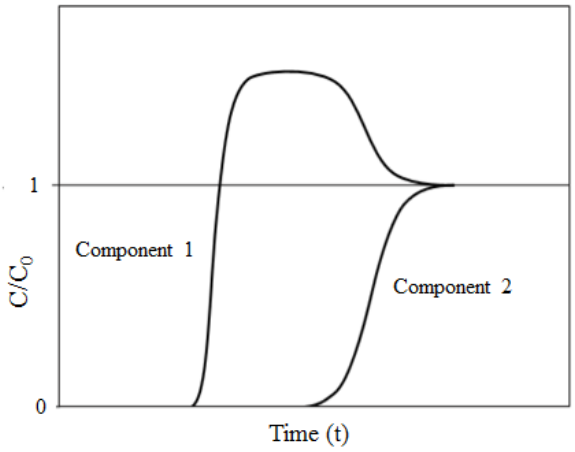

Fig.1.13: Breakthrough curves of a bi-solute adsorbate system. Component 1: weaker adsorbable; component 2: stronger adsorbable.

Later, when the stronger adsorbable component 2 reaches the same layers, a new (bi-adsorbate) equilibrium state is established [2,9]. This is connected with partial displacement of the previously adsorbed component 1. The displaced amount of component 1 equals the difference between the equilibrium adsorbent loadings in single-adsorbate and bi-adsorbate adsorption.

As a result of this displacement process, the concentration of component 1 in the region between both MTZs is higher than its initial concentration.

If the difference between the MTZ velocities of the components is large enough, a plateau zone with a constant concentration of $C>C_0$ will occur.

An analogous behavior can be observed for adsorbate mixtures with more than two components. In multicomponent systems, except for the strongest adsorbable component, all others are subject to displacement processes.

As an example, Figure 1.14 shows the breakthrough curves of a three-component system [2,8-12].

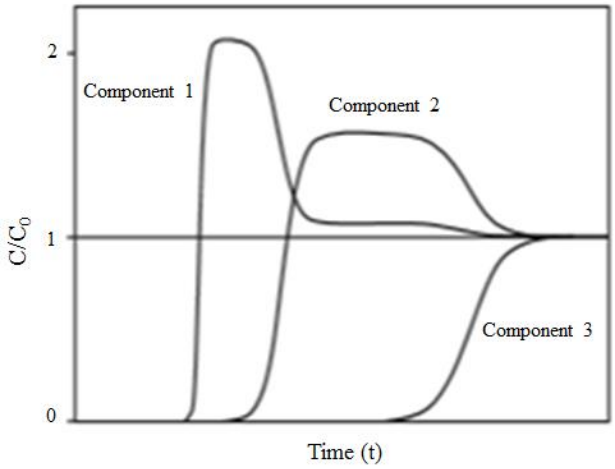

Fig. 1.14: Breakthrough curves of three components adsorbate mixture.

The first component shows two concentration plateaus located above the inlet concentration; the first results from the displacement by component 2, and the second from the displacement by component 3. Component 2 shows one plateau concentration as a result of displacement by component 3. Generally, in a system consisting of N components, the number of plateau zones, P, that can be expected for each component is given by $P = N - K$; where K is the ordinal number of the component in order of increasing adsorbability. In the example given previously, the number of plateaus, P, for component 1 is given by $P = 3 - 1 = 2$, and for component 2 by $P = 3 - 2 = 1$. The different MTZ velocities and the resulting displacement processes are also reflected in the total breakthrough curves that can be obtained by addition of the breakthrough curves of the mixture constituents [2-5,8].

It has to be noted that the plateau zones are only fully developed if the MTZs are completely separated.

This is a special case that does not necessarily occur in practice. Frequently, the MTZs of the components overlap. In particular, overlapping can be expected if one or several of the following factors apply [2,8]:

(a) Short fixed-bed length.

(b) High flow velocity.

(c) Small differences in the adsorption strengths and therefore also in the MTZ velocities.

(d) Large number of components

(e) Slow adsorption processes (broad MTZs)

Figure 1.15 shows the breakthrough curves of a three-component system with overlapping MTZs. A typical effect of MTZ overlapping is that the breakthrough of the better adsorbable component occurs before the concentration plateau of the displaced component is fully established.

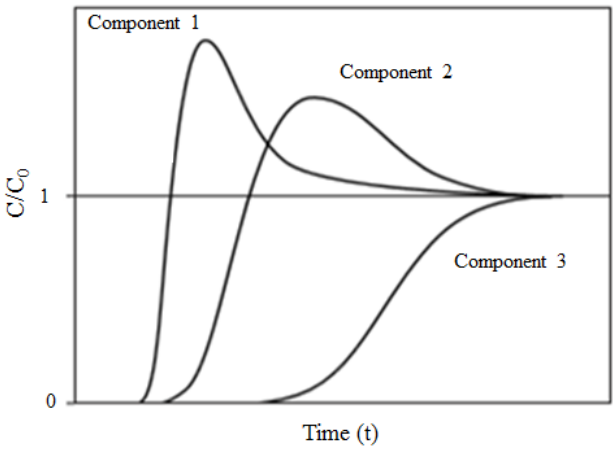

Fig. 1.15: Breakthrough curves of three components adsorbate mixture with overlapping of MTZs.

Consequently, the concentration overshoot is not as high as in the case of completely separated MTZs (Fig.1.14 vs. Fig.1.15). Furthermore, the concentration steps in the corresponding total breakthrough curves are not so clearly visible. For multicomponent systems of unknown composition, only total breakthrough curves can be measured [2-8].

1.10- GAC regeneration

The operating time of an adsorption unit (contactor) is limited by the capacity of the adsorbent. When the adsorbent capacity is exhausted, the adsorbent has to be removed from the reactor and has to be replaced by virgin or regenerated adsorbent material. Since GAC are typically highly refined and expensive products, their regenerability and the regeneration costs are important factors in view of the economic efficiency of the entire adsorption process. This aspect becomes more important the higher the adsorbent costs are and the faster the adsorbent capacity is exhausted. Regeneration of exhausted GAC offers an environmental friendly and cost-saving alternative to the use of fresh activated carbon [5,32-42].

Regeneration have been also referred as reactivation, literature survey suggests that regeneration is better term for reuse of adsorbents as it includes both desorption and activation and also carves difference between desorption and regeneration [35-41].

The chosen regeneration method should ensure:

(a) The highest possible degree of desorption of the adsorbed compound.

(b) The least possible erosion and mechanical destruction of used adsorbent.

(c) Easy access and the ecological safety of used regeneration agent or process.

(d) The easier separation of recovered or removed compounds from the adsorbate.

Techno economic viability of regeneration has to be established. Many methods of regeneration are currently being researched which include: thermal, steam, pressure swing, vacuum, micro wave, ultrasound, chemical, oxidative, ozone and bio-regeneration. Apart from these regeneration methods, combined effects of these methods have been also explored e.g. thermo-chemical regeneration, electro-chemical etc. [34-38,43].

Selection of a regeneration method depends upon the kind and characteristics of the exhausted adsorbent. If adsorbate or both adsorbent and adsorbate recovery is desired,physical means of regeneration are generally employed e.g. thermal, pressure, vacuum, microwave etc.

If adsorbent recovery or adsorbent recovery with destruction of adsorbate is required then oxidative or chemical regeneration may be preferred. However, techno-economics generally dominates the selection of procedure for regeneration [34-38].

Among the regeneration procedures, thermal regeneration is considered one of the most effective methods [30-45].

Various chemical methods can effectively restore the activity of spent carbon from which only single or defined adsorbates need to be removed or recovered. In such cases, appropriate solvents and/or chemicals are used to specifically desorb the target adsorbates.

However, chemical regeneration can restore only partial carbon's activity. Chemical regeneration may restore sufficient activity to the carbon for a few cycles of effective operation; comprehensive thermal regeneration must be applied at regular intervals to restore complete activity. Thermal regeneration effectively restores the activity of carbons loaded with organic adsorbates [2,5,8,43].

1.10.1- Thermal regeneration of exhausted GAC

Regeneration of exhausted GAC is nowadays an important part of the technology of the use of these carbons [10].During adsorption, many organic and inorganic adsorbates can accumulate within the porous structure of activated carbon. Micropores constitute the primary adsorption sites, and therefore tend to become congested to a greater degree than do mesopores and macropores. However, mesopores and macropores also capture adsorbates of relatively high molecular mass and, as a result, there is a progressive decline in adsorption efficiency [8,10,43].

1.10.2-Regeneration steps

The following steps are usual in use in the thermal regeneration of a spent carbon:

(a) **Drying:** highly volatile adsorbates are eliminated (at temperatures of up to about 200°C)

(b)**Thermal desorption**: the volatile adsorbates are vaporized and a decomposition of the thermally unstable adsorbates to form volatile products occurs (from about 200 to 500°C).

(c) **Pyrolysis:** the non-volatile adsorbates are cracked partly or completely (at about 500 to 700°C), which results in the deposition of a carbonaceous residue on the surface of the activated carbon.

(d) **Activation**: selective oxidation of the pyrolyzed residue (at about 700°C and higher) by an oxidizing agent, steam and carbon dioxide.

The first three steps normally proceed with few complications. However, pyrolysis should not be conducted at temperatures higher than 850°C in a non-oxidizing atmosphere, since graphitization of the pyrolyzed residue can occur. Therefore; it would be difficult to remove the residue without extensively damaging the structure of the activated carbon.

The proper activation of carbon in regeneration does not involve direct oxidation of the pyrolyzed residue with oxygen. On the contrary, the atmosphere within that zone of the furnace is deliberately depleted in oxygen so that reactions (III) and (IV) (§1.7.2) must be minimized. In that case C denotes the carbonaceous pyrolyzed residue or the structure of the activated carbon.

Since reactions (III) and (IV) are exothermic, and therefore self-promoting, they would, if allowed to occur, result in aggressive oxidation along the surface of the carbonaceous residue and of the original activated carbon. In practice, this would have the following effects: the pores would widen, the residue would not be removed from deep pores and, in general, the adsorption sites would not be reactivated. The result would be excessive losses of valuable activated carbon.

In an atmosphere consisting of steam or carbon dioxide, endothermic reactions (I) and (II) (§1.7.2) will predominate. An input of energy is required to sustain these endothermic reactions, which constitute the principal reactions that can be effectively controlled in the oxidation and gasification of pyrolyzed adsorbate with minimal damage to the structure of the activated carbon [2,43].

Thermal desorption

In thermal desorption, the temperature dependence of the adsorption process is utilized. Volatile substances are removed from the adsorbent surface.

If necessary, the desorbed substances could be condensed together with the water vapor and can be recovered from the condensate phase [2,8,10].

The kinetics of desorption can be determined either by the intrinsic desorption step or by pore diffusion. The desorption rate is proportional to the substance amount that is still adsorbed at the considered time, "t", and in the case a first order desorption process is considered, the rate equation reads as:

$$\frac{\mathrm{dq_{des}}}{\mathrm{dt}} = \mathrm{k_{des}} \cdot \mathrm{q}_t \tag{1.14}$$

where $\mathrm{q_{des}}$ is the amount of desorbed substance per unit adsorbent mass, q_t is the substance amount still adsorbed at time t, and $\mathrm{k_{des}}$ is the desorption rate constant. The temperature dependence of the rate constant, $\mathrm{k_{des}}$, can be described by the Arrhenius equation[2,8]:

$$\mathrm{k_{des}} = \mathrm{k_A} \cdot \exp\left(-\frac{E_{A,des}}{RT}\right) \tag{1.15}$$

where $\mathrm{k_A}$ is the pre-exponential factor (or frequency factor), $E_{A,des}$is the activation energy of the desorption process, R is the gas constant, and T is the absolute temperature. For a constant heating rate; $\mathrm{r_T}$:

$$\mathrm{r_T} = \frac{\mathrm{dT}}{\mathrm{dt}} = \mathrm{constant} \tag{1.16}$$

the following equation for the temperature dependence of desorption can be derived:

$$\frac{\mathrm{dq_{des}}}{\mathrm{dT}} = \frac{\mathrm{k_A}}{\mathrm{r_T}} \cdot \exp\left(-\frac{E_{A,des}}{RT}\right) \cdot q_t \tag{1.17}$$

The activation energy as well as the pre-exponential factor are functions of the adsorbent loading and have to be determined experimentally. For activated carbons, the required activation energy of desorption increases with increasing molecule size of the adsorbate and decreasing adsorbent loading [2,5,8,43].

This can be explained by the differences in the binding strengths. Larger molecules are more strongly bound to the surface than smaller molecules. Furthermore, in the case of energetically heterogeneous adsorbents, the sites with the highest adsorption energy are occupied at first, which leads to a relatively stronger binding at low surface coverage.

Pyrolysis and activation in regeneration

Where the adsorbent is loaded with a multitude of different substances the recovery of adsorbates is not so interesting, and restoration of the adsorption capacity remains as only objective of the adsorbent treatment. This objective can be efficiently achieved by activation. Carbonization of non-desorbed products that were formed during thermal decomposition or chemisorbed during the adsorption step and surface reactions between carbonaceous residuals and water vapor or oxidizing gases to form gaseous products are the following steps in pyrolysis and activation [5,8,40-61].

Each of these stages comprises several simultaneous steps and is associated with a particular temperature range. The reaction conditions during regeneration are similar to those used for the manufacturing of activated carbons by gas activation, but the objectives are slightly different. In gas activation, a part of the carbon material is transformed to gaseous products by reactions with the activation gases in order to receive an optimized pore structure. In contrast, during regeneration, the adsorbed species should be removed by the previously mentioned reactions with no or only minor altering of the original pore structure. Since the reaction rate of the adsorbate is much higher than the reaction rate of the carbon in the temperature range between 700°C and 850°C, a selective burn-off of the adsorbed material is, in principle, possible[43,2].

However, due to the complexity of the processes and composition of the adsorbed material, it is not easy to find the optimum process conditions, in particular the optimum residence time of the carbon in the reactor. Reactivation is therefore often carried out by the manufacturer of the activated carbon based on long-term experience. Nevertheless, an impact on the carbon structure connected with weight loss and changes in the capacity cannot be completely avoided [2,4,9]. Problems may occur if the residence time in the reactor falls considerably below or exceeds the optimum residence time. If the regeneration is insufficient, the adsorbed material is not completely removed and the capacity decreases. In case of over regeneration time, the micropore walls can be burned out to form mesopores with the consequence that the adsorption capacity for larger molecules increases, but the adsorption capacity for small molecules decreases. For regeneration, different reactors are in use.

Due to the similarities of the gas activation and regeneration processes, the same reactor types can be applied.

The rotary kiln reactors are the most used for regeneration (Fig.1.5 and Fig.S1). Regeneration process can be either carried out on the site (in site) or can be carried off-site depending on the amount of carbon to be regenerated and the factory facilities. Off-site regeneration is generally carried out when the spent adsorption generation is high or considered as a too high investment or too specialized [38-41].

Approximately 5 to 10 percent of the carbon is decomposed in the regeneration process or lost during transport and must be replaced with virgin carbon [33-36].

The capacity of the regenerated carbon is slightly less than that of virgin carbon. Repeated regeneration degrades the carbon particles until equilibrium is eventually reached providing predictable long term system performance. The main advantages and disadvantages of regeneration are [2,33-36,43]:

Advantages

(a) Systems are reliable from a process standpoint.

(b) Reduces solid waste handling problems caused by the disposal of spent carbon.

(c) Saves up to 50 percent of the carbon cost.

Disadvantages

(a) Air emissions from the furnace contain volatiles stripped from the carbon. Carbon monoxide is formed as a result of incomplete combustion. Therefore, afterburners and scrubbers are usually needed to treat exhaust gases.

(b) The induced draft fan of a rotatory kiln may produce a noise problem.

(c) The process is most effective when operated on a 24-hour basis, requiring a continuous operational control.

1.10.3-Response of different compounds to thermal regeneration

In thermal regeneration, the adsorbates associated with a spent carbon can be conveniently classified according to their responses, which are of the following types.

Type I: Volatile organic compounds that were initially adsorbed onto the activated carbon but were not irreversibly bound to active surface sites undergo thermal desorption.

Type II : Organic compounds that are not sufficiently volatile for thermal desorption, and/or that are tenaciously bound to surface sites, undergo thermal decomposition (cracking) and form volatile fragments.

Type III: The remaining compounds are pyrolyzed, and a carbonaceous residue is deposited concomitantly at about 800°C. Compounds that participate in this type of reaction are most critical in the regeneration process, since the carbonaceous residue has to be removed selectively, through endothermic oxidation with steam or carbon dioxide, at comparatively high temperatures (above 800°C).

Within this temperature range, losses of energy increase significantly, equipment specifications become more stringent and equipment more costly, and losses of the activated carbon backbone invariably occur concomitantly with the oxidation of the pyrolyzed adsorbate residues [43].

In reality, many organic adsorbates display different combinations of Types I to III behavior. Based on thermogravimetric analyses, the possible influence of various properties of the adsorbates (boiling point, aromaticity, oxygen content, and molecular mass and chemical functional groups) were considered on their response to thermal treatment [43]. Boiling point and aromaticity (ratio of aromatic carbon atoms to total carbon atoms in a molecule) appear to characterize most significantly the behavior of an adsorbate during (inert) thermal treatment, in particular the extent to which carbonaceous residuals are deposited upon heating to 800°C.

Organic compounds with high boiling points and of appreciable aromatic content are likely to exhibit Type III behavior with substantial carbonaceous residuals at 800°C. Prime examples of such intractable adsorbates are humic acids, lignin, phenol, and substituted phenols [2,5,33-36,43]. Tables 1.3 and 1.4 show the response of some selected adsorbates. If carbon were re-used after pyrolysis alone and the selective-oxidation step were omitted, progressive build-up of the pyrolyzed residues would occur, with a concomitant decline in adsorption efficiency.

Table 1.3: Response of selected adsorbates to thermal treatment at 700°C

Adsorbate	Molecular mass (g/mol)	Boiling Point (°C)	Aromaticity *	Carbonaceous residual fraction at 700 °C	Response to thermal treatment (under N_2)
Toluene	92	110.6	0.75	0	I
Nitrobencene	121	211	1	0	I
Propionic acid	74	141	0	0.01	II
Benzoic Acid	122	249	0.86	0.03	II
Aniline	93	185	1	0.34	II
Phenol	94	182	1	0.36	II
Chlorophenol	129	214	1	0.4	III
Nitrophenol	139	215	1	0.34	III
Resorcinol	110	277	1	0.5	III
2-naphthol	144	288	1	0.62	III

*Ratio of aromatic-to-total carbon atoms in the molecule

Table 1.4: Response of selected adsorbates to thermal treatment at 800°C

Adsorbate	Molecular mass (g/mol)	Boiling Point (°C)	Aromaticity *	Carbonaceous residual fraction at 800 °C	Response to thermal treatment (under N_2)
n-Pentane	72	36	0	0	I
n-Hexane	86	69	0	0	I
n-Decane	142	174	0	0	I
Benzene	78	80	1	0	I
Toluene	92	110.6	0.75	0	I
p-Xilene	106	114	0.75	0.03	II
Butanol	74	118	0	0.02	II
Hexanol	102	157.5	0	0.04	II
Octanol	130	194.5	0	0.03	II
Benzoic acid	122	250	0.86	0.15	III
Lignin	165	-	0.6	0.45	III
Phenol	94	182	1	0.61	III
B-naphthol	144	285	1	0.68	III

*Ratio of aromatic-to-total carbon atoms in the molecule

1.10.4-Regeneration conditions

Operating conditions during regeneration can be controlled to obtain the required degree of regeneration of an exhausted carbon. The following parameters have an important influence on regeneration: furnace atmosphere, presence of inorganic constituents, temperature and residence time.

Furnace applications that employ the use of partial or complete steam atmospheres is the approach most commonly applied. The rule-of-thumb guideline of 1kg of steam per kilogram of activated carbon has often been advanced as the requirement for the complete regeneration of exhausted carbon. In reality, the quantity of steam required depends on the kinetics of selective oxidation (gasification) of the pyrolyzed residue.

The rate of the steam-carbon reaction is likely to be the controlling step in the selective oxidation of carbonized adsorbate residues. Intraparticle diffusion is not likely to affect the over kinetics of regeneration at the temperatures normally employed in such operations. The steam-carbon reaction is relatively insensitive to the flowrate of gas (steam) around the particles, therefore the external mass-transfer rate does not control the overall reaction dynamics [2,5,8-10,43].

Inorganic constituents can catalyze the steam carbon reaction, and can therefore accelerate the gasification of pyrolyzed adsorbate residues, or even of virgin activated carbon. Such inorganic constituents can be present in the original structure of activated carbon, be adsorbed onto the carbon during usage, or be intrinsic parts of organic adsorbates. In the last-mentioned case, a non-volatile inorganic residue will be deposited, together with the carbonaceous residue, during the pyrolysis step of thermal-regeneration operations [8,43].

The influence of temperature and residence time on the selective oxidation of pyrolyzed residues plays an important role. Within strict limits (approximately 650 to 900°C), a trade-off of temperature against residence time can yield optimum thermal reactivation of spent carbon. However, at temperatures above about 950°C, even very short residence times are likely to lead to excessive losses of activated carbon. On the other hand, at temperatures below 650°C, the rate of steam-carbon gasification becomes negligible, and impracticably long residence times may be needed for the proper reactivation of carbon [2,43].

In order to understand the various intraparticle structural changes that occur during progressive thermal treatment of an activated carbon, Van Vliet [2,5,43] tested a new activated carbon based on bituminous coal under a range of regeneration conditions. A plateau region of operating conditions (700 to 850°C peak furnace temperature for 0 to 20 minutes) where evident negligible damage occurred to the intra particle structure was found. Above 850°C and 20 minutes of residence time, structural damage occurred largely by the conversion of smaller pore types to larger ones. The resultant carbon is very soft and fragile.
Van Vliet [43] also tested an exhausted carbon from water treatment under regeneration .During the first few minutes of regeneration; congested micropore volume was substantially restored. The recovery of micropore volume was at a maximum after 8 minutes of residence time and at a peak furnace temperature of 800°C. Equivalent levels of intraparticle structural restoration were achieved at, for example, 800°Cand 10 minutes or 700°C and 60 minutes. However, it was not possible to even approach the overall optimum degree of micropore restoration for any residence time at 950°C, since that temperature affected regeneration conditions that were too intense.
At high temperature and prolonged residence time (e.g. 960° C and 60 minutes), there was excessive loss of micropore volume and an increase in mesopore and macropore volume (according to the mechanisms described earlier), and the resultant carbon particles were very fragile.

1.10.5-Effects of regeneration cycles

As it was discussed previously, regeneration of spent GAC offers the possibility of reusing a valuable resource in adsorption process, while simultaneously eliminating a waste load to landfills [2,5,8,44-75]. Furthermore, reactivation of GAC is typically cheaper than replacement with new GAC. Regeneration strategy can represent roughly one-third of the cost of replacement. According to this, regeneration is an important part for industrial activated carbon markets, as the regenerated carbons can be sold or used in other suitable applications. In addition, activated carbon regeneration is more conductive to protect the environment and conserve resources [76,77]. Moreover, the possibility of using an AC in successive adsorption–regeneration cycles is essential from an economic point of view.

In general, the most attractive option is given by a compromise situation considering both the regeneration efficiency and the number of uses for which the degree of porosity recovery is considered acceptable.

Provided that the target of any regeneration process is the desorption of pollutants concentrated in the GAC without any modification of the initial properties of the adsorbent, which is rarely achieved. The knowledge on the change of the adsorbent properties during adsorption-regeneration operation is mandatory.

The adsorbent is modified regarding both their porosity and surface chemistry, as the number of cycles is increased, becoming more and more vulnerable towards reuse, under certain treatments. Additionally, it has been recognized that GAC pores have often been shown to widen during thermal reactivation, ultimately altering the GAC pore structure [43].

With this in mind, GAC conceptually could only endure a finite number of reactivation cycles before it could no longer be effectively renewed. At such a conceivable point, thermal regeneration of the GAC would produce an unsatisfactory GAC, characterized by a diminished adsorption capacity or high friability.

In short, optimization of the reactivation process offers the possibility to increase the GAC bed life, help minimizing reactivation and operation costs, maximizing the useful life of the GAC. In despite of reports of extensive cycles of regeneration for exhausted GAC used in water treatment, Moore et al.[44] concluded after six regeneration cycles for an exhausted GAC used in water treatment, that the reactivated GAC contained a pore size distribution differing considerably from that of the virgin GAC. The regenerated GAC pores had been widened through the regeneration cycles, resulting in a decreased micropore volume and increased mesopore volume. This type of behavior was also reported in [8,43, 45-75].

The virgin GAC contained a volume of micropores that was roughly twice the amount present in the regenerated GAC. Conversely, the volume of mesopores present in the regenerated GAC was more than two times greater than the volume of mesopores in the virgin GAC. In addition, the regenerated GAC had more total pore volume than the virgin GAC.

1.10.6-Environmental impact of GAC regeneration

There are substantial environmental impacts associated with regenerating GAC. Although substantially less than those of producing virgin GAC. Overall, new produced GAC releases over eight times as much carbon dioxide equivalents as generating GAC (Table 1.5).

Table 1.5: Overall GAC regeneration footprint and comparison to virgin GAC production

	CO_2	NO_X	SO_X	*PM_{10}	**HAP
Pounds emissions per pound of regenerated GAC	0.7	$8.1 \cdot 10^{-4}$	$5.7 \cdot 10^{-4}$	$6 \cdot 10^{-5}$	$1.6 \cdot 10^{-5}$
Pounds emissions per pound of virgin GAC	8.5	0.014	0.034	0.00078	0.0012

*PM_{10} particulate matter with a diameter of 10 microns or less. **HAP hazardous air pollutant.

This conclusion should encourage remedial project managers to use regenerated GAC in their remediation projects [76,77]. Comprehensive environmental footprint calculations also identify opportunities to modify processes to reduce environmental impacts and suggest which specific aspects of these processes have the highest potential for improvement [77].

1.11-Application of GAC in beverages processing

Activated carbon adsorption from liquid phase has found wide applications in several areas of food production and processing industries. The activated carbons remove undesirable odors, colors, and unwanted components of the solution, and improve the quality of the food material. The use of activated carbons in food processing is continuously growing because the food processing and production industries in which the use of activated carbon is well established are expanding. Furthermore, the use of activated carbons is also explored and expanded to areas of the food processes, where it was not previously used [2,8].GAC has been used in the preparation of different wines with special requirements. The carbon should have specific properties so that it can preferentially remove certain color but does not remove components that give desired characteristics to wine.

It should be able to remove undesirable components originating from mildew, cork, yeast, and so on, which may give an unpleasant taste and odor. The activated carbon used should also be able to modify the color of the wine as required [4,8].

Activated carbon is also used in the brewing of beer at a number of stages. For example, it is used for the purification of water, air, and carbon dioxide used in brewing. It is also used directly in the brewing process to improve the quality of a defective beer by modifying the color of the beer and by removing the taste and odor of phenols and coloring matter and also those produced due to the autolysis of yeast and infections [8]. Activated carbon has since long been used in distilleries for refining neutral spirits, increasing its ranges of applications at different stages of the production of alcoholic beverages. In each case, the aim is to remove unwanted components to improve the taste, color, and other properties [8,78-80].In the preparation of rectified spirit, three main fractions are collected during rectification of the crude spirit: the light fraction that contains low boiling aldehydes and other oxygen containing organic compounds; the medium fraction that is the spirit itself; and the heavy fraction that is mainly fusel oil. The middle fraction, rectified spirit, always contains traces of fusel oil, which produces an unpleasant taste and odor. By filtering through a bed of activated carbon, the last traces of fusel oil can be removed by adsorption, and a fine quality spirit, which can be used for preparing alcoholic beverages, is obtained [8,78-80]. In the production of brandies, treatment with activated carbons assist in the removal of undesirable flavors arising from the presence of acids, furfural, and tannins that have been picked up during manufacture and storage. Activated carbon also reduces the amount of aldehydes, fusel oil, and other components in the raw distillate and also accelerates maturing. The addition of about 5 g of carbon per liter of brandy is sufficient to give good quality brandy [8].

1.11.1-Application and management of GAC in Cuban rum production

Cuban rum is derived from the fermentation and distillation of sugar molasses. Distillation columns in continuous process are used to produce the distilled spirit under specific organoleptic parameters which guarantee the optimal quality of the final product.

The distilled spirit (as primary/raw rum) known in Cuba as "Aguardiente", is a colorless liquid with typical organoleptic features such as strong characteristic aroma and intense flavor [78-81,85-88,97,102-104].

These organoleptic characteristics are due to the composition of the aguardiente being a hydro-alcoholic mixture of organic compounds which are mainly produced as sub-products during alcoholic fermentation. The fermentation process plays an important role in the quality of the aguardiente. Therefore, the Cuban rum experts carefully control this operation. As the distilling process is conducted in columns at continuous way, the system has been carefully designed to separate the fusel oil, volatile and heavy compounds that deteriorate the sensorial characteristic in the spirit [102-104]. In order to obtain high-quality Cuban rum, the original sensorial attributes of the aguardiente must be modified and improved. By ageing process in white oak barrels (maturation), the aguardiente changes its original tough sensorial attributes: a light amber color appears; taste softens and a pleasant aroma is produced. During this stage; these sensorial changes are obtained by complex chemical reactions due to the interaction between the aguardiente and the wood [83,84,90-96,98-101]. As rum are complex mixtures of organic substances: 186 organic compounds have been identified. The number of possible reactions during ageing process is enormous [78-81,85-88,97,102-104]. However, after maturation, the aged aguardiente has some original and new organic compounds which must be balanced in order to further refine its organoleptic characteristics to future high-quality rum. In this case, percolation "filtration" of the aged aguardiente using GAC is applied [78-81]. Fig.1.16 depicts the general diagram of rum production process.

The aged aguardiente is refined "filtered" trough a fixed-bed GAC contactor in order to remove / balance some compounds that affects the sensorial attributes of the rum. The rum specialists pay carefully attention to the filtration process where the time of residence of aged aguardiente in contact with the GAC, is a critical variable to achieve the optimal and delicate balance of the key components responsible of the Cuban rum sensorial characteristics. This defines the commercial success and the competitive character of the spirit trading.

The filtered aged aguardiente is mixed and aged again in carefully classified barrels. The final blending is in charge of the rum masters to formulate the final product: The Cuban Rum.

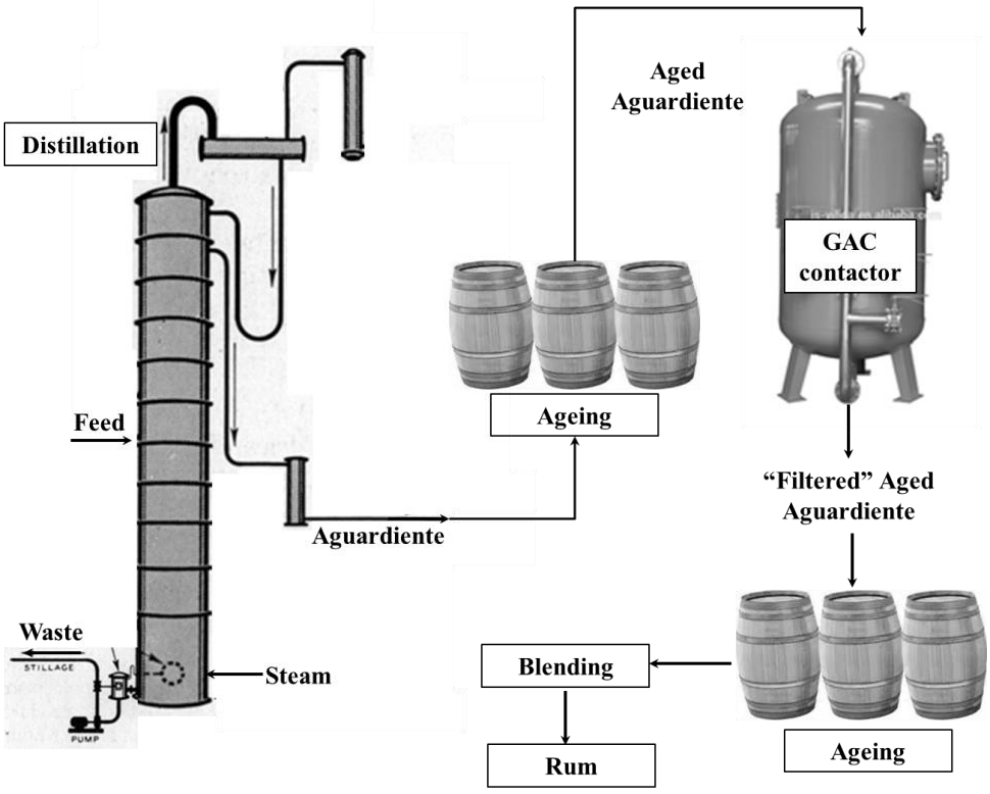

Fig.1.16: Simplified schematic diagram of Cuban rum production process

Besides the influence of fermentation, distillation, ageing and blending, aged aguardiente filtration represents crucial operation in Cuban rum production process. All of them are leaded by the expertise and skills of the Cuban rum masters which have been acquired as traditional legacy for more than a century of Cuban rum production. In rum production process, the multiple contactor system in parallel connection (Fig.1.12) is preferred, due to the operational advantages that this system offers to the rum industry.

Usually, the production rate in a rum factory varies as function of the market demand, thus the parallel system provides operational capacity to process variable amounts of liquid as the total cross sectional area can be adapted to the flow requirements.

As molasses is a natural product, slight sensorial differences in the fresh aguardiente can occur according to the season or the molasses provider. In that case, using the parallel system, sensorial differences can be corrected to reach the standard of quality by mixing the effluents in an elaborated strategy according to the rum master organoleptic expertise.

At present, rum masters determine when GAC needs to be replaced based on the sensorial judgment of the filtered aged aguardiente and not on the exhausted level of the GAC. The GAC quality control is done at industrial scale and is performed empirically. The GAC used is always provided by the same supplier, selected by a board of rum taste experts and only based on the sensorial characteristics of the filtered product. The surface group functionality and its relationship with the effectiveness to achieve the desirable taste and Cuban rum aroma have not yet been studied. The practical evidence gathered for years has been the main (only) criteria to accept the used kind of GAC. When the filtered aged aguardiente quality reaches minimum organoleptic standards, the GAC is completely removed from the filter and replaced by expensive virgin GAC. Although effective, effluent sensorial judgment cannot offer quantitative information about the real exhaustion degree of the GAC in the filter.

As the filtration takes place in fixed bed, a further characterization of the GAC in industrial rum contactors gives the possibility to save a part of the GAC expressed as LUB. As this part has not been saturated, it can be reused in the rum production process.

In order to determine the exhaustion level of GAC a proper and fast analytical technique based on the determination of specific surface area and porosity has to be applied. However, the technological facilities of rum producers are limited. Furthermore, it is found that for detecting the exhaustion degree in exhausted GAC in rum production, the widely applied BET analysis could not be performed. Before BET analysis could be executed, the sample must be outgassed overnight at 300°C in high vacuum [6,25,26]. By this pre-treatment of the sample modifications in the studied GAC were induced: desorption of a part of the absorbed organic compounds took place. Further on, it was even found that this required pre-treatment did not satisfy and even damage of the equipment could take place.

Consequently, an alternative, economic, fast and reliable method to measure the exhaustion level of GAC in rum production and the regeneration degree reached is needed.

While GAC demand in rum production is arising, the future of exhausted GAC is consistently becoming a concern. Under such circumstances reuse by regeneration of the exhausted GAC could give some advantages by stabilizing adsorbents and recovering resource by reutilization.

1.11.2- Relationship between GAC exploitation, characterization and regeneration

Considering the variety of possible applications in which a GAC can be used, it is extremely important to develop a suitable characterization for it. The analytical method used in each case must be selected in order to assess a parameter related as directly as possible to phenomena involved in the application of the porous material, involving physical phenomena similar or close to those involved during the practical application [1,5,7]. Any industry that operates using activated carbon should enable a strategy to permit the control and performance optimization in the use of the adsorbent, which in turn will produce economic and ecological benefits. Additionally, new adsorbents with better adsorptive characteristics or more economically interesting can be explored [70]. On the other hand, costs analysis, and possibility of reactivation should be taken into consideration during the selection of adsorbent of the optimum efficiency [37].

A correct exploitation of the GAC, proper method for characterization and the regeneration process are the three essential steps in which the industry must emphasize to optimize the adsorbent management [70].

Firstly: A proper GAC characterization will permit the assessment of its real exhaustion degree after exploitation. Thus, the strategy of control on the GAC use can be enabled, also it guarantees that all the GAC sent to regeneration is actually exhausted; thus optimizing the energy consumption during the operation and minimizing the number of regeneration cycles, loss of material, damage to the adsorbent , time, etc. Secondly: After regeneration, GAC must be characterized in order to define if still having the adequate porous properties to be reused, If not, other applications could be explored.

For this purpose, the three steps depicted in Fig.1.17 are needed for a correct strategy in the optimized management of the GAC at industrial scale. This figure emphasizes that characterization is one of the three essential steps that should not be omitted [70].

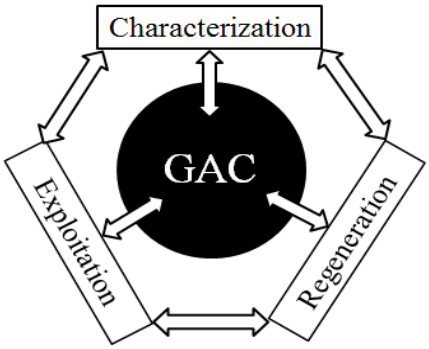

Fig.1.17: Relationship between the exploitation, characterization and regeneration that should always hold in GAC management (adapted from [70].)

1.12- Conclusions of Chapter 1

After analyzing the theoretical bases for characterizing high porous material, the manufacturing, applications and technology of activated carbon for liquid phase adsorption process, focus on the GAC management in Cuban rum production; the following conclusions can be derived:

Insufficient information about the adsorption process with activated carbons in rum production was found. The secrecy involved in spirit industry produces a reduction in the number of allowed publishable researches with useful detailed results.

At present; the management of GAC in Cuban rum industry is incomplete. The possibility of saving a part of the GAC unused, expressed as length of unused bed (LUB), has not been explored yet. Mainly, due to the predominant sensorial nature of the qualitative analysis performed in rum industry without any quantitative analytic counterpart. The landfilled GAC is becoming a concern as the trade of Cuban rum is increasing. In addition, no strategy for GAC regeneration has been addressed.

No specific method to characterize the exhaustion level of the GAC used in rum production was found. Available classical techniques based on gas adsorption isotherms will not provide reliable results as the pre-treatment (outgassing) of the samples imposes severe changes not only to the sample of exhausted GAC to be analyzed but also a serious damage to the analytical instrument during the measurement process can occur. Therefore, an alternative, specific, fast and robust analytical method to determine the exhaustion level of GAC in rum production must be implemented.

Inefficient GAC management in rum production is realized. A proper and specific method for GAC characterization also including in the regeneration process is required in order to optimize its use looking for economic, social and environmental advantages.

Chapter 2-Material and Methods

Chapter 2 gathers all the experimental procedures and analytical techniques performed for this research. As one of the objectives in this study is to provide new analytical approaches for the characterization of GAC used in the rum production, some experimental procedures of novel analytical techniques are actually part of the research results and it will be presented in its correspondent chapters.

2.1-Sampling

Among Cuban rum factories, a target factory of the major rum producer in Cuba was selected for this study. As the GAC thermal regeneration is one of the goals in this work, the selected factory has the most exhausted GAC. According to the expertise of the Cuban rum masters, the exhaustion degree of the GAC depends on the characteristics of the rum factory.

The rum factory with the oldest reserves of aged aguardiente is able to produce the most aged rums. Therefore, according to the rum masters, the GAC contactors used for refining the most aged aguardiente are exploited intensively in comparison with others rum factories which manufacture less aged spirits meant for a different kind of market.

Once the target rum factory was defined, an industrial target GAC contactor "filter" was selected for obtaining the GAC samples to be studied. A rum filter previously declared as: "out of service by exhaustion" by a board of rum taste experts was used as target to obtain the GAC samples at different layers (positions) in the GAC bed. The objective of this sampling is to study the GAC exhaustion profile in the rum filter using different quantitative analytical methods (discussed later) in order to define the LUB in the adsorption process of rum production.

Figure 2.1 presents the schematic diagrams of the superior and frontal views of the target rum filter showing how the sampling process was performed. In Fig.2.1 (a) circles are demarking the radial position where the sample per filter layer was obtained.

In this arrangement, the representability of GAC from different parts of the same layer is guaranteed, avoiding the probability of taking samples from the same place in the layer where possibly a channeling process occurred. In that way, seventeen samples per layer were gathered and mixed to obtain the representative sample at different GAC layers.

According to Fig. 2.1 (b), eight samples (mixing 17 radial samples each) of GAC (0.8 mm) were obtained at different layers (positions) in the GAC bed.

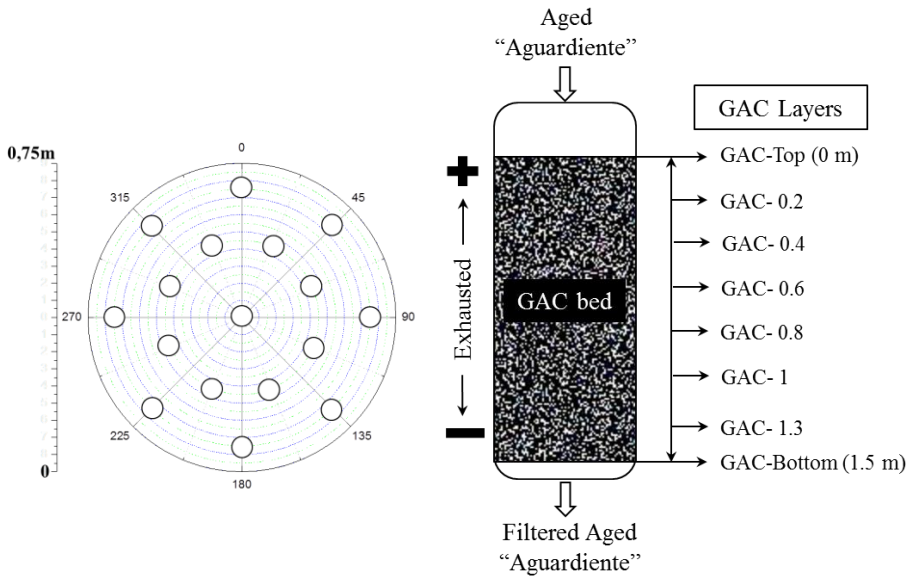

(a) (b)

Fig.2.1: Simplified schematic diagram of the sampling process in the target rum filter: (a) Superior view (radial sampling for each specific GAC layer), (b) Frontal view (longitudinal sampling at different GAC layers).

Using a specific sampler (under patent registration: registration number in Cuba 2016-178) the GAC samples were taken from the top to the filter's bottom (following the sampling pattern Fig.2.2 (a)) according to the subsequent order:

Top (position = 0 m), 0.2, 0.4, 0.6, 0.8, 1, 1.3m and Bottom (position=1.5m).

2.2-Sample preparation

2.2.1-Primary sample preparation (granular)

The sample preparation was performed depending on the type of analytical method. GAC samples were sieved using a WQS vibrating screen (0.3 mm/3000 min-1) in order to eliminate dust and particles smaller than 0.8 mm.

Afterwards a visual inspection was made to eliminate particles bigger than 0.8 mm such as: possible foreign matter as little chips of wood or small fabric pieces which can affect the final results. The samples were dried at 110°C during 3h (explained later) using Boxun BGZ series oven applying ASTM Standard Test Methods for moisture determination in Activated Carbon [107]. Samples were refreshed in a silica-gel desiccator, for weighing a Sartorius analytical balance was used. Samples were kept in sealed envelopes and stored in the silica-gel desiccator prior to analysis.

2.2.2-Secondary sample preparation (grinded)

A representative sample of 2g of GAC (around 2000 grains) (previously prepared according to § 2.2.1) was grinded, about 60 wt % pass through a 325-mesh screen and about 95 wt % pass through a 100-mesh screen (U.S. sieve series). The grinded GAC samples (< 325-mesh) were dried at 110°C during 3 h. Fig.2.2 presents a diagram of the analytical methods used and its correspondent sample preparation strategy.

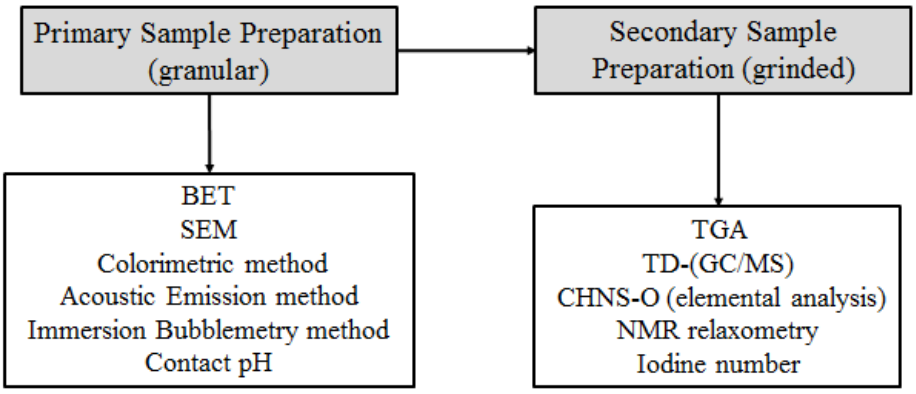

Fig.2.2: Sample preparation strategy according to the analytical procedure

A Boxun oven: (BGZ Series) was used applying ASTM Standard Test Methods for moisture determination in Activated Carbon [107]. Samples were refreshed in a silica-gel desiccator during 2h, labeled, kept in sealed envelopes and stored in the silica-gel desiccator till being measured.

2.3-Sample characterization

2.3.1-Thermo gravimetric analysis (TGA)

Thermogravimetric analysis (TGA) is a thermal analysis method by which the weight loss of a sample (previously prepared as described in section § 2.2.2) is continuously recorded against temperature or time under a controlled heating rate and inert gas atmosphere. The weight loss, caused by volatilization and/or decomposition reaction, provides useful information about the thermal stability of the adsorbed compounds onto the GAC. Differential thermogravimetric (DTG) profiles plot the weight change speed as a function of temperature (time).Thermogravimetric curves (TGA) were obtained using a TA Hi-Res 2950 Thermogravimetric Analyzer. About 7 mg of solid is pyrolyzed under approximately 35 mL/min N_2 gas flow at a heating rate of 20 °C/min from room temperature to 800 °C.

2.3.2-Thermal desorption- gas chromatography/mass spectrometry (TD-GC/MS)

Thermal desorption gas coupled with chromatography/mass spectrometry is a thermo-chemical method useful for the identification of organic volatile and semi-volatile compounds thermally desorbed from a solid matrix by heating the solid at constant temperature. The volatilized compounds are analyzed by gas chromatography (GC) which in turn, is used to separate the mixtures into individual components using a temperature-controlled stationary phase into a capillary column. Mass spectrometry (MS) identifies the various components from their mass spectra. In this research thermal desorption (TD)–GC/MS analyses were performed on a Trace GC Ultra gas chromatograph coupled with a DSQ-II mass spectrometer (Thermo Scientific). GAC samples (previously prepared according § 2.2.2) were introduced in a Double Shot Pyrolizer PY-2020iD (Frontier Lab) in desorption mode (100 – 450°C).

The GC-column was a 30 meter DB-5MS 0.25mm x 0.25µm (Agilent Technologies) and the GC was programmed from 35°C (1 min.), ramped at 12°C/min. to 320°C (for 10 min.). The quadrupole mass spectrometer was scanned 33 – 550 amu in 0.5s, ionization mode was electron impact (EI mode) at 70 eV.

2.3.3-CHNS-O elemental analysis

Elemental analysis is used to determine the C, H, N, S and O content (wt%).The samples (2 – 4 mg) (previously prepared according §2.2.2) were accurately weighed into a small tin container. Vanadium pentoxide (5 - 10 mg) was added as combustion catalyst to obtain sulfur contents as accurate as possible. The apparatus was calibrated using six samples (0.5 – 4.0 mg) of the 2,5-bis (5-tertbutyl-benzoxazol-2-yl) thiophene (BBOT – $C_{26}H_{26}N_2O_2S$) standard. All samples were analyzed in quadruplicate while control (BBOT) and blank samples were measured periodically to ensure proper calibration performance. The elemental composition (C, H, N and S) was determined with a FlashEA 1112 Elemental Analyzer of Thermo Electron Corp. The oxygen content was determined by difference between 100% and the combined hydrogen, carbon, and nitrogen content as the ash content in the sample was no significant thus negligible.

2.3.4-BET and porous structure analysis

As it was explained in Chapter 1, the BET and pore structure analysis are applied to estimate the specific surface area, pore volume and its size distribution of activated carbons from experimental data based on the mathematical modeling of physisorption isotherms using probe gases. Different gases were used to assess the porous characteristics of the GAC. The porous structure of GAC was characterized by N_2 adsorption at 77K and Ar at 87K using the Autosorb-iQS and the Autosorb 1 respectively. The choice of adsorptive is crucial in the characterization of porous materials. Nitrogen at 77K has been widely used, but the interpretation of the isotherm data is not always straightforward. For various reasons, argon adsorption at 87K is considered to be more reliable and is now recommended – particularly for micropore size analysis [6].

Before analysis, the sample was degassed 16 h at 300°C in vacuum. The apparent surface area (S_{BET}) was estimated by the BET equation. The amount of gas adsorbed at the relative pressure of p/p_0 = 0.96 was employed to determine the volume of pores. The micropore volume (V_{DR}) was calculated by applying the Dubinin-Radushkevich equation. The average micropore width (L_0) was calculated using the Stoeckli equation [25].

The quenched-solid-density functional theory (QSDFT) and non-local-density functional theory (NLDFT) were used to determine the pore size distribution [6,26].

2.3.5- Scanning electron microscopy (SEM)

Scanning electron microscopy (SEM) is a method which uses an electron microscope that produces images of a sample by scanning it with a focused beam of electrons. The electrons interact with atoms in the sample, producing various signals that contain information about the sample's surface topography and composition [108-110].To observe the morphology of GAC grains, a Vega®Tescan /TS5130SB/SE detector was used.

2.3.6-Iodine number and contact pH methods

The iodine number is a well-known method that is used to estimate the surface area of activated carbons, and in some cases it is a cost-saving alternative to the BET surface area determination. Their numeric values are comparable although do not have the same meaning. The determination is based on an adsorption experiment with iodine as adsorbate and with defined initial and residual concentrations. The contact pH method is based on the direct measurement of the pH of water after contacting with a sample of activated carbon. The determination of contact pH can be used as a simple and fast measurement technique allowing to determining the initial pH of the water in contact with the carbon. In this study, the GACs samples were also characterized by ASTM, standard test method for determination of iodine number of activated carbons [111] and ASTM, standard test method for determination contact pH of activated carbon [112]; the pH was measured using PHSJ–4A pH meter.

2.4-New GAC characterization methods

2.4.1-Colorimetric method

This novel method is based on the direct spectrophotometric measurement of the change in the color intensity of ammonia solution after contacting with exhausted GAC used in rum production in order to quantify its exhaustion level (discussed later).

Ammonia solution

It was found that an ammonia solution could be used to extract in an optimal way the compounds from the exhausted GAC. This could then be used to determine the concentration of the adsorbed compounds and thus the exhausted level of the GAC. In order to study the ammonia concentration effect on the desorption process; solutions at different concentrations (from 0.125% to 25%) were prepared using Milli-Q water, fulfilling the ASTM specification for reagent water. The ammonia solution of 25% mass (reactant quality) was supplied by Merck®.

Experimental conditions

Wavelength and determination of solid-liquid relation

In order to determine the proper solid-liquid relations (Xi (in g/mL) = mass of GAC per volume of ammonia solution), different Xi were planned. Each Xi sample was put into a hermetically-capped flask in a thermostatic bath at 25 °C. The National Instruments GFL 1086 Gemini (shaker-bath temperature controller) was used to monitor the reaction; gently shaking at 50 rpm for 72 h in order to ensure that the equilibrium state was reached.

Then the extracted solution for each Xi sample was filtered using a PFTE 0.45-µm filter. In order to compare the optical characteristics of each extracted solution (ES) and oak extracted solution (OES), spectra of filtered samples were recorded in the visible range between 380 and 1100 nm. Additionally, an optical study of the industrial amber colorant "caramel color" used in rum production was made, and the results were compared to the optical spectra of ES and OES. The absorption was measured using the Ultrospec 2000 spectrophotometer connected to a computer; a 1-cm quartz cuvette was used.

Reaction kinetic study conditions

Experimental Set-up

For the reaction kinetic study, a specific set-up presented in Figure 2.3 consisted of the following:

The digital temperature controller (1) (Fig. 2.3) was connected to the double jacket experimental reactor (2). The experimental reactor was hermetically capped to avoid ammonia evaporation. The reactor's cap was designed to introduce the mixer (3), and a gently 50 rpm was applied.The reaction liquid was circulated by a peristaltic pump (4) at a flow rate of 10 mL/min. Before the colored solution passes through the spectrophotometer (6), the liquid was filtered using the PTFE 0.45-µm filter (5) to remove possible dust particles coming from the GAC, which may disturb the absorption measurement. The spectrophotometer (6) was coupled to the computer (7). The measured absorption data were stored every 30 s.

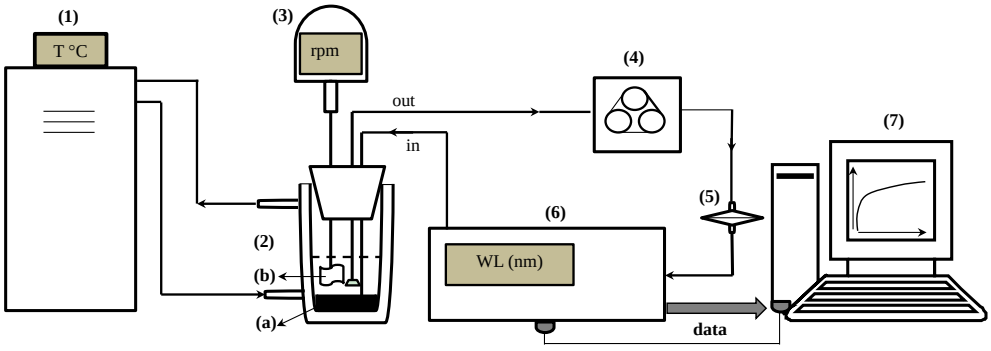

Fig.2.3: Experimental set-up for the kinetic study.

(1) PolyScience Digital temperature controller; (2) double jacket experimental reactor, (a) GAC, (b), propeller; (3) IKA mixer; (4) HeidolphPumpdrive 5001 peristaltic pump (tubing size: 1.7 mm); (5) PTFE 0.45-µm filter; (6) Ultrospec 2000 spectrophotometer (1-cm quartz cuvette); (7) computer. WL = wavelength display.

A GAC sample (a) was uniformly distributed on the reactor's bottom. The suction tube (out) was provided with a 0.2-mm pre-filter to avoid the suction of GAC particles, which may obstruct the peristaltic pump. The suction point was located near the propeller (b) to take advantage of the turbulence and good mixing quality at this point.

The feed-back tube (in) was introduced at the reactor's bottom, below the GAC layer, in order to force the liquid to pass through the GAC bed before being suctioned again. A "blank" circulation time of 5 min was handled for calibration, prior to the introduction of the GAC, as quickly as possible added (this is time zero) into the reactor.

Data Processing

Different models were applied to fit the kinetics of the desorption and to determine its mechanism. To fit the experimental kinetic data, the pseudo-first and pseudo-second order (PFO and PSO) [113], modified pseudo-n order (MPnO) [114] and the mixed order (MOE) [115] rate equations were used.

For the extraction process between ammonia and GAC, a desorption mechanism was considered:

$$q_{e,i} = q_0 - \frac{(C_{e,i} - C_0)w}{m} \quad (2.1)$$

$$q_{t,i} = q_0 - \frac{(C_{t,i} - C_0)w}{m} \quad (2.2)$$

Where $q_{e,i}$ is the equilibrium amount of the colored compound desorbed, q_0 is the maximum amount adsorbed on the GAC that can be desorbed, and $q_{t,i}$ is the desorbed amount of colored compound "*i*" at any time. Both are expressed on a weight/weight (g/g of GAC) basis. The initial concentration of the colored compound, $C_0 = 0$. $C_{e,i}$, is the equilibrium concentration of the colored compound (in g/L). w is the volume of the liquid (in L), and m is the weight of the solid adsorbent (in g). $C_{t,i}$ is the bulk concentration of colored compound "*i*" at any time (in g/L).

According to [113-115]: the integrated form of the PFO desorption rate equation was expressed as:

$$q_t = q_e(1 - e^{-k_1 t}) \quad (2.3)$$

Where k_1 is the PFO rate constant, q_t is the amount of product desorbed at time t and q_e the amount of product desorbed at equilibrium.

For the PSO desorption, the rate equation was defined as:

$$q_t = \frac{t k_2 q_e^2}{1 + t k_2 q_e} \quad (2.4)$$

with k_2 the PSO rate constant.

The MPnO desorption rate equation was expressed as:

$$q_t = q_e(1 - e^{-nk't})^{1/n} \quad (2.5)$$

where $k' = kq_e{}^{n-1}$ and n is the order of the rate equation.

The MOE model was expressed as:

$$q_t = q_e \frac{1 - e^{-k_1 t}}{1 - F_2 e^{-k_1 t}} \quad (2.6)$$

Where F_2 ($F_2 < 1$) was determined as the share of the second order term in the total rate equation:

$$F_2 = \frac{k_2 q_e}{k_1 + k_2 q_e} \quad (2.7)$$

Statistical analyses were performed using the Statgraphics Centurion XV® software. Curve fitting and plots were obtained using Origin 8.1® software.

2.4.2-Acoustic emission method

Acoustic emission method is a novel technique for the characterization of granular activated carbons based on the measurement and analysis of the sound produced by water flooding through a sample of activated carbon. In the sudden contact between water and the GAC sample, the sound produced by bubbles escaping from the carbon pores, slits and cracks, can be used to assess to the pores of the material (discussed later).

Experimental set-up

The GAC acoustic emission experiments were performed in a sound enclosure box (Fig 2.4). The sound enclosure box was built using an external coffer of soft wood which was internally covered with two layers of soft foam and sponge (one inch thick) to absorb not only possible external interferences but also the unwanted resonant vibration produced by the vessel during the measurement process. Internal parts of the sound enclosure box consist of:

1. **Microphone** (Model : G.R.A.S.® microphone, Type 46AF (Frequency Range 3.15 Hz - 20 kHz; Dynamic Range 17 - 146 dB; Sensitivity 50 mV/Pa).
2. **Erlenmeyer flask** (250 ml)
3. **Coaxial cable** for connecting microphone, amplifier and PC
4. **Injection tube**(diameter: 3 mm)
5. **Separator funnel** (100 ml)
6. **Valve**

Working description

The sample of GAC (10 g) is put into the Erlenmeyer flask (2) (Fig 2.4) and distributed uniformly on the bottom. The injection tube (4) is introduced inside of the Erlenmeyer flask and the microphone (1) is adjusted capping the Erlenmeyer flask using a special foam-sponge gasket (a) avoiding the rigid interconnections between the microphone and the vessel reducing the possibility of measuring undesirable vibrations produced during the bubbling process, the microphone was pointed directly towards the GAC layer to take advantages of the microphone's directional characteristics.

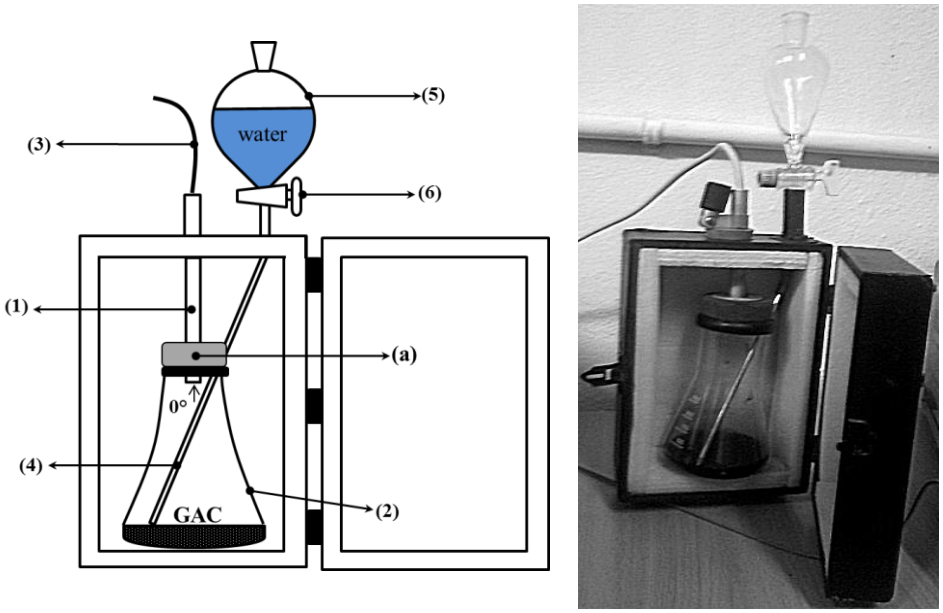

Fig.2.4: Sound enclosure box.

(1) Microphone; (2) Erlenmeyer flask, (3) Coaxial cable ; (4) Injection tube (5) Separator funnel; (6) Valve ; (a) Foam-sponge gasket.

After closing the sound enclosure box, the valve (6) was opened and the sound registration software was started. 40 ml of pure bi-distilled water flows from the separator funnel (5) towards the bottom of the Erlenmeyer. It takes 4s for the water to reach the dispersed GAC.

From the moment the water reached the GAC, immediately bubbles were generated producing a characteristic sound. Each sample was recorded five times to obtain five independent experiments.

Signal capture and processing

The GAC acoustic emission is captured by the microphone (Figs. 2.4 and 2.5) was amplified and digitalized using a NI USB-6211 data acquisition card.

Digital data were recorded in the computer to be processed using MATLAB® software. The signal capture set-up was calibrated using a G.R.A.S.® 42AP Intelligent Pistonphone. The recording time for the GAC sound was 90 s for all the samples.

Fig.2.5: Scheme of the experimental set-up for signal capture and processing

The methodology applied for signal processing and analysis was performed following a similar methodology described in [116, 117]. To select the useful frequency band, the behavior of the energy of the signal in time was taken into account, guaranteeing a similar pattern for all analyzed GAC.

In order to discard any external interference associated with the frequency of interest, a recording at empty sound enclosure box was performed for generating a background signal.

Spectrogram and components of frequency at the range of 1-1.6 kHz were recorded at empty sound enclosure box. No external interferences (noise) were found in the original signal in the selected frequency range.

Finally, the selected cut-off frequency of the band-pass filter was 1.3 kHz (and will be discussed later).

All studied GAC showed a similar behavior of the signal in the frequency range of 1–1.6 kHz, but showing noticeable differences in the signal amplitude in this frequency range. Signal amplitude was used as an interesting parameter to compare the studied GAC samples. Once the signal component in the frequency range of interest was extracted, the next step was to conduct a characterization of the acoustical signals within the time domain, based on the envelope detection, in order to assess the feasibility of its use to estimate the exhaustion degree of GAC samples in different GAC layers of the target rum filter. In this case, the envelope detection was made using the Hilbert Transform of the vibro-acoustical signals in the time domain. The Hilbert Transform of the function x(t) is defined by the equation (5). [116,117]

$$H(x) = \frac{1}{\pi} \int_{-\infty}^{\infty} \frac{x(t)}{x-t} dt \tag{2.8}$$

The Hilbert transform facilitates the formation of the analytical signal, which is useful for band-pass (BP) signal processing. An analytical signal is a complex signal consisting of the original signal x(t) as the real part and the imaginary part as the Hilbert transform of the original signal y(t) [116,117], where

$$y(t) = H(t) \tag{2.9}$$

The Hilbert transform of the signal was found using a Finite Impulse Response (FIR) filter, and it is then multiplied by "i" (the imaginary unit) and added to the original signal, obtaining a new complex signal z(t), named the analytical signal (eq. 2.10) [116,117].

$$z(t) = x(t) + iy(t) \tag{2.10}$$

The original signal is time delayed before being added to the Hilbert transform to match the delay caused by the Hilbert transform, which is one-half the length of the Hilbert filter. The envelope of the signal can be found by taking the absolute value of the analytical signal z(t). The imaginary part is a version of the original sequence with a 90° phase shift.

The Hilbert transformed series have the same amplitude and frequency value as the original data and includes phase information that depends on the phase of the original data. Once the envelope of the acoustical signal has been obtained, and in order to eliminate the rise and smooth of the envelope, the signal is passed by a low pass filter.

The main goal of this filtering is to facilitate the extraction of the signal envelope data in order to correlate them with the GAC characteristics which can define its exhaustion degree. The obtained results establish the relationship between envelopes of GAC acoustical signals generated by water flooding the GAC and its exhaustion degree produced by accumulation of adsorbed organic compounds in the GAC pores.

2.4.3-Immersion "Bubblemetry" method

The immersion "bubblemetry" technique is a novel method for characterizing granular activated carbons in terms of amounts and sizes of produced bubble volumes. The method is based on the microscopic size measurement of the bubbles formed when a GAC grain is immersed in a pure liquid. When the GAC particle is immersed in the liquid, the liquid occupies the available pores in the material displacing the air which leaves the solid in form of bubbles through the bulk liquid. The released air in form of bubbles can give information about the volume of pores (discussed later).

Experimental set-up

The bubble cuvette

The GAC immersion bubble-metric technique experiments were performed in the "bubble cuvette" (Fig 2.6) consisting of:

1- A glass cuvette (25x25x20mm)

2- A glass cover (0.25 mm thickness) forming an angle θ with the bottom of the cuvette which is experimentally determined and function of the physical properties (viscosity, molecular size, surface tension, …) of the immersing liquid used.

3- An immersion liquid and GAC particle just trapped within the angle between the glass cuvette bottom and the glass cover.

3.75 mL of liquid is injected at 25°C in the cuvette, not only covering the GAC particle (one grain (rod) each time) within 3s, but reaching a 6 mm of liquid level (Fig 2.6).The experiment was performed using glycerol (Alfa Aesar ® reactant quality 99.9%) as immersing liquid at 25°C (discussed later).

Few seconds after completing the total immersion process, the bubbles appear as the result of air escaping from the GAC pores and slits. Bubbles of different size are formed and some of them coalescence.

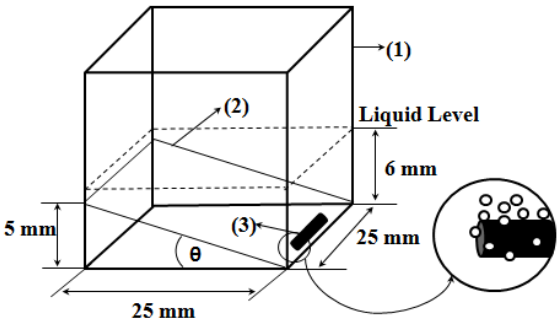

Fig.2.6: Bubble cuvette characteristics.

The formed bubbles slowly appear from the solid but remain separately trapped by the glass cover in the liquid. The first produced bubbles are gently pushed away by the next one.

The viscosity of glycerol guaranties a slow motion process and diminishes the bubble coalescence. When all the bubbles have been formed, which can last 3-10 min, depending on the exhaustion level of the measured GAC particle, the combination of the glycerol properties (transparency, viscosity and surface tension) and the used glass cover position retains all formed bubbles making clear microscopic pictures of the formed bubbles possible.

The aim of the glass cover with specific slope is (1) to block the bubble's movement giving the possibility to do size measurement (2) to retain separated bubbles and to diminish overlapping and coalescence effects and (3) to fix properly the GAC particle in the same position. In this way an optimal condition is realized for correct microscopic observations of the bubble formation process.

Working description

The experimental set-up is presented in Figure 2.7. The optical microscope (1) is coupled with the digital camera (3) which is connected to the computer (4). A microscopic model ruler (0.1 mm scale) was used for calibrating the size of the bubbles in the microscopic images.

The Scope Image Dynamic UTHSCSA-Image Tool software is used to transform the image dimension in pixels into mm using a conversion factor obtained by applying a microscopic model ruler (0.1 mm scale).

The calibration process takes place at the same optical adjustment for observing the formed bubbles. When the GAC bubbling process is finished in the bubble cuvette (2), a digital picture of all formed bubbles is taken and the bubble sizes and amounts are measured and counted. The volume of each bubble is determined and the total volume of air released can be obtained by knowing the number of formed bubbles and its sizes.

Bubble size measurement

A specific own software (under copyright protection process) was created to detect (counting) and analyzed (bubble size) the bubbles in the images. The software was developed in MATLAB® applying the Hough transform [118-124] as algorithm to the circular pattern recognition. After detection and recognition the circular shapes (bubbles) in the images, the software automatically determines the independent radius and volume of each detected bubble, based on the pre-calibration transforming pixels into mm using the calibration microscopic ruler. All the data (radius and bubble volume) are saved in a excel file for further processing.

During the bubbles detection process, the software is equipped with several options to correct possible mistakes such as "false detection" or "not detected". In that case, a "delete" and "manual detection" options are available to eliminate possible errors using the interactive graphic software interface, e.g. before saving the data, the user can see all the changes made and rectify the initial detection by the software.

Different immersing liquids were tested: lactic acid, phosphoric acid, paraffin and glycerol because of their viscosity and transparency that permits to observe the formed bubbles at "slow motion" giving the possibility of fixing proper microscopic pictures of the bubbles for further analysis. However only for glycerol the observed formed bubbles could be evaluated and gave reliable results (discussed later).

Using glycerol as immersing liquid, the software performance took into account the following parameters:

- Efficiency for detecting automatically the real number of bubbles: 90%
- Efficiency for calculating the total volume of the bubbles (considering the detected ones): 97.5%
- Total of detected bubbles with the option of "manual detection": 100%

Data processing for determining the total volume of pores by immersion bubblemetry method

Thirty five (35) grains (one by one) per GAC sample (according to Fig. 2.1 (a)) were independently analyzed. The size and the number of the formed bubbles were determined and its volume (in cm^3) was calculated using the software described above. The used data are given in Table 2.1.

Table 2.1: Weight (in mg) for the calibration curves of the GAC particles.

Samples	Np=	25	50	75	100	125
GAC-Top (0 m)		35.0	73.4	108.1	141.0	174.9
GAC-0.2 m		36.8	71.6	105.5	137.9	168.3
GAC-0.4 m		33.3	69.9	100.5	135.8	171.2
GAC-0.6 m		33.4	68.1	100.6	131.6	165.3
GAC-0.8 m		34.8	65.4	97.8	129.3	163.5
GAC-1.0 m		31.2	61.7	97.7	130.2	162.4
GAC-1.3 m		32.9	61.8	91.9	129.0	166.8
GAC-Bottom (1.5 m)		28.9	58.2	89.7	125.9	161.9
GAC-Virgin		27.0	56.1	82.1	109.5	134.3

The number of particles (Np) per GAC sample was plotted versus the total weight of GAC and a linear correlation was obtained.

In order to express the volume of air bubbles released per gram of GAC in cm^3/g as for the total volume of pores V_T, a weight calibration curve was recorded. Different number of particles (Np) (previously prepared according to (§2.2.1) per GAC sample were weighed: i.e. 25, 50, 75, 100 and 125.

The slope value is the main weight for a single GAC grain, S_w(in g/GAC particle), being more accurate than weighing particles individually. The specific weight for a single GAC particle S_w is similar within the analyzed GAC samples (Table 2.2).

Table 2.2: Average weight of a grain for each GAC sample

Sample	Sw(g/GAC particle)	error(Sw)
GAC-Top (0 m)	$1.41 \cdot 10^{-3}$	$+/-3 \cdot 10^{-5}$
GAC-0.2 m	$1.37 \cdot 10^{-3}$	$+/-4 \cdot 10^{-5}$
GAC-0.4 m	$1.36 \cdot 10^{-3}$	$+/-1 \cdot 10^{-5}$
GAC-0.6 m	$1.33 \cdot 10^{-3}$	$+/-1 \cdot 10^{-5}$
GAC-0.8 m	$1.31 \cdot 10^{-3}$	$+/-1 \cdot 10^{-5}$
GAC-1.0 m	$1.30 \cdot 10^{-3}$	$+/-1 \cdot 10^{-5}$
GAC-1.3 m	$1.30 \cdot 10^{-3}$	$+/-2 \cdot 10^{-5}$
GAC-Bottom (1.5 m)	$1.26 \cdot 10^{-3}$	$+/-2 \cdot 10^{-5}$
GAC-Virgin	$1.08 \cdot 10^{-3}$	$+/-1 \cdot 10^{-5}$

However a clear tendency of increasing S_w from the GAC-Bottom to the GAC-Top (Fig.2.1 (b)) can give the first evidence for differences in exhaustion degree between samples.

Calculation

The calculation procedure was conducted firstly by obtaining the total volume of air contained in a number of experimentally detected (counted) "k" bubbles (V_{Tb} (in cm^3)) released per GAC sample which was determined as:

$$V_{Tb} = \sum_{i=1}^{k} V_i \tag{2.11}$$

being (V_i (in cm^3)) the volume of each spherical single bubble (data from the software).

The immersion total volume of released bubbles per gram of GAC ($V_{T\ "imm"}$ (in cm^3/g)) was determined as:

$$V_{T"imm"} = \frac{V_{Tb}}{Np \cdot S_w} \tag{2.12}$$

with Np = number of GAC particles (in this case (35) per GAC sample).

Bubble shape analysis

Considering that the formed bubbles are captured using the glass cover (Figure 2.6), they suffer from a deformation (flattened), introducing errors in the real measured dimension of the bubble. In this condition bubbles are not totally spherical as the initial formed bubbles are freely suspended into the bulk glycerol.

An analysis about the differences between the radiuses of the original formed bubble and the flattened one is proposed. Nevertheless the observed bubbles can be considered as "spherical" as will be proved.

According to Figure 2.7, a simplified model of bubble deformation can be presented. An original free bubble of radius: "*r*" and volume: "V" escaping from the GAC ascends to reach the glass cover.

We can accept that the flattening process is equivalent to a formation of a new spherical bubble of fictitious radius: "r_1" and fictitious volume: "V_F". An equivalent spherical sector of volume: "V_S", with base radius: "r_2" and altitude: "a" can be assumed as the loss section of the fictitious spherical bubble (Figs.2.7 and 2.8).

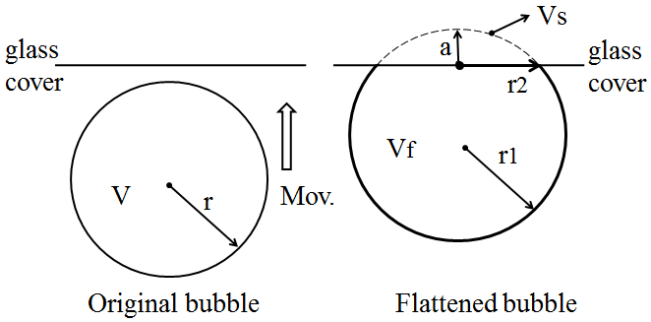

Fig. 2.7: Steps of bubble deformation

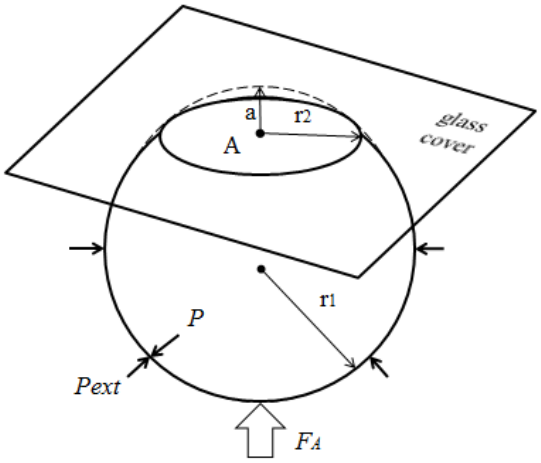

Fig. 2.8: Simplified 3D model of bubble deformation

As the volume of air inside of the original bubble does not change by deformation, the relation between volumes of original and flattened bubble can be expressed as:

$$V = V_F - V_S \tag{2.13}$$

eq.(2.13) can be rearranged and expressed in term of radius relation as:

$$\frac{4}{3}\pi r_1^3 = \frac{4}{3}\pi r^3 + V_S \tag{2.14}$$

where: $r_1 > r$

The external static pressure of the liquid: "P_{ext}" is equal to the pressure "P" of the air inside of the flattened bubble also in equilibrium with the bubble ascending force "F_A" according to Archimedes and Pascal laws as follows:

$$P_{ext} = \rho g h = P = \frac{F_A}{A} \tag{2.15}$$

Being "A" the circular area of deformation which is the basis of the equivalent spherical sector V_S, ρ the liquid density, g the acceleration of gravity and h the immersion depth of the bubble.(Fig.2.8)

As the gas density is much smaller than the liquid density, according to the Archimedes law, the ascending force on a formed bubble is expressed as:

$$F_A = V\rho g \tag{2.16}$$

combining eqs. (2.15) and (2.16) gives:

$$\rho g h = \frac{4\pi}{3A} r^3 \rho g \tag{2.17}$$

simplifying and reordering eq.(2.17)

$$A = \frac{4}{3}\pi \frac{r^3}{h} \tag{2.18}$$

As the basis of the spherical sector "A" can be considered as circular, eq.(2.18) can be expressed as:

$$\pi r_2^2 = \frac{4}{3}\pi \frac{r^3}{h} \tag{2.19}$$

Thus

$$r_2 = \sqrt{\frac{4}{3}\frac{r^3}{h}} \tag{2.20}$$

The volume of the spherical sector can be calculated as:

$$V_S = \frac{\pi}{6} a(3r_2^2 + a^2) \tag{2.21}$$

where

$$a = r_1 - \sqrt{{r_1}^2 - {r_2}^2} \tag{2.22}$$

Combining equations (2.14) and (2.21) gives:

$$\frac{4}{3}\pi r_1^3 = \frac{4}{3}\pi r^3 + \frac{\pi}{6}a(3r_2^2 + a^2) \tag{2.23}$$

Combining eqs. (2.20) and (2.23), after simplifying gives:

$$r_1 = \left(r^3\left(1 + \frac{a}{2h}\right) + \frac{a^3}{8}\right)^{\frac{1}{3}} \tag{2.24}$$

also combining equations (2.20) and (2.22):

$$a = r_1 - \sqrt{{r_1}^2 - \left(\frac{4}{3}\frac{r^3}{h}\right)} \tag{2.25}$$

Equations (2.24) and (2.25) give the mathematical model to determine the radiusr_1, of the flattened bubble. The radius of the flattened bubble depends on the size of the original bubble and the immersion depth. By calculating r_1, it is possible to know how much larger the radius of the flattened bubble is in comparison with the original spherical bubble initially formed. The volume obtained by measuring the fictitious bubble dimension can now be corrected into a real bubble volume with radius r.

Some possible bubble radiuses of original bubbles were proposed and the radiuses of its correspondent flattened formed bubbles were calculated according to eqs. (2.24) and (2.25). Results are presented in Table 2.3. For h, a value of 6 mm depth was considered according to the liquid level in the bubbling cuvette (Fig. 2.6).

According to the results presented in Table 2.3, original bubbles with radiuses lower than 0.5 mm do not present significant differences in comparison with the radius and volume of its flattened version. Additionally, for an original bubble radius into the range of 1 to 2.5 mm the experimental error increases, however, for bubble radius less than 2 mm the involved error is less than 5 %.In conclusion, the bubble flattening process does not affect considerably the bubble size measurement below 1 mm in radius. According to the experimental error involved, the fact to consider "spherical" shapes for the observed bubbles is quite correct in the explored radius range of 0-1 mm. Indeed, bubble radius measured maximize for all GACs investigated at around 0.15 mm (see further).

The presented bubble shape analysis was done considering flat position of the glass cover: θ= 0; in this case using glycerol, the retention angle θ=11.3° diminishes also the flattening process.

Table 2.3: Results of the differences between flattened and original bubble volumes and graph of the error involved as function of the original bubble radius.

r(mm)	a(mm)	r1(mm)	V(mm^3)	Vf (mm^3)
0.05	0.0003	0.0500004	0.0003	0.0003
0.1	0.0011	0.100003	0.0024	0.0024
0.15	0.0025	0.15001	0.0079	0.0079
0.2	0.0044	0.20003	0.0188	0.0188
0.5	0.0286	0.5004	0.2944	0.2951
1	0.1176	1.0033	2.3550	2.3784
2	0.4997	2.029	18.840	19.672
2,5	0.8060	2.558	36.797	39.418

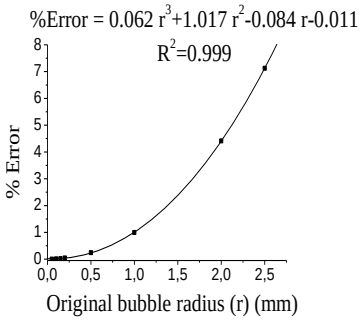

The percent of error ($Error$ (%)), was calculated as:

$$Error(\%) = \frac{(V_f - V)}{V} 100$$

Fig.2.9 presents a forces diagram when the retention angle "θ" is different from zero. In this case, the ascending force on the bubble is just a component of the total Archimedes force: (F_A); according to the diagram, the force that dominates the bubble deformation degree is: $F_{A(y)} = F_A cos\theta < F_A$. The bubble is retained statically in a specific position due to the equilibrium between the viscous and tensional forces of the liquid (F_v) and the component of the Archimedes force $F_{A(x)}$; thus this equilibrium mathematically can be expressed as: $F_{A(x)} = F_v$.

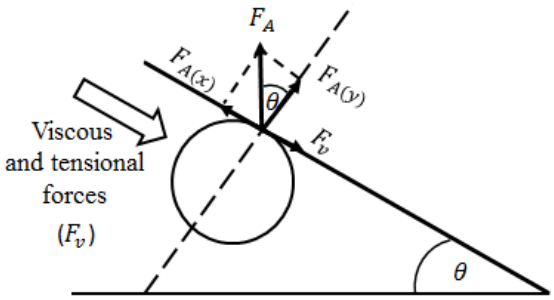

Fig.2.9: Forces diagram for $\theta \neq 0$

Concluding, as $F_{A(y)} < F_A$ the flattening process diminishes when $\theta \neq 0$ in comparison with the flat position: θ =0 , which is the critical condition (maximal) for bubble deformation. The greater θ, the smaller the deformation of the bubble will be. In view of the applied technique, the use of a spherical shape for the observed bubbles is thus quite correct.
Using different immersing liquids, the flat position of the glass cover has to be adapted and can give extra information on the pore sizes and total volume in the GAC.

2.5 -NMR relaxometry

Relaxometry is a tool to determine the pore size distribution of a porous material using NMR based on the fact that the ^{1}H NMR spin-lattice and spin–spin relaxation time of a liquid confined in a porous material changes according to the pore environment [125-142].

2.5.1-NMR relaxometry experiments

The T_{2H} (spin-spin relaxation) decay times were determined by means of solid-state ^{1}H-wideline solid-echo NMR measurements carried out at ambient temperature on a Varian Inova 400 spectrometer equipped with a dedicated 5 mm wide line probe. Hereto, on-resonance Free Induction Decays (FIDs) were acquired with 200 accumulations by the solid-echo method (90°x' - tse - 90°y' - tse - acquire) to overcome the effect of the dead-time of the receiver. The 90° pulse length t90 was set to 2 µs and spectra were recorded with a spectral width of 2 MHz (0.5 µs dwell time) allowing an accurate determination of the echo maximum. The echo maximum is formed at τ = (3t90/2 + 2tse) = 9 µs and this time point is calibrated to time zero. These FID's were then converted into ASCII files and the signal intensity was analyzed as a function of the acquisition time t with the sum of a Gaussian function (T_2Hs ; rigid fraction) and a Lorentzian (exponential) function (T_2Hl ; mobile fraction) according to the equations 3.21 and 3.22 discussed in Chapter.3). A preparation delay of 5 sec (≥ 5 times the T_1H relaxation decay time) was always respected between successive accumulations to obtain quantitative results. The data were analyzed by a non-linear least-squares fit (Levenberg-Marquardt algorithm).

2.6 –Thermal regeneration experiments

2.6.1-Regeneration set-up

The GAC regeneration experiments were performed in the set-up depicted in Fig.2.10 consisted of the following: (1) Tubular quartz reactor; (2) Nabertherm horizontal oven ; (3) Gas-flowmeter automatic valve; (4)Programmable FGH 1000 temperature controller.; (5)Programmable Schott TR 100 automatic burette; (6)PC.

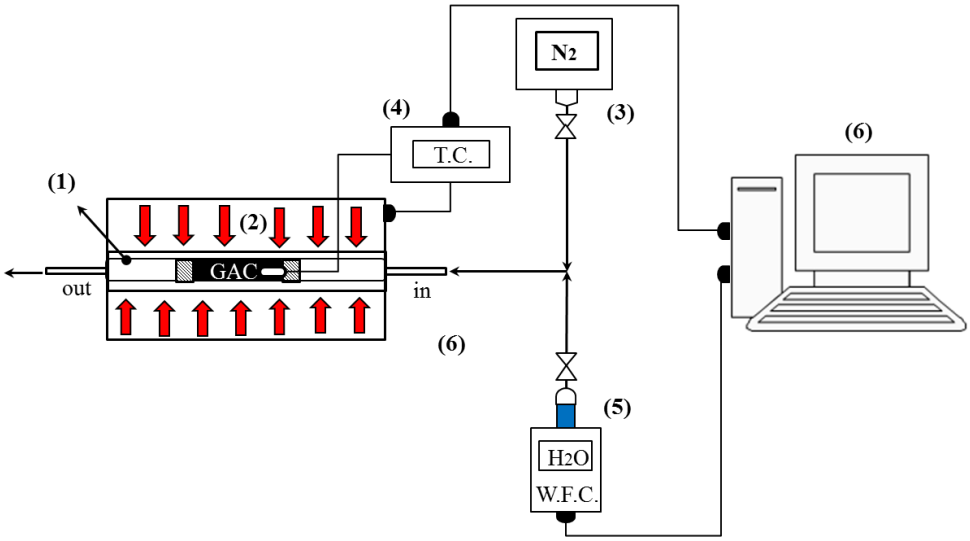

Fig.2.10: GAC regeneration set-up. T.C.: temperature controller; W.F.C.: water flow controller.

Working description

The reactor (1) is a horizontal tubular quartz reactor designed for the horizontal Nabertherm oven (2). 20g of GAC sample (previously prepared according to §2.2.1) is put into the quartz reactor and attached in the center of the quartz tube using two gaskets of glass wool. The quartz reactor is introduced into the Nabertherm horizontal oven.

Once the oven and the reactor are prepared, a constant flow of nitrogen at 70 mL/min is supplied by the gas-flowmeter automatic valve (3) to ensure an oxygen-deficient environment during the initial stages of the GAC regeneration process (drying and thermal desorption).

Flushing N_2, the oven is switch-on to heat the sample at certain temperature with a predetermined heating rate previously programmed in the Programmable FGH 1000 temperature controller (4).Once the temperature for the third stage (pyrolysis) in regeneration process has been reached, the N_2 injection to the reactor is switched to steam in order to induce the proper oxidant atmosphere for the activation process. The selected activation temperature is held isothermally. During steam pyrolysis and activation, water is injected directly into the quartz reactor, with subsequent steam formation.

The water flow is supplied by the programmable Schott TR 100 automatic burette (5) which is controlled by the PC (6). The heating process is controlled automatically by the programmed FGH 1000 controller. Temperature feedback to the controller is supplied by a type K thermocouple, inserted directly in the regenerating volume.

2.6.2- Regeneration experimental planning

The regeneration process was planned taking into account a real industrial plant for producing activated carbon in Cuba using a rotatory kiln. This approach was introduced with the intention to perform the thermal regeneration of exhausted GAC in rum production at industrial scale in this plant (it will be discussed in Chapter 4).

The industrial rotatory kiln (similar design of Fig.1.5) has a maximum load capacity of one ton of material. The residence time in the kiln can be adjusted between 0.5-3 h depending on the precursor to produce the activated carbon. The steam flow for the activation is supplied by a boiler in a range of 1-3 ton/h. The heating rate of the industrial kiln is 2°C/min to reach a maximum steam activation temperature of 850°C.More information about the technological characteristics of the rotatory kiln used for the regeneration at industrial scale in the activated carbon plant in Cuba and a further comparison with other rotatory kiln systems can be found in supplementary materials (Fig. S1).

According to the observed operational parameters in the industrial kiln to be used in the thermal regeneration, the experiments were conducted to reproduce as close as possible the reality in order to obtain the highest regeneration degree, with the maximum yield and efficiency based on the process carried out in this plant.

Table 2.4 presents the main operational parameter ranges for the industrial reactor. According to the operational ranges, a regeneration of GAC exhausted in rum production can be conducted in this reactor under different conditions. Therefore, the experiments were prepared to explore the regeneration variables based on the industrial reactor range parameters. According to [43], 1kg of steam per kilogram of activated carbon has often been advanced as the requirement for the complete regeneration of exhausted carbon.

In that case, the ranges of the variables involved in the regeneration experiments are presented in Table 2.5.

Table 2.4: Main operational parameters of the industrial rotatory kiln in Cuban activated carbon plant.

Parameter	**Unit**	**Values**
Temperature	°C	400-850
Residence time	h	0.5-3
Load capacity (max.)	ton	1
Heating rate	°C/min	2
Steam flow generation capacity	ton/h	1-3
Steam/carbon ratio	(kg of seam/kg of GAC)	0.5-6

Table 2.5: Experimental parameters range for GAC regeneration at lab scale

Parameter	**Unit**	**Explored values range**
Temperature	°C	450-850
Residence time	min	20-100
Load capacity	g	20
Heating rate	°C/min	5
Steam flow	g/min	(2/11)-(1/2)
Steam/carbon ratio	(g of seam/g of GAC sample)	1

Experimental planning is summarized in Fig. 2.11. In the "x" axe, the time and "y" axe the temperature. Two colored lines are presented; the yellow one represent N_2 injection to the reactor and the blue lines are referred to the process with steam atmosphere.

The diagonal line symbolizes the heating process with rate of 5°C/min and horizontal lines are representing isothermal regeneration process. Each regeneration experiment is symbolized with a red circle.

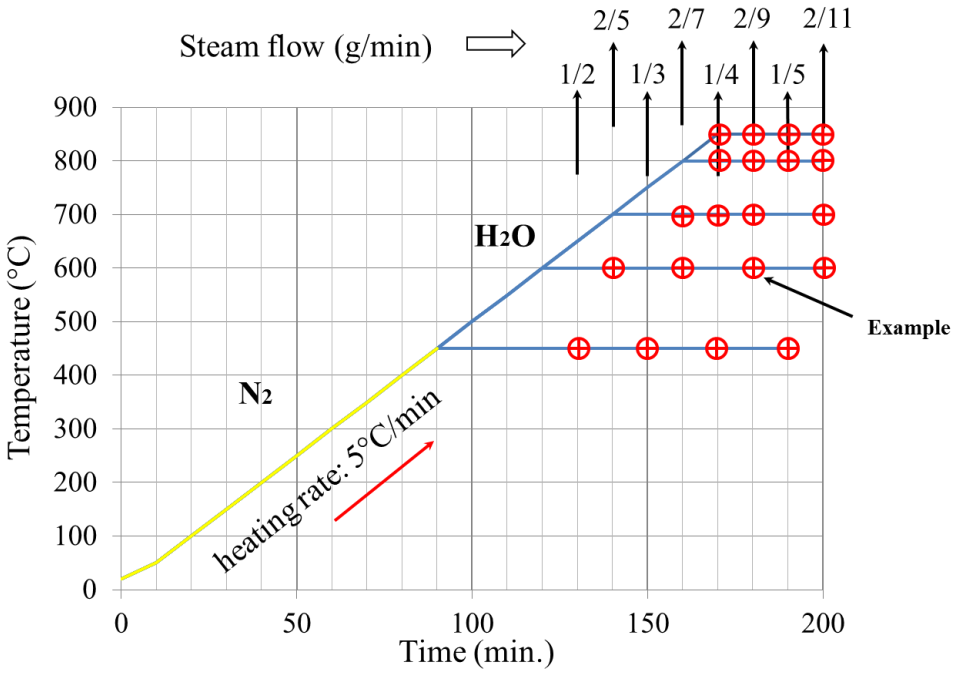

Fig.2.11: Graphical planning of GAC regeneration experiments. Red circles (experiments), yellow line (Process under N_2 atmosphere), blue line (Process under steam atmosphere).

We can take the regeneration experiment indicated in Fig. 2.11 as "example". The heating process starts: time "zero" at room temperature flushing N_2. The first 50 minutes, high volatile compounds and water are desorbed (drying)[2,5,8,43], 50-90 min thermal desorption occurs approaching to the pyrolysis stage, due to the nature and variety of adsorbed compounds in rum production [78-81,85-88,97,102-104] in the exhausted GAC, in order to avoid the graphitization process during pyrolysis [2,5,8,43] at 450°C the N_2 atmosphere is switched to steam (the temperature of 450°C was selected based on TGA and TD-(GC/MS) analysis which that will be discussed later).

The temperature still increasing but in that case under a steam–oxidizing environment. When the temperature of treatment has been reached (e.g. 600°C) the process is kept isothermally until the time of regeneration has been covered. When the isothermal process has been stablished, the regeneration process starts, (i.e. zero residence time).

Following "example", the experiment was performed: heating till 450°C (90 min) under N_2 , switched to steam and heated till 600°C (+30 min), and kept isothermal at 600°C (+ 60 min = residence time). Thus, for "example" the regeneration was performed at 600°C during 60 min.

According to Fig. 2.11, the experimental matrix is shown in Table 2.6. The regenerated GAC is indicated as: RAC followed by a code which is referred to the conditions of the experiment in terms of temperature and residence time applied RAC (T;t). Five independent regenerations were performed for each experimental condition and the material was mixed to create one homogeneous sample. Each regenerated-mixed sample was further analyzed.

Table 2.6: Experimental matrix for GAC regeneration

		Residence time (min)							
	T(°C)	1	2	3	4	5	6	7	8
		5	**10**	**20**	**30**	**40**	**60**	**80**	**100**
1	**450**	x	x	x	x	RAC(1;5)	RAC(1;6)	RAC(1;7)	RAC(1;8)
2	**600**	x	x	RAC(2;3)	x	RAC(2;5)	RAC(2;6)	RAC(2;7)	x
3	**700**	x	x	RAC(3;3)	RAC(3;4)	RAC(3;5)	RAC(3;6)	x	x
4	**800**	x	RAC(4;2)	RAC(4;3)	RAC(4;4)	RAC(4;5)	x	x	x
5	**850**	RAC(5;1)	RAC(5;2)	RAC(5;3)	RAC(5;4)	x	x	x	x

The higher the temperature, the shorter is the residence time. This strategy has two main purposes: (1) to minimize possible structural damage to the GAC grain for a long exposure to high temperature [2,5,8,43] and (2) to find the better combination between residence time and temperature in order to obtain a proper regeneration degree with the higher yield at the lower cost.

2.7- Sensorial analysis

The sensorial analysis was performed based on the Triangle Test Method according to the legal regulations NC-ISO 4120:2006 of the Cuban National Bureau of Standards.

The triangle test method describes the procedure to determine perceptible sensorial differences between two products. This method is applied to detect differences or similarities in sensorial attributes of a product.

In this case, the goal is to demonstrate that two products (refined aged aguardiente) are (or not) statistically different based on its sensorial attributes. Three coded cups (blind) with samples of filtered aged aguardiente (two cups containing the original standard filtered aged aguardiente and one containing filtered aged aguardiente but using the regenerated carbon (RAC) are tasted for each rum expert in the sensorial board .

They have to detect which cup contains the filtered aguardiente using the RAC (the different product). The results are statistically processed to define if the product presents or not sensorial differences based on "true or false" detection.

Chapter 3 –Characterization of the GAC applied in rum production based on different methods. Development of new methods of GAC characterization: Acoustic Emission, Colorimetry and Immersion Bubblemetry.

This chapter focusses on the development of novel analytic methods to assess the porous characteristics of the GAC used in the rum production process. The obtained results applying the novel methods are correlated and compared with other well-stablished conventional analytical techniques not only in terms of feasibility, robustness and efficacy but also the suitability for rum producers.

3.1- A colorimetric method for the determination of the exhaustion level of GAC used in rum production.

The primary rum, known in Cuba as Aguardiente, is a colorless liquid that is aged in barrels of white oak wood during a timed period in order to transform and improve its sensorial characteristics. The ageing process (maturation) results in changes of the Aguardiente: a light amber color appears; taste softens; and a pleasant aroma is produced [78]. During this stage; these sensorial changes are obtained by complex chemical reactions, which can be summarized in four simultaneous general steps (Fig. 3.1) [78; 81-84]:

(1) Reaction between the different original compounds in the Aguardiente

(2) Substance extraction from the oak wood to the alcoholic bulk liquid

(3) Oxidation of both kinds of compounds (extracted and original compounds)

(4) New reactions between the original, extracted and the oxidized compounds.

However, apart from this general scheme, taking into account the amount of compounds "n" in each phase and other collateral reactions, an enormous number of possible reaction mechanisms and products can be found. Chemically speaking, the study of the ageing process is really complicated. Rums are a complex mixture of organic substances: 186 organic compounds have been identified [79, 80, 85-89]. Additionally, research to understand the sensorial characteristics of rums based on the composition of white oak wood has been performed. The problem is complicated because volatile and non-volatile compounds from the wood have also important contributions. Non-volatile compounds are precursors improving rum's flavor. Volatile compounds contribute to rum's aroma [90–93].

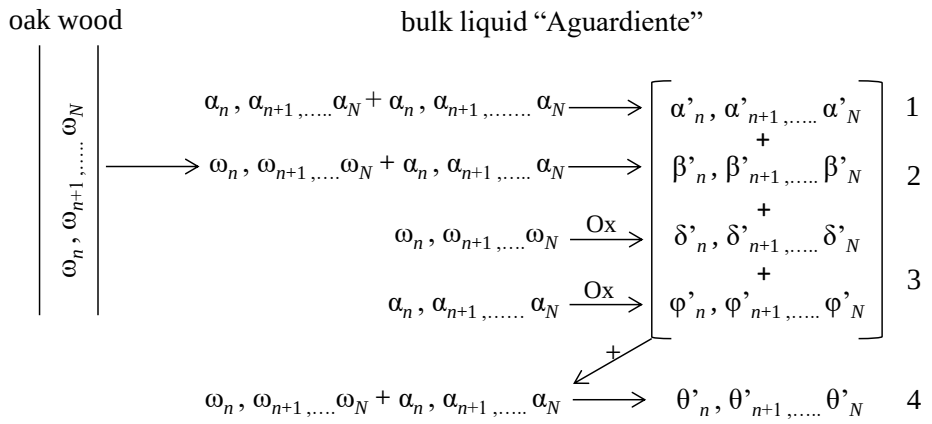

Figure 3.1: Reduced scheme of the main reactions in the rum ageing process. (α, ω represent the original compounds of Aguardiente and wood, correspondently, and α', β', δ', φ', θ' the probable obtained compounds; "*n*" represents the different types of organic compounds involved in each possible particular reaction).

Table 3.1 presents the basic composition of white oak wood [78, 94]. The hemicellulose is constituted by polymers of monosaccharides, mainly represented by pentoses and polyuronics. The last can be easily extracted from the wood and hydrolyzed to pentoses (arabinose, xylose) and hexoses (fructose, glucose and galactose), which improve the flavor of the rum, giving its sweetness [95].

Table 3.1: Basic composition of white oak wood.

Component	**% of Total Dry Weight**
Cellulose	40–45
Hemicellulose	20–35
Lignin	20–33
Extractable compounds	2–10

Extractable compounds are important contributors in the organoleptic features of rums, giving aged rum the typical amber color and odor of oak wood. Extractable compounds present in rum include: wood resins, fatty acids, terpenes, carbohydrates, polyhydric alcohols, nitrogenized compounds (wood amino-acids and proteins), phenolic compounds and inorganic constituents.

The effect of the white oak wood proteins and amino acids on rum taste and color has been studied. In the ageing process, amino acids lose the amino group, which is substituted by a carbonyl group. During the ageing, the pyrocatechol and pyrogallol intensify the dis-amination of the amino acids [78, 82,85, 88, 91, 92, 96–103]. The color increment in aged Cuban rum has been studied and its linear correlation with the ageing time in months presented [78]. In the ageing process, the total acidity increases, and a close relationship between the improvement of the rum quality and its acidity exists. Oak wood is an important source of non-volatile acids that contributes to the total acidity in rums and other aged beverages [78,104].

When the GAC has been used in rum production (specifically for refining aged Aguardiente), it was found that a reaction between the exhausted GAC and an ammonia solution (in a wide concentration range) resulted in an almost instantaneously amber color appearing (Figure 3.2). The more exhausted the GAC is, the darker the produced amber color. If the GAC has not been used in aged Aguardiente treatment, the reaction does not occur.

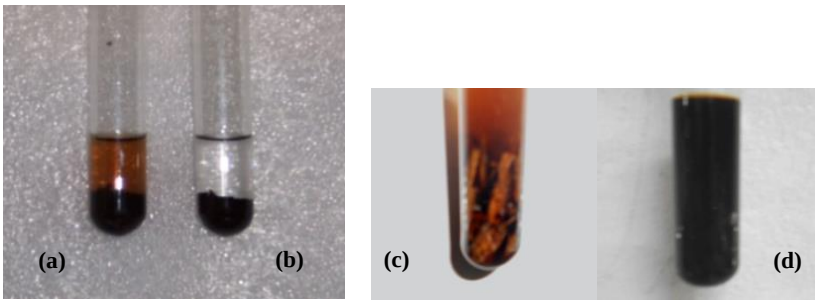

Figure 3.2: Samples of activated carbon in contact with ammonia solution (25%). (a) Exhausted granular activated carbon (GAC) from the rum production process and (b) virgin GAC; white oak wood chips after (c) 15 min and (d) 12 h.

Additionally, from our pre-studies, the same reaction feature occurred between chips of white oak wood and ammonia solution. The amber color appeared much darker than the amber color obtained with GAC (Figs3.2c and d). The reaction between ammonia with different type of woods or wood "ammonia fuming" is a well-known practice among the techniques for aesthetic wood modification in furniture and wood flooring [143-147].

Several authors have pointed that ammonia treatment for darkening of wood is attributable to ammonia-tannin reaction [143-145].The compounds present in the white oak wood are responsible for the amber color in the rum. The compounds are adsorbed onto GAC during rum production. The exhausted GAC reacts with the ammonia solution, releasing the amber-colored compounds, as is shown in Fig. 3.2a. According to Figure 3.3, the reaction with ammonia occurs when the white oak is introduced in the scenario of rum production. The compounds responsible for coloring the ammonia solution are coming from the wood fibers as extractable compounds. The concentration of these substances in the wood is high enough to obtain a very intense dark amber color by reacting with ammonia (Figure 3.2d).

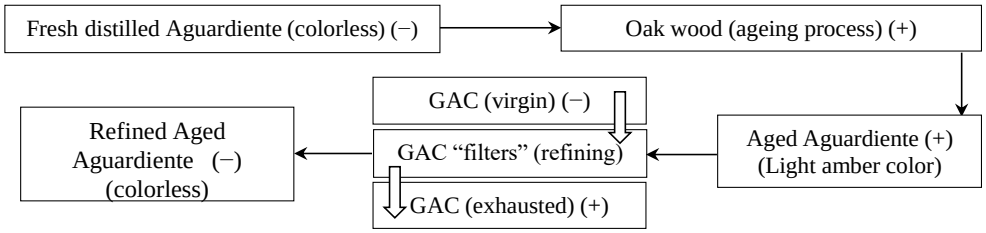

Figure 3.3: Diagram of the color reaction. The "(+)" represents when the reaction with the ammonia solution occurs (amber color) and "(–)" when the color does not appear.

When the Aguardiente is aged, the colored extractable compounds are present in the liquid [78, 82,85, 88, 91, 92, 96–103] (Step 2 in Figure 3.1), but its concentration is so low in comparison with the oak wood that the reaction produces just a pale amber color. However, in the Aguardiente refining process, GAC adsorbs these color compounds among other substances [78,105,106].

Our study was conducted to develop an in-depth specific, reliable, robust and fast colorimetric method to analyze the exhausted level of different GAC samples used in the rum production process. A quick qualitative pre-evaluation of the exhausted degree can be performed based on an on-sight color intensity evaluation by a simple extraction test of used GAC with ammonia. In order to establish the proper conditions and experimental parameters to perform the colorimetric method, an initial comparison between the GAC samples in the rum

filter (showed in Fig.2.1 and sampled as is described in §2.1) and the virgin GAC must be done.

Table 3.2 displays the iodine number and contact pH of the samples. Five experiments were performed, and statistical parameters were determined for each sample. Based on the iodine number, GAC-Top is the most exhausted. The pH trend was consistent with the obtained order by the iodine number. Comparable trend of both parameters as function of the GAC layer position in the rum filter is presented in Figs.S2 (a) and (b) (supplementary materials).

Table 3.2: Iodine number and contact pH of the GAC samples.

	Iodine Number			**Contact pH**		
Samples	$\bar{x}$	$\sigma(x)$	V.C. (%)	$\bar{x}$	$\sigma(x)$	V.C. (%)
GAC-Top	472	23	4.9	3.94	0.09	2.3
GAC-0.2	496	37	7.5	4.04	0.11	2.7
GAC-0.4	537	31	5.8	4.11	0.04	1.0
GAC-0.6	805	72	8.9	4.89	0.06	1.2
GAC-0.8	1035	36	3.5	5.41	0.03	0.6
GAC-1.0	1213	98	8.1	5.61	0.02	0.4
GAC-1.3	1193	83	7.0	5.61	0.01	0.2
GAC-Bottom	1259	90	7.1	5.63	0.03	0.5
GAC-virgin	1515	115	7.6	6.23	0.01	0.2

V.C.: variability coefficient, $\bar{x}$: averaged value, $\sigma(x)$(standard deviation).

This indicates that the lower the iodine number, the more acidic the GAC sample. Iodine number and the measured pH correlated with the adsorption capacity of the GAC: the more exhausted the GAC, the lower the pH value. According to other researchers [78,96–103], the acidity increases during the ageing process in rum production. After filtering the Aguardiente through the GAC, adsorption of a variety of acids occurs. The longer the GAC is used in the rum production process, the higher the adsorbed concentration of these acid compounds onto the GAC is (beside the adsorption of other compounds) and, thus, the more acidic these GAC become.

Results are also consistent with the direction of the mass transfer zone MTZ displacement through the GAC bed and the adsorption wave theory described in §1.9.1 [8-11,17,32] the most exhausted GAC in the target rum filter is located at the filter's top.

A linear correlation (R^2 = 0.993) is obtained by plotting the iodine number vs. the pH (Table 3.2). The reduction of the adsorption capacity involves an increment of adsorbed compounds onto GAC grains (including extractable and formed acids during the ageing process (Steps 2–4, Figure 3.1) [78,96–103]. It can be suggested that the iodine number and the contact pH can be equally used to determine the exhaustion level of a GAC sample, once the value of the initial GAC is known.

However, the iodine number must be carefully interpreted when an exhausted GAC in rum production is tested applying this method. Firstly, the iodine number method is originally used on fresh carbons [111]. Also it was found that iodine can react with some adsorbed organic compounds which were detected in exhausted GAC used in rum production applying TD-GC/MS (discussed later). Such reactions between iodine, alcohols and phenolics compounds have been reported by different authors [148-150].Therefore, testing exhausted carbon by iodine number method has to be analyzed just as a relative parameter in order to compare GAC samples.

Figure 3.4 displays SEM images of GAC samples: "virgin" (a) and GAC-Top "most exhausted" (b) before and after use in a rum production process.

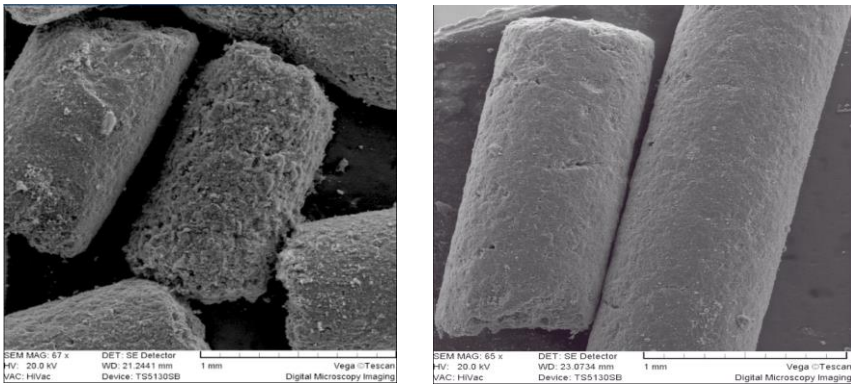

(a) (b)

Figure 3.4: Digital microscopic images of samples of "virgin" GAC (a) and "exhausted" GAC-Top (b) before and after use in a rum production process.

Differences can be seen in the external surface of the GAC particle. "Virgin" GAC (a) shows more roughness in its surface in comparison to "exhausted" GAC (GAC-Top (b)).

The diminished external roughness of the used GAC in the rum production process can be associated with increased amounts of adsorbed organic compounds.

Fig. 3.5 displays the CHNS-O elemental analysis expressed as element ratio between the GAC samples and the virgin GAC. The element ratio(R) of a GAC layer can be expressed as:

$$R = \frac{(\%\ Element)_i}{(\%\ Element)_{virgin}} \tag{3.1}$$

where $(\%\ Element)_i$ and $(\%\ Element)_{virgin}$ are the element percent of "i" and "virgin" GAC sample respectively.

The horizontal line located at R=1 represents an equal ratio in comparison with the virgin GAC. The percent of carbon in the eight GACs is almost the same in comparison with the GAC virgin, thus located very close to the R=1 line.

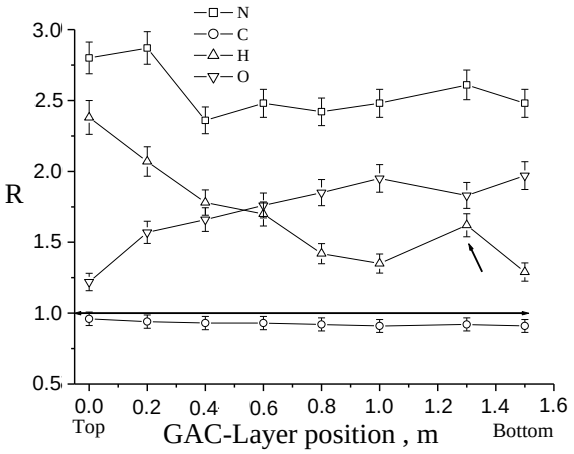

Fig 3.5: CHNS-O elemental analysis data expressed as element ratio (R) between the GAC layers and the virgin GAC. No sulphur was found.

The nitrogen content in the samples is ranging between 2.4-2.7 times higher than the virgin GAC. For the samples GAC-Top and GAC-0.2 the nitrogen content is slightly higher in comparison with the other GACs which have almost the same nitrogen content, but slightly increasing as a function of the layer position.

After GAC-1.3 the N-content decreases again. The nitrogen content can be associated with amino acids and proteins from the oak wood [78,82-84].

The hydrogen content decreases from the top to the bottom being almost 2.5 and 1.2 times higher compared with the virgin GAC respectively. According to Fig. 3.5, the hydrogen content for the GAC-Top is almost two times higher than the hydrogen content in the three last layers near to the filter bottom. As the oxygen content was calculated by difference, obviously a complementary tendency is observed. The increment of the hydrogen content in the top can be related with a higher concentration of adsorbed organic compounds, resulting in a higher H/C ratio. In contrast, the GAC layers near to filter's bottom have less adsorbed organic compounds, thus a much lower hydrogen content, tending to the value of the virgin GAC. Based on Fig. 3.5, the hydrogen content for GAC-1.3 (indicated by the arrow) is higher than the hydrogen content observed in the sample GAC-1, indicating an apparent change in adsorption behavior of the GAC in that filter part. This behavior is also observed with other techniques further on. A systematic decreasing trend with the increment of the GAC layer position to the bottom is expected. However, the GAC-1.3 is more exhausted than GAC-1. This behavior is related with the characteristics of the rum filtration process.

The aged aguardiente is applied at the top of the column, flows downward through the carbon bed, and is withdrawn as "filtered aguardiente" at the bottom of the column (Fig.2.1 (b)). The process is carried out under batch condition at atmospheric pressure and the liquid crosses the GAC bed by gravity force. A defined amount of aged aguardiente is filtered each day according to the production demand in the factory. This filtration is carefully monitored by the rum masters to guarantee optimal flow velocity. At the end of the batch operation process, the filter retains a certain amount of aged aguardiente trapped into the GAC bed (bed porosity: around 40%). Slowly the filter is drained and a certain volume of liquid retained in the bed.

As the hydraulic pressure depends on the liquid level, the draining process is faster at the beginning, but as the liquid level decreases the draining process slows down, meaning that an amount of primary rum is retained for longer time in the GAC layers near to the bottom. This effect results in a longer contact time around the GAC-1.3 in comparison with the GAC-1 layer, explaining the apparent change of hydrogen content at 1.3 m.

Based on contact pH, iodine number and elemental analysis, GAC-Top is the most exhausted GAC; therefore, was used as the target GAC in developing the colorimetric method. Afterwards, samples GAC 0.2-Bottom were measured with the optimal colorimetric method conditions.

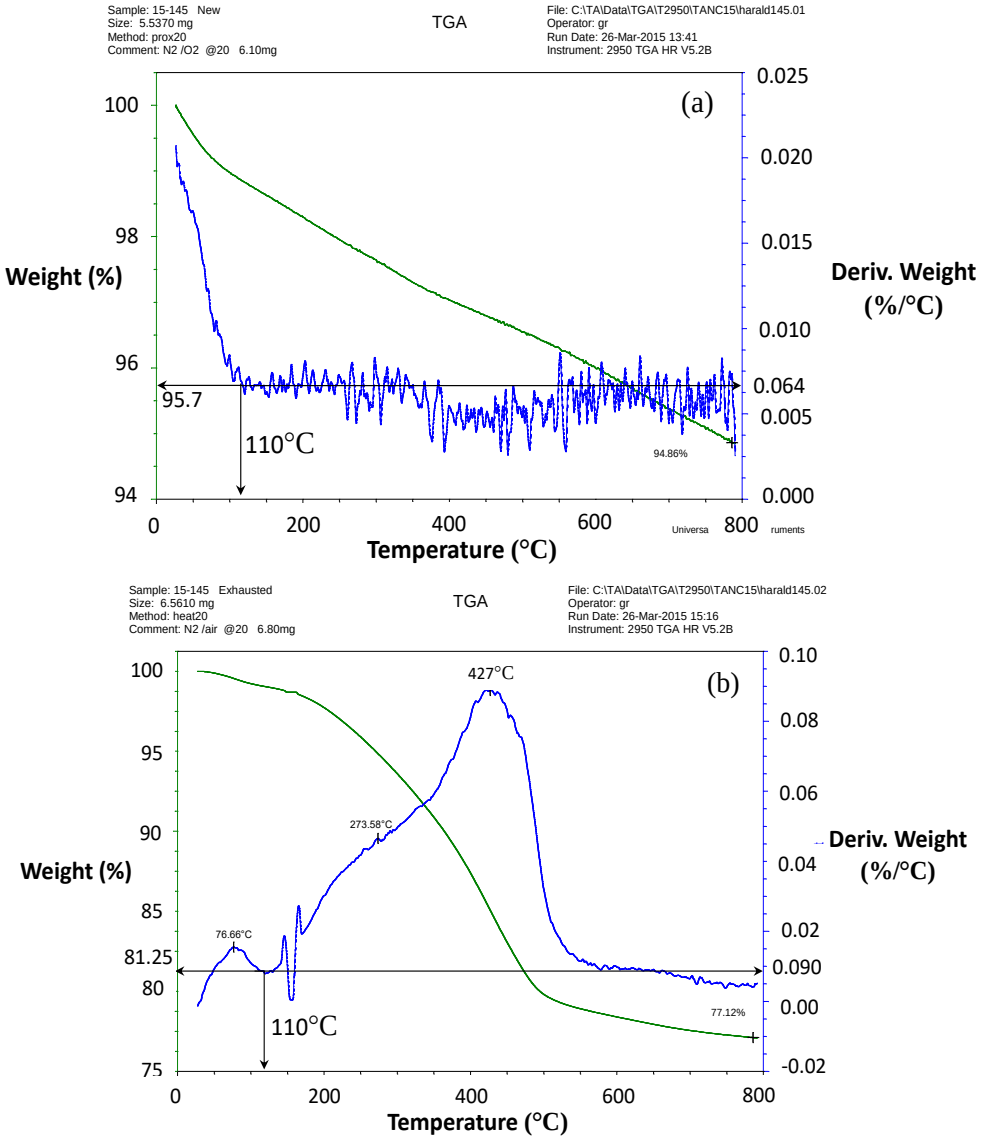

Figure 3.6: Thermogravimetric (TG) curves and derivative weight loss (DTG) curves for GAC-Virgin (a) and GAC-Top (b) in N_2 atmosphere.

Figure 3.6 displays the thermogravimetric analysis (TGA) results for the virgin and the most exhausted samples: GAC-Virgin (a) and GAC-Top (b) correspondently.

According to Figs. 3.6 (a) and (b), the loss of weight for GAC-Virgin was about 6% and for the GAC-Top around 20%. Above 110 °C, minor weight loss occurred in a continuous way due to in situ-formed volatiles for GAC-Virgin upon further heating. Comparing TGA results, Figs 3.6 (a) and (b), great differences between the exhausted samples and virgin GAC are noticeable.

At 110 °C, the loss of water and low MW volatile compounds ends. Additionally, based on this TGA, a thermal treatment just above 500 °C for GAC-Top could result in a removal of most of the adsorbed organic compounds featured by an desorption peak at 427°C. Thermal desorption in the absence of oxygen could point to a possible recycling strategy.

3.1.1- Sample preparation for the colorimetric method

Drying

According to Figure 3.6 (b), the drying process for the samples of exhausted GAC-Top must be handled carefully in order to release only moisture. Therefore, preparing GAC for the colorimetric method, a drying curve was recorded in order to determine the proper drying time at 110 °C.

The moisture content for GAC-Top was determined [107] and plotted versus time. After 3 h, the moisture content did not significantly change. According to the drying curve (Fig.S3) and TGA results, the drying process must be carried out at 110 °C for 3 h.

Solid-Liquid relation "Xi" (g/mL)

The solid-liquid relation "Xi" (grams of GAC per volume of ammonia solution) represents an important variable to be fixed. Xi affects the intensity of the obtained color of the extracted solution (ES). The higher the Xi value is, the darker the color. An optimal Xi to perform the colorimetric method was determined in combination with an optimal wavelength to measure the color intensity according to the Xi value. Initially, the experiments were performed using 20.0 mL of 25% ammonia solution, with masses of GAC equal to: 0.2; 0.4; 0.6; 1.0; 1.6; 3.2 and 6.0 g.

Wavelength

Figure 3.7 displays the absorbance spectra of ES at different Xi combinations. Absorbance spectra are almost identical for all Xi combinations.

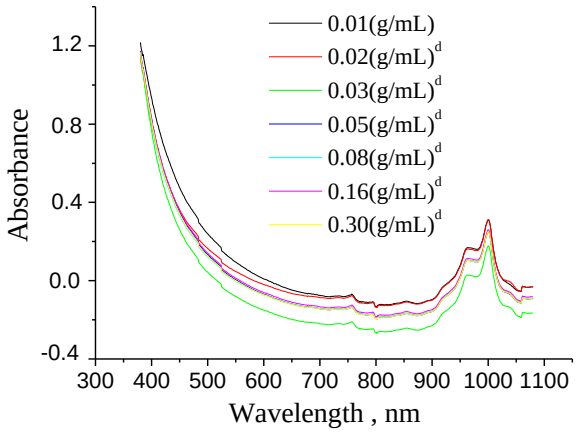

Figure 3.7: Spectra of the extracted solution (ES) at different Xi (T = 25 °C/stirring rate = 50 rpm/extraction time = 72 h/20.0 mL ammonia solution (25%)/batch experiment). "d": after proper dilution.

From these spectra, it is clear that no optimal wavelength can be selected. Therefore, a strategy was explored to measure at the most proper wavelength. First, a proper dilution of all ES solutions was made to account for all Xi values of the VIS spectrum (380–1100 nm), making spectra comparison possible.

Measurement scale

According to the instrumentation and measurement criteria, any measurement should be done at 50%–75% of the equipment maximal scale value in order to minimize the measurement errors. The spectrophotometric measurement range of absorbance was 0–2 absorbance units. Thus, an accurate measurement in the range of 1–1.5 absorbance units was possible. For each absorption spectrum of ES at different Xi values, the selected wavelength must give an absorption value in this range. The value of 1.25 absorbance units was selected. Hereafter, each sample of ES at different Xi values was spectrophotometrically analyzed without dilution.

Table 3.3 displays the values of the wavelength determined by processing statistically the optical data close to 1.25 absorbance units. Five independent experiments for each value of Xi were performed. The more intense the color is, the higher the obtained wavelength.

The minimal standard deviation $(\sigma(x))$ was observed at 634 nm at Xi = 0.16 g/mL. A representative amount of GAC particles per volume of ammonia solution has to be used in order to obtain an optimal extraction condition. However, when the Xi value is higher than 0.16 g/mL, the color (dark-amber) is so intense that the optimal wavelength is loaded again with a larger error.

Table 3.3: Wavelengths of direct absorbance measurements for each solid-liquid relation (Xi) value.

Xi (g/mL)	0.01	0.02	0.03	0.05	0.08	0.16	0.30
λ_i (nm)	440	480	514	549	583	635	670
	436	488	516	550	582	634	669
	437	482	515	549	583	635	671
	440	480	514	549	581	633	667
	438	484	518	552	584	635	673
$\sigma(x)$ (nm)	1.8	3.3	1.7	1.3	1.1	0.9	2.2
$\bar{\lambda}$ (nm)	438	483	515	550	583	634	670

Notes: λ_i(wavelength values at each Xi combination), $\bar{\lambda}$(average wavelength value), $\sigma(x)$(standard deviation).

Concluding: a representative Xi value with a proper amount of GAC, but also proper color intensity and the lowest error is for 0.16 g/mL of GAC (3.2 g/20 mL) to be measured at 634 nm.

3.1.2-Kinetics

Effect of ammonia concentration

A 25% ammonia solution was used to determine the optimal Xi and wavelength to develop the spectrophotometric measurement. To evaluate the effect of the ammonia concentration, seven different ammonia concentrations were explored: 25%; 12.5%; 6.25%; 3.125%; 1.25%; 0.25% and 0.125%. Three-point-two grams of GAC-Top and 20 mL of ammonia solution were loaded in the kinetic set-up (Fig. 2.3). For each ammonia concentration, five independent experiments were performed at 25 °C, and absorption was measured at 634 nm after every 30 s.

Figure 3.8 displays the kinetic data plotted at different ammonia concentrations. Kinetic plots for ammonia concentration at 25%, 12.5% and 6.25% are grouped together showing a similar extraction rate. By contrast, kinetic plots for ammonia concentrations 3.125%–0.125% were different: different extraction rates and different extracted amounts.

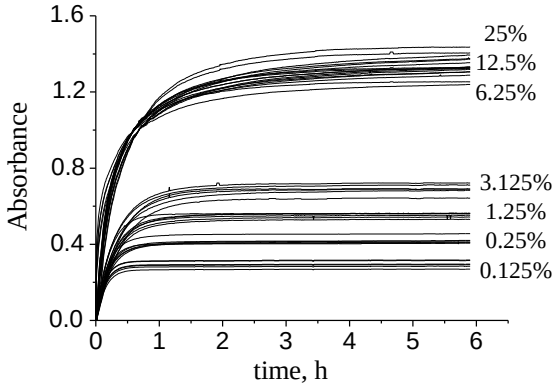

Figure 3.8: Plots of the experimental kinetics data for different ammonia solution concentrations at 25°C.

The lower the concentration of ammonia used, the faster the extraction occurred, but a lower maximum absorption value is reached or fewer amounts of compounds are desorbed. An ammonia concentration of 6.25% needed 6 h of contact for maximum absorption.

Table 3.4 presents the results of the statistical comparison between the final absorbance values reached at 25 °C for each ammonia concentration.

Table 3.4: Statistical comparison of the equilibrium absorbance value reached for each
ammonia concentration.

Concentration of NH_3	$\overline{A^*}$	σ(x)
0.125%	0.296	0.01
0.25%	0.420	0.03
1.25%	0.552	0.04
3.125%	0.690	0.07
6.25%	1.332	0.09
12.5%	1.326	0.09
25%	1.349	0.11

Method: 95.0 percent lower significant difference (LSD). $\bar{A}^*$ is the mean of the absorbance in equilibrium (in absorbance units). σ(x) is the standard deviation.

The multiple comparison method was applied to determine statistical differences between the mean of the samples using Fisher's lower significant difference (LSD) method. In this case, there was no statistical difference in the equilibrium absorbance value reached between 25%, 12.5% and 6.25% of ammonia. In addition, all spectra recorded for ES at different ammonia concentrations were identical to those displayed in Figure 3.7.

According to Lambert-Beer's law, the absorbance value is directly proportional to the concentration of a component "A". As rum is a complex mixture of organic substances [79, 80, 85-89], it is difficult to determine the specific extractable compound responsible for ES color (an analytical procedure to determine the family of extractable compounds responsible for the obtained color is presented later). Therefore, an alternative way to assume the linear correlation between the absorption value and the concentration of the color can be proposed. An industrial amber color from sugar cane (known as caramel color) was therefore used. This colorant is produced at industrial scale, and its quality parameters are strictly guaranteed and regulated. The amber color from the caramel color is very similar to the color of the ES and the color from the oak extracted solution (OES) presented in Figs.3.2 (c) and (d).

Figure 3.9 presents the absorbance spectra of ES, OES and the caramel color. The spectra are similar in the 380–900 nm range.

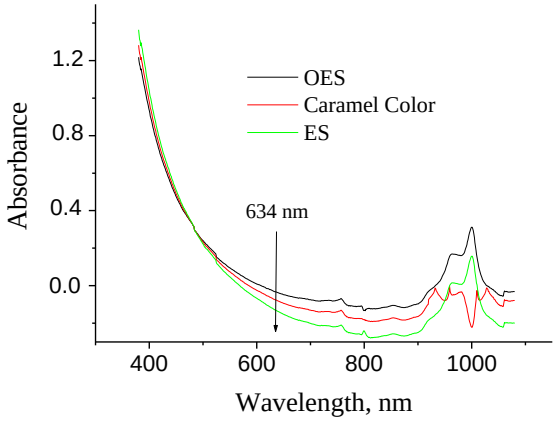

Figure 3.9: Optical scans of ES, OES and the caramel color.

As the measurements take place at 634 nm, the caramel color can be used as a representative or equivalent substance to evaluate the linear correlation between the absorbance value and the color concentration.

After 900 nm, the optical pattern of the caramel color is somewhat different from the ES and OES patterns. A linear calibration curve between measured absorbance and the concentration of the caramel color at 634 nm was obtained. Accordingly, for ES, an equivalent linear correlation at 634 nm can be stated and is used to calculate "color" concentration or C_{eq} for ES and OES.

The model that describes the relationship between absorbance (*Abs*) and the color concentration C_{eq} (in g/L) is proposed as:

$$Abs = 0.0464 \cdot C_{eq} \qquad (R^2 = 0.999) \qquad (3.2)$$

Figure 3.10 presents the experimental and fitted kinetic data for only two different ammonia concentrations at 25 °C.

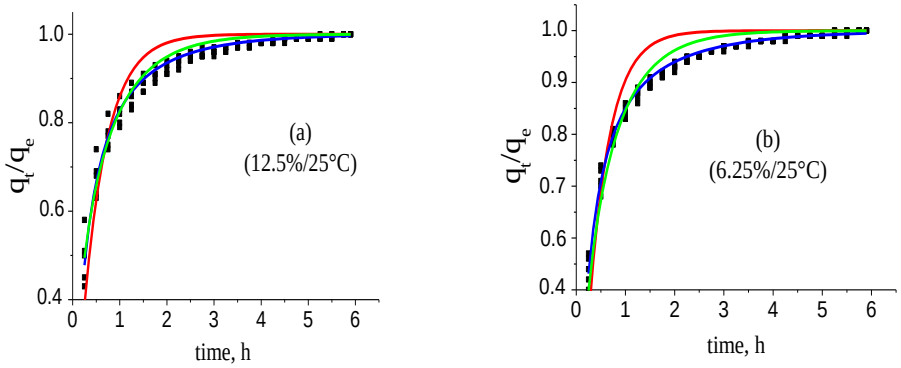

Figure 3.10: Experimental and fitted kinetics data at two different ammonia concentrations (GAC-Top; 3.2 g/20 mL NH_3 solution). Red: pseudo-first order (PFO); green: modified pseudo-"n" order (MPnO) and blue: mixed order (MOE).

All of the data were used in the fitting process using the q_t/q_e ratio versus t according to the PFO, PSO, MPnO and MOE models. q_t and q_e data were obtained by transforming the absorbance values into equivalent caramel color concentration C_{eq}. At all ammonia concentrations, the PSO model had a correlation coefficient lower than 0.80, and they were therefore not restrained.

For 25%, 12.5% and 6.25% of ammonia concentration, a lower regression coefficient was found for the PFO model fitting compared to MPnO and MOE (Table 3.5).

Table 3.5: Parameters and characteristics of experimental data fitted at different ammonia concentrations for the studied kinetic models (temperature at 25 °C).

		Conc. NH_3 (wt%)						
		25	**12.5**	**6.25**	**3.125**	**1.25**	**0.25**	**0.125**
PFO (red)	k_1	2.35	1.96	2.35	2.55	3.43	4.77	6.90
	$\sigma(k_1)$	±0.07	±0.05	±0.06	±0.03	±0.05	±0.07	±0.08
	R^2	0.85	0.86	0.84	0.98	0.96	0.95	0.95
MPnO (green)	n	2.44	1.96	1.80	1.34	1.41	1.6	1.8
	σ(n)	±0.09	±0.09	±0.03	±0.05	±0.08	±0.1	±0.2
	k’	0.44	0.59	0.75	1.55	1.87	2.1	2.7
	σ(k’)	±0.03	±0.05	±0.01	±0.10	±0.09	±0.2	±0.3
	R^2	0.98	0.96	0.95	0.98	0.96	0.95	0.95
MOE (blue)	k_1	0.59	0.61	0.60	1.70	2.3	3.0	4.2
	$\sigma(k_1)$	±0.05	±0.04	±0.03	±0.08	±0.2	±0.2	±0.3
	k_2	21	17	21	19	32	62	159
	$\sigma(k_2)$	±1	±2	±2	±1	±2	±5	±17
	R^2	0.97	0.98	0.99	0.98	0.96	0.96	0.95

Notes: Conc. = NH_3 concentration in wt%

However, the PFO model fits the data for all lower ammonia concentrations quite well; MPnO and MOE models fit the data for all ammonia concentrations at 25 °C very well. In all examined models, the rate coefficient increased with a decreasing ammonia concentration, which was in accordance with the kinetic results (Figure 3.8). The lower the concentration of ammonia, the faster the equilibrium absorption value is reached. The desorption velocity increases as the ammonia concentration decreases. According to Tables 3.4 and 3.5, the ammonia concentration in the range of 25% down to 6.25% affects the reaction parameters, but does not affect the equilibrium absorption value reached.

Effect of temperature

For determining the effect of temperature, three different temperatures were explored: 10, 25 and 40 °C. Three-point-two grams of GAC-5 and 20 mL of a 6.25% ammonia solution were loaded in the kinetic set-up (Figure 2.3).

For each temperature, five independent experiments were performed: the absorption value was recorded at 634 nm every 30 s.

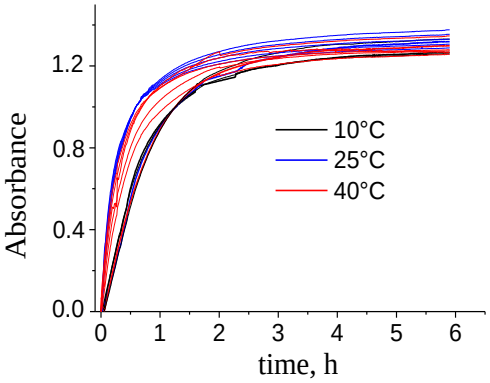

Figure 3.11: Plots of the experimental kinetic data for different temperatures (GAC-Top; 3.2 g/20 mL of a 6.25% ammonia solution).

Figure 3.11displays the obtained plots for the experimental kinetic data at different temperatures. Only some minor differences in the plots can be noticed. The equilibrium absorbance values reached are very similar.

Table 3.6 presents the results of the statistical comparison between the final absorption values reached at equilibrium for each temperature. There are no statistical differences between 10, 25 and 40 °C.

Table 3.6: Statistical comparison of the equilibrium absorbance value reached for each temperature.

Temperature (°C)	$\overline{A^*}$	$\sigma(A^*)$
10	1.294	0.10
25	1.332	0.10
40	1.285	0.09

Method: 95.0 percent LSD.

It can thus be concluded that temperature does not affect the final absorbance value at equilibrium in the range of 10–40 °C.

However, in terms of reaction rate, 25 °C seems to be the most optimal temperature. Further on, the recorded spectra of the different ES (not shown) at the different temperatures are again comparable with each other, as found in Figs 3.7 and 3.9.

Figs.3.12a and b (and 3.10 b) display the experimental and fitted kinetic data at different temperatures for a 6.25% ammonia solution. At 25 °C, the lowest correlation coefficient was for the PFO model (Table 3.5, Figure 3.10 b).

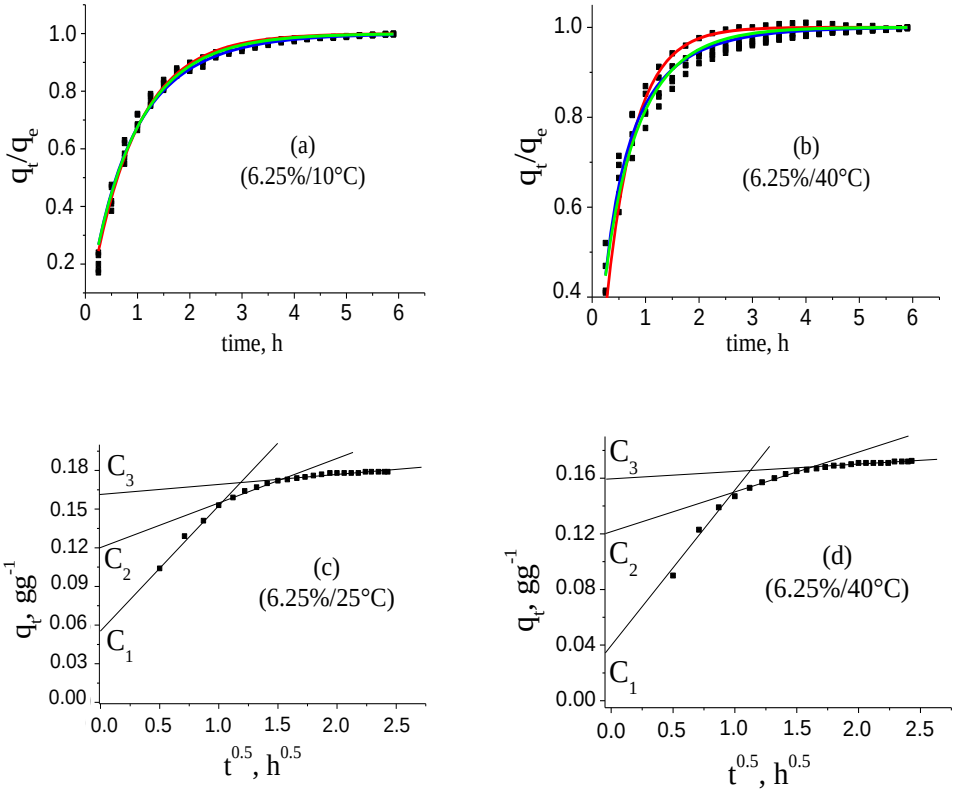

Figure 3.12: (a,b) Experimental and fitted kinetics data at two different temperatures (ammonia concentration 6.25%); (c,d) q_t vs. $\sqrt{t}$ at two different temperatures (6.25% of ammonia concentration), C_1, C_2 and C_3 are the boundary layer thickness (g/g), respectively, the larger the greater the effect.

MPnO and MOE models present satisfactory goodness of fit for all temperature ranges. For the 10 °C kinetic study, all of the other models fit the data equally well. At 25 °C, the MOE model fits the data better than the MPnO model. At 40 °C, again, all models were comparable, but MOE is superior towards MPnO. PFO has the lowest correlation coefficient. The temperature affects the reaction rate constant, but does not affect the equilibrium absorbance value.

At 25 °C, the rate constant is different from the other temperatures for all of the explored kinetics models.The effect of temperature on the behavior of the rate constant value is a typical feature of heterogeneous reactions controlled by the desorption velocity of the reactant from the solid surface [151–153]. It can be noticed from Table 3.7 that at 25 °C for all kinetic models compared to the 10 °C and 40 °C experiments, the rate constants clearly drastically change.

Table 3.7: Parameters and characteristics of experimental data fitted at different temperatures for the studied kinetics models (6.25 % ammonia concentration).

		Temperature (°C)		
		10	**25**	**40**
PFO (red)	k_1	1.13	2.35	1.85
	$\sigma(k_1)$	±0.01	±0.06	±0.04
	R^2	0.99	0.84	0.93
MPnO (green)	n	1.11	1.80	1.42
	σ(n)	±0.03	±0.03	±0.08
	k’	0.93	0.75	1.0
	σ(k’)	±0.07	±0.16	±0.1
	R^2	0.99	0.95	0.96
MOE (blue)	k_1	0.88	0.60	0.96
	$\sigma(k_1)$	±0.04	±0.03	±0.07
	k_2	2.5	20.6	2.2
	$\sigma(k_2)$	±0.2	±2.01	±0.2
	R^2	0.99	0.99	0.97

For the PFO model k_1 maximize at 25°C, although having the lowest correlation coefficient at this temperature. For the MPnO model a same trend was noticed, a maximal n-value and a corresponding minimal k’ value at 25°C, with a better correlation value. For the MOE model, $k_1$minimize at 25°C with a great maximal k_2 value and the highest correlation coefficient. Nevertheless, the above formulated features cannot explain these changes as a function of temperature, indicating a more complex desorption mechanism. The study of the kinetics in the colorimetric method, as well as the compounds involved in the reaction can be very interesting for addressing a strategy of the GAC regeneration process in rum production.

A pretreatment using ammonia solution as the extraction solvent prior to thermal regeneration could be an attractive procedure to reduce the energy consumption in the GAC regeneration. The ammonia as a solvent can be easily recovered and reused due to its high volatility and solubility in water.

Beyond the practical use of the colorimetric method for determining the exhaustion level of GAC, this method can be potentially applied for the recycling of GAC in rum production. For all considered temperatures and certainly for the 10 °C experimental conditions, no acceptable data fitting according to the intra-particle diffusion model can be proposed. For the 25 °C and 40 °C data, a fitting can be proposed for the desorption points at the start of the process and at the end of the desorption process (Table 3.8, Figs. 3.12 c and d).

Table 3.8: Results of linear fittings for the q_t vs. $\sqrt{t}$ curves (6.25% ammonia concentration).

T (°C)	k_1	C_1	R^2	k_2	C_2	R^2	k_3	C_3	R^2
25	0.097	0.057	0.99	0.03	0.12	0.97	0.008	0.16	0.96
40	0.115	0.036	0.96	0.03	0.12	0.97	0.007	0.16	0.94

Notes: k_1,k_2,k_3 (intra particle diffusion rate constants), C_1, C_2, C_3 (boundary layer thickness (g/g)).

The results indicated that, as formulated previously, a complex desorption mechanism of the colored compound(s) even in competition with other adsorbed molecules must be proposed, which is clearly temperature dependent.

Effect of temperature and vessel size on the ammonia concentration in the liquid phase

Ammonia is a volatile compound and thus in equilibrium with its partial pressure in the gas phase. To that effect, a hermetic capping of the experimental vessel is needed in order to avoid the volatilization of ammonia during the experiment and consequently a reduction of its concentration in the liquid phase, which could affect the final results.

However, it was found that the increment of the temperature resulted in a statistical minor effect. Additionally, the free space in the experimental set-up is very small, closed and constant. Therefore, the amount of loss in ammonia can be neglected. Furthermore, results in Table 3.6 indicate the very small effect on the absorption value recorded, when changing drastically the ammonia concentration in the range of 25%–6.25%.

3.1.3- Experimental conditions for the final proposal of the colorimetric method and correlation with other methods.

The same procedure as described in section 3.1.1can be applied for the other GAC samples (0.2-Bottom) i.e.:

Three-point-two gram (3.2 g) of GAC (previously prepared according to §2.2.1) is added to 20 mL of 6.25% ammonia solution, gently stirred at 50 rpm in batch conditions at 25 °C for 6 h in a 100-mL capped glass vessel. The brownish GAC extracted solution is filtered using a 0.45 µm PFTE filter and the absorbance is measured using a 1 cm quartz cuvette at 634 nm.

Fig. 3.13 presents a picture of the brownish color profile observed in the extracted solution for the different GAC layers in the target rum filter according to the colorimetric method. In concordance with the presented plots (iodine number, contact pH and elemental analysis), the samples are ordered from the left to the right beginning from the GAC-Top (darker).

Fig. 3.13: Color profile of extracted solutions of the different GAC samples in the rum filter. The color intensity is decreasing from the top (left) to the rum filter's bottom (right).

A quick inspection of Fig. 3.13 is enough to notice evident differences in the color intensities between the samples. The three last samples present an abrupt change of color. However, the inflection point at GAC-1.3 is also noticeable by direct inspection (see Figs 3.5 and Fig. S1 as later Figs. 3.15, 3.26, 3.29, 3.33 and 3.37). The color in the GAC-1.3 extract (solution at the second right position of Fig. 3.13) is slightly more intense than GAC-1 and GAC-Bottom.

The possibility to detect this behavior in the GAC layers using the colorimetric technique gives an evidence of sensitivity, representability, reliability and accuracy of the proposed method. For studying the rum filtration process it can directly be applied to detect the exhaustion degree of the used GAC.

Table 3.9 presents the mean absorbance values ($\overline{A^*}$) for the extracted solution of the GAC samples.Five experiments were performed, and the statistical parameters were determined. According to the equilibrium absorbance (Table 3.9), the samples can be ordered in terms of exhaustion degree as follows:

GAC-Top > GAC-0.2 > GAC-0.4 > GAC-0.6 > GAC-0.8 > GAC-1.3≥ GAC-1.0≥ GAC-Bottom

This order is consistent with the iodine number, contact pH, and hydrogen content. The darker the obtained extracted solution was, the more exhausted the GAC.

Table 3.9: Absorbance values at 634 nm for the extracted solution of the GAC samples.

GAC-Layer	**Top (0)**	**0.2**	**0.4**	**0.6**	**0.8**	**1.0**	**1.3**	**Bottom (1.5)**
$\overline{A^*}$	1.2	1.0	0.87	0.28	0.061	0.012	0.015	0.011
$\sigma(\overline{A^*})$	0.1	0.1	0.08	0.03	0.005	0.002	0.001	0.001

$\overline{A^*}$: mean of equilibrium absorbance values (in absorbance units) for five independent experiments and $\sigma(\overline{A^*})$: standard deviation.

Figure 3.14 shows the relationship between the equilibrium absorbance values and the contact pH. The shape of the curve suggests a non-linear fitting; the parameters could be fitted using models as power or exponential.

However, according to other reports [151–153], it is demonstrated that the fractional coverage θ of the GAC can be given by:

$$\theta = a \cdot C_i^m \quad (3.3)$$

a, m are specific constants, C_i is the concentration of colored compound i.

This has basically the form of the Freundlich isotherm, which often provides a good fit to adsorption/desorption data, especially in liquids [153].

Considering that the absorbance value is linear correlated with C_A, θ can be expressed as:

$$\theta = \beta \cdot (A^*)^m \quad (3.4)$$

β is a proportional factor.

Applying the logarithm in both terms:

$$\mathrm{Ln}\,\theta = \mathrm{Ln}\,\beta + m \cdot \mathrm{Ln}\,A^{*} \tag{3.5}$$

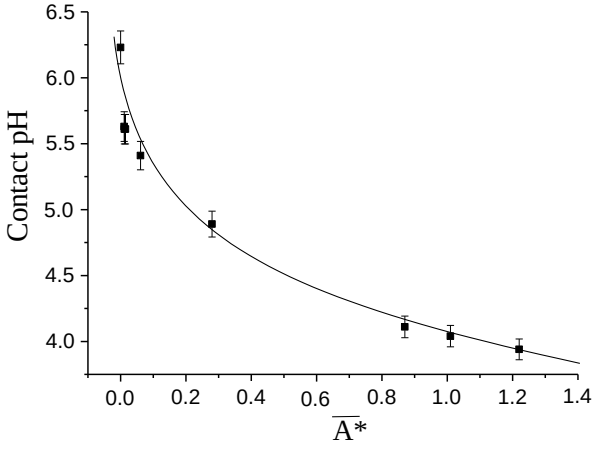

Figure 3.14: Relationship between the equilibrium absorbance values and the contact pH.

As the color increment in aged Cuban rum has a linear correlation with the ageing time [78] and the total acidity due to the presence of non-volatile acids contributed by the oak wood during ageing process [78,104], the contact pH can be considered as a direct function of the concentration of colored compounds adsorbed onto GAC and taking GAC-1 (virgin) as the "model GAC" with the maximum pH value free of adsorbed color compounds , then for the other used samples (GAC-0.2–Bottom) the fractional coverage (θ) can be expressed as:

$$\theta = 1 - \frac{\text{Contact pH}_i}{\text{Contact pH}_\text{m}} \tag{3.6}$$

With Contact pH_i: contact pH of the used GAC "*i*"; and $\text{Contact pH}_\text{m}$: contact pH of the virgin GAC, being 6.23 (Table 3.2).

According to the obtained mean of the contact pH for the samples (Table 3.2), the fractional coverage can be calculated as:

$$\theta = 1 - \frac{\text{Contact pH}_i}{6.23} \tag{3.7}$$

Table 3.10 presents the values of$\mathrm{Ln}\,\theta$, $\overline{A^{*}}$ and $\mathrm{Ln}\,\overline{A^{*}}$ for each example. Applying double logarithm arrangement, a quite good linear correlation (R^2 = 0.997) was found for $\mathrm{Ln}\,\theta$ vs. $\mathrm{Ln}\,A^{*}$.

Table 3.10: parameters for the fitting process.

Samples	$\boldsymbol{\theta}$	$\mathbf{Ln}\boldsymbol{\theta}$	$\overline{\boldsymbol{A^*}}$	$\mathbf{Ln}\overline{\boldsymbol{A^*}}$
GAC-Top	0.368	-1.00	1.22	0.20
GAC-0.2	0.352	-1.05	1.01	0.01
GAC-0.4	0.340	-1.08	0.87	-0.14
GAC-0.6	0.215	-1.54	0.28	-1.28
GAC-0.8	0.132	-2.03	0.061	-2.80
GAC-1.0	0.100	-2.31	0.012	-4.20
GAC-1.3	0.100	-2.31	0.015	-4.42
GAC-Bottom	0.096	-2.34	0.011	-4.51
GAC-Virgin	0.00	-	0.00	-

Note: θ = fractional coverage, $\overline{A^*}$: mean of equilibrium absorbance values (in absorbance units) for five independent experiments.

$\mathrm{Ln}\,\theta = (-1.08) + 0.29 \cdot \mathrm{Ln}\,A^*$

$\mathrm{Ln}\,\beta: -1.08 \pm 0.04$

$\mathrm{m}: 0.29 \pm 0.02$

Finally, the equation that correlates the fractional coverage of colored compounds and the equilibrium absorbance value in the colorimetric method can be expressed as:

$$\theta = 0.34 \cdot A^{*\,0.29} \qquad (0 \le A^* \le 2) \qquad (3.8)$$

The absorbance value at equilibrium can thus be used to determine θ and can be applied to determine and quantify the exhaustion level of GAC used in the rum production. This means that for GAC-Bottom, around 10% of the porous space or sites are occupied by colored compounds and that in the case of the GAC-Top, these compounds represent about 40 % of the total occupied sites.

In other words, using the colorimetric approach, the exhaustion can be quantified. Taking into account that also other compounds are adsorbed and a completely exhausted GAC can be determined using colorimetric measurement, the results can be used to define the end-of-life state of a GAC in the rum production process.

Fig.3.15 displays the profile of the GAC exhaustion degree at different layer positions in the rum filter based on the colorimetric method taking the fractional coverage as parameter. In the GAC layers near to the top (in the range Top-0.4m) a linear decrease of the color intensity is observed.

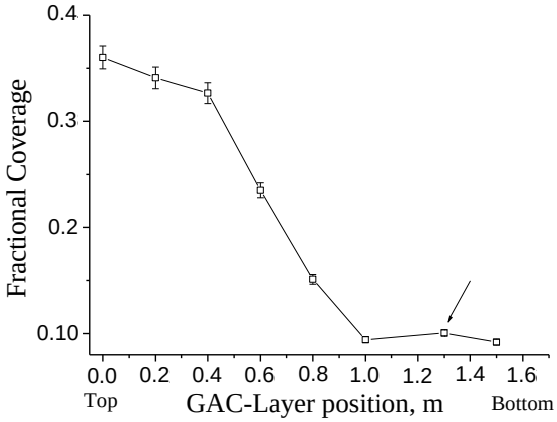

Fig. 3.15: Profile of the degree of GAC exhaustion at different locations in the rum filter based on the colorimetric method.

After GAC-0.4, an abrupt decrease of color intensity is found. The last three GAC layers near to the filter bottom have the lowest color intensity and almost the same fractional coverage value. The inflexion point at GAC-1.3 (arrow) is also observed as in Fig. 3.5.

Fig.3.16 presents the TD-GC/MS chromatograms of the different GAC samples in the rum filter, systematically ordered from the Top to the bottom. As complement, Fig.3.17 presents the same TD-GC/MS chromatograms also ordered from the Top to the bottom to properly appreciate in a comparative way the sequential adsorption process of some compounds in rum production manufacturing .The figure Fig.3.17 was divided in two parts: (2-11 min and 11-19 min). Different thermal desorption experiments were conducted at 300°C, 450°C and 500°C based on the obtained TGA experiments. At 300°C it was found that this temperature was too low to obtain comparable chromatograms. At 500°C, the original adsorbed compounds from the rum production process already show a thermal decomposition trend, making a proper comparison of the original adsorbed compounds in the different GAC samples not possible. It was found that at 450°C very reliable chromatograms were recorded for all GAC samples. In general, for all the studied GAC samples the same predominant family of compounds were found but with different relative abundance.

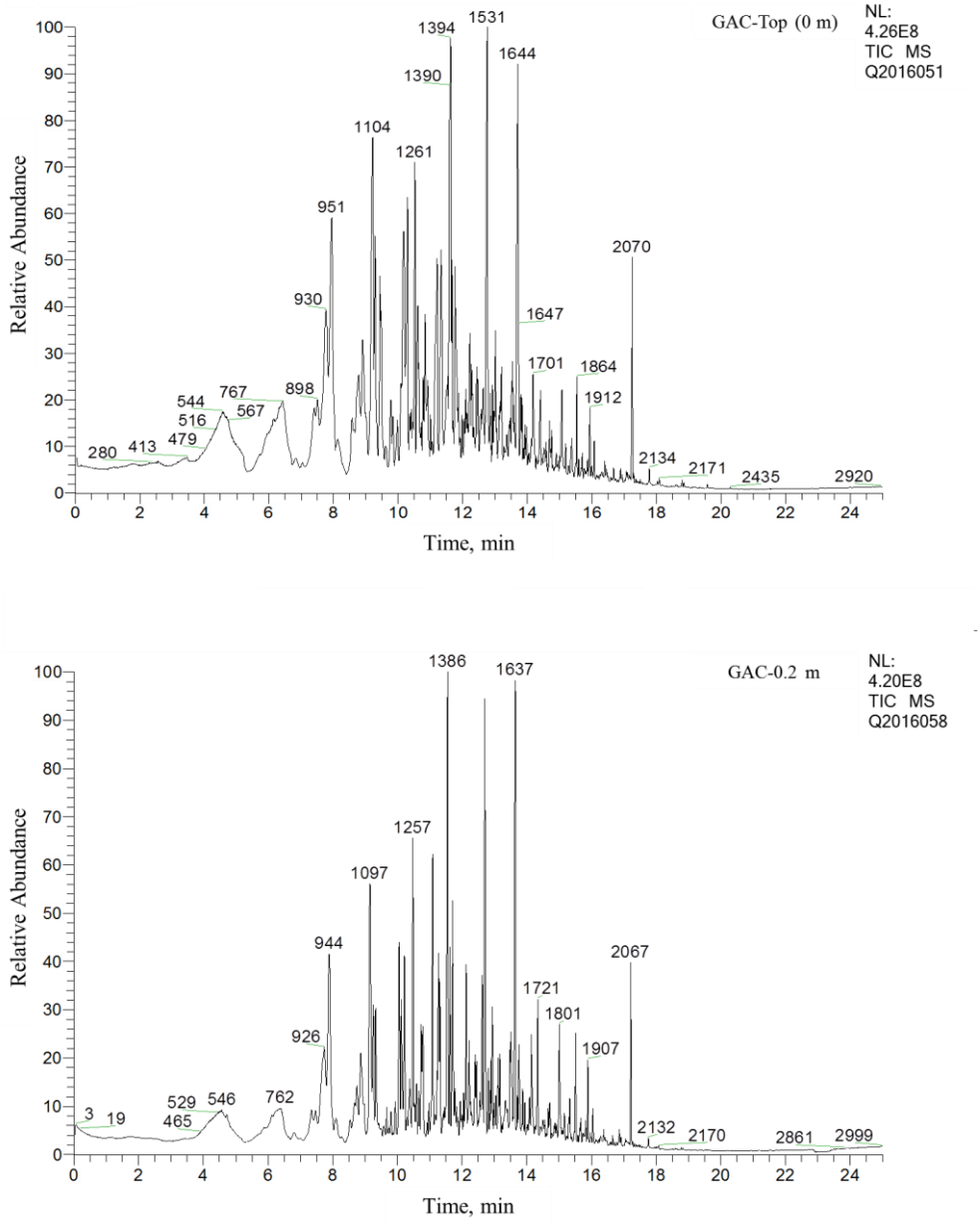

Fig. 3.16: TD-GC/MS chromatograms of the different GAC samples in the rum filter: (1 of 4).

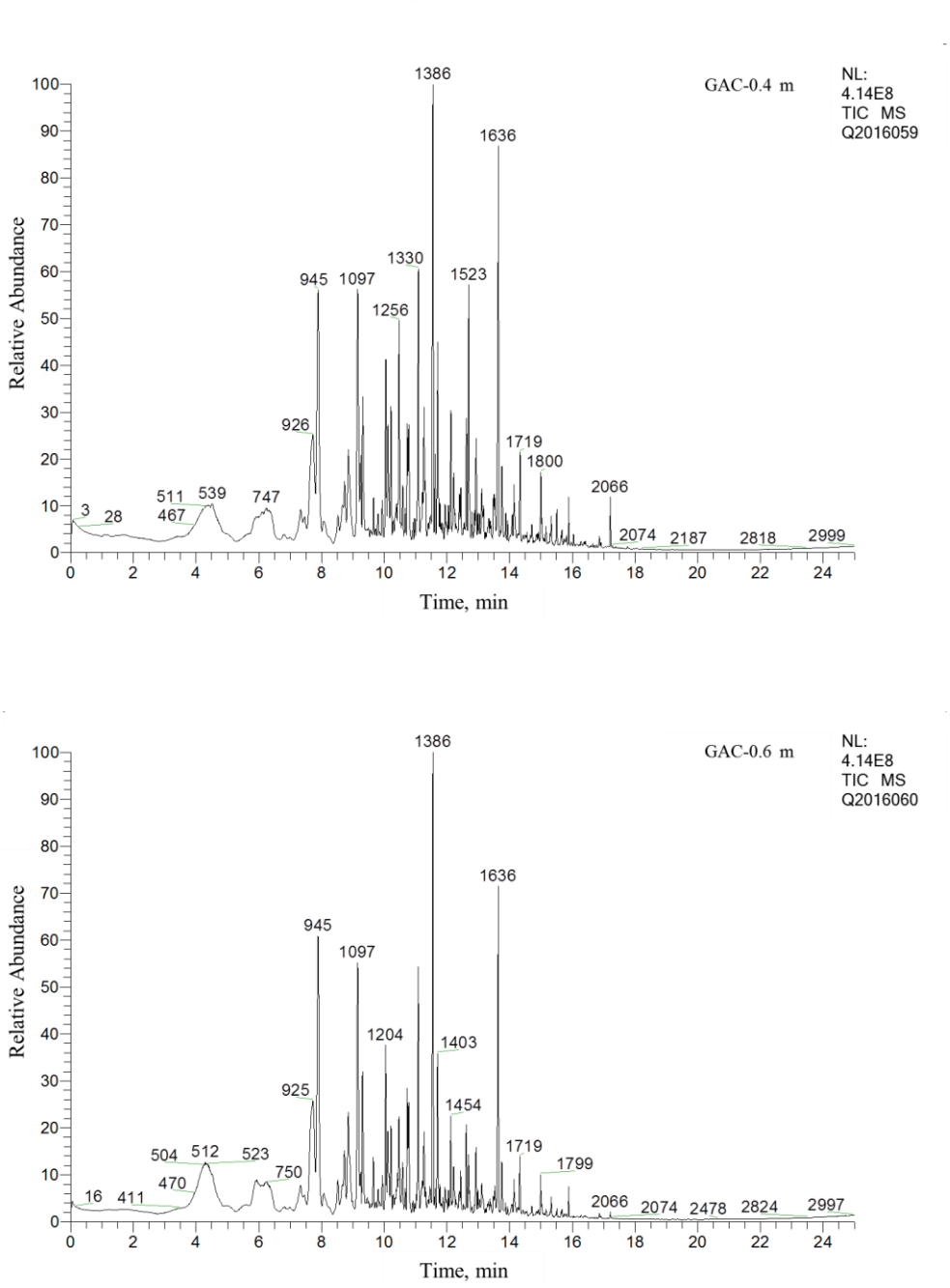

Fig. 3.16: TD-GC/MS chromatograms of the different GAC samples in the rum filter:(2 of 4).

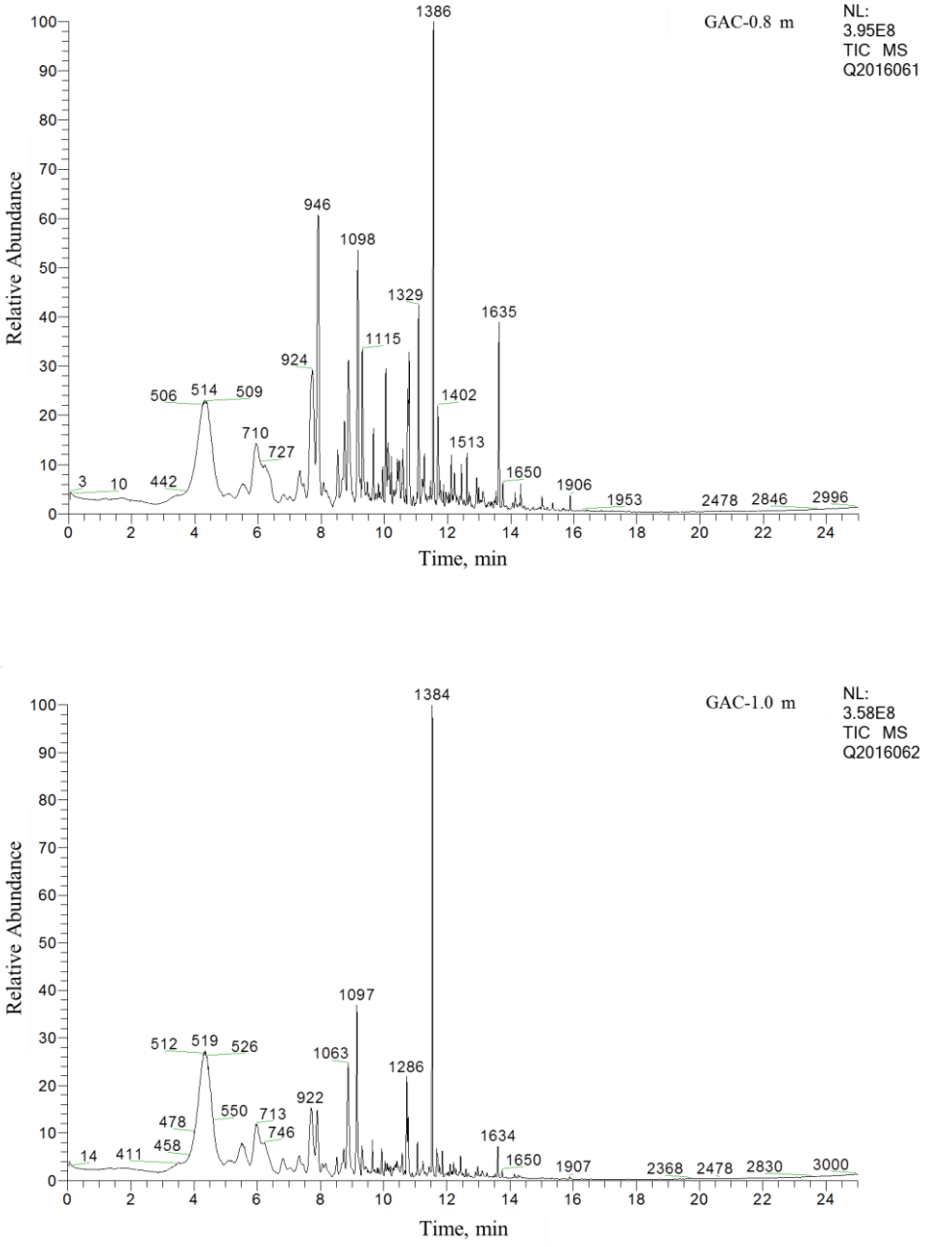

Fig. 3.16: TD-GC/MS chromatograms of the different GAC samples in the rum filter:(3 of 4).

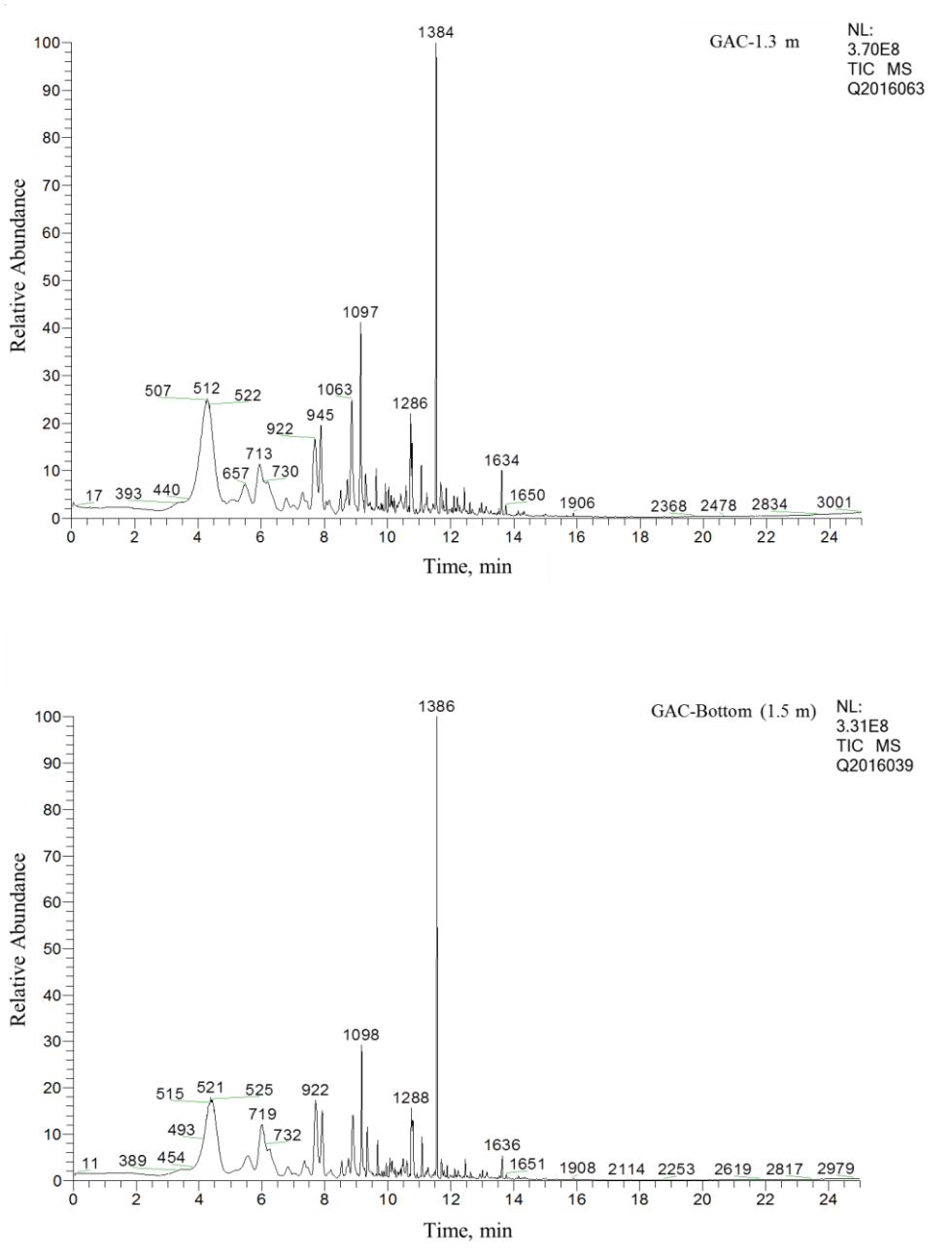

Fig. 3.16: TD-GC/MS chromatograms of the different GAC samples in the rum filter: (4 of 4).

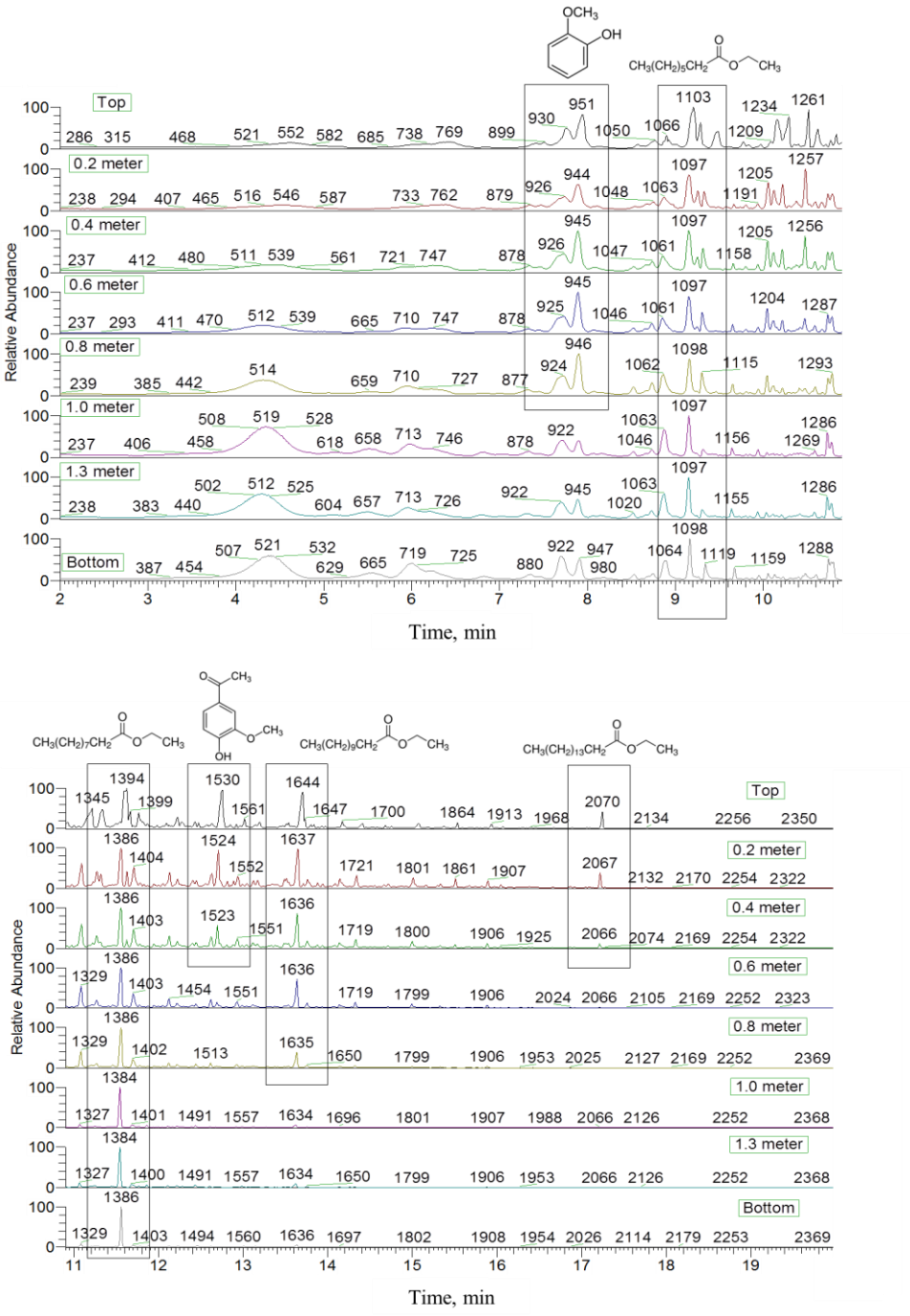

Fig. 3.17: TD-GC/MS chromatograms of the different GAC samples in the rum filter (sequential).

Table 3.11 presents the predominant compounds found in all the GAC layers in the rum filter. The tabulated compounds (Table 3.11) have been found in aged Cuban rums and were reported in detail by Pino et al. and Maarse in [79-81]. The significant role of fatty esters, phenolic compounds and vainilloids on the improvement of the aroma and bouquet not only in aged rums but also in other aged distilled beverages as whiskies has been widely discussed by different authors [78-81].

Table 3.11: Predominant compounds detected in the rum filter GAC by TD-GC/MS analysis

Compound	**Family**	**(m/z)**
Ethyl decanoate	Fatty ester	(1384-1394)
Ethyl hexadecanoate	Fatty ester	(2066-2070)
Ethyl dodecanoate	Fatty ester	(1635-1644)
Ethyl octanoate	Fatty ester	(1097-1104)
2-Methoxyphenol (Guaiacol)	Phenolics	(922-951)
3-Methoxy-4-hydroxy acetophenone (Acetovanillone)	Vainilloids	(1523-1531)

In Cuban rum production, the GAC acts as a sensorial modulator of certain "key components" that define the sensorial characteristics in rums; the proper balance of these compounds is crucial to obtain the desirable sensorial typical characteristics in the final product. The rum filtration process is designed to let just pass the correct amounts of each compound in a delicate balance, where the contribution of each compound is optimal to reach the proper sensorial characteristics. Therefore, the same compound can usually be found before and after filtering with GAC but at different concentration levels.

The GAC-Top shows higher concentration of the main adsorbed compounds. The evolution of the sum of the peak areas is decreasing from the top to the bottom reaching the lowest value for GAC-bottom. The clustered behavior between GAC-1, 1.3 and bottom is also clearly noticeable by direct comparing chromatograms in Fig. 3.16. Also, the special exhaustion degree of GAC-1.3 can be observed, an increment in peak area distribution of dedicated compounds can be detected.

As can be clearly observed in Fig 3.17, ethyl decanoate is dominantly present in all the GAC layers and in enhanced concentration after GAC-0.8. The vainilloids are present in the top GAC layers.

However, their relative fraction drops abruptly after GAC-0.4. A similar behavior is observed for the phenolics, although present in all the GAC layers, their relative normalized peak areas decays from 60% in the GAC-Top to about 20% in GAC-1, but being rather constant at this value till the GAC-Bottom sample.

In general the family of esters is decreasing in relative abundancy from the top to the bottom.

However, their decay can be associated to the molecular weight change. The heavier members of this family decay faster in relative abundance than the light esters. For instance ethyl hexadecanoate is present in GAC-Top around 50% but is nearly undetectable after GAC-0.4. The presented results suggest that the involved mechanisms in rum "filtration" and its relationship with the sensorial features of rum are rather complex and must be further studied.

Apart of the predominant compounds discussed, Fig 3.18 depicts the profile of the main compounds adsorbed in the filter bed. Fatty acids decay from the top to the filter's bottom, following a similar pattern of a series of fatty esters. However for ethyl octanoate and ethyl decanoate after a steep decay as low increase as a function of GAC-layer position can be noticed.

The phenolic compounds have different behavior; in the case of 2-methoxy-4-propyl-phenol a systematic decadent tendency is observed, the rest presents a concentration overshoot in GAC layers around 0.2 and 0.4 m. This overshoot is a typical feature of a multi-solute adsorbate system, each MTZ travel with different velocities through the adsorbent bed.

This is a result of the competition for GAC pores and adsorption sites and subsequent displacement for the adsorbates during the adsorption process (previously presented in §1.9.5/ Fig.1.14).

According to Fig 3.18, 2-methoxy-4-propyl-phenol seems to be stronger adsorbed than the rest displacing them to other GAC layers. In addition, dianhydro glucopyranose was only found in the GAC-Top; probably as rest of a heavier pyrolyzed carbohydrates coming from the oak wood during ageing process. Carbohydrates are essentially non-volatile compounds at low concentration and undetectable by TD-GC/MS analysis.

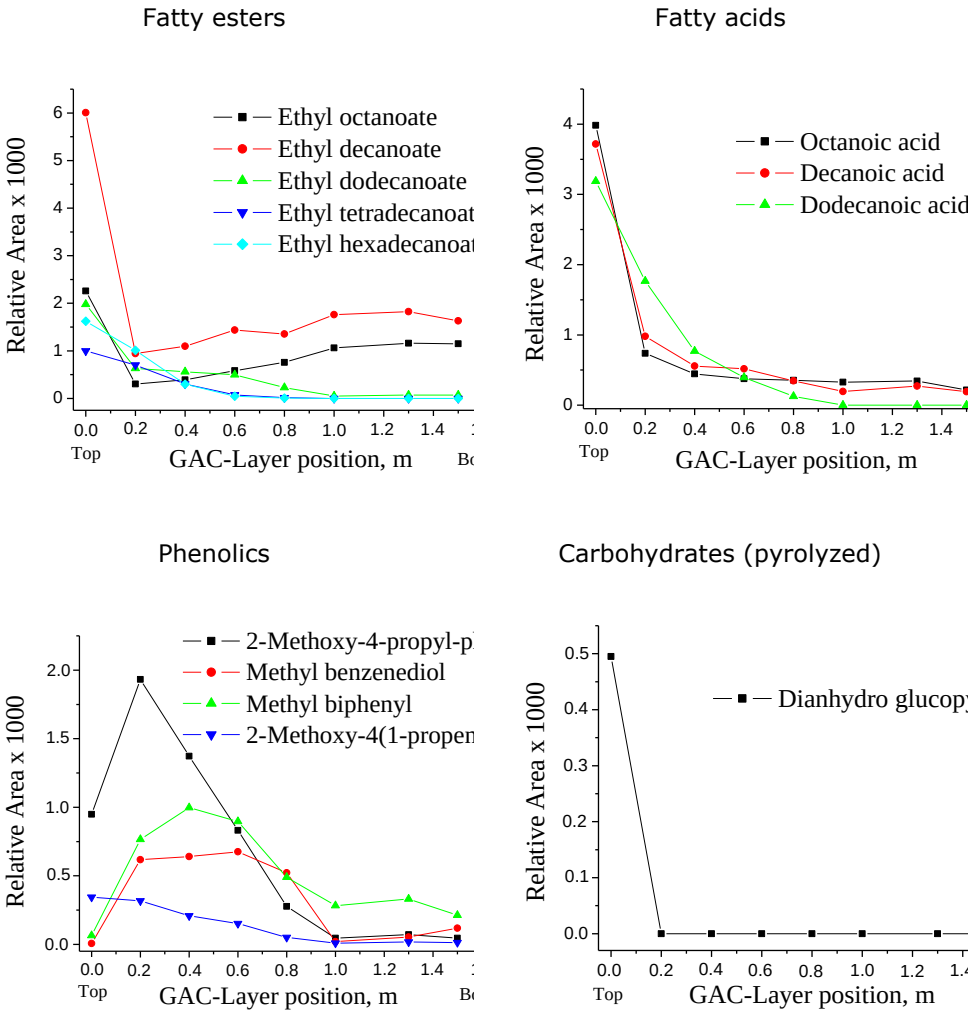

Fig. 3.18: Profile of main adsorbed compounds through the filter bed detected by TD-GC/MS.

In the case of GAC-Top, its concentration is high enough to produce pyrolyzed residues that can be volatilized and thus detected. The presence of these carbohydrates suggests that regeneration of the exhausted GAC must be conducted at high temperature to remove possible pyrolyzed residues which could accumulate in GAC pores leading to a narrowing process and consequently a poor regeneration degree (discussed later).The clustered behavior of the three last GAC layers is also observed in Fig. 3.18 for the phenolics.

3.1.4-Compounds involved in the reaction between ammonia and exhausted GAC

In view of the determination of the compound(s) involved in the colorimetric reaction and addressing to a possible regeneration strategy of the exhausted GAC and based on the TGA, colorimetry and CHNS-O elemental analysis results of the different GAC samples according their layer position in the rum filter, GAC-Top is treated with ammonia. GAC-Top and ammonia treated GAC-Top are compared with each other using TGA and TD-GC/MS.

Fig. 3.19 displays the TG and DTG curves in N_2 atmosphere for GAC-Top before and after a treatment with a 6.25% ammonia solution. Differences in both TG and DTG profiles can be observed.

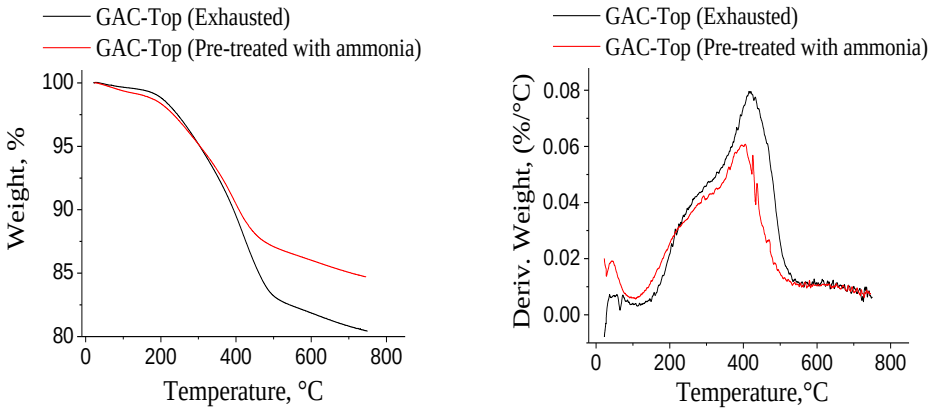

(a) (b)

Fig. 3.19: TG (a) and DTG (b) profiles in N_2 atmosphere for GAC-Top before and after been treated with ammonia solution.

Comparing the TG curves in Fig. 3.19 (a), the decrease in mass loss of ammonia treated GAC-Top is around 5% less than untreated GAC-Top. In Fig. 3.19(b) DTG curves of GACs are also different, a decrease in the maximal desorption rate peak is found, clearly indicating the removal of adsorbed organic compounds by the ammonia solution. A combined ammonia and thermal treatment in absence of oxygen could point to a possible GAC recycling strategy. Fig. 3.20 displays the TD-GC/MS chromatograms of GAC-Top (most exhausted) before and after the treatment with ammonia solution of 6.25%.

The chromatographic signals have comparable values but in the case of ammonia treated GAC they are slightly lower in relative abundance, thus indicating a smaller concentration of adsorbed organic compounds.

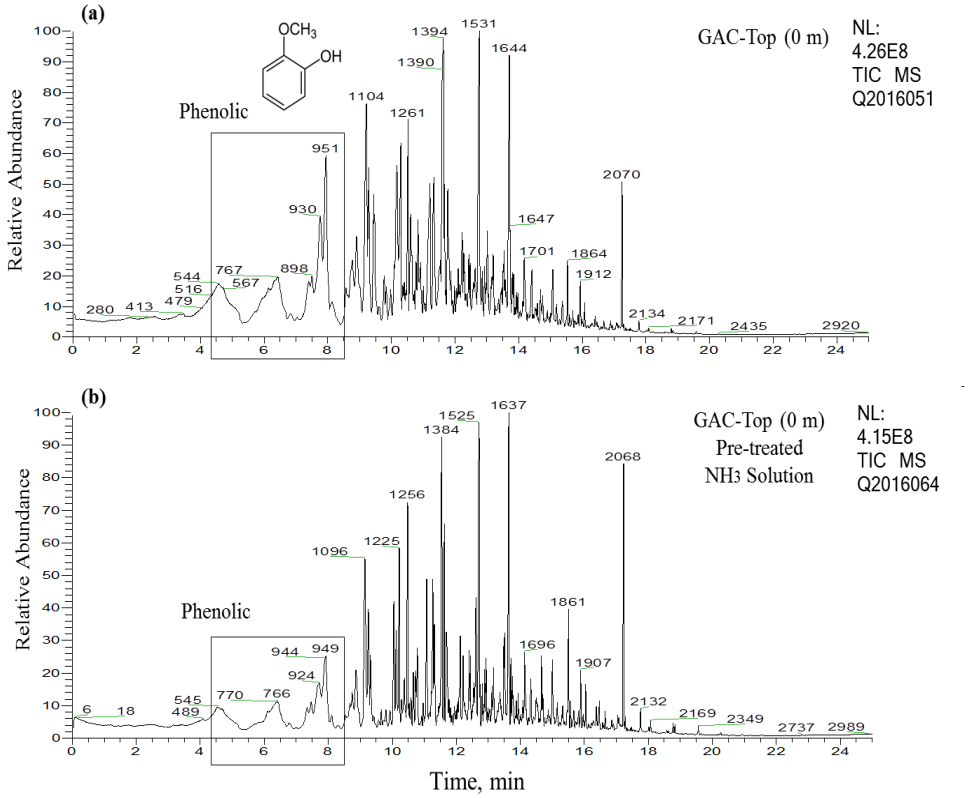

Fig 3.20: TD-GC/MS chromatograms for GAC-Top before (a) and after (b) to be treated with ammonia solution.

The square demarcation zone in the chromatograms indicates the most significant reduction of compounds after the ammonia treatment, and refers to phenolic compounds. The observed reduction of relative abundance was between 27% and 60%. However, no significant changes were detected for the other compounds, being the same families of predominant esters.

The differences detected in the chromatograms suggest the extraction of the phenolic compounds by ammonia. As tannins are basically polyphenols, these results are in accordance with results reported by other authors in the ammonia fuming reaction with oak wood [143-147].

According to the results presented by Pino et al [78-80], phenolic compounds have not been detected in fresh distilled rums. However, they have been reported in several distilled beverages after the ageing process [78-86,88, 90-102,104]. Based on the TD-GC/MS results, the involvement of oak wood extractable compounds adsorbed on the GAC during rum production and extracted by the ammonia solution is confirmed.

3.2-Characterization of GAC based on acoustic emission analysis method

The acoustic emission analysis is a new method for the characterization of granular activated carbons based on flooding a GAC sample with water. It results in a sound emission by bubbles formation through the bulk water and exploding at the liquid surface. The GAC sound is produced by the bubbles escaping from the GAC cracks and pores when water molecules occupy the air filled voids inside of the GAC by displacing the present air. The amount of produced bubbles is closely related to the porosity of the GAC. The bubble volume fraction and rate at which the bubbles appear by approaching the water surface influence sound parameters as frequency and signal amplitude [154-165]. The acoustic emission is produced in audible spectra and can be analyzed by a proper acoustic signal analysis technique. In the case of GAC used in the rum production process, large amounts of organic compounds with different molecular sizes adsorb, and block cracks and pores of GAC, creating an important reduction of pore volume and specific surface area. Exhausted GAC therefore result in a reduction of bubbling potential and consequently in a reduction and a change in the sound signal amplitude. The use of acoustic measurements makes it possible to determine the overall porosity but also to characterize the porous structure of GAC according to the sound patterns obtained (it will be further discussed in chapter 4).

Fig.3.21 presents a simplified bubble model of a GAC-virgin (a) and exhausted (b) GAC-Top in the rum production. The red color represents the adsorbed compounds onto GAC pores. Virgin GAC has all the pores clean and the volume of air trapped into the GAC particle is larger. When the water fills the pores, different sizes of bubbles are formed at the same time but the rate of bubble production and the tortuous characteristics of the pores connections is a favorable condition to the bubble coalescence to form bigger bubbles.

When the organic compounds from the rum production process are adsorbed (b) the pores are blocked, its volume is reduced and its interconnections are narrowed or completely sealed. In this case, the rate of formed bubbles and porous characteristics are not favorable conditions as such, nor to the coalescence process, thus generating a lower signal power. It is reasonable to accept that the porosity characteristics of carbons (a) and (b) are different and because of the compounds will modify its texture, affecting the characteristics of the formed bubbles.

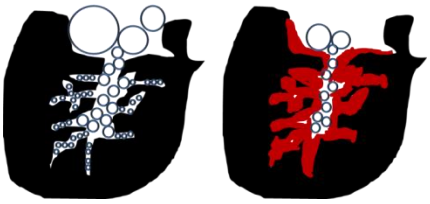

Fig.3.21 Simplified bubbling model in virgin (a) and exhausted (b) GACs. Red color represents the adsorbed organic compounds onto AC pores.

The explosion of the bubbles on the water surface appears thus randomly and chaotically, therefore they cause a great increase in pressure pulsation and a turbulent sound in a wide frequency range [166]. The higher the number of exploding bubbles at the water surface, the higher the amplitude and intensity of the recorded acoustic signal.

This behavior of GAC bubble production depends on the GAC resistance to the water intrusion in the cracks and pores to displace the air. The bigger the size of the pores and cracks, the easier water has access inside the particle resulting in a quick removal of the air in the form of bigger bubbles. The less accessible the pore, the narrow and tortuous the way to remove the air inside of the particle and the rate of bubble production decreases as well as their size.

Bubbles and its corresponding sound patterns are in general widely studied, theoretically analyzed and applied in many scientific fields[154-169].The analysis of acoustic and vibrating signals to characterize mechanical events such as pump cavitation, cavity effects in gas-jet impingement propellers and stir spot welding process has proven to be accurate and sensitive techniques [116,117,154-169]. Recorded data can be correlated with GAC properties and more specific in the determination of its exhaustion degree.

In this research the set-up presented in Fig.2.4 (§2.4.2) is applied for the characterization of GAC. The GAC acoustic signal is processed using MATLAB® following a similar way as is presented in other researches (but focused on mechanical engineering applications [116,117]) allowing the characterization of the GAC acoustic emission phenomenon and its features. In general, the propagation of sound waves in a bubbly liquid is a complex process, which involves the dynamics of the individual bubbles and their interactions. Each bubble acts as a resonator in which the gas acts as the spring and the moving mass is the liquid adjacent to the bubbles [167].Therefore, resonant components during the bubbling process appear intrinsically produced by the process itself. This feature is independent of the acoustic characteristic of the used set-up.

Due to the complexity involved in bubble acoustic and mechanical vibration modeling, a previous knowledge about signal processing, math and physics is needed to face a deep interpretation of obtained results.

3.2.1-GAC exhaustion profile in the target rum filter based on acoustic emission method

Figs.3.22 (a) and (b) show the relative amplitude power of the signal (RMS) of the acoustic signal of GAC-Top (a) and GAC-Bottom (b). Comparing both figures it is possible to see evident differences between the samples located at extreme points in the rum filter. The signal power produced by GAC-Bottom is more intense than GAC-Top. Figs.3.22 (c) and (d) present the spectrograms of the signals of GAC-Top (a) and GAC-Bottom (b). The wide range of observed frequency components is a typical feature of the bubbling process and the resonator nature of the exploding bubbles [163,167].

A typical frequency component around 1-1.5kHz and its harmonics can be observed in both samples but with different intensities (arrows in Figs.3.22(c) and (d)).

The GAC-Bottom sound, presents more intensity than GAC-Top, giving evidence of different exhaustion degree of the GAC in the rum filter. At the beginning of the sound recording process, the spectrograms shown no external interferences (noise) which is in correspondence with the noise characterization recording at empty enclosure box explained in §2.4.2.

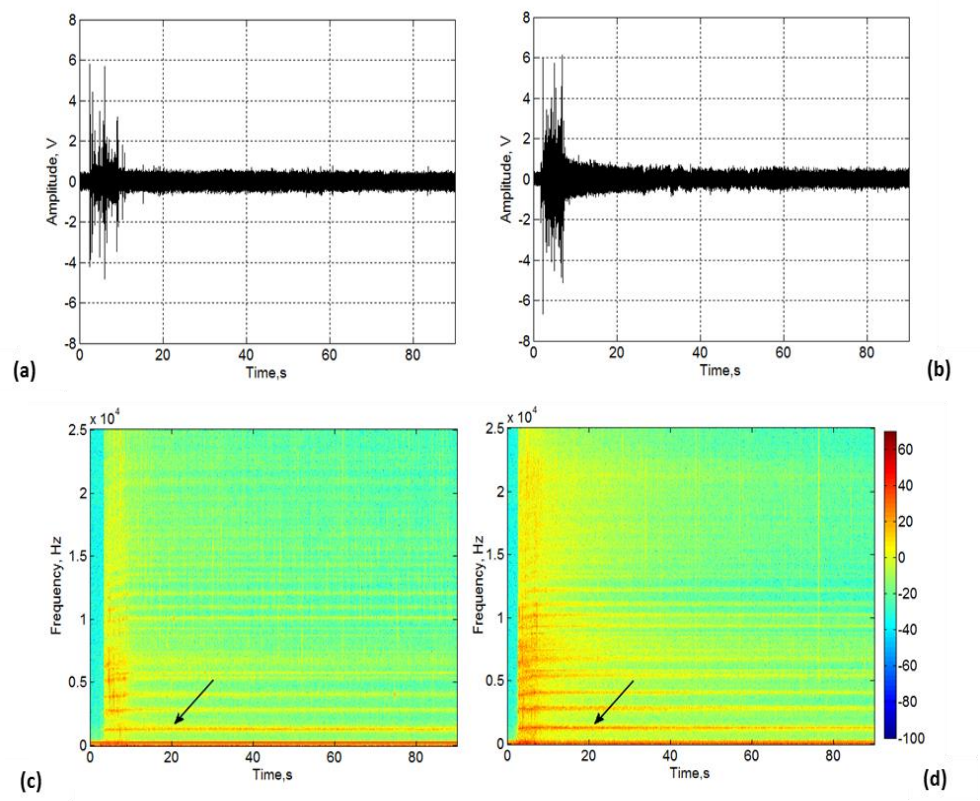

Fig.3.22: Relative amplitude power of the signal (RMS) of the GAC acoustic signal: (a) GAC-Top, (b) GAC-Bottom and spectrograms of the GAC acoustic signal: (c) GAC-Top and (d) GAC-Bottom

Fig.3.23 shows the frequency component distribution found in the signals of GAC-Top (a) and GAC-Bottom (b). A magnification of the spectral range with the peak of interest is presented in Fig.3.23: (c) GAC-Top and (d) GAC-Bottom.

Analyzing Figs.3.23 (a) and (b), two zones can be clearly defined. Zone I: (0-0.3 kHz) defined by a great number of frequency components which can be associated not only with the phenomena of GAC sound production but also to the noise interferences produced during water injection, GAC particles colliding and unwanted resonant components. Actually, Zone I is not a good range to select any frequency component because of all these interferences. Zone II (0.3-1kHz) is defined by a clear absence of frequency components.

After Zone II, an interesting feature was found: a peak in the frequency domain around 1.3 kHz and its resonant components.

There are two important aspects to select the 1.3 kHz frequency component as the frequency of interest for characterizing the exhaustion degree in GAC used in the rum production process. The component is observed in both GAC samples at extreme layers in the fixed bed filter and its amplitude is clearly different in intensity.

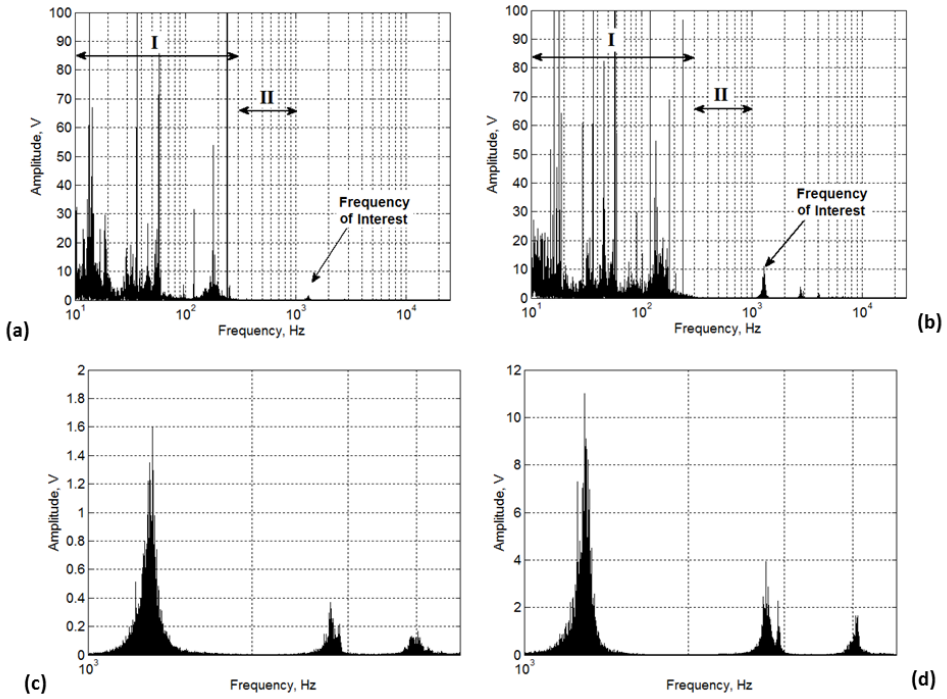

Fig.3.23: Frequency component distribution of GAC acoustic signal: (a) GAC-Top and (b) GAC-Bottom. Magnification of the frequency component distribution at the frequency of interest: (c) GAC-Top and (d) GAC-Bottom.

The amplitude value can be correlated with the GAC porous characteristics and is free of interferences. According to the obtained results, 1.3 kHz was selected as the cut-off frequency to the band-pass (**BP**) signal filtering.

Fig.3.24 displays a section of the filtered (at 1.3 kHz) signal envelopes for the GAC-Top and GAC-Bottom. Significant differences are found between the GAC in terms of the shape of the envelope curves and the signal amplitude in the time domain.

According to this, analyzing the envelope features, a characterization of the GAC can be obtained and clear differences in the GAC exhaustion degree can be observed.

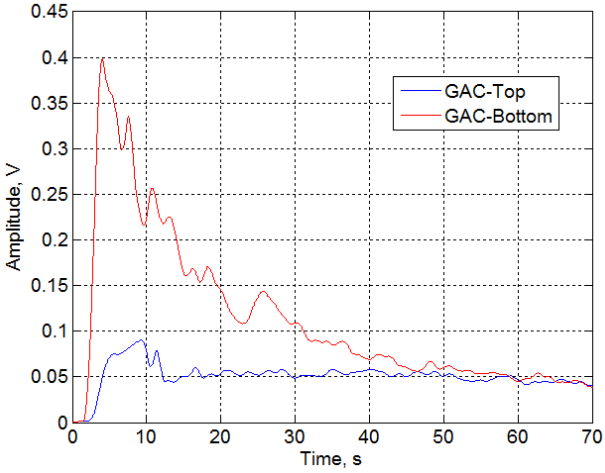

Fig.3.24: Signal envelopes of GAC-Top and GAC-Bottom after being filtered at 1.3 kHz.

The remaining GAC were analyzed following the same procedure. Fig. 3.25 presents the signal features of the GAC samples at different layers of the rum filter. Differences between samples were found in terms of amplitude of the RMS signal (Fig. 3.25(a)), signal frequency spectrum amplitude (Fig. 3.25(b)) and signal envelope (Fig. 3.25(c)) at 1.3 kHz (c).

Differences are more evident by comparing the signal amplitude and envelope. The envelope maximal peak amplitude (EMP) and the area under the signal envelope curve integral or "sound surface" (SS) at 1.3 kHz increase systematically from the top (GAC more exhausted) to the filter's bottom, giving a strong correspondence between the exhausted behavior of GAC layers and the sound amplitude in the frequency of interest.

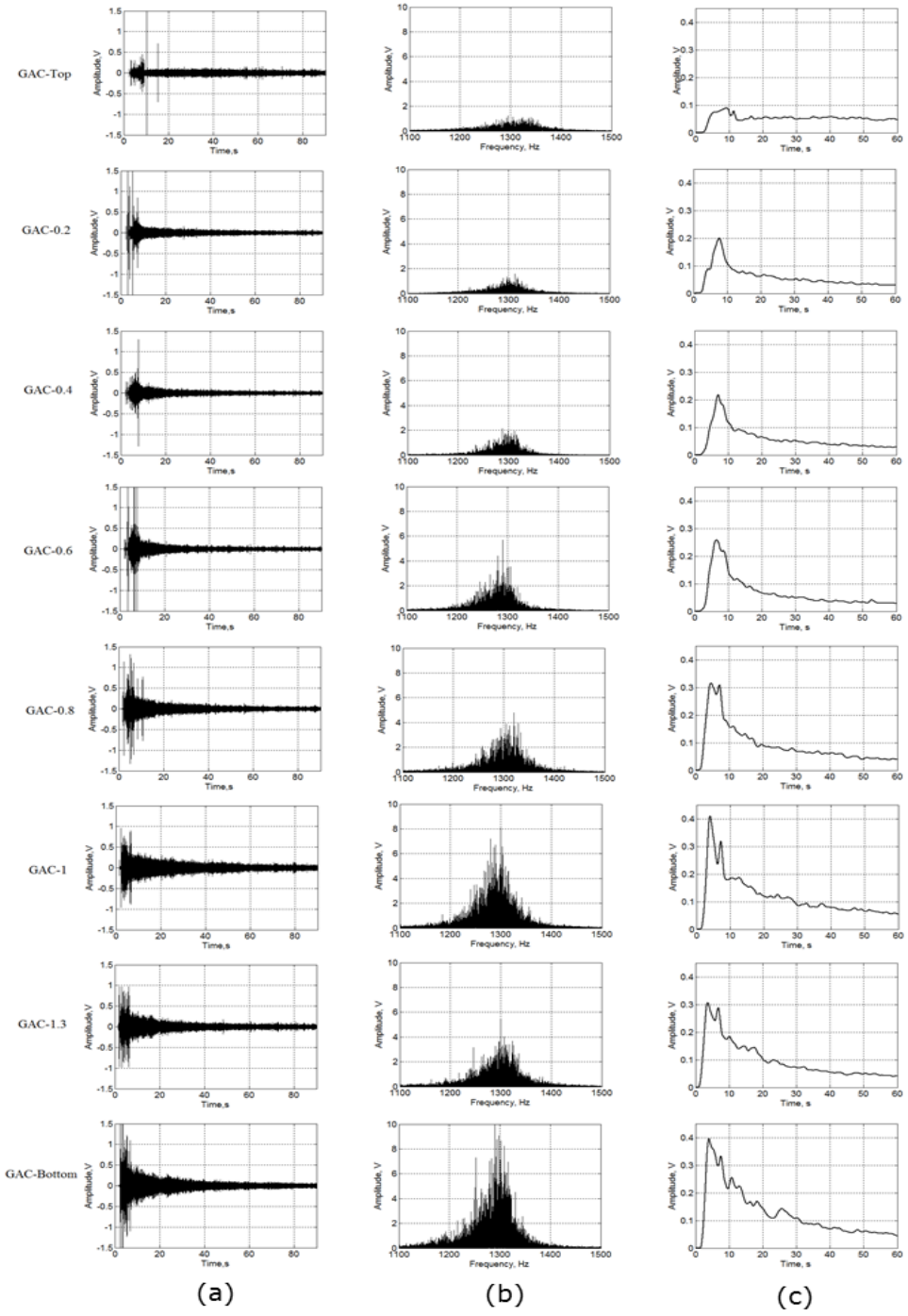

Fig. 3.25: Evolution of the acoustic emission signal generated by GAC samples at different layers in the rum filter.

Table 3.12 shows the values of the envelope maximal peak amplitude (EMP) and Sound Surface (SS) of the signal in line with the plots presented in Fig.3.25. The Multiple Comparison Method was applied to determine statistical differences between the mean of the samples.

Table 3.12: EMP and SS values of the signal.

Samples	**GAC Top**	**GAC 0.2**	**GAC 0.4**	**GAC 0.6**	**GAC 0.8**	**GAC 1**	**GAC 1.3**	**GAC Bottom**
$\bar{x}\,(\mathrm{EMP},\mathrm{V})$	0.095	0.209	0.226	0.253	0.279	0.357	0.311	0.401
$\sigma(x)$	0.005	0.006	0.005	0.004	0.013	0.033	0.002	0.004
$\bar{x}\,(\mathrm{SS},\mathrm{V}\cdot\mathrm{s})$	3.781	4.052	4.233	5.262	7.160	8.714	7.821	9.216
$\sigma(x)$	0.283	0.301	0.323	0.394	0.544	0.655	0.597	0.693

*Method: 95.0 percent LSD/ $\bar{x}$ is the mean of the EMP and SS values of five independents experiments

The applied method was the Fisher's lower significant difference method. Based on statistical analysis, significant differences between EMP and SS of samples were found.

Fig. 3.26 shows the profile of the GAC exhaustion degree at different layers position in the rum filter based on the acoustic emission results considering as parameter the envelope of maximal peak amplitude and SS values at 1.3 kHz. A model fitting can be proposed with a proper correlation coefficient.

However, based on Figs. 3.25 and 3.26 analyzing the behavior of the EMP and SS values at 1.3 kHz, the amplitude found for GAC-1.3 is lower than the amplitude observed in the sample GAC-1, which is consistent with the inflection point observed at 1.3 m by the elemental analysis, TD-GC/MS and colorimetric method. Therefore, according to acoustic emission analysis, the GAC exhaustion profile in the rum filter can be divided in three zones (Fig.3.26).

Zone I : (near to the Top) with a rather linear behavior; **Zone II** : (layers above 0.4 and next to 1m) featured by a polynomial tendency and **Zone III**: (above 1m to the bottom) where a behavior of the GAC exhaustion degree is observed characterized by an inflection point in between due to the specific characteristics of the rum-ending production process.

The possibility to detect this behaviour in the GAC layers using the presented acoustic technique gives evidence of sensitivity and selectivity of the proposed method.

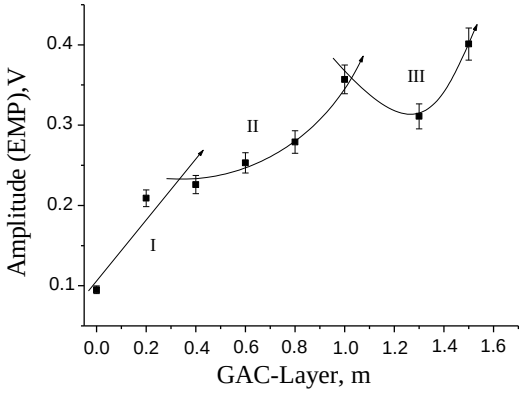

(a)

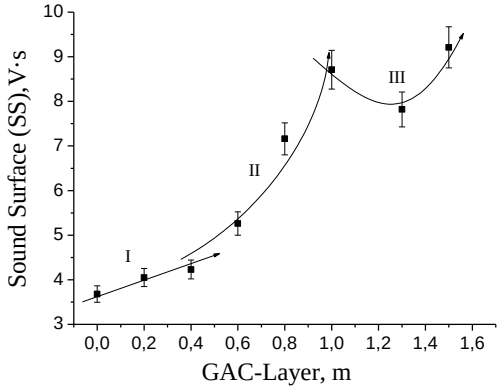

(b)

Fig.3.26: Profile of the GAC exhaustion degree at different layers position into the rum filter based on the acoustic emission using the envelope of maximal peak amplitude (EMP) (a) and SS (b) values at 1.3 kHz as parameter.

Fig.3.27 displays the surface plots of the signal envelope behavior in terms of amplitude (color scale), GAC layer depth and the time. Taking advantage of the three dimension figure and the color scale, differences in the amplitude and intensity of the GAC sound signal are more visible.

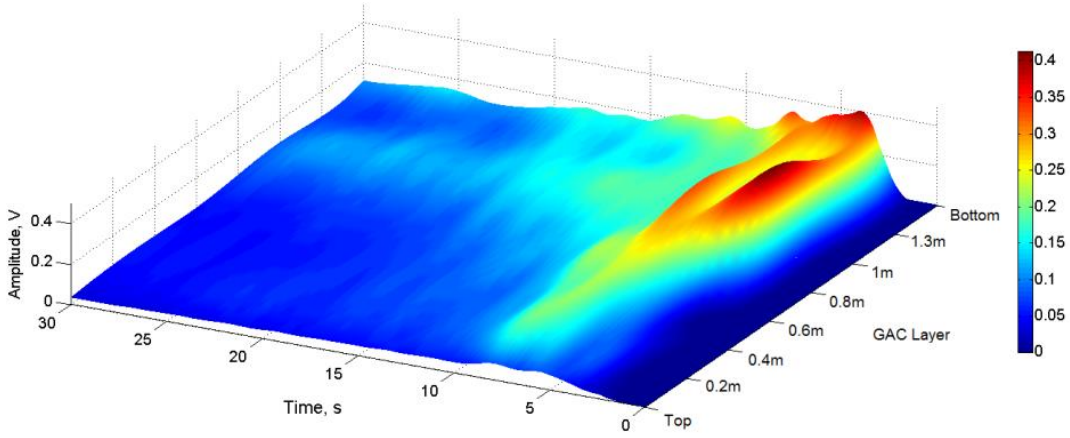

Fig 3.27: Surface plots of the signal envelope behavior

Fig.3.28 (a) displays the thermogravimetric curves (TG) of weight loss (in wt%) vs temperature for all studied samples. According to the graphs, the weight loss for GAC-Top has the highest value (about 18-20%), for the other samples a systematic decreasing value is observed to reach the lowest value for the GAC layers near to the bottom (about 13-15%). The GAC 1, 1.3 and Bottom are clearly clustered and separated from the other samples as their exhaustion degree is less and comparable between each other.

On the other hand, Fig 3.28 (b) displays the derivative weight loss in (wt%/°C) vs temperature (DTG curves) for the studied samples. Comparing DTG curves evident differences between the GAC can be noticed. Based on Fig 3.28 (b), the maximal desorption rate is located in the range of 325-500 °C for all the samples.

Comparing the peak temperatures, a systematic shift towards lower temperatures can be found from GAC-Top towards GAC-Bottom. The GAC near the top presented a systematic increment in derived weight loss from GAC-0.8 up to GAC-Top. As could be expected, GAC-1, GAC-1.3 and GAC-Bottom are clustered. The differences observed in the peak temperature and weight loss can be attributed to the amount and the kind of adsorbed organic compounds on the GAC. The more the GAC is exhausted, the more time it takes for the organic compounds to be released from the GAC.

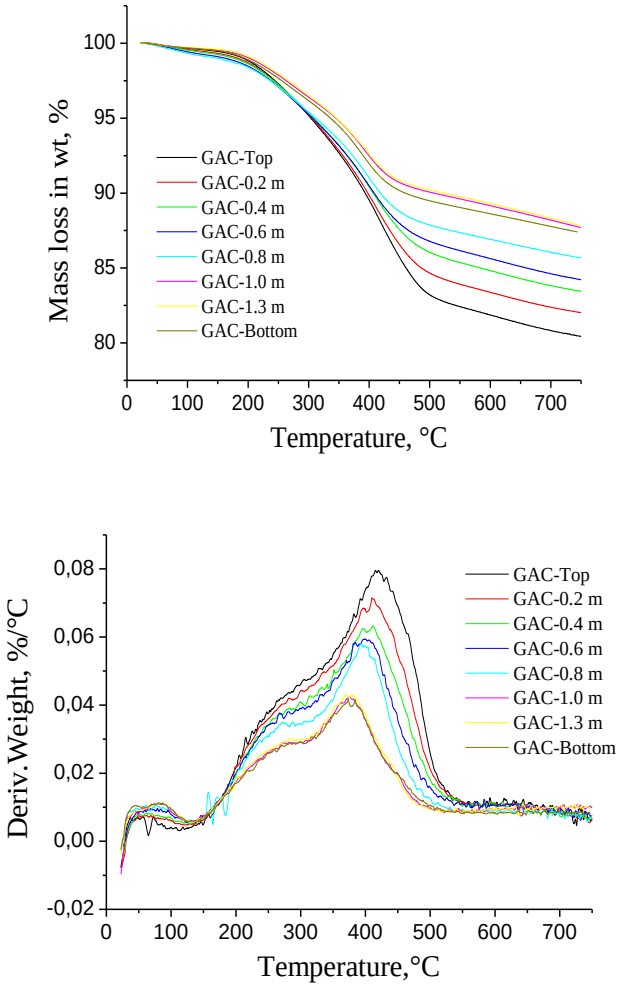

Fig 3.28: (a) TG curves and (b) DTG curves for GAC in N_2 atmosphere.

The behavior of the DTG curves in the vicinity of the maximal point is almost the same. A proper data fitting by a second order polynomial gives satisfactory results as shown in Table 3.13.

As the desorption rate is proportional to the substance amount that is still adsorbed [2], the derivative of weight loss can be associated with the mass of adsorbed compounds in GAC pores during the filtering process, the maximal desorption rate (Y_{max}) at the peak in the DTG curves can be used as a parameter to compare the exhaustion degree of the GAC used in rum production process.

Table 3.13: Parameters and characteristics of the DTG curves fitted to second order polynomial in the vicinity of the peak of maximal desorption rate.

Samples	**GAC Top**	**GAC 0.2**	**GAC 0.4**	**GAC 0.6**	**GAC 0.8**	**GAC 1**	**GAC 1.3**	**GAC Bottom**
A	-1.43	-0.97	-1.23	-1.42	-2.00	-0.94	-0.79	-0.66
e(A)	±0.01	± 0.01	±0.01	±0.02	±0.03	±0.01	±0.02	±0.02
$B1 \cdot 10^3$	7.2	5.1	6.4	7.4	10.0	5.2	4.4	3.7
$e(B1) \cdot 10^5$	±4.8	±6.5	±5.2	±8.4	±13	±7.6	±9.1	±1.2
$B2 \cdot 10^6$	-8.6	-6.3	-8.0	-9.4	-13.1	-7.0	-5.9	-4.9
$e(B2) \cdot 10^7$	±5.7	±8.2	±6.3	±1.0	±1.2	±1.0	±1.2	±1.6
Xmax.	**420**	**407**	**403**	**398**	**396**	**374**	**377**	**377**
$Ymax. \cdot 10^2$	**7.96**	**6.81**	**6.16**	**6.00**	**5.60**	**4.24**	**4.37**	**3.98**
R^2	0.98	0.93	0.97	0.98	0.95	0.96	0.97	0.94

e = parameter error $y = A + B1 \cdot x + B2 \cdot x^2$ and $(X_{max}; Y_{max})$ $\therefore$ $\frac{dy}{dx} = 0$

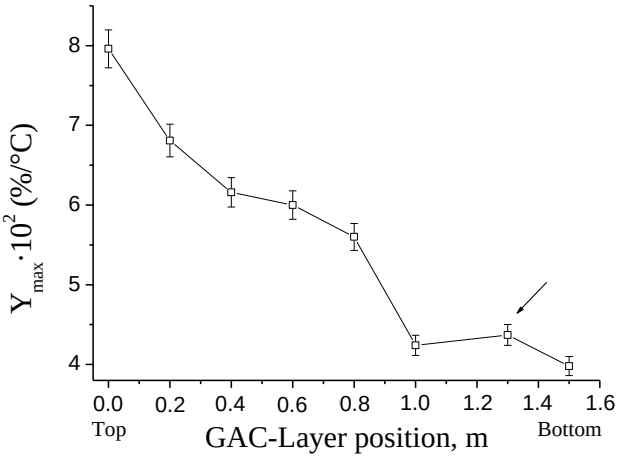

Fig.3.29: Profile of the GAC exhaustion degree at different layer positions into the rum filter based on the DTG analysis using the maximal desorption rate as parameter.

Fig. 3.29 shows the profile of the GAC exhaustion degree at different layer positions into the rum filter based on the DTG analysis using the maximal desorption rate as parameter. So far, similar trends between Figs.3.5, S1, 3.15, 3.26 and 3.29 are clearly noticeable. The inflection point is detected for all the cases. The three distinctive zones in the rum filter profile detected by the acoustic and colorimetric methods are also observed using the TGA analysis.

3.3-Characterization of GAC based on immersion "bubblemetry" method

In porous characterization of activated carbons, some methods only have access to open pores (e.g. those methods using a fluid), whereas other methods may access both open and closed pores (e.g. methods using adsorption or scattering of electromagnetic radiation). Moreover, for a given method, the value determined experimentally depends on the size of the molecular probe (fluid displacement, adsorption) or of the gauge (stereology). Thus, a measured value of porosity is a reflection of both the physical state of the material and the experimental method used for its determination. To distinguish these three cases, it should be noted whether the specific pore volume, is due to the open pores (leading to the "open porosity"), the closed pores (leading to the "closed porosity"), or both types of pores together (leading to the "total porosity") [9].

One of the fluid displacement techniques widely used is immersion micro-calorimetry. Immersion micro-calorimetry is based on the fact that when a solid is immersed into a non-reacting liquid, a given amount of heat is evolved. This "heat of immersion" or "heat of wetting" is related to the formation of an adsorbed layer of molecules of the wetting agent on the solid surface. The heat of immersion of a given solid into different liquids is usually different [10]. Characterization of microporous adsorbents by immersion calorimetry is not as straightforward as for non-porous adsorbents. Atkinson et al. measured the heat of immersion of a microporous carbon cloth and a microporous activated carbon in a series of organic liquids and, for a given solid, obtained a significant dependence of the heat of immersion with the liquid used. They concluded that the heat of immersion is a measure of the volume of pores accessible to the molecule of the immersing liquid, thus opening the possibility of using immersion calorimetry as a tool to obtain pore size distribution in AC [9,10,13,17]. Furthermore, molecules larger than some pores will not be able to access internal surfaces as smaller molecules do. Thus, the use of liquids with different molecular sizes permits the estimation of the pore size distribution of a porous solid. The shapes of the adsorbing molecule and pore shapes are also important factors [3,5,9]. The most important feature is the assumption of simple proportionality between the surface area and the enthalpy of immersion,

irrespective of the role played by micropores in the enhancement of the adsorption potential.

It is established that, for slit-shaped micropores in which only one molecule of the wetting liquid can be accommodated, there is a twofold increase of the adsorption potential as compared with that in an open surface [5,9,10,13,17].

Figure 3.30 shows the set-up, at a stage which is just prior to the immersion of the solid. Here, the sample (1) is located in a glass bulb (2) with a fragile tip (3). The sample has already been outgassed, out of the micro-calorimeter, and has been left either under vacuum or under a given vapor pressure of the immersion liquid. The bulb has been sealed off and attached, through fitting (4), to a thin glass rod.

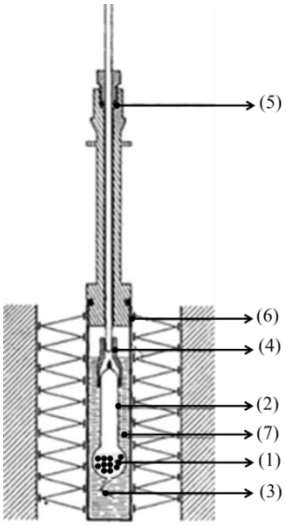

Fig.3.30: Set-up for immersion micro-calorimetry. (Adapted from [3])

This assembly has been introduced into the micro-calorimeter cell and tightly closed. The glass rod is able to slide down through an O-ring (5) (located outside the calorimeter to avoid detecting friction effects). The heat flowmeter (6) (a Tian-Calvet thermopile) surrounds the micro-calorimetric cell containing the immersion liquid (7) and the glass bulb. With the above set-up, the essential steps for a safe and convenient experiment are as follows:

1- Introduction and weighing of adsorbent in immersion bulb.

2- Outgassing of adsorbent.

3- If pre-adsorption is required, equilibration of sample with desired relative vapor pressure of immersion liquid.

4- Sealing of ampoule neck at 2 cm above the bulb if necessary immersed in cooling bath to protect the sample.

5- Determination of weight of sealed bulb.

6- Connection of top of sample bulb to glass rod (3 mm diameter) by means of Teflon plug.

7- Introduction of sample bulb (2) into stainless steel calorimetric cell already filled with immersion liquid (7).

8- Tight closure of this set-up, with some lubricant on O-ring (5) and with end of capillary tip of sample bulb circa 5 mm above bottom of microcalorimetric cell.

9- Allowance of time for temperature equilibration in the microcalorimeter (this may require 3 hours for high sensitivity).

10-Breaking of capillary tip by slowly and gently depressing glass rod until microcalorimetric signal starts to respond.

11- Recording of microcalorimetric signal until it returns to baseline (this usually requires c. 30 min).

12- Careful removal of sample bulb and broken tip from microcalorimetric cell.

13-Determination of weight of sample bulb filled with immersion liquid (only wiped outside), together with broken tip.

14- Determination of dead volume V of sample bulb from the information gained in Steps 5 and 13, knowing mass and density of immersion liquid.

15-Determination of total experimental heat of immersion by integration of the whole microcalorimetric signal (including the small endothermal peak due to vaporization of the first droplet of immersion liquid into dead volume) just before immersion proper.

16- Calculation of correction terms and, finally, of the energy of immersion.

The immersion process can be performed according to various types of wetting. The four major types of wetting are as follows (the first three following Everett's definitions, 1972) [3,5,8,9,13]:

1. **Immersional wetting**: (which we simply call immersion and denote by subscript 'imm') is a process in which the surface of a solid, initially in contact with vacuum or a gas phase, is brought in contact with a liquid without changing

the interface area. Here, a solid-gas (or solid-vacuum) interface is replaced by a solid-liquid one of the same area.

2. **Adhesional wetting**: is a process by which an adhesional union is formed between two pre-existing surfaces (one of them being solid and the other liquid). Here, two initial interfaces (solid-gas and liquid-gas) are replaced by one (solid-liquid).

3. **Spreading wetting**: is a process in which a drop of liquid spreads over a solid substrate (the liquid and solid being previously in equilibrium with the vapor). Here, the solid-vapor interface is replaced by two new interfaces (solid-liquid and liquid-vapor) of the same area.

4. **Condensational wetting**: is a process in which a clean solid surface (initially in vacuum) adsorbs a vapor up to the formation of a continuous liquid film. Here, the solid-vacuum interface is replaced by two new interfaces (solid-liquid and solid-vapor) of the same area, as in spreading wetting. The difference between condensational and spreading wetting is the initial state, the liquid film being formed from a vapor in one case and from a drop in the other case.

If properly used, immersion calorimetry is a versatile, sensitive and accurate technique which has many advantages for the characterization of porous solids and powders. It should be kept in mind that any change in surface area, surface chemistry, or micro-porosity will result in a change in the energy of immersion. Immersion calorimetry is quantitative and sensitive method, and it can be used for quality testing. The preliminary outgassing requires the same care as for a BET measurement, but, from an operational standpoint, energy of immersion measurements are probably less demanding than gas adsorption measurements. When a particle of a porous material is immersed into a liquid, the air trapped in pores and cracks of the particle is removed in form of bubbles by the liquid which occupy the "empty" spaces in the particle. This behavior was observed when particles of GAC used in the rum production were immersed in different liquids. The GAC is initially in contact with a gas phase (air), creating a solid-air interface, when putting in contact with the liquid the solid-gas interface is replaced by a solid-liquid one. This replacement occurs by the capillary action involved in filling the pores and slits in the GAC particle. In the interface replacement process, the air is removed in form of bubbles which escape through the bulk liquid.

Measuring the size of the formed bubbles and calculating its volume, the total volume of released air and correspondently, the volume of with liquid occupied open pores and slits can be determined.

The bubbles production rate and its characteristics, depend on the porous characteristics of the solid and the physical properties of the immersing fluid. In this case, glycerol was used as immersing liquid because of its physical properties (discussed later) permits to observe the formed bubbles at "slow motion" giving the possibility of fixing proper microscopic pictures of the bubbles, to be further analyzed. In this work the set-up and procedures presented in §2.4.3 were applied to determine the bubbles size and amounts produced in an immersing process with glycerol for GACs used in the rum production. If a comparison between immersion micro-calorimetry and immersion "bubblemetry" methods is done; immersion "bubblemetry" method can be classified as fluid displacement technique to determine the porous characteristic of GAC. According to the set-ups and procedures presented in §2.4.2 and §2.4.3 and the immersion micro-calorimetry basis, the acoustic emission and "bubblemetry" methods take place under the same basic principle: the sudden contact between the liquid and solid phases. Differences are present in the measured parameter; for "acoustic emission" it is the bubbles sound, for "immersion micro-calorimetry" it is the heat of adsorption and in "bubblemetry" it is the size of the bubbles.

Immersion "bubblemetry" technique is an important tool to understand the relationship between the acoustic emission measurements and the GAC bubble process when the GAC is suddenly immersed in a pure and inert liquid. Glycerol was used as immersing liquid due to its transparency and viscosity that permits not only to obtain well defined microscopic images but also to understand the GAC bubble process in water since the bubble process in glycerol occurs slowly. The intensity of the bubble process and the fast rate of bubble formation make the bubble characterization impossible when water is used as immersing liquid (this will be discussed later).

Fig. 3.31 displays digital microscopic images of the typical bubble production patterns of GAC grains from three specific layers positions in the rum filter immersed in glycerol.

Differences in the GAC bubble pattern are noticeable giving the first evidence that the number and the total volume of produced bubbles are in correspondence with the GAC sound pattern observed in Figs.3.25 and 3.26, being higher for the bottom than for the top GAC, following a systematic trend.

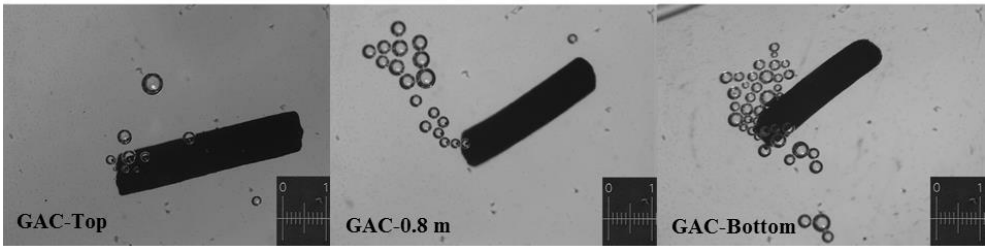

Figure 3.31: Digital microscopic images of bubble GAC samples immersed in glycerol from three specific layers positions in the rum filter.

Fig.3.32 presents the GAC bubble diameter distribution. No significant differences are found between the plots of GAC samples from GAC-0.2 to GAC-Bottom. For these GAC, the majority of formed bubbles are distributed around 0.2 - 0.4 mm in diameter.

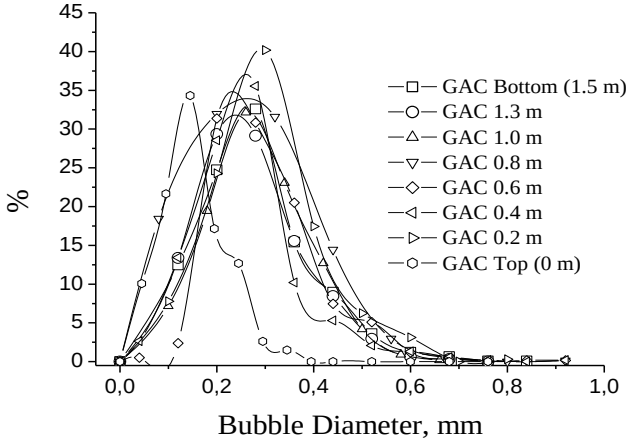

Fig. 3.32: Bubble diameter distribution

However the GAC-Top diameter distribution is located between 0.1-0.2 mm in diameter, it is almost half of the bubbles observed in the rest of the GAC layers, and such phenomenon can be associated with the concentration of adsorbed

compounds on the GAC grain. If the concentration of these compounds is high enough, the carbonaceous primary matrix of the GAC can change by overloading.

Therefore, the interaction solid-immersing liquid in the replacement process of the solid-air phase is different; consequently a different bubble pattern appears. In this case, smaller bubbles are mainly present when the GAC is totally exhausted; this is an interesting and quick-assessment parameter to detect the "complete exhaustion degree" of a GAC in the rum process. According to this observation, the bubble process is not simple and depends not only on the immersing liquid properties but also on the GAC surface characteristics, which must be further studied.

Table 3.14 shows the fitting parameters of the Gaussian model obtained for the different GAC plots. According to the regression coefficient, the Gaussian model fits quite well the found bubble diameter distribution.

Table 3.14: Fitting parameters of Gaussian model for GAC bubble diameter distribution.

Samples	**GAC Top**	**GAC 0.2**	**GAC 0.4**	**GAC 0.6**	**GAC 0.8**	**GAC 1**	**GAC 1.3**	**GAC Bottom**	**GAC Virgin**
y_0	0.83	1.44	0.92	0.53	0.43	0.31	0.58	0.53	0.10
$e(y_0)$	±2.2	± 1.0	±0.8	±1.3	±1.7	±0.1	±0.9	±1.3	±0.4
x_c	0.143	0.287	0.245	0.268	0.257	0.275	0.248	0.269	0.268
$e(x_c)$	±0.01	±0.01	±0.01	±0.01	±0.01	±0.01	±0.01	±0.01	±0.01
w	0.121	0.181	0.159	0.269	0.230	0.205	0.202	0.174	0.260
$e(w)$	±0.02	±0.01	±0.01	±0.03	±0.02	±0.01	±0.02	±0.02	±0.01
A	4.62	8.66	7.02	7.43	12.2	7.82	7.73	7.42	10.0
$e(A)$	±0.8	±0.7	±0.5	±0.9	±1.4	±0.6	±0.6	±0.9	±0.5
R^2	0.942	0.985	0.976	0.936	0.970	0.989	0.982	0.956	0.983

$e(i)$: error associated to the parameter "i"

$$y = y_0 + \frac{A}{w \cdot \sqrt{\pi/2}} \cdot e^{-2 \cdot \frac{(x-xc)^2}{w^2}}$$

When comparing the parameters: $\boldsymbol{x_c}, \boldsymbol{w}$ and $\boldsymbol{A}$, no significant differences between GAC bubble diameter distribution into the range (GAC-0.2 to GAC-Bottom and virgin) can be found. However $\boldsymbol{x_c}$ and $\boldsymbol{A}$ in the GAC-Top differ significantly from the rest, confirming the graphical comparison.

The bubble diameter defines the frequency of the produced sound during the bubble process. The smaller the bubble, the higher the obtained frequency is [154,155,158,160,161,166-168]. Taking into account the bubble behavior when glycerol is used as an approach to the water immersion, the results between Fig.3.25 (b) and Fig.3.32 are comparable. If the bubble diameter distribution is almost the same, the frequency distribution must be the same as observed in Fig.3.25 (b). However, comparing the shape of the spectra at 1.3 kHz (Fig.3.25 (b).) it is noticeable that the peak of the amplitude distribution for the GAC-Top spectrum is not well defined in comparison with the other samples. Additionally, the distribution around 1.3 kHz for GAC-Top is slightly displaced to the right (higher frequencies) indicating smaller bubble contributions to the GAC sound.

Table 3.15 presents the results of total volume, $V_{T"imm"}$, by immersion "bubblemetry" technique. Each presented value was obtained by adding the total bubble volume of 35 independent particles per GAC sample analyzed individually as described in eqs. (2.11) and (2.12) presented in §2.4.3.

Table 3.15: Immersion total volume of the GAC

Sample	V_{Tb}(cm^3)	k	$V_{T"imm"}$ (cm^3/g)
GAC-Top (0 m)	$6.6 \cdot 10^{-3}$	268	0.13
GAC-0.2 m	$7.0 \cdot 10^{-3}$	319	0.15
GAC-0.4 m	$8.1 \cdot 10^{-3}$	529	0.17
GAC-0.6 m	$11.6 \cdot 10^{-3}$	590	0.25
GAC-0.8 m	$13.3 \cdot 10^{-3}$	776	0.29
GAC-1.0 m	$18.6 \cdot 10^{-3}$	1099	0.41
GAC-1.3 m	$15.2 \cdot 10^{-3}$	955	0.33
GAC-Bottom (1.5 m)	$19.6 \cdot 10^{-3}$	1081	0.45
GAC-virgin	$21.2 \cdot 10^{-3}$	987	0.56

The values of total volume of the "k" experimentally counted bubbles (V_{Tb}) are different. For GAC-Bottom the highest value of V_{Tb} was found and correspondingly, the lowest value was observed for GAC-Top following a systematic tendency of increasing volume from the top to the filter bottom, which matches with the rum production process using fixed bed "filters" (Fig.2.2).

The amount of the experimentally counted bubbles released ("k") is quite high and characteristic for high-porosity materials. The high amount of total released bubbles "k" disables the bubble counting for more than one particle each (number "k" of counted bubbles varied between 268=>1081).

Additional, if too many bubbles are formed (testing more than one GAC grain), they coalescence, overlap partially each other or are even invisible, leading to inaccurate counting and measurement results. The obtained V_T*"imm"* values are comparable with the porous characteristics of activated carbon in terms of pore volume.

Fig. 3.33 presents the profile of the GAC exhaustion degree at different layer positions in the rum filter based on the immersion bubblemetry method.

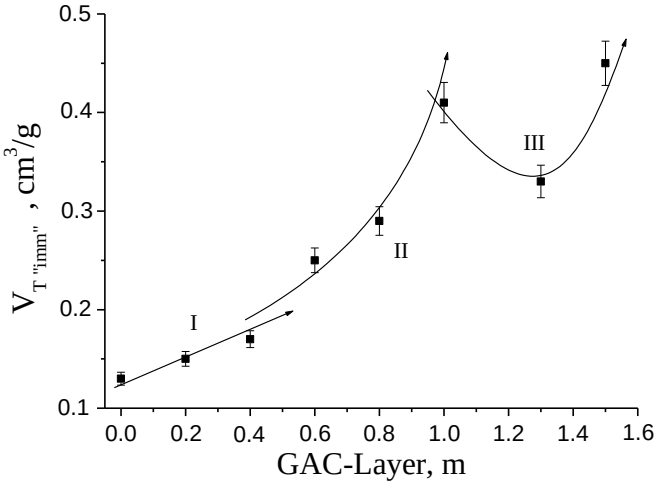

Fig.3.33: Profile of the GAC exhaustion degree at different layers position into the rum filter based on immersion bubblemetry method.

Comparing Fig. 3.26 and 3.33, quite similar trends can be found. The acoustic emission results are highly correlated with immersion total volume of the GAC. This confirms the relationship between acoustic emission and porous characteristics of the GAC.

Experiment with an immersion liquid of smaller molecular size (more pore accessibility) will result in higher V_T*"imm"* values.

This can be proved as follows: Supposing that two immersing liquids (1) and (2) have different pores accessibility and considering that: (1) represents the liquid with higher accessibility; then the total volume of bubbles formed in both liquids (1) and (2) can be expressed according to eq. (3.9).

$$V_{Tb_1} = \sum_{i=1}^{k_1} V_{i_1} \quad \text{and} \quad V_{Tb_2} = \sum_{i=1}^{k_2} V_{i_2} \tag{3.9}$$

being:

k_1 ; k_2: Number of experimentally counted bubbles with volume $V_{i_1}; V_{i_2}$in liquids (1) and (2).

$V_{i_1}; V_{i_2}$: The volume of a single bubble formed in liquids (1) and (2).

Fig. 3.34 presents a gas bubble into an immersing liquid of density "ρ". The gas bubble is statically located at depth "h" under the liquid level.

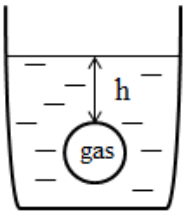

Fig.3.34: Gas bubble immersed into the liquid

The gas pressure "*P*" inside of the bubble is equal to the external static pressure of the liquid P_{ext} , therefore the gas pressure into the bubble can be calculated as:

$$P = P_{ext} = \rho g h \tag{3.10}$$

according to the ideal gas law

$$PV = nRT \tag{3.11}$$

For any single formed bubble V_i gives:

$$V_i = \frac{n_i R T_i}{P_i} \tag{3.12}$$

Where n_i is the amount of air (mol) contained into a single bubble of volume V_i

Combining eqs. (3.10) and (3.12) and considering the same conditions of T, ρ and depth h for all the formed bubbles suspended into an independent liquid:

$$V_i = n_i \left(\frac{RT}{\rho h}\right) \tag{3.13}$$

The differences in the final results obtained by applying different immersing liquids (1) and (2) can be presented in form of ratio as:

$$\frac{V_{Tb_1}}{V_{Tb_2}} = \frac{\sum_{i=1}^{k_1} V_{i_1}}{\sum_{i=1}^{k_2} V_{i_2}} \tag{3.14}$$

Combining the equations (3.13) and (3.14):

$$\frac{V_{Tb_1}}{V_{Tb_2}} = \left(\frac{\sum_{i=1}^{k_1} n_{i_1}}{\sum_{i=1}^{k_2} n_{i_2}}\right)\left(\frac{T_1}{T_2}\right)\left(\frac{h_2}{h_1}\right)\left(\frac{\rho_2}{\rho_1}\right) \tag{3.15}$$

The total amount of air (in mol) displaced by the liquid: (n_T) in form of "k" bubbles can be determined as:

$$n_T = \sum_{i=1}^{k_1} n_i \tag{3.16}$$

Combining eq.(3.15) and (3.16) gives:

$$\frac{V_{Tb_1}}{V_{Tb_2}} = \left(\frac{n_{T_1}}{n_{T_2}}\right)\left(\frac{T_1}{T_2}\right)\left(\frac{h_2}{h_1}\right)\left(\frac{\rho_2}{\rho_1}\right) \tag{3.17}$$

Equation (3.17) presents the parameters which can modify the final results using different immersing liquids and experimental conditions. In this case, analyzing the terms of the equations, the total volume of released air by a particle depends on: 1) the pore accessibility of the liquid (related with the molecular size, surface tension and viscosity of the liquid), 2) the liquid temperature, 3) the immersion depth and 4) the liquid density. Using this equation, it is possible to predict the effect of changes using different immersing liquids and different experimental conditions in terms of the total volume of released bubbles and correspondently on the total volume of pores determined by immersion "bubblemetry". The use of other liquids like water or ethanol to obtain the bubbles was also explored, but the results were not satisfactory. The bubbling process using these liquids is so fast that it was not possible to capture the bubbles in a picture. Due to their low viscosity, coalescence phenomena occur making the measurement of the sizes of produced bubbles impossible. Other liquids such as: phosphoric acid, lactic acid and paraffin were also researched (they're also transparent and their viscosity is higher than water), but again no satisfactory results were obtained: the counting process was quite difficult and not accurate because of the enormous number of produced bubbles, bubbles coalescence and attached on the GAC surface (see Figure 3.35).

Further on, only one side of the particle is visible under the microscope; more bubbles remain hidden at the other side of the GAC being thus non-detected. Therefore, using these liquids, around 30-50% of the information about the number of produced bubbles and its volume is unknown/lost, introducing a significant error in the measurement process. Comparing the obtained features (Figure 3.35) with the images obtained using glycerol (Figure 3.31) as immersing liquid, these cited problems didn't occur. Up to now, glycerol is the best immersing liquid to detect and process the bubbles. However, the chemical and physical property of the liquids and the relationship with the GAC bubbling feature must be further studied.

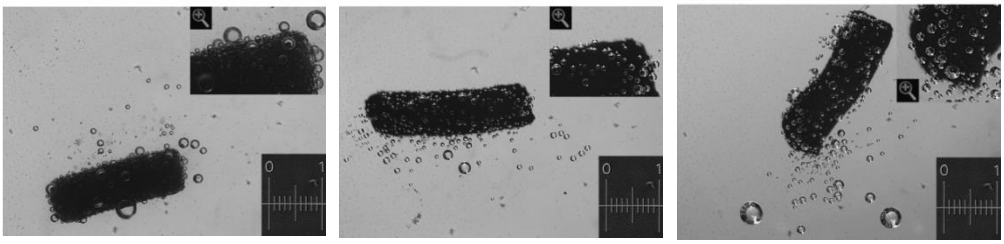

Phosphoric acid Lactic acid Paraffin

Figure 3.35: Bubbling features of GAC-Bottom particles immersed in different liquids.

This correlation is not simple; liquids with similar physical properties (surface tension, density and viscosity) produce different bubbling patterns. The bubbling pattern of a GAC depends not only on the chemical-physical properties (or one individual property) of the used liquid but also on the chemical-physical characteristics of the GAC surface and its interaction with the immersing liquid.

3.4- Determination of the exhaustion level of GAC used in rum production based on NMR relaxometry.

NMR has been extensively applied for the study of porosity and pore-liquid interactions in different porous media. It is a non-invasive and non-destructive method that can be successfully used for the characterization of phase morphologies and pore spaces [125]. Therefore, NMR provides a convenient way of quantifying the pore size distributions and can give information on the nature of interaction of a fluid with the porous material confining it [126].

NMR relaxometry is a tool to determine the pore size distribution of a porous material on the basis of the relaxation behavior of a liquid (like water) confined in the pores. It was first described in the paper of Brownstein and Tarr (1979) [125,127].

Measurements of the 1H NMR spin-lattice (T_1) and spin–spin or transverse (T_2) relaxation time have been used for the characterization of the pore size distribution for different porous media. Since the observed transverse relaxation times are strongly dependent on pore size, T_2 measurements have been proven to be highly correlated to surface area and pore size distribution [126].

According to the Brownstein-Tarr theory, the transverse relaxation time (in μs) for a pore "i" with volume V_i and surface S_i, will be:

$$\frac{1}{T_{2,i}} = \frac{1}{T_{2,bulk}} + \left(\frac{S_i}{V_i}\right)\rho_i \tag{3.18}$$

in which $T_{2,bulk}$ (in μs) is the transverse bulk relaxation time of water, S_i/V_i (in m^2/m^3) the surface area-to-volume ratio of the pore, and ρ_i (in m/μs) the surface relaxivity. This model has proven to be widely applicable [128]. Because $T_{2,bulk}$ has values around 1-3 s, thus being >> $T_{2,i}$, the inverse can be neglected in equation (3.18), resulting in the following approximate equation:

$$\frac{1}{T_{2,i}} = \left(\frac{S_i}{V_i}\right)\rho_i \tag{3.19}$$

In porous media, the T_2 relaxation of water is accelerated by the collisions with pore walls [129]. As is presented in eq. (3.19), the relaxation time is inversely proportional to the surface area-to-volume ratio, thus directly proportional to the pore radius [130,131]. The stronger a water molecule is in interaction with the pore walls, the shorter theT_2 relaxation decay time [125]. Moreover, since the amplitude of a NMR water signal is proportional to the amount of water present [130], it allows to quantify the different water mobility distributions present in the specimen via an exponential decay time analysis by curve fitting. The resulting relaxation time distributions can then be correlated with the distributions of pore sizes present in the system [132]. For spherical pores, the pore size diameter (d_i) can then be estimated from the equation developed by Davies et al. [133-135]:

$$d_i = \left(\frac{6V_i}{S_i}\right) \tag{3.20}$$

As said above, the T_2 relaxation is affected by the strength of the interaction between the water molecules and the pore surface. A T_2 relaxation time shift towards shorter values (faster relaxation) indicates water movement into smaller pores (or more strongly bound water). The longer the T_2 relaxation time, the less restricted (more free) the water movement.

However, although the boundary conditions are not well defined, as a general rule one can differentiate between water in micropores or tightly bound water having short relaxation decay times ($T_2 \leq$ 60 ms), mesopores or loosely bound water having medium relaxation times ($T_2 \approx$60 - 300 ms) and water in macropores having long relaxation times ($T_2 >$ 300 ms). [136]

If extending the "single-pore" relaxation model (eq. 3.18) to a "multiple-pore" model, the water transversal magnetization M(t) is described by a combination of a Gaussian and exponential function or by a combination of exponential functions [134,137,138].

$$M(t) = m_0^1 e^{\left(-\frac{t}{T_{2,1}}\right)} + m_0^2 e^{\left(-\frac{t}{T_{2,2}}\right)} \quad (3.21)$$

or

$$M(t) = m_0^1 e^{\left(-\left(\frac{t}{T_{2,1}}\right)^2\right)} + m_0^2 e^{\left(-\frac{t}{T_{2,2}}\right)} \quad (3.22)$$

where m_0^i represents the normalized magnetization of water in pores of type "i".

These m_0^i magnetization values are proportional to the molar fractions of water molecules in the different pore environments [138]. Material porosity can therefore be described by the normalized fractions of the measured NMR transverse relaxation decay time in the samples. Or in other words, the observed T_2 fractional distribution represents the pore size distribution in the material [139]. Therefore, NMR relaxometry measurements are evaluated in order to determine the exhaustion profile of GAC in the target rum filter.

3.4.1- NMR data processing

According to the Brownstein–Tarr relaxation models, the values $T_{2,1}$ and $T_{2,2}$ can be interpreted as two main pore size types in the GAC samples [125-139]. An activated carbon is a highly porous material and the overall porosity is formed by the contribution of pores of different sizes. The distribution of amounts of these pores in the material defines its porous characteristics such as: specific

surface, total volume of pores and volume of present macro, meso and micro pores [1-29]. Therefore, the total area-to-volume ratio for an activated carbon can be expressed as a contribution of the area-to-volume ratio of the different pores, considering that the matrix is the same for all the examined pores in the carbon. The magnetization fractions or intensity m_0^i represents the population of different pore size types in a defined sample mass [139].

Thus, the detected fractional distribution of the pores in the GAC samples represents the fractional contribution of two pore size distributions, size type 1 and 2, corresponding to the $T_{2,1}$ and $T_{2,2}$ relaxation times according to the Gaussian-exponential model (eq. 3.22), where the fractional contribution $x_{2,i}$ of each pore size type to the total porosity can be expressed as function of the magnetization fraction according to the following equation :

$$x_{2,i} = \frac{m_0^i}{\sum_{i=1}^{2} m_0^i} \tag{3.23}$$

As the $T_{2,i}$ relaxation time is proportional to V_i/S_i (which in turn is proportional to the pore size) [125-139] the fractional contribution of each $T_{2,i}$ can be used to determine the pore size distribution in the GAC [139-142].

Table.3.16 presents the T_2 relaxation times and their fractional contributions, representing the water fractions in the different types of pores. According to the T_2 values, all the pores can be associated with tightly bound surface water in small pores (micropores) having short relaxation times [136].

Table 3.16: Values of T_2 and the graph of fractional contribution for the GAC samples

Samples	$T_{2,1}$ (μs)	$x_{2,1}$	$T_{2,2}$ (μs)	$x_{2,2}$
GAC-Top	18.3	0.457	22.6	0.543
GAC-0.2	18.5	0.429	22.0	0.571
GAC-0.4	18.5	0.430	22.1	0.570
GAC-0.6	18.3	0.391	22.6	0.609
GAC-0.8	18.6	0.371	24.3	0.629
GAC-1.0	18.7	0.347	28.1	0.653
GAC-1.3	18.9	0.351	28.0	0.649
GAC-Bot.	17.9	0.344	26.0	0.656

Bot. =Bottom

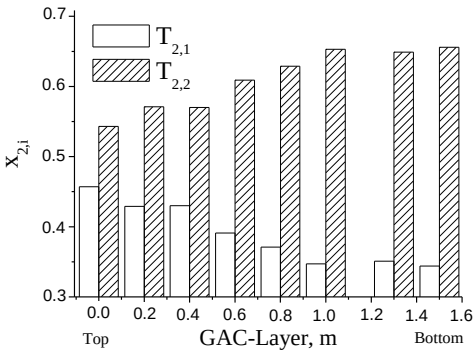

Water of which the T_2 relaxation has to be described by a Gaussian function is very strongly bound as is for $T_{2,1}$. The pore size type represented by this $T_{2,1}$=18-19 μs is present in all the samples but its fractional contribution $x_{2,1}$ decreases from the Top to the Bottom of the filter.

The second $T_{2,2}$ decay time, corresponding to a second pore size type, is more variable and can be split in two groups: 22-24 μs and 26-28 μs. Water of which the $T_{2,2}$ decay time has to be described by a Lorentz (exponential) function is more free and the longer the T_2 decay time, the more free is the water.

A systematic increase of $T_{2,2}$ is found from the top to the bottom but an abrupt change can be noticed again for GAC-1, GAC-1.3 and GAC-bottom. The fractional $x_{2,2}$ contribution of the pores represented by $T_{2,2}$ clearly increases from the Top to the Bottom of the filter.

According to the relaxometry model, $T_{2,2}$ represents "wider" pores than those represented by $T_{2,1}$ which can be considered as "narrow" pores. As these GAC samples have been used in rum production, they are loaded with organic molecules that block the pores, cracks and slits. Therefore, it is acceptable that the term: "wider" pores is related with unblocked, clean or "available" pores, while "narrow" pores can be associated with blocked or "occupied" pores.

Fig.3.36 displays a simplified model of pores from the extreme samples: GAC-Top (most exhausted) and GAC – Bottom (low degree of exhaustion). Based on the T_2 relaxation behavior and the fractional contributions presented in Table 3.16, the micropores of the GAC can be divided into three groups as presented in Figs. 3.36 (a), (b) and (c).

The adsorption of organic compounds during rum refining using GAC is a complex process where the adsorption occurs under quite different mechanisms which involve competition for adsorption sites and randomly molecules accommodation to create a non-uniform deposition or coverage of adsorbed substances into the GAC pores [28]. In Fig. 3.36; for (a), (b) and (c) pores, the black irregular shapes are representing the adsorbed impurities which occupy the available active sites into the pore creating a reduction of its volume with an irregular pattern and presents a more realistic pore filling than the uniform ring deposition.

According to the relaxation time values, the volume of the pores still available for adsorption of organic compounds can be ordered as: (a) < (b) < (c).

The fractional contribution ratio (FCR) is calculated in the following way:

$$FCR = \left[\frac{x_{2,2}}{x_{2,1}} - 1\right] \cdot 100 \tag{3.25}$$

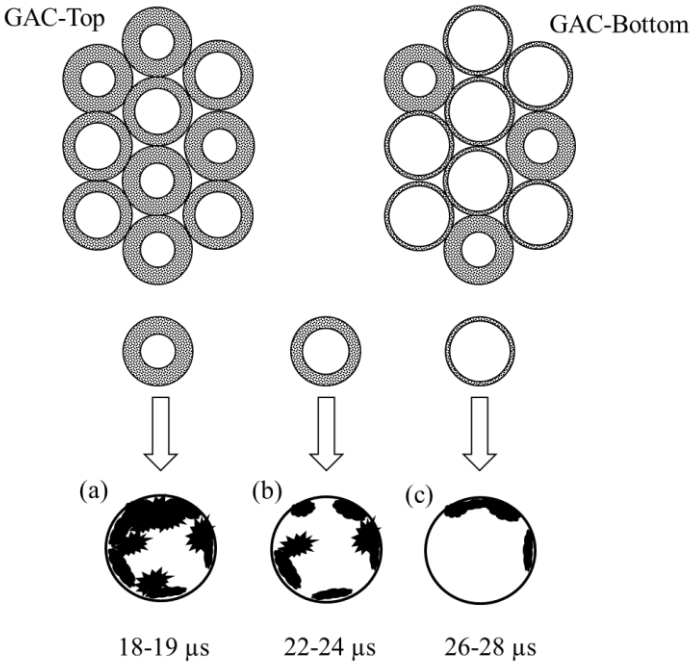

Fig. 3.36: Simplified model of pores from the extreme samples GAC-Top and GAC-Bottom and the T_2 relaxation characteristics of the main pore types detected.

Fig. 3.37 displays the plot of FCR in percent versus the GAC-layer position in the rum filter. FCR represents how many times (in percent) the amount of the "available" pores is bigger than the "occupied" pores per mass of sample.

This function, evaluates how different are the fractional contribution of the different types of pores present in the GAC sample in term of the "available pores" represented by $T_{2,1}$ and $T_{2,2}$.

Fig. 3.37 can be interpreted as the profile of the GAC exhaustion degree at different layers position into the rum filter based on NMR relaxometry considering the FCR as parameter.

Based on Fig. 3.37, the value found for GAC-1.3 is lower than the value observed in the sample GAC-1 creating the inflection point in the systematic growing plot trajectory (indicated by the arrow).

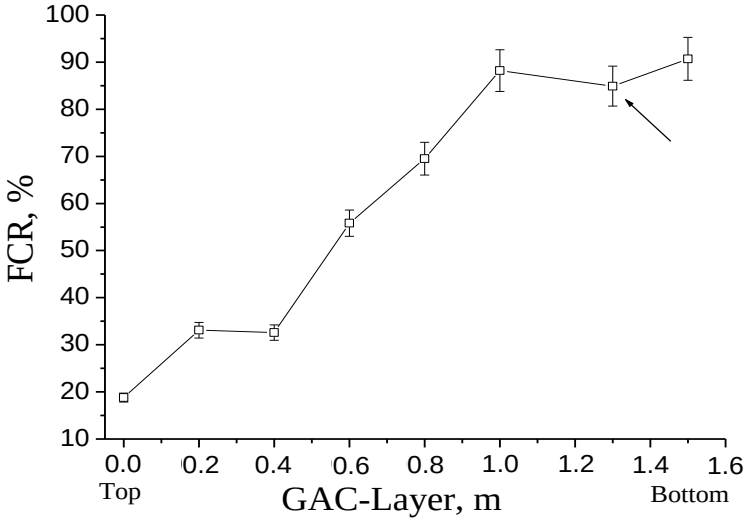

Fig. 3.37: Fractional contribution rate (FCR) trend according to the GAC-Layer position

However, the last three points near to the filter's bottom have almost similar FCR values (about 90%).This pattern is in line with the results from colorimetry, TGA/DTG, TD-GC/MS, CHNS-O elemental analysis, acoustic emission, bubblemetry, iodine number and contact pH.

3.5- Conclusions of Chapter 3

Three novel methods for the characterization of granular activated carbon used in rum production have been presented and compared with other analytical techniques.

It can be stated that the colorimetric method generated an amber color from used activated carbon in rum production with ammonia solution is a very specific and useful method in quantifying the exhaustion level of the GAC. The brownish color is produced by the reaction between the ammonia with phenolic compounds coming from the oak wood during the ageing process and adsorbed onto GAC during the filtration of aged aguardiente.

According to the kinetic results, the extraction reaction of the ammonia solution from the GAC demonstrated that the final absorbance value at equilibrium was not affected by the applied temperature range of 10–40 °C, nor by the ammonia concentration in the range of 25% down to 6.25%.The optimal measurement conditions were: an ammonia concentration of 6.25%, working temperature of 25 °C and 3.2 g of GAC for 20 mL of ammonia, gently shaking at 50 rpm in a tight capped (100mL) vessel for 6 h. The extracted solution is filtered using a PFTE filter (0.45µm) and measured at 634 nm in 1x1 cm quartz cuvette.

The acoustic emission method, based on signal processing of sound produced by GAC flooded with water, is a sensitive technique for determining the exhaustion degree of granular activated carbons used in the rum production process. It is a fast and correct predicting method for the detection of the exhaustion level of used GAC at different depth within the fixed bed filter.
An experimental set-up and software to capture, to process and to characterize the GAC sound was proposed. It is proved that the maximal peak amplitude and the area under the curve of the GAC sound signal envelope in the time domain obtained by BP filtering at 1.3 kHz give the most optimal and very reliable results. The immersion "bubblemetry" technique using glycerol as immersing liquid proved to give analogue and complementary information as the acoustic technique.

It can be stated that the acoustic emission, immersion "bubblemetry" and colorimetric methods demonstrated to be suitable and sensitive tools to determine the exhaustion degree of GAC used in rum production. The results can be satisfactory correlated with iodine number, contact pH, TGA, CNHS-O elemental analysis, TD-GC/MS and NMR results. The facilities and advantages of all proposed methods for analyzing the exhausted level of GAC form very interesting complementary analytical techniques to characterize GAC beyond the sensorial judgement traditionally performed by rum specialists.

The colorimetric method has some advantages in comparison with the iodine number and contact pH methods. To determine the iodine number, GAC must be grinded, and a higher amount of reagents is needed, more experimental steps are involved, and this is thus more time consuming. Additionally, the experimental error for the iodine number method was higher than the others (around 10%) [111]. In addition, the possibility of reaction between iodine and organic adsorbed compounds onto exhausted GAC disables the correct interpretation of iodine number results furthermore as a comparative parameter when an exhausted GAC is tested. On the other hand, the contact pH method is very simple and had a good confidence limit of around 2.4% [112]. However, the amount of GAC sample to be tested must be 10 g (dry weight); the results are highly dependent on the working temperature, correct calibration procedure and the quality of the used water.

In contrast, the colorimetric method is fast, specific and requires minimal reactants. It is not affected by changes of temperature or ammonia concentration. The error for the colorimetric method was around 5.3%.Additionally, even only on sight, a quick qualitative inspection of the color intensity can be performed by a simple ammonia extraction test, giving a very fast indication about the exhausted level of the used GAC. A combined ammonia extraction and thermal regeneration of used GACs gives interesting perspectives for reducing rum production costs and is beneficial for the environment, in reducing landfill deposition of exhausted GAC. The ammonia reacts with the phenolics compounds, inducing desorption from the exhausted GAC.

In contrast with the colorimetric method, which is just specifically applied for exhausted GAC used in rum production (or others which have been in contact with aged spirits), the acoustic emission and immersion "bubblemetry" methods can be applied for the characterization of GAC in general. These methods (acoustic and bubblemetry) are intrinsically linked by the same physical phenomenon: the bubbling process, its differences are in the measured parameter and the way to process the experimental results. In acoustic emission, the sound produced by bubbles exploding at the surface of the flooding liquid is the magnitude to be measured and in the bubblemetry method, the amount of air displaced in form of bubbles from the GAC using an immersing liquid. On the other hand, as the colorimetric method is based on a specific reaction between wood tannins and ammonia, the use of this method to characterize the exhaustion level of the GAC is quite specific, limited and useless for comparing virgin or regenerated GAC samples. Additionally, colorimetry cannot give direct information about the porous characteristics of the GAC as in the case of the acoustic and bubblemetry methods. Actually, using the acoustic emission and bubblemetry methods the virgin GAC can be characterized and also compared with other GAC which has been regenerated (this will be discussed in chapter 4). According to this fact, although this study is focused on GAC used in rum production, acoustic and "bubblemetry" methods shows its wider potential in the assessment of features of different adsorption systems. The simplicity and advantages of these proposed methodologies can be very interesting as complementary analytical methods to characterize high-porosity materials in order to explore the GAC pores characteristic.

The above mentioned new GAC characterization techniques offer in this particular case several advantages in comparison with well-known conventional techniques such as gas adsorption (BET). They are sensitive and non-destructive methods which can be performed quickly and thus are less time consuming. It does not need special experimental conditions or special reactants. Additionally, it is found that for detecting the exhaustion degree in used GAC the BET analysis could not be performed. Before BET analysis could be executed, the sample must be dried overnight at 300°C in vacuum.

In this case, the pre-treatment of the sample induces modifications in the studied GAC, desorption of a part of the absorbed organic compounds took place. It was even found that this required pre-treatment did not satisfy and could damage the equipment. Therefore, the measured BET results on exhausted GAC are not presented. The other proposed techniques are more reliable to determine the real exhaustion level, being an interesting tool for the control and management of GAC in the rum production process and analogue applications.

According to the results derived from all the applied methods, the exhaustion degree of the GAC at different layer positions in the rum filter reveals the following order:

GAC-Top > GAC-0.2> GAC-0.4> GAC-0.6> GAC-0.8> GAC-1.3≥GAC-1.0≥GAC-Bottom

An inflection point in the exhaustion level at GAC-1.3 in the rum filter was detected by all the performed methods. The possibility to detect this behaviour in the GAC layers using the novel methods confirms the sensitivity and accuracy of the measurements to study the GAC exhaustion process in rum production.
According to the lower exhaustion degree observed in GAC-1, GAC-1.3 and GAC-Bottom, a possible reuse of these GAC layers to the rum filtration can be proposed. Around 30% of the GAC as the length of the unused bed (LUB) fraction in the rum filter can be efficiently reapplied in a complete new contactor, mixed with virgin GAC.
In that case, the filling of a new rum filter should be started at the bottom using 70% of virgin GAC and then completed with partially exhausted GAC at the top. This possibility is more cost-effective than removing all the GAC and replacing by expensive virgin GAC. This aspect must be further evaluated and validated by rum specialists by sensorial judgment. If successful, it could be a very attractive proposal for reducing the costs in the rum production process.

Chapter 4-Thermal regeneration of the exhausted GAC used in Cuban rum production

Process of adsorption with GAC has been widely used in many industries at large scale for purification, separation and compliance purposes. The fact that adsorption can be used with liquid and gas process streams with high efficiency, low cost and friendly operation has made it a favorite process among industrial and compliance units. Industries are always in search of an adsorbent which has high surface area and is also specific to the target compounds. This desire has initiated enormous research in the field of adsorption. However, depending on their adsorption capacity, they become saturated after some time.

While adsorption facilities are being picked up at different industrial and commercial levels, the future of spent adsorbents is consistently becoming a concern.

Considering all above arguments it is evident that spent adsorbent needs to be stabilized after being discarded. Because of involvement of high cost of production, stabilizing or proper disposal of adsorbents, it seems an unwilling operation. Under such circumstances reuse by regeneration of adsorbent could prove double rewarding by stabilizing adsorbents and by recovering resource via reutilization and thereby minimizing the demand for virgin adsorbents. One of the cheapest and most versatile methods of regenerating activated carbons is thermal treatment in a given atmosphere.

In this study, thermal regeneration of exhausted GAC applied in rum production is investigated. Thermal regeneration experiments were conducted following the experimental planning presented in section §2.6.2.

According to experimental matrix for GAC regeneration (Table 2.6) different temperatures (450-850°C) and residence times (5-100 min.) were explored based on reported experiences in activated carbon regeneration loaded with different organic adsorbates [2,5,8,43]. As it is the most exhausted activated carbon found in rum production, GAC-Top was used for the regeneration experiments. The regenerated GAC samples (RAC) were characterized using the acoustic emission method presented and discussed in sections §2.4.2 and §3.2.1 respectively.

During thermal regeneration, the porous structure and pore size distribution of the GAC change and if regeneration conditions were too extreme (high temperature and long residence time) resultant carbon particles would be soft and very fragile [2,5,8,43]. Thus, in principle the acoustic behavior of the regenerated GAC could be different from the virgin GAC like a "new" activated carbon. Considering the relationship between the porosity, size of formed bubbles and the acoustic emission pattern, the parameters and conditions to perform the acoustic measurements must be adjusted in order to optimize the signal analysis process as it was discussed in §3.2.1 for the characterization of the exhaustion level of GAC in the rum filter, if the regenerated GAC were severely damaged during the regeneration process. Therefore, the cut-off frequency (frequency of interest) to assess the regenerated GAC has to be determined to ensure the correct acoustic characterization to make a proper evaluation of the regeneration process.

According to the effect on the regeneration temperature on the GAC porous characteristic of the and the residence time, a frequency spectrum comparison between the GAC-Top (exhausted), GAC-virgin and the regenerated activated carbon (RAC) at the most extreme experimental conditions at 850°C/30 min. (RAC (5;4))(see Table 2.6) was done.

Fig.4.1 shows the RMS, spectrograms and frequency component distribution of the GAC acoustic signal for the regenerated GAC (RAC (5;4)) and GAC-virgin.

Comparing the RMS between regenerated, virgin GAC and exhausted GAC-Top (Figs. 4.1 (a), (d) and 3.22 (a)) it is possible to see evident differences between the samples. The signal power produced by GAC-virgin is more intense than RAC and GAC-Top. However, the RMS of the RAC acoustic signal is closer to GAC-virgin, giving an initial evidence of porosity and regeneration degree. In contrast, the spectrograms depicted in Figs. 4.1 (b), (e) and 3.22 (c) present very similar features in terms of frequency distribution within a wide range of observed frequency components due to the resonator nature of the exploding bubbles [163,167]. The same frequency component around 1-1.5 kHz and its harmonics can be observed in RAC, GAC-virgin and exhausted samples but with different intensities (arrows in Figs. 4.1 (b), (e) and 3.22 (c)). The GAC-virgin sound is the most intense as expected for a virgin adsorbent.

The exhausted, regenerated and virgin condition of each sample can be noticed just by direct comparison between spectrograms.

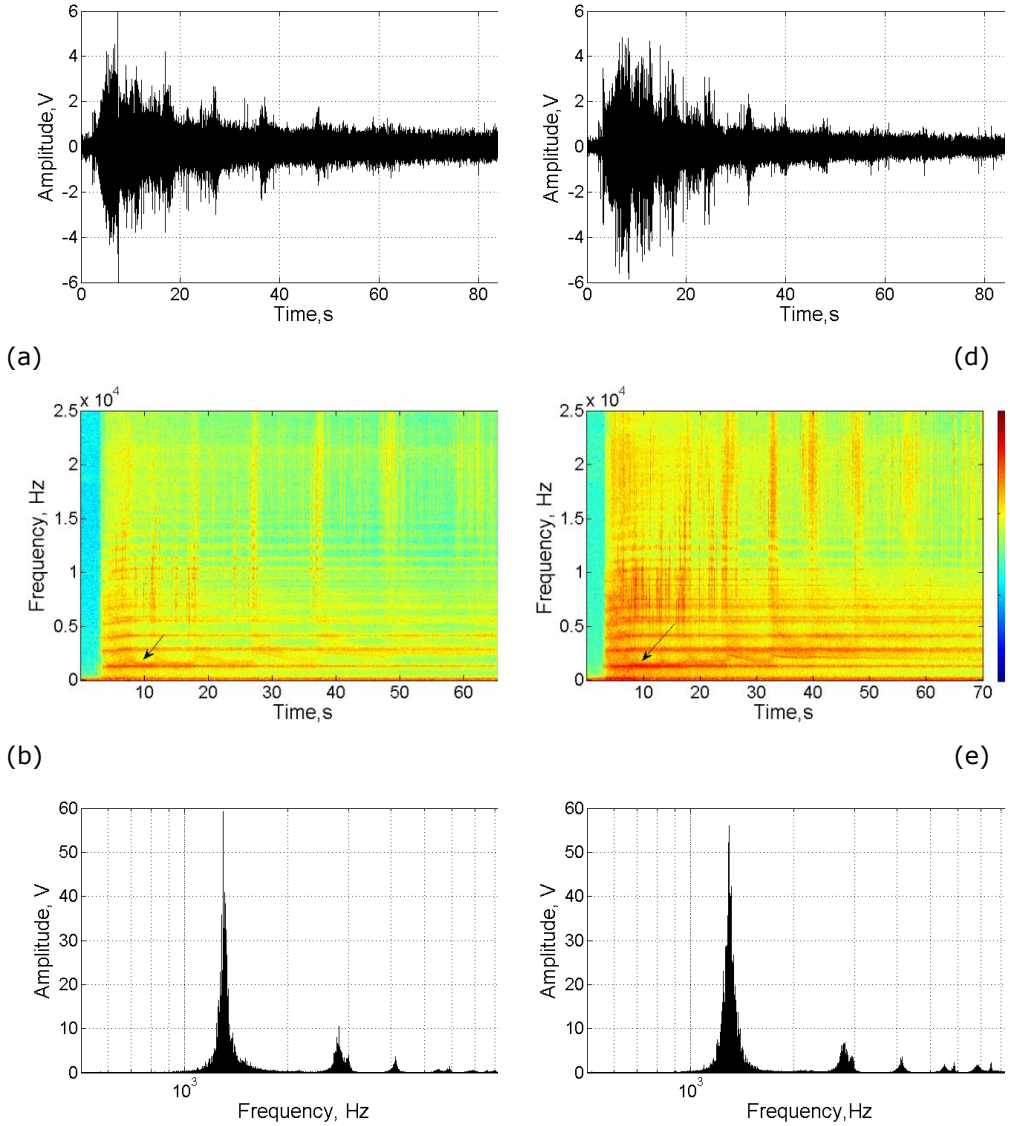

Fig.4.1: RMS of the GAC acoustic signal: (a) RAC (5;4) and (d) GAC-virgin, spectrograms: (b) RAC (5;4) and (e) GAC-virgin and frequency component distribution: (c) RAC (5;4) and (f) GAC-virgin.

Figs.4.1 (c) and (f) show the magnification of the spectral range with the peak of interest in RAC and GAC-virgin sound signal respectively. The same frequency components distribution featured by a peak in the frequency domain around 1.3 kHz was found. Comparing the amplitude of the dominant frequency peaks in the case of RAC and GAC-virgin, similar values can be observed, which is in line with the regenerated conditions of RAC. Both, RAC and GAC-virgin have a clearly higher intensity than the intensity of the frequency peak for GAC –Top (exhausted) (Fig.3.23 (c)).

As conclusion, the same procedure for signal analysis described in §2.4.2 and performed in §3.2.1 can be used to characterize the regeneration degree for the exhausted GAC used in rum production

Table 4.1 displays the values of the total integrated area under the signal envelope curves (sound surface: SS) for all the regenerated GAC at different experimental conditions, exhausted and virgin GAC. Table 4.1 uses the same format of Table 2.6 to easily decode the regenerated samples (RAC (T;t)) in terms of temperature and residence time combinations applied.

Table 4.1: SS values of the RAC (T;t) signal

		Residence time (min)								
	T(°C)	0	1	2	3	4	5	6	7	8
	-	**0**	**5**	**10**	**20**	**30**	**40**	**60**	**80**	**100**
1	**450**	3.78*	x	x	x	x	7.47	9.72	9.23	**9.25**
2	**600**	3.78	x	x	12.55	x	15.03	15.56	**15.32**	x
3	**700**	3.78	x	x	15.37	16.42	16.71	16.40	x	x
4	**800**	3.78	x	17.59	18.28	18.09	**18.23**	x	x	x
5	**850**	3.78	14.25	19.95	21.86	21.78	x	x	x	x

GAC-Virgin: SS = 24.01 (±1.3) V·s

* This value is referred to the SS value obtained for GAC-Top (before regeneration; see Table 3.12)

Five independent regenerations for each RAC (T;t) were performed and the material was mixed to create one homogeneous sample. Each RAC (T;t) mixed sample was acoustically measured in five independent experiments. A normal distribution for the results was confirmed. The averaged value of the SS for each sample is presented in Table 4.1.

The Multiple Comparison Method was applied to determine statistical differences between the mean of the samples. The applied method was the Fisher's Lower Significant Difference (LSD) method. Based on statistical analysis, significant differences were found between the RAC sound surface values in terms of temperature and residence time applied (the effect of both parameters will be further discussed later).

Porous characteristics of four representative RAC samples were analyzed using BET method. Two probe gases (argon 87 K and nitrogen 77 K) were applied in order to compare the results and to correlate with acoustic emission measurements. Although acoustic emission method and gas sorption analysis are performed under quite different conditions, the phenomenological correlation between both methods assessing the porous characteristics of activated carbons can be deduced (it will be discussed later).

The selected RAC samples are underlined and bolded in Table 4.1: RAC (1;8), RAC (2;7), RAC (4;5) and GAC-virgin. The selection was made in order to cover low, medium and high regeneration temperature ranges at maximum residence time for each temperature. Two main objectives were addressed with this selection; firstly, to make an initial exploration about the more suitable regeneration temperature range and secondly; to provide representative data as diverse as possible in terms of porous characteristics to correlate with acoustic measurement in a wide range, covering different regeneration degrees.

Fig. 4.2 presents the N_2 sorption isotherms of the selected samples. The isotherms for all carbons are **type I** with a hysteresis loop **type H4** according to IUPAC classification [6], indicating a microporous nature of adsorbents. The hysteresis loops for the RAC samples are similar and broader than the GAC-virgin loop. This behavior can be more associated with the filling of micropores than with capillary condensation in mesopores according to the value of the "C" BET constant related to the energy of monolayer adsorption [6] depicted in Table 4.2.

Fig. 4.3 presents the sorption isotherms of the samples using argon at 87K as gas probe. In concordance with N_2 results, the isotherms for all carbons are **type I** with a hysteresis loop **type H4** according to IUPAC classification [6], confirming the microporous nature of adsorbents.

However, the followed pattern by the volumes adsorbed and the extent of the isotherms is somewhat different from the N_2 results.

As reported by IUPAC [6], argon at 87K is a more suitable probe gas than N_2 at 77K. In contrast to nitrogen, which has a quadrupolar moment; argon does not interact with the surface functional groups. Argon at 87K provides more reliable results than N_2 for the porous characterization in high porosity microporous materials [6]. This will be discussed later in more detail.

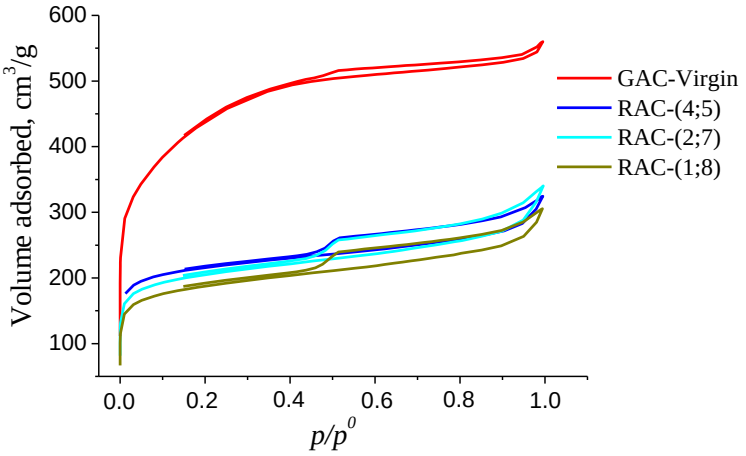

Fig. 4.2:N_2 sorption isotherms at 77 K of activated carbons.

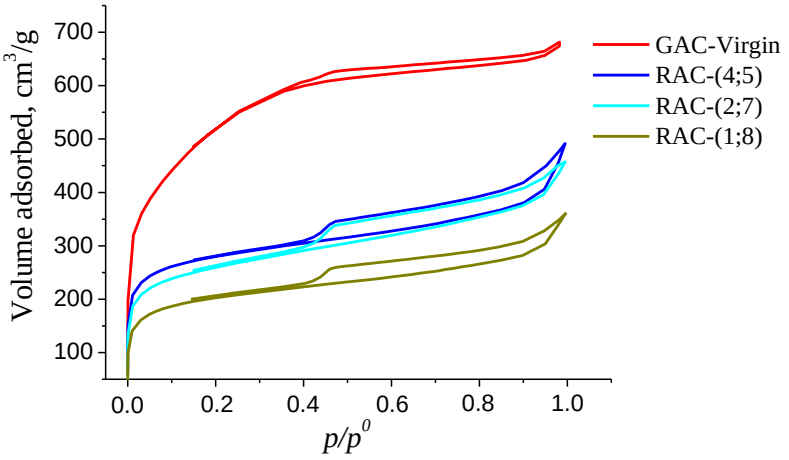

Fig. 4.3: Ar sorption isotherms at 87 K of activated carbons.

Table 4.2 displays the porous structure of the four GAC samples using N_2 and Ar as probe gases. For GAC-virgin, the highest apparent surface area is measured and is around 1570 and 1640 m^2/g for nitrogen and argon respectively. The apparent BET area of the regenerated carbons follows a growing trend according to the regeneration temperature applied. However, based on gas sorption results, the GAC-virgin apparent surface area is almost two times larger than the RAC-(4;5) which is the explored regenerated sample with higher BET apparent surface area.

Table 4.2: Characterization of porous structure of activated carbons using N_2 (77K) and Ar (87K) sorption.

Samples	Pore Shape	S_{BET} m^2/g		C*		Micropore Volume (V_{DR}) cm^3/g		Pore width (L_0) nm NLDFT		Pore width (L_0) nm QSDFT	
		N_2	Ar	N_2	Ar	N_2	Ar	N_2	Ar	N_2	Ar
RAC (1;8)	Slit	694	655	1266	373	0.30	0.27	1.23	0.27	0.61	0.59
RAC (2;7)	Slit	761	824	1590	663	0.32	0.34	1.23	0.34	0.61	0.59
RAC (4;5)	Slit	810	912	1701	539	0.34	0.37	1.29	0.37	0.79	0.59
GAC-virgin	Slit	1573	1644	191	114	0.67	0.56	1.23	0.56	0.79	0.75

*related to the energy of monolayer adsorption; degassing conditions: 16h/300°C/high vacuum. Decoded: (1;8)= (450°C/100 min), (2;7)= (600°C/80 min), (4;5)= (800°C/40 min).

When assessing the porosity data in combination with table 4.1, temperature confirms to be the most determining parameter to obtain higher regeneration degrees. The "C" BET constant is quite different between regenerated and virgin samples suggesting a higher energy of interaction for the regenerated samples (between 7 and 9, and between 3 and 5 times higher than in GAC virgin in the case of N_2 and Ar correspondently). As argon has more accessibility to the carbon pores with no specific interaction between the adsorbed molecules at 87K and the surface functional groups, the results are different in comparison with N_2 sorption analysis [6]. In the case of N_2, a systematic increase in "C" value can be noticed for RAC samples. In the case of Ar the RAC (2;7) sample shows the highest "C" value. The C-value for Ar is lower in comparison with N_2 results, not only considering the magnitude of the constant but also in the differences observed between regenerated and virgin GAC, coinciding with the absence of a quadrupolar moment in Ar, limiting specific interactions with the surface.

Nevertheless, the "C" values for all the regenerated samples are high, indicating gas adsorption in narrow micropores [6]. Although significant differences between the regenerated and the virgin GAC in terms of specific surface area and volume of pores are noticeable, results are more descriptive using Ar as probe gas. In this case, a systematic increment in the specific surface area and volume of pores is observed in correspondence with the regeneration temperature.

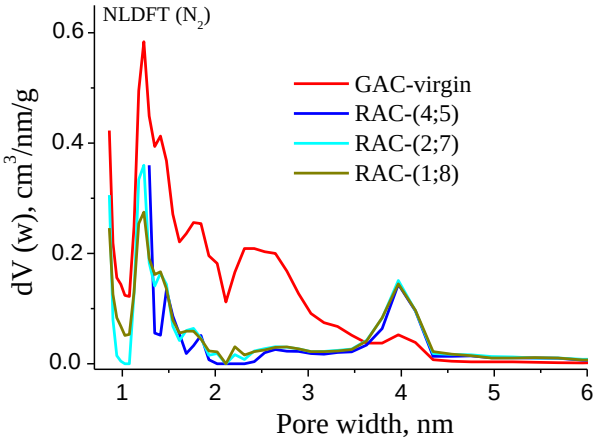

(a)

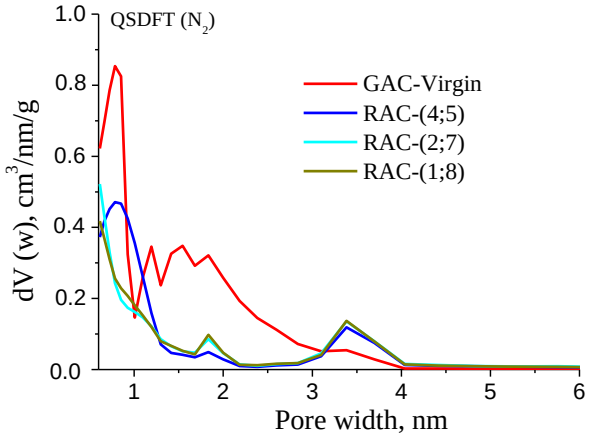

(b)

Fig. 4.4: Pore size distribution determined by NLDFT (a) and QSDFT (b) methods using N_2 at 77K.

Fig.4.4 (a) and (b) presents the pore size distribution in the carbon samples according to NLDFT and QSDFT respectively and slit shaped pores as model using N_2 at 77K. Based on QSDFT and NLDFT theories, the pore width is ranging between super-micro and micropores respectively.

In general, the pores have comparable sizes. GAC virgin has larger pores than the other samples and much more porosity based on N_2 sorption. In this case, clearly two maxima are found: one around 0.7 nm (QSDFT) and 1.2 nm (NLDFT) and a broader second one around 1-2 nm (QSDFT) and 1.7-2.7 nm (NLDFT).

Additionally, the first peak of GAC virgin (NLDFT) is broader compared to the regenerated samples located at the same region. The pore sizes between 1.2 and 3 nm are clearly lesser present for RAC with different regeneration level pointing to preferential adsorption of organic compounds in the pores with a size within this range. According to [43] and considering the types of adsorbed compounds found in the exhausted GAC in rum production (TD-GC/MS) discussed in § 3.1.3, this could be caused by pyrolyzed depositing of carbonaceous residues [43]. The pore size distributions of the regenerated samples are quite similar, indicating the presence of larger porosity visible as slit shaped pores and the appearance of a broader second peak in the range of 3-4 nm (QSDFT) and 4 nm (NLDFT).

As it was discussed in acoustic emission experiments (§3.2), the wider distribution of pores in the virgin GAC can be translated in a sustained higher bubble production with stronger sound amplitude than other regenerated samples.

In the case of pore size distribution based on Ar sorption presented in Fig.4.5 (a) and (b), results are comparable with the N_2 pore size assessment. The first peak around 0.7 nm (QSDFT) and 1.2 nm (NLDFT) are confirmed. However, the broader region between 0.7-3 nm (NLDFT) and 1.2-2 nm (QSDFT) is larger for the GAC-virgin than the regenerated samples.

Average pore width values for Ar are consistent with the regeneration process and comparable between NLDFT and QSDFT methods leading to more homogeneous results than N_2. GAC-virgin presents wider pores than regenerated carbons according to Ar.

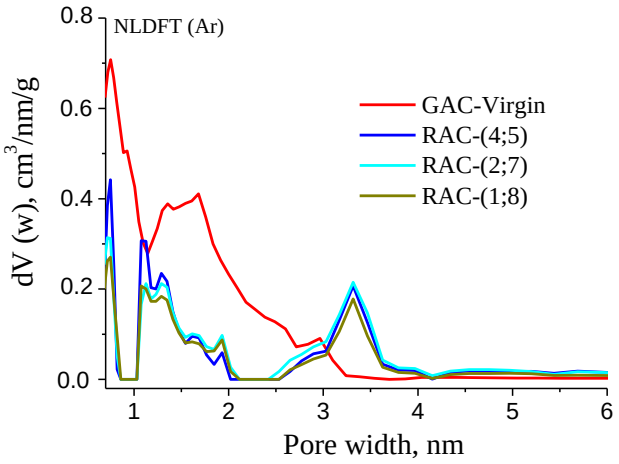

(a)

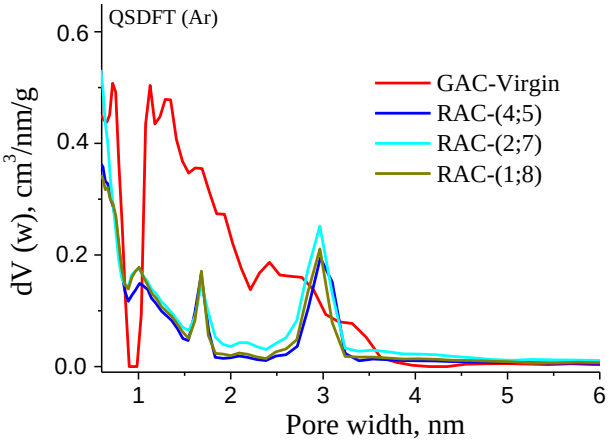

(b)

Fig.4.5: Pore size distribution determined by NLDFT (a) and QSDFT (b) methods using Ar at 87K.

According to the gas sorption results, the significant effect of the applied temperature on the restoration of the porous characteristics in the regenerated GAC is confirmed. Based on Ar, at 450°C the recovering of apparent S_{BET} area and V_{DR} represents about 40 and 46% respectively from the original parameters in the virgin GAC.

In contrast, at 800°C the restoration of the porous characteristics is around 53% for apparent S_{BET} area and 66% for V_{DR}. Similar values can be obtained from N_2 results.

This suggests in the case of the GAC regeneration in rum production, the process must be performed at temperatures at least at 800°C and probably higher than 800°C to obtain larger apparent surface area and volume of pores closer to the virgin material (will discussed later).

A more effective removal of pyrolytic residues could be possible if regeneration was conducted over 800°C as reported in [43] for the regeneration of GAC loaded with organic compounds which in our case produce carbonaceous residues. According to TD-GC/MS results presented in §3.1.2 (Table 3.11 and Figs. 3.16 and 3.17), the found adsorbed compounds in the exhausted GAC in rum production can be classified as **Type III** according to the response to thermal treatment during regeneration [43]. BET analyses confirmed narrow micro-porosity in RAC samples and lack presence of pores in the range of 2-3 nm. Among the predominant compounds detected, phenolics have a significant contribution which was also demonstrated by the colorimetric method. In addition, the presence of tannins and lignin derivated from the oak wood during ageing process can produce a high carbonaceous residual fraction at 800°C according to Tables 1.3 and 1.4.

All detected phenolics and tannins as polyphenols are mainly responsible for the residue deposition in a significant fraction [43]. The presence of dianhydro-glucopyranose in the exhausted GAC as pyrolyzed fraction of carbohydrates suggests the deposition of carbonaceous residues by non-volatile compounds like lignin.

Fig.4.6 shows the signal envelopes generated for the explored RAC samples and GAC-virgin acoustic signals filtered at 1.3 kHz (also including the signal envelope of GAC-Top exhausted). According to Fig 4.6, all the explored samples present a multi-peak pattern in the signal envelope. The virgin GAC is the most complex one. First a shoulder around 5-6 s on the first main multi peak around 9-13 s, with again a shoulder at 14 s can be noticed. A second peak can be observed around 16 s, followed by a broad third one centred at 23 s and a fourth weak one at 34 s, referring to a very variable porous structure, confirming N_2 and Ar probe gas adsorption-desorption results for GAC virgin.

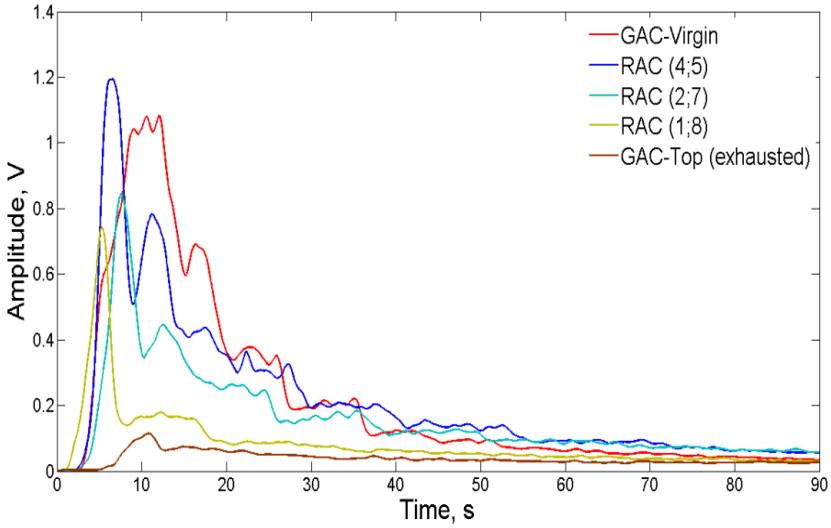

Fig.4.6: Signal envelopes of explored samples (filtered at 1.3 kHz)

In contrast, for the RAC samples, a main initial peak (around 5-7 s) is obtained with high amplitude in comparison with the other peaks; this main peak is associated with the first water – GAC contact. The air is massively released from the GAC pores in a sudden and intense process.

On the other hand, the signal envelope patterns of RAC samples are divers, pointing to differences in surface characteristics. Comparing the envelope pattern of the exhausted GAC with the regenerated and virgin GAC, further significant differences can be noticed. The shape of the pattern and the time window where the main peak is observed for the exhausted GAC-Top gives the first evidence of sensitivity for detecting differences in the porous characteristics between the GAC samples.

After this first broad and less intense peak (around 10 s, with a small preceding shoulder at 5-7 s), the amplitude decays by a rather monotonic slow decreasing amplitude at a function of time. According to Fig.4.6, all peak characteristics depend on the regeneration conditions, the higher the temperature and the residence time applied, the higher the amplitude of the registered peaks. The air released from the GAC pores are related to these peak features. The found results for RMS are more detailed and divers compared to the results of N_2 and Ar probe gas adsorption-desorption experiments.

Differences in shape and signal amplitude are noticeable between samples. Regenerated carbons present a main peak sharper than GAC-virgin which is broader (still bubbling for longer time) and displaced in time. A relationship between the regeneration temperature and the main peak amplitude can be observed. The higher the regeneration temperature, the higher is the main peak. During thermal regeneration, the porous structure and pore size distribution of the GAC change [43], opening new and wider pores and cracks giving water an easier access to the more internal porosity (micro and mesopores).

The pore widening process enhances the fast removal of the air in form of bubbles from the internal pores which in turn creates a sound signal of higher amplitude. The fast filling process of the small pores (via wider pores) produces fast increasing and decreasing of signal amplitude with high slope. Although with apparently different phenomenological nature, actually, the results of both methods, acoustic emission and the volumetric sorption analysis are linked and can not only be correlated but are also complementary. The volumetric sorption analysis is indicating a narrowing process at micro-pore scale, in contrast, the acoustic signal indicates a pores widening process occurring at the same time. An evidence of this phenomenon is presented in Figs.4.4 (a), (b) and 4.5 (a), (b) where a peak for pores distribution around 3-4 nm in the regenerated samples was detected. The structural damage during regeneration is visible in the change in the hysteresis loop, resulting in wider pores (e.g. macro-pores), slits and cracks, and in a larger pore distribution profile in regenerated than in virgin GAC [6,43].

It is a well-known fact that in activated carbons the micro and mesoporosity represents practically the total pore volume and the largest total apparent surface area. In contrast, macropores are not of considerable importance for textural characterization in activated carbons because their contribution to the surface area and pore volume is very small. However, in the adsorption process, macropores enable adsorbate molecules to pass rapidly to smaller pores situated deeper within the particles of active carbons being primarily relevant for the mass transfer into the interior of the adsorbent particles [1-10].

Based on the GAC porous characteristics described above, we can accept that the volume of air displaced by the flooding water which produces the GAC sound in the acoustic emission method is mainly coming from the micro and mesoporous structure of the carbon. As the macropores do not significantly contribute in the total volume of pores in the GAC, their direct contribution to the acoustic signal amplitude in terms of the produced volume of air escaping in form of bubbles can be neglected. Nevertheless, the GAC macroporosity plays an important role in defining the pattern of the acoustic signal envelope. Regarding the significance of GAC macroporosity to give water an easier access to smaller pores enhancing the mass transfer process, in terms of the acoustic emission method, the volume of air in form of bubbles coming from the macro and mesopores finds a fast way out from the carbon particle using the macropores, slits and cracks of the GAC. Therefore producing a massive release of bubbles with a consequent acoustic signal of high intensity with a main peak of high amplitude which abruptly drops after the air is completely removed due to micro and mesopores water filling.

In conclusion, the relationship between the acoustic signal envelope feature and the porous characteristics of the GAC can be summarized in the following types of patterns:

Type I: GAC with high microporosity and macroporosity: A broad main peak of high amplitude followed by a systematic decreasing trend featured by secondary peaks of comparable amplitude. The larger the volume of micropores, the broader is the signal peak.

Type II: GAC with high microporosity and low macroporosity: A broad main peak of moderate amplitude and delayed in time scale followed by a smooth decreasing trend slope featured by secondary peaks of comparable signal intensity which are gradually attenuated.

Type III: GAC with low microporosity and high macroporosity: A sudden and sharp main peak of very high amplitude followed by an abrupt decreasing trend featured by fewer secondary peaks of low amplitude. The lower the volume of micropores, the shorter is the initial main peak.

Type IV: GAC with low microporosity and macroporosity: A broad main peak of very low amplitude and delayed in time scale followed by a monotonic smooth decreasing trend slope without significant secondary peaks.

At relative low regeneration temperature (450-600°C) the main and second peaks for RAC (Fig. 4.6) indicate that the adsorbed compounds are not being efficiently desorbed at this temperature range, keeping part of the pores blocked or/and maybe producing carbonaceous residues giving a **Type III** signal envelope pattern. Therefore, a broader and higher second peak for RAC indicates better restoration of internal porosity. At 800°C, the behavior of the envelope curve for RAC (4;5) follows a different pattern. In this case, the main and second peaks are higher than the other RAC samples trending to a **Type I** signal envelope behavior. The difference is more noticeable if the second peaks are compared. As the intensity of the peak amplitude can be associated to the accessibility to the pores with a consequent massive air release in form of bubbles, we can accept that at 800°C the adsorbed compounds and carbonaceous residues were better removed from the pores but creating a widening process in the original GAC porous structure at macro scale.

The initial peak of the exhausted GAC-Top can give us evidences that relate the main peak with the water accessibility to the internal porosity (pattern **Type IV**). The main peak slope of the GAC-Top is not so high; the water takes more time to get access to inner pores as adsorbed organics compounds are blocking and narrowing the majority of the pores. As the GAC virgin has not been regenerated, keeping its original integrity, the signal intensity is higher than the one of the regenerated samples, because of loss in and less accessible pore structures thus describing a **Type I** pattern.

Taking into account the second peak amplitude; differences between RAC samples are more noticeable. According to this, the second peak can be interpreted as the formation of "internal" less accessible (narrow) porosity in the material, at 800°C (RAC (4;5)) the regeneration was better than at 450°C (RAC (1;8) describing a **Type III** pattern) and more available pores were formed. In the case of GAC virgin, the main peak is sharing the same time-space scale of the second peak for regenerated samples, it can be assumed that GAC virgin contains more internal pores. In regenerated samples, a visible third peak is only found after regeneration at 800°C.

Based on gas adsorption and acoustic emission analyses, the regenerated GAC samples are structurally different from the virgin GAC and exhausted GAC samples. The regeneration process produces changes in the GAC grain and in its porous structure. From one side; carbonaceous residues of adsorbed organic compounds found in exhausted GAC (e.g. aromatics, phenolics and carbohydrates which were classified as **Type III** according to the carbonaceous residue deposition after regeneration [43] see Table 1.3 and 1.4 in §1.10.2) lead to narrowing micropores; while the thermal treatment under steam-oxidizing environment produces structural damages in the GAC particles, opening wider pores (at meso and macro scale), slits and cracks in the regenerated carbons [43]. The area under the envelope curve "integral" (sound surface (SS) expressed in V·s) was used as parameter to correlate with the gas sorption characterization. The integral area under the envelope curve (SS) can give information about the total rate of produced bubbles and its volume. Thus, it provides information about the bubble potential produced by GAC during the whole bubbling process in time domain. As these air bubbles are formed by air escaping from the GAC pores, SS value can be correlated with the volume of pores of granular activated carbons.

In Figs. 4.7 (a) and (b), the correlations between V_{DR} and S_{BET} with SS are depicted for both gases. According to the plots presented in Fig.4.7, satisfactory non-linear correlation between SS and the porous structure parameters of GAC can be proposed.

In both cases (Ar and N_2) a decreasing polynomial or exponential decay model can be fitted in order to estimate the apparent S_{BET} surface and V_{DR} based on acoustic measurements.

The non-linear correlation found between both methods is not unexpected considering that the acoustic phenomenon obeys to a logarithmic function.

Table 4.3 displays the parameters and characteristics of experimental data fitted at exponential decay first order (eq. 4.1). Comparing the correlation coefficients between N_2 and Ar; a better correlation was found for argon. Additionally, by a comparative inspection on the plots presented in Fig.4.7, based on the sequential trajectory and the distribution of the data points, a more sensitive correlation for Ar can be noticed, especially in the case of V_{DR}.

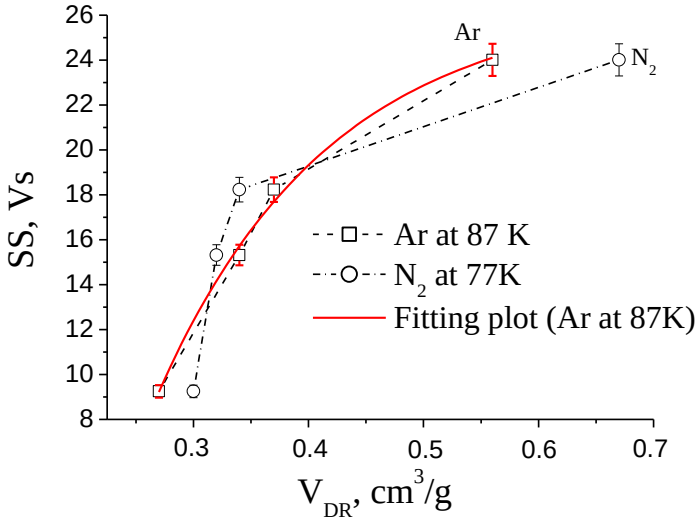

(a)

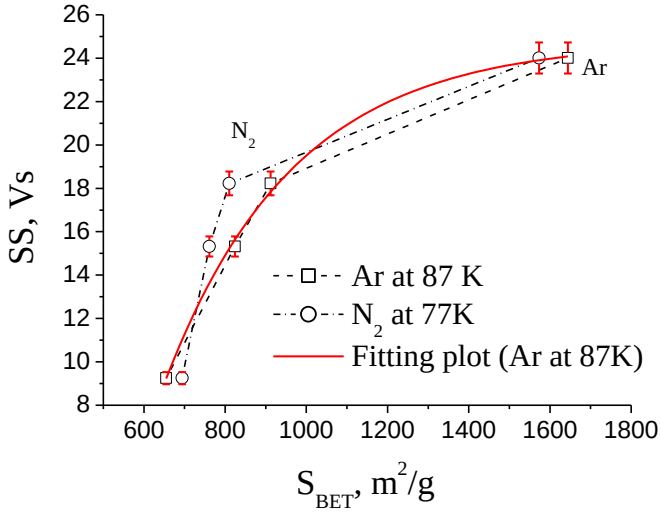

(b)

Fig.4.7: Correlation between the porous characteristics of GAC samples using two probes gases and the sound surface SS. (a) volume of pores and (b) apparent surface area.

Table 4.3: Parameters of experimental data fitted at exponential decay first order (eq.4.1).

Gas		y_0	e (y_0)	A	e (A)	t	e (t)	R^2
Ar	$\mathbf{V_{DR}}$ (cm^3/g)	26.3	± 1.6	-113	± 37	0.14	± 0.03	0.996
	$\mathbf{S_{BET}}$ (m^2/g)	24.7	± 0.7	-127	± 29	311	± 37	0.999
N_2	$\mathbf{V_{DR}}$ (cm^3/g)	25.3	± 5.2	-204	± 87	0.11	± $8{\cdot}10^{-3}$	0.873
	$\mathbf{S_{BET}}$ (m^2/g)	25.1	± 3.1	-293	± 7	229	± 80	0.939

e (i) : error associated to the parameter

$$y = y_0 + A \cdot e^{-\left(\frac{x}{t}\right)} \tag{4.1}$$

The drastic change in the curve slope (Fig. 4.7 (a) and (b)) in the section between 18 and 24 Vs for N_2 is not observed in the case of Ar. The abrupt change in the tail of the curve makes a less linear correlation between the parameters of both methods visible, being difficult to estimate porous characteristics in this zone as a small increment in the SS value, representing an important change in the volume of pores and the apparent surface area. In contrast, the found correlation with Ar and V_{DR} (Fig. 4.7 (a)) is rather smooth in terms of the data distribution, giving a less abrupt change in the curve tail, thus, more suitable to predict porous characteristics in this zone than N_2.
This plot behavior when Ar is applied is in line with the suitability of argon at 87 K as probe gas to correlates with acoustic emission method instead of N_2 at 77K. Therefore in figure 4.7 only the fitting plot for Ar is shown.

According to both results, the order in the regeneration (activation) degree in the explored samples can be proposed as follows:

GAC-virgin > RAC (4;5) > RAC (2;7) > RAC (1;8) > GAC-Top.

According to the BET analysis and acoustic emission method, the regeneration of the GAC used in rum production must be conducted at temperatures higher than 800°C (and lower than 950°C [43]) in order to remove the carbonaceous residues damaging as less as possible the carbon structure and its mechanical properties.

Based on reported results [2,5,8-10,43]; regeneration at 850°C under steam atmosphere usually provides an optimal activation degree in carbons loaded with organic molecules. Therefore, regeneration was also conducted at this temperature (RAC (5;4) in Table 4.1).

Fig.4.8 depicts the kinetic behavior of the regeneration performance at different temperatures based on the sound surface (SS) as parameter. The plots were performed using the data presented in Table 4.1.

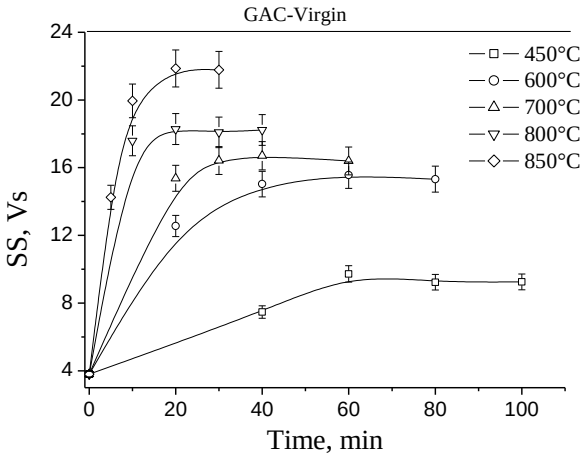

Fig.4.8: Kinetic curves of the regeneration process at different temperatures based on SS as parameter.

The line located at 24.01 Vs represents the sound surface of the virgin GAC as model. In this case, samples regenerated at 850°C are now analyzed and compared with the others. The error involved in each measurement has been presented in the plots as error bars. Significant statistic differences in the SS values at different regeneration temperatures were found between RAC samples. However, the residence time was statistically significant in a specific range for each temperature applied. Initially in the regeneration process, the residence time plays an important role on the regeneration degree reached.

This initial stage is different according to the applied temperature. Comparing plots presented in Fig.4.8 after this period, the regeneration degree expressed as SS is basically the same (no significant statistical differences were found) creating a plateau with a statistically constant value of SS.

This plateau is indicating that the thermal removal of adsorbed compounds has ended at that temperature. In that point, independent of the applied residence time, the regeneration degree does not change any more. Therefore, an optimal/minimal residence time can be found for each temperature; e.g. 450°C/60 min; 600°C/60min; 700°C/40min; 800°C/20min and 850°C/20min.

Based on these results, the higher the temperature applied, the faster is the regeneration process. This is in line with the influence of temperature over the thermal desorption and activation rates discussed in §1.10.2 [2,8,10,43].

Analyzing Fig. 4.8 another interesting feature can be observed by comparing the curves. Differences in the regeneration kinetics curves at 450°C and 600°C are quite noticeable with a significant gap between SS values at optimal residence time. This difference (gap) is not so large between 600 and 700°C neither between 700 and 800°C. In the range of 800-850°C again a quite significant gap is observed.

In order to properly compare the effect of temperature over the regeneration process based on acoustic analysis; a derivative SS in function of temperature (DSST in Vs/°C; homologous to TDG in %/°C in TGA analysis) can be enabled; thus DSST can be calculated as:

$$\mathrm{DSST} = \left(\frac{\Delta \mathrm{SS}}{\Delta \mathrm{T}}\right) \tag{4.2}$$

DSST represents the change of the regeneration degree reached as a function of the temperature gradient expressed in terms of SS.

Fig.4.9 presents the DSST values for different ranges of regeneration temperatures applied. DSST was calculated using the data presented in Table 4.1 according to the optimal residence time for each temperature.

In the range 450-600°C, DSST is higher than DSST for 600-700°C and 700-800°C. In contrast, the highest value of DSST is observed for 800-850°C.This confirms the strong influence of temperature in the regeneration process and conclusions formulated in the discussion part of Fig. 4.8.

Fig.4.9 suggests that at 600°C a thermal desorption of the majority of adsorbed volatile and semi-volatile compounds occurs. Between 600 and 800 °C pyrolysis of non-volatile compounds occurs but leaving carbonaceous residue.

The removal of these pyrolytic residues, take place above 800°C increasing the RAC porosity; thus, larger SS values are obtained. The same conclusion can be deducted if the signal envelope curves presented in Figs.4.6 and 4.10 are compared.

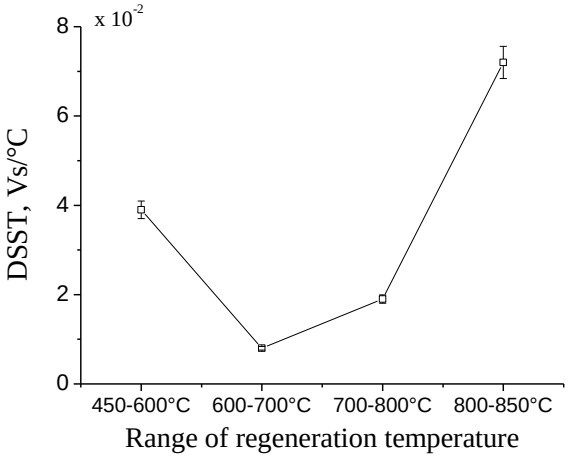

Fig.4.9: DSST for different temperature ranges

Fig.4.10 depicts the signal envelopes at 1.3 kHz for regenerated samples at different temperatures. In order to have a sequential and general overview about the regeneration process, GAC-Top (exhausted) and GAC-virgin have also been included.

The effect of the temperature on the regeneration process can be noticed by comparing the signal envelope curves not only in terms of the amplitude and integrated area "SS" but also in terms of the curve shapes.

The GAC exhausted presents almost no sound surface in comparison with the rest, the first peak is not well defined and delayed in time (pattern type IV). This behaviour is consistent with a poor accessibility of water to inner pores for displacing the air, the lack accessibility is due to adsorbed organic compounds which are blocking pores, slits and cracks thus creating a resistance to the water intrusion into de particle and reduced volume of air displaced.

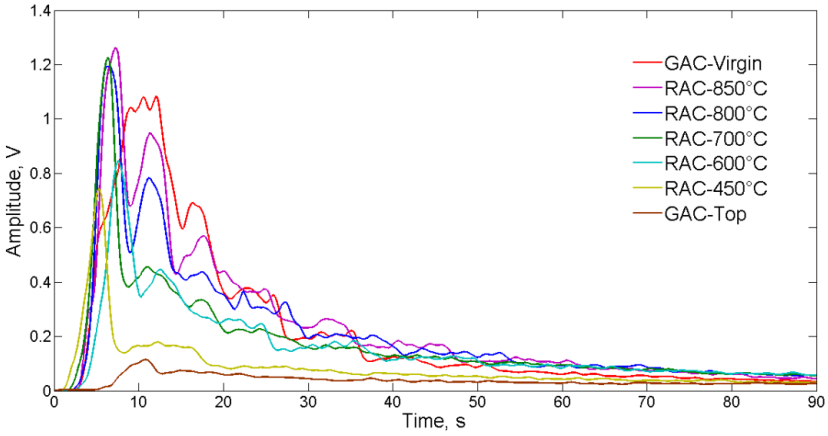

Fig.4.10: Signal envelopes of regenerated carbons at different temperatures

Comparing envelopes at 800°C and 850°C some differences can be found. The first peak has similar amplitude; therefore 850°C seems not affect structurally the GAC particles more than when 800°C is applied. However, the second peak found in the 850°C signal is significantly higher than the second peak in the 800°C signal, approaching the amplitude of the GAC-virgin peak. The third peak for the 850°C signal is substantially higher than the peaks observed for the rest of regenerated samples with a similar shape to the second peak of GAC-virgin but with less amplitude. Actually, the RAC at 850°C presents more similar envelope shape in comparison with GAC-virgin than the other RACs. However, despite the increment of regeneration temperature, evident differences between virgin and regenerated GAC remain obvious.

Fig.4.11 presents the signal envelopes of RAC at 850°C at different residence times. After 20 min, no statistical differences between the regeneration degrees reached in terms of SS were found, corresponding with the kinetic curves of the regeneration process at different temperatures presented in Fig.4.8. However, a third peak with of relative high amplitude and delayed in time space in around 18 s is noticeable for RAC after 20 min of thermal regeneration at 850°C. This can be associated with a better repair of the internal porosity trending to the type I pattern of the signal envelope.

Based on the results obtained by BET and acoustic emission analysis, the regeneration of the exhausted GAC in rum production must be conducted at 850°C, optimum/minimum residence time: 20 min feeding to the reactor about 1kg of steam/kg of exhausted GAC.

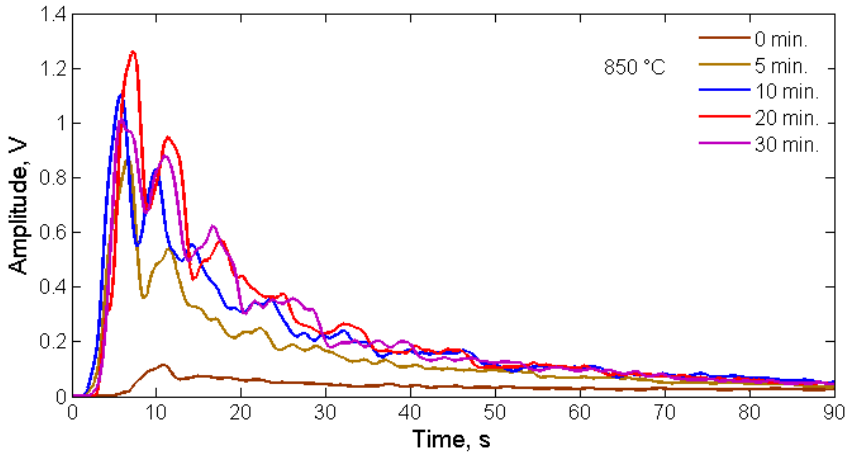

Fig.4.11: Signal envelopes of RAC at 850°C at different residence times.

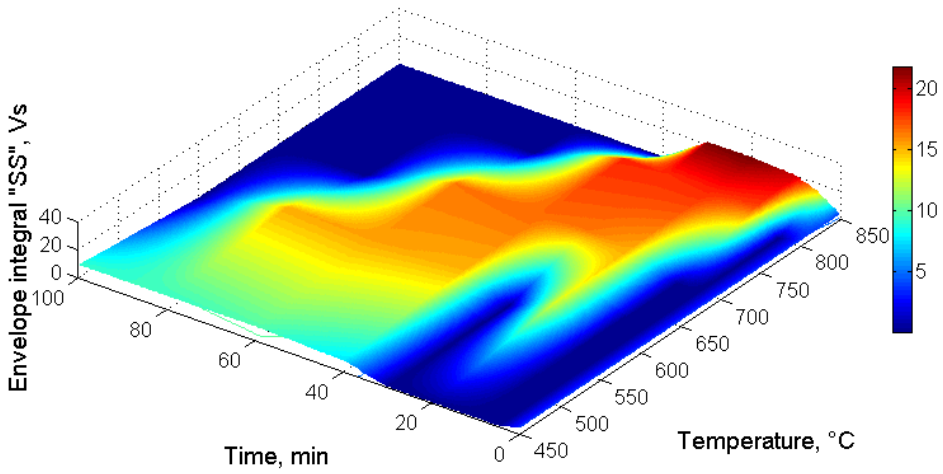

Fig 4.12: Surface plots of the signal envelope behavior

Fig.4.12 displays the surface plots of the signal envelope behavior in terms of integral sound surface (color scale), temperature and time.

At 850°C and 20 min of residence time, the regeneration degree is the highest in terms of SS. Under such conditions (850°C/20 min), the regenerated carbon (RAC) produces a sound with a SS value of around 21.8 Vs. (Table 4.1).
According to the exponential decay model presented in eq.4.1 and fitted parameters in Table 4.4, the porous characteristic of the regenerated GAC (S_{BET} and V_{DR}) can be estimated by SS:

SS correlation for Ar at 87K (eq.4.1)
V_{DR} = 0.48 (± 0.06) cm^3/g and S_{BET} = 1268 (± 52) m^2/g
SS correlation for N_2 at 77K (eq.4.1)
V_{DR} = 0.47 (± 0.07) cm^3/g and S_{BET} = 1105 (± 43) m^2/g

The estimated porous characteristics of the RAC at 850°C based on acoustic analysis for both gases are showing an increment of the regeneration degree at this temperature. However, the estimated values of V_{DR} and S_{BET} are still lower than found values for the GAC-virgin. In contrast, based on acoustic estimation, at 850°C better restoration of the porous characteristics is obtained in comparison with the other regeneration conditions explored. In that case, considering the found correlation between SS and the porous characteristics determined by gas sorption, a restauration of about 77% of the apparent surface area and around 86% of the volume of pores in terms of Ar at 87K was found. Analogous results were obtained for the porous characteristic in terms of N_2 at 77K based on the acoustic analysis correlation: about 70% of apparent surface area and volume of pores were restored after regeneration at 850°C.

4.1- Regeneration at industrial scale of the exhausted GAC in the rum production

According to studies reported, [1,2,4,43] on-site regeneration is generally not cost-effective unless the carbon exhaustion rate is over 910 kg per day. Off-site regeneration is considered if the spent adsorbent generation rate is less than 225 kg per day.In case of thermal regeneration, which is most common, the temperature of regeneration determines the place for the regeneration process. Off-site regeneration is preferred when regeneration temperature is between 700-950^{0}C, moreover because of liability and economic concerns, many design manuals recommend that regeneration should be done off-site whenever

possible, regardless of whether land and utilities are available on-site [1, 43]. The adsorbent losses due to attrition have been estimated as 5-10% for in on-site regeneration and 10-15% for off-site regeneration [1,2,4,43].

Therefore considering the GAC exhaustion rate in Cuban rum factories (10-12 ton/year =27-33 kg/day) and the range of the needed regeneration temperature (850°C); the off-site regeneration is more suitable than its on-site counterpart. In this case, the regeneration cost is highly dependent on the cost of the off-site regeneration service.

Analytical methodologies presented in chapter 3 demonstrated that a fraction (about 1/3) of the total amount of the GAC in the rum filters can be saved and reused back to the primary rum (aged aguardiente) filtration process. The other fraction can be regenerated off-site paying the regeneration service in an activated carbon manufacturing plant.

As it was presented in section §2.6.2, the regeneration process at industrial scale was performed off-site in the industrial plant for producing activated carbon using a rotatory kiln located in the municipality of Baracoa (eastern of Cuba).The main technological characteristics and operational parameters of this plant were previously presented in Table 2.4 (§2.6.2) and Fig.S1 in supplementary materials.

According to the gas sorption and acoustic emission results in terms of temperature and optimal residence time at experimental scale to be applied, 20 min at 850°C feeding 1kg of steam/kg of GAC produces a better restoration of the porous characteristics.

Based on these results, the industrial rotatory kiln in the plant was prepared to reproduce as close as possible the optimal regenerating conditions. The main operational parameters of the rotatory kiln to perform the regeneration process at industrial scale are depicted in Table 4.4.

The rotatory kiln was loaded with 432 kg of exhausted GAC. The exhaustion level of the material was confirmed based on the methods proposed in chapter 3 (colorimetry, acoustic emission and bubblemetry).

After regenerating the GAC exhausted in the industrial reactor according to the parameters depicted in Table 4.4, a yield of 234 kg of RAC was obtained. The general aspects of the material balance found in the regeneration process at industrial scale are presented in Table 4.5.

Table 4.4: Main operational parameters of the rotatory kiln to perform the regeneration process at industrial scale

Parameter	**Unit**	**Value**
Temperature	°C	850
Residence time	min	30
Load capacity	kg	432
Heating rate	°C/min	2
Steam flow	ton/h	1
Steam/carbon ratio	(kg of steam/kg of GAC)	1.16

Table 4.5: General aspects of the material balance of the regeneration process at industrial scale

	Mass of material (kg)	**Apparent density** (kg/m^3)	**Volume*** (m^3)	**Efficiency in terms of:** (%)	
Exhausted GAC (in)	432	550	0.8	**Mass**	**Volume**
Regenerated GAC (out)	234	395	0.6	54.2	75.4

***** The volume of material was calculated using the apparent density.

Concerning to the material balance, the apparent density of the carbon is an important aspect not only for the technological analysis but also from the economic view point (it will be discussed further on). According to Table 4.5, the apparent density of the material before and after regeneration is quite different. As expected, the regenerated carbon has less apparent density (about 30% less) than the exhausted GAC.

This result is in line with the TG curves performed in an inert N_2 atmosphere presented in Fig. 3.6. Based on TGA results, the exhausted carbon presented a mass loss of 20% above 500°C and the other 10% can be attributed to the selective burn-off of the adsorbed material and part of the carbonaceous matrix to create new porosity during the pyrolysis and activation stages in regeneration (§1.10.2).

In contrast, comparing the yield of volume of material after regeneration, results are not as different from the reported typical loss as in the case of the mass yield. The regeneration efficiency in terms of mass and volume of material depicted in Table 4.5 indicates that after regeneration, a loss of about 50% and 25% occurs in term of mass and volume of carbon respectively.

Both parameters in the material balance (mass and volume) are quite different from the range of 10-15% of loss during off-site regeneration (§1.10.2).

However, the relative high value in the loss of material during the regeneration of the GAC exhausted in rum production can be justified by analysing the different losses during the process. The main losses which influence the relative low yield in this first regeneration at industrial scale are:

1- **High amount of adsorbed organic compounds in the GAC exhausted**.

They represent about 20% of total mass of the GAC exhausted.

2- **Operating conditions in the industrial reactor.**

Oxidizing atmosphere enhances the burn-off process of the adsorbed material and part of the carbonaceous matrix during pyrolysis and activation which induces structural damage occurred largely by the conversion of smaller pore types to larger ones. Additionally, the rotatory movement of the industrial kiln (different from the static reactor at experimental conditions) produces mechanical attrition of the material (mainly on fragile GAC grains which has been previously damaged by exploitation in the rum production process), thus creating dust which is continuously removed from the reactor using the exhaust gas extraction system installed in the kiln.

3- **Insufficient amount of material to be processed.**

The reactor was designed for 1 ton of circulating material. In this first regeneration experiment at industrial scale, the reactor was loaded at less than 50 % of its operational loading capacity. Before the regeneration process, the reactor was completely cleaned in order to avoid contamination with remains of other activated carbons usually produced in the plant from other precursors such as: coconut shell or wood which can contaminate the regenerated material, thus producing erroneous results. The rotatory kiln is equipped with a screw conveyors system to feed the carbonaceous precursor into the rotatory reactor tube. The conveyors are specially designed to transport granulated material within a particle size range of 5-20 mm, considering the size of the exhausted GAC to be regenerated (0.8 mm), an amount of the material is retained in the conveyor system specifically in the gap formed between the screw and the conveyor's bottom. The fraction of retained material in the transport system is more significant as less as the amount of processed material.

This loss of material in the conveyor system has a constant value, thus its influence on the yield of the regenerated GAC can be neglected if the GAC feed to the reactor is high enough. Then, taking into account the amount of processed GAC and the size of the reactor employed, the loss of material attributable to the conveyor system has to be considered.

Based on the material balance analysis focused on the loss of GAC, the yield in the regeneration process can be improved by increasing the amount of material to be regenerated. However, considering the TGA results, the amount loss in the regeneration of exhausted GAC in rum production will never reach a value less than 20% in term of mass, correspondently; the maximum expected yield will be 80%.

On the other hand, the volume yield is more important for rum producers than the mass yield. The rum filters (cylindrical contactors) must be filled to prepare the GAC bed independently of the mass of the material used. The optimum filtration flow, liquid velocity and contact time between the aged aguardiente and the GAC to obtain the desirable organoleptic characteristics in the rum, are parameters highly dependent not only on the GAC characteristics but also on the GAC bed height. Therefore, the mass of material in the GAC bed has a minor influence during the rum filtration design.

The regenerated GAC at industrial scale (234 kg) was stored in paper bags of 10 kg and sent back to the rum factory in order to prepare an experimental industrial rum filter for refining aged aguardiente (Fig.S4).

The regenerated GAC at industrial scale was characterized using the acoustic emission method. Each bag with regenerated GAC was sampled. Twenty four samples of 10 g (240g in total) were mixed to create one homogeneous sample of industrially regenerated GAC. The regenerated-mixed sample was acoustically measured in five independent experiments. The parameters to perform the acoustic measurements and analysis were also confirmed. The cut-off frequency (frequency of interest) to assess the regenerated GAC at industrial scale was determined (1.3 kHz) to ensure the correct acoustic characterization. After the regeneration process in the industrial reactor, the sample showed a very similar feature of RMS, spectrogram and frequency component distribution (Fig.S5) in comparison with the other GAC samples presented in the Fig.4.1.

Fig.4.13 presents the acoustic signal envelopes filtered at 1.3 kHz of the regenerated GAC at industrial scale, GAC-virgin and GAC exhausted.

According to Fig 4.13, the multi-peak pattern in the signal envelope of the regenerated GAC is again observed. A sharp main peak around 6 s at high amplitude related with a fast and intense bubbling process is suggesting a widening process in the original GAC porous structure. Comparing the main peak of the industrially regenerated GAC with the regenerated GAC under controlled conditions in the laboratory, differences can be noticed.

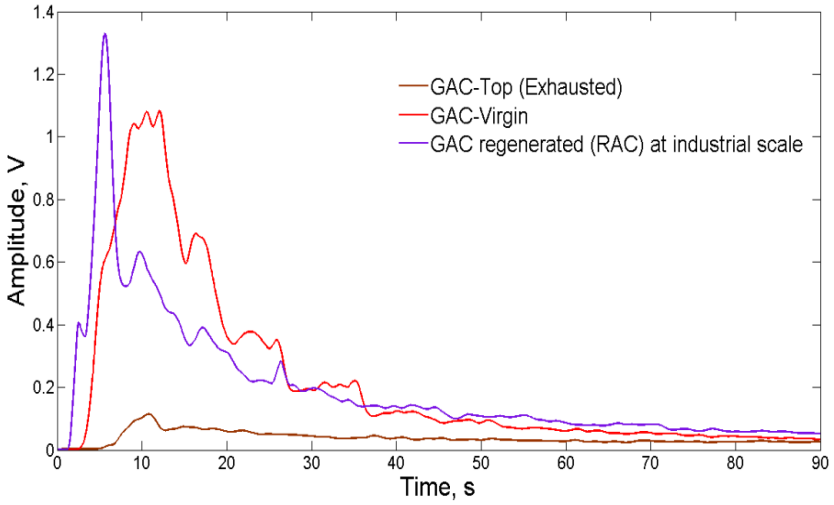

Fig.4.13: Signal envelopes of the regenerated GAC at industrial scale, GAC-virgin and GAC exhausted (filtered at 1.3 kHz)

The regenerated GAC at industrial scale presents the sharpest main peak which abruptly decayed in amplitude. Although the signal envelope pattern of the industrially regenerated GAC shows a recovering of porous characteristics, the found pattern is closer to Type III than Type I as in the case of GAC lab-scale regenerated which behaves trending to the virgin GAC pattern. The bubbling production for the industrially regenerated carbon starts almost immediately in a very sudden process after contact water-GAC. This initial behavior can be associated not only with the formation process of new and wider pores but also with an extra structural damage of the GAC particles because of the technological characteristics of the used reactor (discussed in supplementary

materials, Fig.S1(c)) and the mechanical stress during the rotation movement of the kiln thus creating a colliding and attrition effect between the GAC particles.
The mechanical stress enhances the formation of slits and cracks in the external surface of the carbon particle creating easier access to the water, therefore producing an initial intense bubbling process which is translated in a high and sharp main peak.
A second peak around 10 s and 0.6 V of intensity is observed. This peak is shorter than the second peak found for the lab-scale regenerated GAC in analogous conditions (850°C/20 min) (Fig.4.11) and it is somewhat later visible than 11 s and with different shape. Consequently, the decay slope to reach the third peak (16-18 s) is not as abrupt as in the case of the GAC lab-scale regenerated. This signal envelope behavior of the industrial generated GAC pointing to the removal of adsorbed compounds and carbonaceous residues is different compared to the regeneration performed in the lab at the same temperature. Certainly the continuous mixing of the GAC in the industrial installation compared to the lab-scale one, being not moved, will influence the carbon external surface in a different way.
The sound surface (SS) of the signal envelope for the industrially regenerated carbon was also calculated. A normal distribution for the acoustic emission results was confirmed. The averaged value of the SS for the regenerated GAC at industrial scale was:
SS=18.79 V·s (+/- 0.6 V·s)
According to the exponential decay model presented in eq.4.1 and fitted parameters in Table 4.4, the porous characteristic of the industrially regenerated GAC (S_{BET} and V_{DR}) can be estimated by SS as follows:

Porous characteristics estimated for Ar at 87K (eq.4.1)
V_{DR} = 0.39 (±0.04) cm^3/g and S_{BET} = 966 (±41) m^2/g
Porous characteristics estimated for N_2 at 77K (eq.4.1)
V_{DR} = 0.36 (±0.03) cm^3/g and S_{BET} = 842 (±38) m^2/g

Based on the estimated porous characteristics using the acoustic method, the repair of textural properties at industrial scale is lower than the regeneration results found in the lab experiments at the same conditions of temperature and residence time, but with different motion conditions.

The industrially regenerated carbon shows a restoration of about 60% of the apparent surface area and around 70% of the volume of pores in terms of Ar at 87K. The porous characteristic in terms of N_2 at 77K based on the acoustic analysis correlation showed about 54% of restoration of apparent surface area and volume of pores. Nevertheless, an adjustment of the operational parameters in the regeneration process at industrial scale can be considered in order to improve the porous repair of the regenerated carbon. Parameters such as residence time and rotating velocity in the reactor have to be further studied to improve the structural characteristics of the RAC particle.

4.1.2- Sensorial judgment of the filtered aged aguardiente using the regenerated GAC

The industrially regenerated GAC (232 kg/ 0.6 m^3) was placed in an industrial rum contactor (industrial experimental filter) at the same target rum factory (Fig. S4). The filter was connected to the rum production process under the operational supervision of the rum masters. The triangle test method described in § 2.7 was applied to detect if the refined aged aguardiente presents sensorial differences when filtered using RAC.

A board consisting of 11 rum taste experts was engaged for the triangle test. 4/11 members detected the different product (refined aged aguardiente using RAC). In this case, for 11 experts in the board, the minimum of correct detections needed to conclude that the products are statistically different is 6 (using 80 % of statistical significance/ risk level: α=20%). Therefore, the products had not perceptible organoleptic differences and the RAC can be effectively reused in the rum production process (considering just one regeneration cycle so far).

4.2- Economic assessment and facilities for the regeneration process at industrial scale

As described in §4.1, the regeneration at industrial scale was performed off-site. Therefore, the cost to regenerate GAC basically depends on the payment to the AC factory for the regeneration service. Additionally, to properly evaluate the economic benefits of the new proposed of GAC management, not only the regeneration has to be considered.

The performed methods for characterizing the exhaustion level of the GAC in the rum filter demonstrated that a fraction (about 30%) of the total amount of the GAC in the rum filters can be saved and reused back to filtration process.

Therefore, the economic assessment for the new GAC management in the rum production process must cover the analysis of the combined strategy of regenerating and GAC saving. An economic model has been created based on a material balance for the new GAC management proposal.

Economic model for the new proposal of GAC management

The filtration of aged aguardiente in rum production is a non-continuous process, after certain period (depending on the rum factory production rate) the exhausted GAC is removed and replaced by virgin GAC. However, according to this cycle of exploitation of the activated carbon in the industry, a consideration of continuity can be proposed.

At present, a certain amount of activated carbon is required for filling the volume capacity (V_0 (in m^3)) of the GAC contactors, this volume of virgin GAC ($V_V = V_0$) is exhausted in a time t_v (in years). Therefore, at the current GAC management conditions in rum industry, the overall volumetric flow of virgin GAC Q_v' (in m^3/year) can be calculated as:

$$Q_v' = \frac{V_v}{t_v} = \frac{V_0}{t_v} \tag{4.3}$$

Fig. 4.14 (a) depicts the present model of GAC exploitation in Cuban rum factories. In that case, as no strategy of reusing or regeneration of exhausted GAC is applied, the produced volumetric flow of exhausted GAC: Q_e (in m^3/year) = (V_e / t_v) = Q_v'. Fig.4.14 (b) shows the schematic diagram of the new GAC management proposal.

After the GAC is declared as exhausted by the rum specialists, a fraction of this volume of GAC ($x_s \cdot V_0$) is saved as "saved activated carbon" (SAC) as its exhaustion degree is less (determined by methods discussed in Chapter 3). The other fraction of exhausted GAC, ($(1-x_s) \cdot V_0 = V_e$) is sent to the off-site regeneration process. During regeneration, a part (V_L) of the total volume of exhausted carbon feed to the regeneration reactor is lost. The amount of regenerated GAC (RAC) (V_r) is sent back to the rum production process.

A volume of virgin GAC (VAC) (V_v) must be introduced in the process to complete the required GAC amount to restore the loss incurred during regeneration.

Then, the volume V_0 of "new" GAC material in the process will be a mixture (V_m) composed by SAC+RAC+VAC. Therefore, the volume of mixture can be expressed as $V_m = V_s + V_r + V_v$.

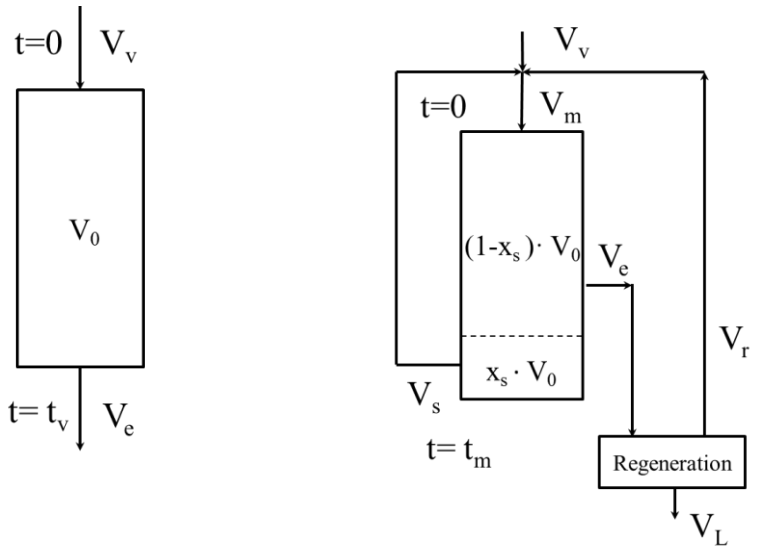

(a) (b)

Fig.4.14: Management of GAC in rum production. (a) at present time, (b) proposal for saving and regenerating GAC .

Additionally, the steps for filling up the filter with the GAC mixture must be performed as presented in Fig. 4.15.

Firstly, following the original process, the rum filter is filled with virgin GAC ready to be used in aged aguardiente refining (a) in a time $t_0 = 0$. After a period of exploitation (t_1), the filter is declared "out of service by exhaustion" applying the sensorial judgement of rum specialists (b).

The next step is to perform quantitative methods (colorimetry, acoustic emission or bubblemetry) to determine the GAC exhaustion level in the filter's bed.

After determining the exhaustion profile in the rum filter, the exhausted GAC is send to a regeneration installation and the partially exhausted GAC (located near to the filter's bottom) is saved to refill the contactor according set-up (c).
Initially, the first volumetric fraction of the filter is filled with virgin material followed by the regenerated carbon.

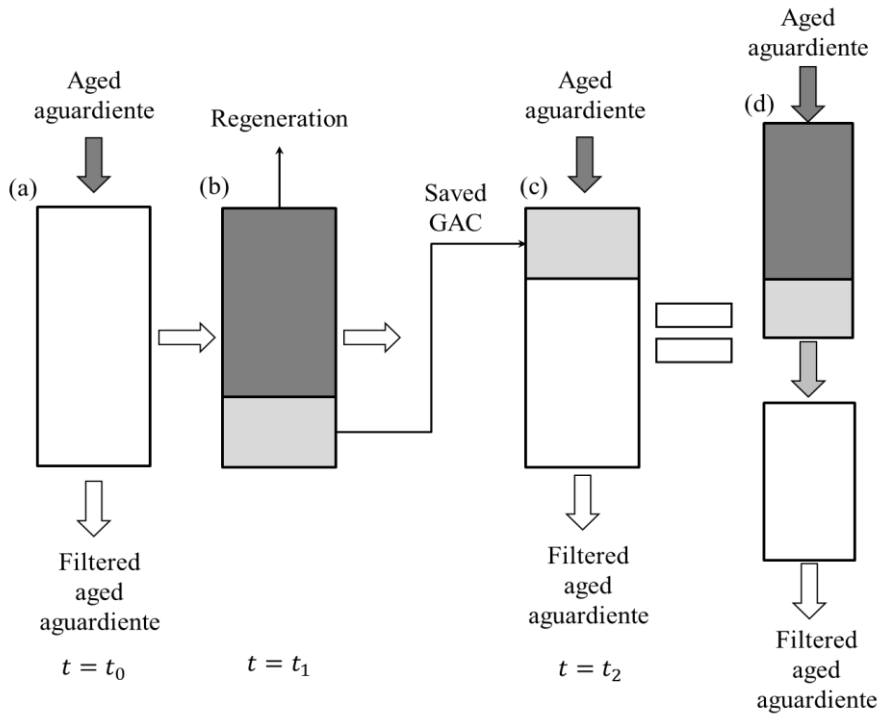

Fig.4.15: Scheme of the GAC saving strategy in rum production. White: virgin and/or regenerated GAC. Dark gray: Exhausted GAC. Clear gray: partially exhausted GAC (saved).

The partially exhausted GAC (saved) will then be placed in the top layer. The GAC layers must be placed in the filter following a sequential order according to the GAC adsorption potential. Actually, the GAC layer order proposed in (c) is equivalent to a fresh GAC contactor in a series arrangement below the effluent of the exhausted rum filter (d). In this way, an extensive, better and more efficient use of the GAC can be obtained compared with other possible GAC layer arrangements based on the adsorption wave theory.

The time of exploitation of this contactor (c) will be different and shorter than the one in (a), being t_2

However, the consumption rate of this mixture depends on the time-of-exploitation (t_m) in operation of the new mixed material.

Hence:

$$Q_m = \frac{V_m}{t_m} = \frac{V_0}{t_m} \tag{4.4}$$

Taking a reference of GAC volume " V_0" , and working at the same liquid flow regime, each type of carbon introduced in the process will have a capacity of time-of-exploitation " τ_i" (in year/m^3). According to this, τ_i can be expressed as:

$$\tau_i = \frac{t_i}{x_i \cdot V_0} \tag{4.5}$$

where

t_i : Time-of-exploitation of a part of volume V_0 of an "i" GAC (in year)

If each type of material is a fraction of the total amount of adsorbent, the time-of-exploitation in the mixture (t_m) can be assumed as:

$$t_m = \sum_{1}^{n} (x_i \cdot V_0) \cdot \tau_i \tag{4.6}$$

Being "n", the number of type of adsorbents, in our case: 3

In this case:

$$t_m = (x_s \cdot \tau_s + x_r \cdot \tau_r + (1 - x_s - x_r) \cdot \tau_v) \cdot V_0 = t_s + t_r + t_v \tag{4.7}$$

t_s , t_r , t_v : Time-of-exploitation of a volume $x_i \cdot V_0$ of saved, regenerated and virgin GAC respectively (in year).

x_s , x_r : Volumetric fraction of saved and regenerated GAC respectively

Taking the GAC virgin as model, the time-of-exploitation of each adsorbent can be expressed in terms of τ_v as follows:

$$\tau_i = \beta_i \cdot \tau_v \tag{4.9}$$

With β_i is the fractional capacity of time-of-exploitation in terms of τ_v of the material "i". As expected, the virgin GAC presents more adsorption capacity than the regenerated and saved GAC. Therefore, the value of the fractional capacity of time will be ranging: $0 < \beta_i \leq 1$

Taking all this into account and combining eqs. (4.4), (4.8) and (4.9), equation (4.10) is obtained:

$$Q_m = \frac{V_0}{(x_s \cdot \tau_s + x_r \cdot \tau_r + (1 - x_s - x_r) \cdot \tau_v) \cdot V_0} = \frac{1}{(x_s \cdot \beta_s + x_r \cdot \beta_r + (1 - x_s - x_r)) \cdot \tau_v} \quad (4.10)$$

Hence, combining eq.(4.3) and (4.10), one obtains
[as $Q_v' = V_0/t_v = V_0/(\tau_v \cdot x_v \cdot V_0)$ with x_v equal 1 and thus $Q_v' = 1/\tau_v$]

$$Q_m = \frac{Q_v'}{(x_s \cdot \beta_s + x_r \cdot \beta_r + (1 - x_s - x_r))} \quad (4.11)$$

The cost of the original operational process (Fig.4.14 (a)) C_0 (in \$/year) can be calculated as:

$$C_0 = Q_v' \cdot P_0 \quad (4.12)$$

Being P_0 (in \$/m^3) the total purchase cost of the virgin activated carbon (VAC). P_0 Includes: the cost of transportation, workers salary, energy consumption and others)

For the proposal (Fig.4.14 (b)), the cost of the mixed GAC for adsorption C_m (in \$/year) combining: SAC+RAC+VAC can be written as:

$$C_m = Q_m \cdot P_m \quad (4.13)$$

Being P_m (in \$/m^3) the total purchase cost to prepare the new GAC filters. As the new material is a fractional combination of different GAC.

$$P_m = x_s \cdot P_s + x_r \cdot P_r + (1 - x_s - x_r) \cdot P_0 \quad (4.14)$$

Where:

P_s (in \$/m^3) is the total purchase cost of the SAC.

P_r (in \$/m^3) is the total purchase cost of the RAC. (P_r includes the cost of the off-site regeneration service, transportation, workers salary, and others)

As SAC is recovered directly from the process, its cost can be neglected and eq.(4.14) can be simplified as:

$$P_m = x_r \cdot P_r + (1 - x_s - x_r) \cdot P_0 \quad (4.15)$$

In order to analyze the reduction in the total cost by comparing the original process (Fig.4.14 (a) with the new proposal Fig.4.14 (b), the rate $\left(\frac{C_m}{C_0}\right)$ as parameter for the economical assessment can be applied as follow:

$0 < \left(\frac{C_m}{C_0}\right) < 1$ Economically feasible: the closer to zero, the higher is the profit.

$\left(\frac{C_m}{C_0}\right) = 1$ Breakeven

$\left(\frac{C_m}{C_0}\right) > 1$ Economically no feasible.

Combining eqs. (4.11), (4.12), (4.13) and (4.15) gives:

$$\left(\frac{C_m}{C_0}\right) = \frac{x_r \cdot P_r + (1 - x_s - x_r) \cdot P_0}{\left(x_s \cdot \beta_s + x_r \cdot \beta_r + (1 - x_s - x_r)\right) \cdot P_0} \quad (4.16)$$

In the case for the economic assessment without regeneration incorporated, just saving the carbon (where: P_r=0, x_r=0 in eq. 4.16); a simpler model can be obtained (eq.4.17).

$$\left(\frac{C_m}{C_0}\right) = \frac{(1 - x_s)}{\left(1 + x_s \cdot (\beta_s - 1)\right)} \quad (4.17)$$

It is well known that during each regeneration cycle, the GAC material is structurally damaged (it was observed by applying the acoustic emission method) and also the GAC adsorption capacity decreases [2,8,43]. Therefore, this produces changes in the original variables such as fractional time–of–exploitation and saved amount of SAC creating a reduction on the economic advantages of the new proposal. That imposes a limited number of regenerations, thus after determined number of cycles, all the GAC must be completely removed and replaced for virgin GAC. The obtained model (eqs. 4.16 and 4.17) is a very useful tool for a fast-assessing of the effect of number of possible cycles on the process profitability.

Simulation Data

Based on sensorial results, no loss in the quality of the produced rum could be detected by the rum master experts using the above concept, its taste withstood without any problem the reference ones.

As this is an important precondition to use the above strategy a simulation calculation for this concept can be proposed, despite the missing of exact knowledge for a number of parameters after a first saving and regeneration of GAC. According to the increment of the number of cycles "n", all the parameters certainly decay; the economic data simulation was performed under the following assumptions:

1- The GAC particle is deteriorated by attrition/abrasion due to the mechanical stress during the rotatory movement in the kiln and thermal damage during regeneration, that increase the loss of material; thus, diminishing the regeneration efficiency.
2- After each regeneration cycle, a destruction of pores occurs due to the severity of the treatment; also pyrolyzed residues of non-volatile adsorbed organic compounds can block pores reducing the time-of-exploitation of the regenerated GAC expressed as fraction (βr) of the virgin GAC.
3- In each regeneration cycle, the mixture of activated carbon will have less time-of-exploitation because the accumulative loss of GAC adsorption capacity after regeneration but also the saved GAC losses in adsorption efficiency by each cycle, additionally with a decreasing amount. According to all this, the fractional time-of-exploitation (βs) of GAC saved will be less.

Taking into account the regeneration process performed at industrial scale, the total purchase cost of the RAC regenerated off-site in the AC plant in Baracoa was P_r = 920 \$/m^3 . On the other hand, the current total purchase cost of the virgin activated carbon for the Cuban rum factories P_0 =2670 \$/m^3
The economic index (C_m/C_0) was obtained applying the economic model (eqs.4.16 and 4.17) under the more likely expected variation of the presented parameters influencing the rum filter performance using the GAC mixture.

A simulation of the changes on the GAC parameters performance in the rum production process as function of number or regenerations is presented in Table 4.6. The economic index was calculated considering that P_r and P_0 are fixed values (no influence of the trade prices).

It is important to clarify that other possible economic fluctuation in the GAC market or/and extra cost associated with industrial services were not considered for simulation in order to simplify the analysis and to show how to proceed for the economic assessment applying the model.

Table 4.6 Simulation data based in the expected changes in the GAC performance as function of the number of regeneration cycles.

n	xs	βr	βs	(Cm/C0)	(Cm/C0)*
0	-	-	-	1	1
1	0.3	0.80	0.50	0.48	0.82
2	0.28	0.77	0.48	0.53	0.84
3	0.25	0.75	0.45	0.61	0.87
4	0.21	0.68	0.40	0.69	0.90
5	0.15	0.50	0.31	0.84	0.95
6	0.10	0.45	0.20	0.94	0.98

note: n=0 is referred to the original process (no regeneration applied), * process without regeneration, just saving the GAC

However, the presented economic model can be applied under whatever change in economic and/or industrial parameters. Additionally, it was demonstrated that for the first regeneration about 1/3 of the GAC amount can be saved, thus x_s=0.3 for n=1. The rest of the parameters were simulated according to its expected behavior after increasing the number of regeneration cycles.

Fig.4.16 presents the plots for the data simulation (Table 4.6) of the economic index $\left(\frac{C_m}{C_0}\right)$ behavior for a possible number of cycles. Additionally, the $\left(\frac{C_m}{C_0}\right)$ index was simulated for the same number of cycles but without regenerating (just saving the fraction less exhausted) which was calculated based on eq.4.17.

Analyzing Fig. 4.16, the maximal economic benefit by applying the new management (regeneration and saving) is expected in the first cycle, also for the rum production process without considering the regeneration, only saving GAC. Conforming the number of cycles increase, the damage to the GAC particle increases, loss of material increases and the regeneration degree reached is lower. Therefore, the time-of-exploitation of the material is less, thus diminishing the economic benefits derived from the regeneration practice which is represented by the approaching of $\left(\frac{C_m}{C_0}\right)$ curve to the profit line.

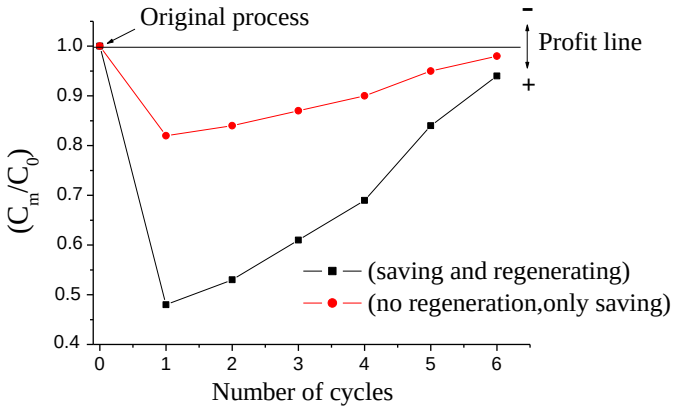

Fig. 4.16: Economic impact of the number of cycles based on the model simulation.

Comparing the model behaviors (Fig. 4.16) in the case of $\left(\frac{C_m}{C_0}\right)$ for the process with and without regeneration, noticeable differences can be found. Although the pattern in both cases are quite similar and featured with a maximal profit in the first cycle followed by a rather linear profit decreasing tendency, the economic benefit in the case when the regeneration is not considered (just saving) is considerably less than the profit obtained using the combined strategy (regenerating and saving).

In the first cycle, the associated cost of the process is about 80% of the original cost by only saving the GAC. In contrast, a great cost reduction of around 50% than the original cost can be observed when the strategy of saving and regenerating is implemented.

At the simulated conditions, in the sixth cycle, the economic advantage derived of both strategies is almost the same representing about 3 up to 6 % of cost reduction. At such conditions, based on the analysis of the proposed economic model, the best option for rum produces is rather less than six cycles of combining saving and regenerating. After the fifth cycle, the GAC should be completely removed from the filter and replaced by fresh GAC starting the proposed saving and regenerating cycles again.

This economic analysis is just an example to use the deducted model in the future in order to evaluate the GAC management strategy. At the moment, all the variables for calculating $\left(\frac{C_m}{C_0}\right)$ were simulated based on assumptions according to the expected impact of numbers of cycles on the regeneration process. Although the proposed model has been created according to the material balance; the parameters after the second regeneration cycle are yet unknown. Several years have to pass using regenerated and saved activated carbon in rum industry in order to properly know the changes in these parameters with the number of cycles. Nevertheless, economic and industrial reality will be more complex.

The change in economic index patterns, dependent on the economic conditions, will be for sure obtained in the future. However, the material balance basis which supports the found economic model, guaranties the robustness and accuracy of economic assessment at whatever real conditions. The presented model is a powerful, efficient and fast-predicting tool to help rum produces to take important economic decisions concerning the profitability of the new proposal of GAC management to face future changes in the economic and/or industrial scenarios.

4.3- Conclusions of Chapter 4

It can be stated that the acoustic technique based on signal processing of sound produced by GAC flooded with water is a sensitive method for determining porous characteristics of granular activated carbons, specifically for assessing the (exhausted and) regeneration degree of granular activated carbons used in the rum production process. It is demonstrated that the integrated area under the curve of the GAC sound signal envelope (SS) in the time domain obtained by BP filtering at 1.3 kHz can be satisfactory correlated with BET and V_{DR} results using N_2 and Ar as probe gases, although not linearly.

The regeneration process of exhausted GAC used in rum production modifies the porous structure of the material. A pore narrowing process apparently by pyrolytic residues deposition and the formation of wider pores by structural damage taking place at the same time during the regeneration process.

The repair of the porous characteristics in the regenerated GAC is highly dependent on the applied temperature. The higher the temperature, the larger is the apparent surface area and volume of pores obtained. According the regeneration kinetics based on acoustic emission method, the better conditions for the reestablishment of the GAC porous parameters were found at 850°C and 20 min of residence time in the reactor. A recovering of 70-77% of the apparent surface area and around 70-86% of the volume of pores in terms of Ar (87K) and N_2 (77K) by correlating with the acoustic method were estimated at laboratory scale.

An industrial regeneration of 432 kg of exhausted GAC was performed off-site in a rotatory kiln in an activated carbon factory located in the municipality of Baracoa. The GAC regeneration was conducted following as close as possible the best regenerating conditions determined at lab scale. In contrast with the lab scale results, the reestablishment of the GAC porous characteristics regenerated at industrial scale was lower; it just reached about 54-60% of the apparent surface area and around 55-70 % of the volume of pores in comparison with the virgin material possibly because of insufficient removal of pyrolytic residues but certainly because of rotational movement in the industrial reactor.

Based on the acoustic emission results, the industrially regenerated GAC also presented wider pores and more structural damage of the GAC particles in comparison with the GAC regenerated at lab scale. This can thus be explained by the mechanical stress during the rotational movement of the reactor creating an abrasion/attrition effect on and between the GAC particles.

At industrial scale, a yield of 54.2 and 75.4% in terms of mass and volume of regenerated GAC was respectively obtained. The apparent low regeneration efficiency in terms of mass is mainly because the differences in the apparent density of the material after regeneration due to desorption of the adsorbed organic compounds and the pores burn-off effect during regeneration. In contrast, the regeneration yield in terms of volume was quite acceptable. One of the main causes of loss of volume (and mass) of material was the carbon dust which is produced by mechanical stress, abrasion and attrition of soft GAC particles during the rotatory movement in the reactor and subsequent carbon dust removal from the reactor by the gas extracting system.

The industrially regenerated GAC was placed in an industrial rum contactor (filter) at the same target rum factory and connected to the aged aguardiente refining process. The filtered aguardiente using RAC was compared against a standard product using the Triangle sensorial test method. According to the results for a board of 11 rum master experts, the RAC can be successfully applied in the rum production process.

A math model for the economic assessment of a better GAC management was created. Based on simulation under expected hypothetical parameters (except for the first cycle) the proposed GAC management strategy produces a maximum projected cost reduction of about 50% in the first cycle in the saving and regeneration of GAC case. It was demonstrated that an increment of the number of cycles will produce a reduction in the economic advantages derived from the new management proposal. The presented model is an efficient, suitable and fast-predicting tool which offers significant advantages to rum produces in order to take important economic decisions concerning the economic assessment and profitability of the new GAC management proposal to face changes in the economic and/or industrial scenarios.

According to the presented results, the sub-questions II and III which were formulated at the beginning of this research can now be answered: the thermal regeneration can be successfully applied for the exhausted GAC in rum production. Additionally, it was demonstrated that it is possible to improve the management of GAC in rum production at the current conditions by introducing the GAC regeneration and saving strategy complemented with new, innovative, robust and more suitable analytical methods to characterize the GAC.

Summary and general conclusions

Cuban rum is regarded among the best global brands of rum with a sustained growing in the international market. **To reach its desirable organoleptic features, the operation of percolation "filtration" of aged aguardiente using a proper granular activated carbon (GAC) is essential**. Fixed bed of GAC is placed in cylindrical contactors where the aged aguardiente is applied at the top of the filter, flows downward through the carbon bed, and is withdrawn as "filtered aged aguardiente" at the bottom of the column. **When the filtered aged aguardiente quality reaches minimum organoleptic standards, the GAC is completely removed from the filter and replaced by virgin material**. Specialized rum taste experts determine when GAC needs to be replaced only based on the sensorial judgment of the filtered aged aguardiente and not on the exhausted level of the GAC. **At present in Cuban rum industry, an estimate of 10-12 tons per year of exhausted GAC from rum production is landfilled without any treatment.** Therefore, the same amount of **expensive fresh GAC for replacing is imported. The landfilled GAC creates a solid waste problem** which grows proportionally to the spirit production rate. For this reason, a **regeneration process of the exhausted GAC should be applied and the effectiveness of regenerated GAC must be guaranteed.**

Based on that, the following **problems in the current GAC management in Cuban rum production were found**:

The sensorial judgment on the filtered aguardiente cannot offer quantitative information about the real exhaustion degree of the GAC in the rum "filter". Therefore, the predominant sensorial nature of the qualitative analysis performed in rum industry without any quantitative analytic counterpart makes the recovering of part of the GAC unused in the process impossible.

No specific quantitative analytical method to characterize the exhaustion degree of the GAC used in rum production is implemented. Furthermore, it is found that for detecting the exhaustion degree in exhausted GAC in rum production, the widely applied BET analysis could not be applied as a pretreatment is needed which changed the GAC characteristics.

Adsorbed organic compounds were desorbed at the applied conditions of 300°C in vacuum during an overnight period. Thus changing the exhaustion degree of the GAC. Additional the pretreatment conditions were not successful, insufficient, even still damaging the experimental set-up.

At present, the regeneration of the exhausted GAC has not been considered yet as an alternative not only for mitigating the environmental problem that the exhausted GAC generates but also as an attractive idea in order to diminish the cost associated with the imported GAC consumption.

Although conventional techniques based on gas adsorption isotherms can be effectively applied for the characterization of the regenerated activated carbons, these methods are not available in rum industry due to limited technological facilities of rum producers. Consequently, an alternative, economic, fast and reliable method to measure the regeneration degree reached is needed.

Insufficient information about the adsorption process with activated carbons in rum production, regeneration procedures or analytic methods to determine the exhaustion level of the GAC used in rum production was found. The secrecy involved in spirit industry produces a reduction in the number of allowed publishable researches with useful detailed results.

In this thesis, the **main objective** is to present **a new and improved proposal of GAC management in rum production based on the thermal regeneration of the exhausted GAC complemented with novel, robust, accurate and suitable analytical methods to determine its porous characteristics.**

In order to solve the found insufficiencies in the GAC management in Cuban rum production and fulfilling the main objective proposed in this research, the first sub-question that arose was:

When is a GAC exhausted in rum production?

This sub-question is crucial and creates the basis of this study. According to the main objective, the new GAC management proposal includes the thermal regeneration of the exhausted GAC.

Thermal regeneration involves important energy consumption, loss of material and damage to the adsorbent occurs during the process. Consequently, before the regeneration process is considered, a proper characterization of the exhaustion degree of the GAC to be regenerated must be performed. Only the sensorial judgment of rum masters as tool for detecting organoleptic changes in the filtered product is insufficient to define when the GAC is exhausted. Actually, the sensorial judgment is just suitable to detect when the rum filter is "out of service" and the aged aguardiente operation using this filter is over. It does not mean that all the GAC in the filter's bed is exhausted enough to be replaced or regenerated, this is only possible by performing quantitative analytic methods for directly analyzing the GAC characteristics.

Having this sub-question as elemental basis in this thesis, samples of **GAC from an industrial rum filter and the unused GAC (GAC-virgin) were characterized using different methods.** Among Cuban rum factories, **a target factory of the major rum producer in Cuba was selected for this study**.

A rum filter previously declared as: "out of service by exhaustion" by a board of rum taste experts was used as "target filter" to obtain the GAC samples at different layers (positions) in the GAC bed. Using a specific sampler (Cuban patent registration: N_0: 2016-178), **the GAC samples were taken from the top to the filter's bottom according to the subsequent order:**

Top (position = 0 m), 0.2, 0.4, 0.6, 0.8, 1, 1.3m and Bottom (position=1.5m).

As an initial exploration, the GAC samples were assessed using two well-known and relatively simple techniques: the iodine number and contact pH methods. After performing the experiments, it was found that **the contact pH and iodine number trends were consistent with a comparable behavior of both parameters as function of the GAC layer position in the rum filter**. A linear correlation (R^2 = 0.993) was obtained by plotting the iodine number vs. the contact pH. **The iodine number increased from the top to the filter's bottom** ranging between 452 and 1259 respectively. Following a similar trend, the contact pH at different layer positions augmented from 3.94 (top) to 5.63 (bottom). This indicated that **the lower the iodine number, the more acidic the GAC sample**.

The observed trend is consistent with the features of the rum production process. The acidity increases in the aged aguardiente during the ageing process in rum production. Therefore, after filtering the aguardiente through the GAC bed, adsorption of a variety of acids occurs. The longer the GAC is used in the rum production process, the higher is the adsorbed concentration of these acid compounds onto the GAC (beside the adsorption of other compounds) and, thus, the more acidic these GAC become. Results are also consistent with the direction of the mass transfer zone displacement through the GAC bed and the adsorption wave theory. Iodine number and the measured pH correlated with the adsorption capacity of the GAC: **the more exhausted the GAC, the lower the pH value**. The GAC-virgin was also characterized based on these methods giving as result values of 1515 and 6.23 of iodine number and contact pH respectively. Based on these results, **the GAC sample located at the filter's top (GAC-Top) is the most exhausted** and the GAC-Bottom trends to the GAC-virgin characteristics.

Scanning electron microscopy was used to compare the sample's surface topography. **Differences were found in the external surface of the GAC particles of top and virgin samples.** The virgin GAC showed more roughness in its surface in comparison to "the most exhausted" GAC (GAC-Top).**The diminished external roughness of the used GAC in the rum production process is associated with increased amounts of adsorbed organic compounds.**

According to the elemental analysis performed to determine the C, H, N, S and O content (wt%), **the nitrogen content in the rum filter's samples is ranging between 2.4-2.7 times higher than the virgin GAC.** While for the samples GAC-Top and GAC-0.2 the nitrogen content was slightly higher in comparison with the other GACs which had almost the same nitrogen content, but slightly increasing as a function of the upward layer position. The nitrogen content is associated with amino acids and proteins from the oak wood. On the other hand, **the hydrogen content decreased from the top to the bottom being almost 2.5 and 1.2 times higher compared with the virgin GAC respectively**. **The hydrogen content for the GAC-Top was almost two times higher than the hydrogen content in the three last layers near to the filter bottom**.

The increment of the hydrogen content in the top is related with a higher concentration of adsorbed organic compounds, resulting in a higher H/C ratio. In contrast**, the GAC layers near to filter's bottom presented less adsorbed organic compounds, thus a much lower hydrogen content**, tending to the value of the virgin GAC. **The hydrogen content for GAC-1.3 was higher than the hydrogen content observed in the sample GAC-1**, **indicating an apparent change in adsorption behavior of the GAC in that filter part**. This behavior (inflection point) was also observed with other techniques and discussed further on.

Although a systematic decreasing trend of the hydrogen content with the increment of the GAC layer position to the bottom was expected, the GAC-1.3 showed more exhausted condition than its preceding layer (GAC-1). This behavior featured by the inflection point (which was confirmed by other methods) and is related with the characteristics of the rum filtration process.

As it was already explained, the aged aguardiente is applied at the top of the column, flows downward through the carbon bed, and is withdrawn as "filtered aguardiente" at the bottom of the column. **The process is carried out under batch condition at atmospheric pressure and the liquid crosses the GAC bed by gravity force. A defined amount of aged aguardiente is filtered each day according to the production demand in the factory. This filtration is carefully monitored by the rum masters to guarantee optimal flow velocity.** At the end of the batch operation process, the filter retains a certain amount of aged aguardiente trapped into the GAC bed **(bed porosity: around 40%).** Slowly the filter is drained and a certain volume of liquid retained in the bed. **As the hydraulic pressure depends on the liquid level, the draining process is faster at the beginning, but as the liquid level decreases**, the draining process slows down meaning that an amount of aged aguardiente is retained for longer time in the GAC layers near to the bottom**.**

This effect results in a longer contact time around the GAC-1.3 in comparison with the GAC-1 layer**, explaining the apparent change of hydrogen content at 1.3 m,** thus creating this deviation in the exhaustion trend.

In this research it was found that an ammonia solution could be used to extract in an optimal way the phenolics compounds from the exhausted GAC**. When the GAC has been used in rum production (specifically for refining aged aguardiente), it was observed that a reaction between the exhausted GAC and an ammonia solution (in a wide concentration range) resulted in an almost instantaneously amber color appearing. The more exhausted the GAC is, the darker the produced amber color.** If the GAC has not been used in aged aguardiente filtration, the reaction does not occur. This was used to determine the concentration of the colored adsorbed compounds and thus the exhausted level of the GAC. Additionally, from our pre-studies, the same reaction feature occurred between chips of white oak wood and ammonia solution. The amber color appeared much darker than the amber color obtained with GAC.

The phenolic compounds present in the white oak wood are responsible for the amber color in the rum. These compounds are adsorbed and accumulated onto GAC during the filtration of aged Aguardiente. The exhausted GAC reacts with the ammonia solution, releasing the amber-colored compounds.

The described phenomenon was the origin of a novel colorimetric method which is based on the direct spectrophotometric measurement of the change in the color intensity of ammonia solution after contacting with exhausted GAC used in rum production in order to quantify its exhaustion level. Our study was conducted to develop an in-depth specific, reliable, robust and fast colorimetric method to analyze the exhausted level of the GAC samples used in the rum production process. A quick qualitative pre-evaluation of the exhausted degree can be performed based on an on-sight color intensity evaluation by a simple extraction test of used GAC with ammonia. The experimental conditions to perform the colorimetric method were studied and optimized. The best results are obtained under the following conditions:

Three-point-two gram of GAC (free of dust and foreign matter and dried at 110°C/3h) is added to 20 mL of 6.25% ammonia solution, gently stirred at 50 rpm in batch conditions at 25 °C for 6 h in a 100-mL capped glass vessel. The brownish GAC extracted solution is filtered using a 0.45 µm PFTE filter and the absorbance is measured using a 1 cm quartz cuvette at 634 nm.

According to the kinetic results, the extraction reaction of the ammonia solution from the GAC in **the colorimetric method** demonstrated that the final absorbance value at equilibrium **is not affected by the applied temperature range of 10–40°C, or by the ammonia concentration in the range of 25% down to 6.25%**.

The colorimetric method was applied to characterize the rum filter samples. **The brownish/amber color profile observed in the extracted solution for the different GAC layers in the target rum filter was in concordance with the results applying the iodine number, contact pH and elemental analysis methods**. A quick inspection is enough to notice evident differences in the color intensities between the samples. **The GAC-Top showed the highest color intensity** (darker) in comparison with the color intensities observed for the other GAC layers. **The three last samples presented an abrupt change of color and sequence (clearer)**.**The inflection point at GAC-1.3 was also noticeable by this inspection**. The possibility to detect this behavior in the GAC layers near to the filter's bottom using the colorimetric method gives an evidence of sensitivity, representability, reliability and accuracy of the proposed method.

It was found that the fractional coverage of colored compounds ($\boldsymbol{\theta}$) and the equilibrium absorbance value in the colorimetric method ($\boldsymbol{A^*}$) can be correlated by the following equation:

$$\theta = 0.34 \cdot A^{*\,0.29} \qquad (0 \leq A^* \leq 2) \qquad R^2 = 0.997$$

The **absorbance value at equilibrium** can thus be used to determine θ and **can be applied to determine and quantify the exhaustion level of GAC used in the rum production**. Based on that, it was demonstrated that for GAC-Bottom, around 10% of the porous space or sites are occupied by colored compounds and that in the case of the GAC-Top; these compounds represent about 40 % of the total occupied sites. The colorimetric exhaustion profile showed a linear decrease of the color intensity in the GAC layers near to the top (in the range Top-0.4m). After GAC-0.4, an abrupt decrease of color intensity was found.

The last three GAC layers near to the filter bottom had the lowest color intensity and almost the same fractional coverage value but featured by the inflexion point at GAC-1.3.

Using the colorimetric approach, the exhaustion level of the GAC can be quantified. Taking into account that also other compounds are adsorbed and not necessary contribute to the color, but which amounts can be correlated with the colored compounds, the exhausted degree of the GAC can therefore be determined using colorimetric measurement. **The colorimetric results can be used to define the end-of-life state of a GAC in the rum production process**.

Thermal gas desorption coupled with chromatography/mass spectrometry (TD-GC/MS) method was performed for the identification of organic volatile and semi-volatile compounds thermally desorbed from the GAC in the rum filter at different layers. Different thermal desorption experiments were conducted at 300°C, 450°C and 500°C. At 300°C it was found that this temperature was too low to obtain comparable chromatograms. At 500°C, the original adsorbed compounds from the rum production process already showed a thermal decomposition trend, making a proper comparison of the original adsorbed compounds in the different GAC samples not possible. It was found that at 450°C reliable chromatograms were recorded for all GAC samples.

Based on TD-GC/MS analysis, **for all the studied GAC samples the same predominant family of adsorbed compounds were found but with different relative abundance.** The predominant compounds found in all the GAC layers in the rum filter were: **fatty esters such as: ethyl decanoate, ethyl hexadecanoate, ethyl dodecanoate and ethyl octanoate; phenolics such as: 2-methoxyphenol (Guaiacol) and vainilloids such as: 3-methoxy-4-hydroxy acetophenone (Acetovanillone) all of them have also been found in aged Cuban rums.**

According to the TD-GC/MS chromatograms, it was found that **the GAC in the rum production acts as a sensorial modulator of certain "key components" that defines the sensorial characteristics in rums**; the proper balance of these compounds is crucial to obtain the desirable sensorial typical characteristics in the final product.

The rum filtration process is designed to let just pass the correct amounts of each compound in a delicate balance, where the contribution of each compound is optimal to reach the proper sensorial characteristics. Therefore, the same compound can usually be found before and after filtering with GAC but at different concentration levels.

The GAC-Top showed higher concentration of the main adsorbed compounds. **The evolution of the sum of the peak areas was decreasing from the top to the bottom reaching the lowest value at GAC-bottom**. The clustered behavior between GAC-1, 1.3 and bottom was also clearly noticeable by direct comparing the TD-GC/MS chromatograms. Also, **the special exhaustion degree (inflection) of GAC-1.3 was observed**, an increment in peak area distribution of dedicated compounds was detected.

It was found that the ethyl decanoate is dominantly present in all the GAC layers and in enhanced concentration after GAC-0.8. The vainilloids are present in the top GAC layers. However, their relative fraction dropped abruptly after GAC-0.4. A similar behavior was observed **for the phenolics**, although present in all the GAC layers, **their relative normalized peak areas decayed from 60% at the GAC-Top to about 20% at GAC-1, but being rather constant at this value till the GAC-Bottom sample.** In general, **the family of esters decreased in relative abundancy from the top to the bottom. However, their decay can be associated to the molecular weight change.** The heavier members of this family decayed faster in relative abundance than the light esters. For instance ethyl hexadecanoate was present in GAC-Top around 50% but was nearly undetectable after GAC-0.4. The TD-GC/MS results suggest that the involved mechanisms in rum "filtration" and its relationship with the sensorial features of rum are rather complex and must be further studied.Apart of the predominant compounds, **other adsorbed substances such as fatty acids decayed from the top to the filter's bottom, following a similar pattern of a series of fatty esters**. However for ethyl octanoate and ethyl decanoate after a steep decay, a low increase as a function of GAC-layer position was found. The phenolic compounds had different behavior; in the case of 2-methoxy-4-propyl-phenol a systematic declining tendency was observed, the rest presented a concentration overshoot in GAC layers around 0.2 and 0.4 m.

This overshoot is a typical feature of a multi-solute adsorbate system, each mass transfer zone (MTZ) travel with different velocities through the adsorbent bed. This is a result of the competition for GAC pores and adsorption sites and subsequent displacement for the adsorbates during the adsorption process.

The compound 2-methoxy-4-propyl-phenol gave the impression to be stronger adsorbed than the rest displacing them to other GAC layers. In addition, **dianhydro glucopyranose was only found in the GAC-Top**; probably as rest of a heavier pyrolyzed carbohydrates coming from the oak wood during ageing process. **The presence of these carbohydrates suggests that regeneration of the exhausted GAC must be conducted at high temperature to remove possible pyrolyed residues which accumulates in GAC pores leading to a narrowing process and consequently a poor regeneration degree. The clustered behavior of the three last GAC layers (GAC-1 – bottom) was also observed in the phenolics profile.**

TD-GC/MS chromatograms of GAC-Top (most exhausted) before and after the treatment with ammonia solution of 6.25% showed comparable values of the chromatographic signal but in the case of ammonia treated GAC was slightly lower in relative abundance, thus indicating a smaller concentration of adsorbed organic compounds after the ammonia treatment.

The most significant reduction of compounds after the ammonia treatment resulted for the phenolic compounds. The observed reduction of relative abundance was between 60% before and 27% after ammonia treatment. However, no significant changes were detected for the other compounds, being the same families of predominant esters.

The differences detected in the chromatograms pointed to the extraction of the phenolic compounds by ammonia. As tannins are basically polyphenols, these results were in accordance with results reported for the ammonia fuming reaction with oak wood. The TD-GC/MS results confirmed the involvement of oak wood extractable compounds adsorbed on the GAC during rum production and extracted by the ammonia solution in the colorimetric method.

The acoustic emission analysis method was a new method developed in this research for the characterization of granular activated carbons based on the measurement and analysis of the sound produced by flooding a GAC sample with water. It results in a sound emission by bubbles formation through the bulk water and exploding at the liquid surface.

In the sudden contact between water and the GAC sample, the GAC sound is produced by the bubbles escaping from the GAC pores and slits when water molecules occupy the air filled voids inside of the GAC by displacing the present air. **The amount of produced bubbles is closely related to the porosity of the GAC. Therefore, the acoustic signal produced by the escaping bubbles can be used to access the GAC porosity**

The acoustic emission is produced in audible spectra and was analyzed by a proper acoustic signal analysis technique. In the case of GAC used in the rum production process, large amounts of organic compounds with different molecular sizes adsorb, and block pores and cracks of GAC, creating an important reduction of pore volume and specific surface area. Exhausted GAC therefore resulted in a reduction of bubbling potential and consequently in a reduction and a change in the sound signal amplitude.

This behavior of GAC bubble production which is the basis of the acoustic emission method depends on the GAC resistance to the water intrusion in the pores to displace the air. The bigger the size of the pores and slits, the easier water has access inside the particle resulting in a quick removal of the air in the form of bubbles. The less accessible the pore, the narrow and tortuous the way to remove the air inside of the particle and the rate of bubble production decreases as well as their size. **The use of acoustic measurements not only makes it possible to determine the overall porosity but also to characterize the porous structure of GAC according to the sound patterns obtained.**

The GAC acoustic emission experiments were performed in a specific set-up in order to guaranty proper experimental conditions for GAC sound measurement and analysis. The GAC sample (10 g) is put into the acoustic set-up equipped with a water injection system to feed 40 mL of pure bi-distilled water for flooding the GAC sample in 4 seconds.

From the moment the water reaches the GAC, immediately bubbles are generated producing a characteristic sound which is captured by a professional microphone amplified and digitalized using a data acquisition card. Digital data is recorded in the computer to be processed using MATLAB® software. The process takes place into an enclosure sound box. The recording time for the GAC sound was 90 seconds.

Evident differences between the samples located at extreme points in the rum filter were found by the acoustic emission method. The relative amplitude power of the signal (RMS) of the acoustic signal of GAC-Bottom was more intense than GAC-Top. A wide range of frequency components were observed for both samples. This is a typical feature of the bubbling process and the resonator nature of the exploding bubbles.

The frequency component distribution found in the signals of GAC-Top and GAC-Bottom showed two zones clearly defined: Zone I: (0-0.3 kHz) defined by a great number of frequency components associated not only with the phenomena of GAC sound production during water injection but also to the noise interferences produced by GAC particles colliding and unwanted resonant components. No frequency components in Zone I was considered for the acoustic analysis because of all these interferences. **Zone II (0.3-1kHz) was defined by a clear absence of frequency components. After Zone II, an interesting feature was found: a peak in the frequency domain around 1.3 kHz and its resonant components. The 1.3 kHz frequency component was observed in both GAC samples at extreme layers in the rum filter and its amplitude was clearly different in intensity.**

According to the frequency component distribution results, **1.3 kHz was selected as the frequency component of interest** (the cut-off frequency to the band-pass (**BP**) signal filtering) for characterizing the exhaustion degree in GAC used in the rum production process.

The signal envelopes for the GAC-Top and GAC-Bottom filtered at 1.3 kHz were obtained. Significant differences were found between the GAC samples in terms of the shape of the envelope curves and the signal amplitude in time domain. The signal envelope in time domain curve filtered at 1.3 kHz of the GAC samples at different layers of the rum filter (GAC-0.2-1.3m) were also evaluated.

Differences between samples were found in terms of amplitude of the RMS signal, signal frequency spectrum amplitude and signal envelope. Detected differences were more evident by comparing the signal amplitude and envelope. **The maximal peak amplitude (EMP) and the area under the signal envelope curve integral or "sound surface" (SS) at 1.3 kHz increased systematically from the top (GAC more exhausted) to the filter's bottom, giving a strong correspondence between the exhausted behavior of GAC layers and the sound amplitude in the frequency of interest. The behavior of the EMP and SS values at 1.3 kHz revealed that the amplitude found for GAC-1.3 was lower than the amplitude observed in the sample GAC-1, which was consistent with the inflection point observed at 1.3 m** by the elemental analysis, TD-GC/MS and colorimetric method. The possibility to detect this behaviour in the GAC layers using the presented acoustic method is an evidence of sensitivity and accuracy of the proposed technique.

Thermogravimetric analysis (TGA) is a thermal analysis method by which the weight loss of the GAC is continuously recorded against temperature or time under a controlled heating rate and inert gas atmosphere. The weight loss, caused by volatilization and/or decomposition reaction, provides useful information about the thermal stability of the adsorbed compounds onto the GAC. Differential thermogravimetric (DTG) profiles are obtained for TGA, which plots the weight change velocity as a function of temperature (time). **GAC-virgin showed a weight loss of about 6%.** Above 110 °C, minor weight loss occurred in a continuous way due to in-situ presence of volatiles upon further heating. **Great differences between the GAC-Top and virgin GAC in terms of weight loss and DTG profiles were noticeable.**

Additionally, based on this TGA, a thermal treatment just above 500 °C for GAC-Top could result in a removal of most of the adsorbed organic compounds featured by a desorption peak at 427°C. For the GAC-Top (most exhausted), at 110 °C the loss of water and low MW volatile compounds ended. According to TGA analyses, increasing the temperature above 110°C for an exhausted GAC sample, desorption of water and also other volatile substances will occur.

According to this, **the drying process for sample preparation before further analytic procedures of exhausted GAC must be handled at 110°C as maximum** in order to desorb only moisture.

The GAC samples from the rum filter were assessed using TGA analysis. **The weight loss for GAC-Top had the highest value (about 18-20%), for the other samples a systematic decreasing value was observed to reach the lowest value for the GAC layers near to the bottom (about 13-15%).** The GAC-1, 1.3 and Bottom were clearly clustered and separated from the other samples as their exhaustion degree is less and comparable between each other.

DTG curves showed evident differences between the GAC samples in the rum filter. The maximal desorption rate (DTG peak) was located in the range of 325-500 °C for all the samples. Comparing the DTG peak temperatures, a systematic shift towards lower temperatures can be found from GAC-Top towards GAC-Bottom. The GAC near the top presented a systematic increment in derived weight loss from GAC-0.8 up to GAC-Top. As could be expected, GAC-1, GAC-1.3 and GAC-Bottom were clustered. **The differences observed in the peak temperature and weight loss can be attributed to the amount and the kind of adsorbed organic compounds on the GAC. The more the GAC is exhausted, the more time it takes for the organic compounds to be released**; thus, the peak temperature, maximal desorption rate and weight loss increases according to the exhaustion level of the GAC.

As the desorption rate is proportional to the substance amount that is still adsorbed, the derivative of weight loss (DTG) was associated with the mass of adsorbed compounds in GAC pores during the filtering process, **the maximal desorption rate at the peak in the DTG curves was used as a parameter to compare the exhaustion degree of the GAC** used in rum production process.

Similar trends in the exhaustion profile for the GAC in the rum filter were clearly noticeable by comparing the DTG maximal desorption rate with contact pH, iodine number, CHNS-O elemental analysis, TD-GC/MS, colorimetry and acoustic emission methods. **The inflection point at 1.3 m was detected for all the cases**. **The three distinctive zones in the rum filter profile were detected by the different methods applied.**

The GAC exhaustion profile in the rum filter can be divided in three zones: Zone I: (near to the Top) with a rather linear behavior; **Zone II: (layers above 0.4 and next to 1m) featured by a polynomial or exponential tendency and Zone III: (above 1m to the bottom) where a similar exhaustion degree of the GAC is observed characterized by an inflection point in between due to the specific characteristics of the rum-ending production process.**

The immersion "bubblemetry" technique is a novel method specially developed for characterizing granular activated carbons in terms of amounts and sizes of produced bubble volumes.

The method is based on the microscopic size measurement of the bubbles formed when a GAC grain is immersed in a pure liquid. When the GAC particle is immersed in the liquid, the liquid occupies the available pores in the material displacing the air which leaves the solid in form of bubbles through the bulk liquid. The released air in form of bubbles can give information about the volume of pores.

The bubbling behavior was observed when particles of GAC used in the rum production were immersed in different liquids. In the bubbling process, the GAC is initially in contact with a gas phase (air), creating a solid-air interface, when putting in contact with the immersing liquid the solid-gas interface is replaced by a solid-liquid one. This replacement occurs by the capillary action involved in filling the pores and slits in the GAC particle. In the interface replacement process, the air is removed in form of bubbles which escape through the bulk liquid. Measuring the size of the formed bubbles and calculating its volume, the total volume of released air and correspondently, the volume of with liquid occupied open pores and slits can be determined. The bubble production rate and its characteristics, depend on the porous characteristics of the solid and the physical properties of the immersing liquid. In this case, **glycerol was used as immersing liquid because of its physical properties permitted to observe the formed bubbles at "slow motion"** giving the possibility of fixing proper microscopic pictures of the bubbles, to be further analyzed.Immersion "bubblemetry" method can be classified as fluid displacement technique to determine the porous characteristic of GAC.

The acoustic emission and "bubblemetry" methods take place under the same basic principle: the sudden contact between the liquid and solid phases. Differences are present in the measured parameter; for "acoustic emission" it is the bubble sound and in "bubblemetry" it is the size of the bubbles.

Immersion "bubblemetry" is an important tool to understand the relationship between the acoustic emission measurements and the GAC bubble process when the GAC is suddenly immersed in a pure and inert liquid. Glycerol was also selected as immersing liquid due to its transparency and viscosity that permits not only to obtain well defined microscopic images but also to understand the GAC bubble process in water since the bubble process in glycerol occurs slowly. The intensity of the bubble process and the fast rate of bubble formation make the bubble characterization impossible when water is used as immersing liquid.

The bubblemetry method was performed in a specific set-up. The immersion liquid (3.75 mL) is injected in the bubbling cuvette, not only covering the GAC particle (one grain (rod) each time) within 3s, but reaching a 6 mm of liquid level. The experiment was performed using glycerol as immersing liquid at 25°C (discussed later).

Few seconds after completing the total immersion process, the bubbles appear as a result of air escaping from the GAC pores and slits. Bubbles of different size are formed and some of them coalescence.

The formed bubbles slowly appear from the solid but remain separately trapped by a glass cover in the liquid. The viscosity of glycerol guaranties a slow motion process and diminishes the bubble coalescence. When all the bubbles have been formed, which can last 3-10 min, depending on the exhaustion level of the measured GAC particle, the combination of the glycerol properties (transparency, viscosity and surface tension) and the used glass cover position retains all formed bubbles making clear microscopic pictures of the formed bubbles possible.

When the GAC bubbling process is finished a microscopic digital picture of all formed bubbles is taken and the bubble sizes and amounts are measured and counted. The volume of each bubble is determined and the total volume of air released can be obtained by knowing the number of formed bubbles and its sizes.

A specific own software (under copyright protection process) was created to detect (counting) and analyses (bubble size) the bubbles in the images. The software was developed in MATLAB® applying the Hough transform as algorithm to the circular pattern recognition. After detection and recognition the circular shapes (bubbles) in the images, the software automatically determines the independent radius and volume of each detected bubble, based on the pre-calibration transforming pixels into mm using the calibration microscopic ruler. All the data (radius and bubble volume) are saved in a excel file for further processing.

Apart of glycerol, different immersing liquids were tested: lactic acid, phosphoric acid, and paraffin because of their viscosity and transparency that also permits to observe the formed bubbles at "slow motion" and giving the possibility of fixing proper microscopic pictures of the bubbles.

However only for glycerol the observed formed bubbles could be evaluated and gave reliable results.

Digital microscopic images of the typical bubble production patterns of GAC grains from the layer positions in the rum filter immersed in glycerol showed noticeable differences in the GAC bubble pattern, giving the first evidence that the number and **the total volume of produced bubbles was in correspondence with the GAC sound pattern observed, being higher for the bottom than for the top GAC**, following a systematic trend.

No significant differences in the GAC bubble diameter distribution were found between GAC samples from GAC-0.2 to GAC-Bottom. For these GAC, **the majority of formed bubbles were distributed around 0.2 - 0.4 mm in diameter**. However **the GAC-Top diameter distribution was located between 0.1-0.2 mm in diameter**, it was almost half of the bubbles observed in the rest of the GAC layers.

Such phenomenon can be associated with the concentration of adsorbed compounds on the GAC grain. If the concentration of these compounds is high enough, the carbonaceous primary matrix of the GAC can change by overloading. Therefore, the interaction solid-immersing liquid in the replacement process of the solid-air phase is different; consequently a different bubble pattern appears.

In this case, **smaller bubbles are mainly present when the GAC is totally exhausted; this is an interesting and quick-assessment parameter to detect the "complete exhaustion degree" of a GAC in the rum process**. According to this observation, **the bubble process is not simple and depends not only on the immersing liquid properties but also on the GAC surface characteristics**, which must be further studied.

The values of **immersion total volume of pores** determined by immersion bubblemetry **for the GAC samples in the rum filter and the GAC-virgin were different**. **The obtained values of immersion total volume of pores were comparable with the porous characteristics of activated carbon in terms of pore volume. For GAC-virgin the highest value of immersion volume of pores (0.56 cm^3/g) was found**.

On the other hand, **in the rum filter, the higher value of total immersion volume was 0.45cm^3/g for the GAC-Bottom and the lowest value was observed for GAC-Top (0.13cm^3/g) following a systematic tendency of increasing volume from the top to the filter bottom**. It matched also with the results obtained by TGA, TD-GC/MS, elemental analysis, colorimetry and acoustic emission methods. **In turn, it was in line with the rum production process using fixed bed "filters". The same exhaustion profile** of the GAC in the rum filter **was detected, featured by the inflection point at 1.3 m**.

Acoustic emission and bubblemetry methods were compared and quite similar trends were found. **The acoustic emission results were highly correlated with immersion total volume of the GAC.** This confirmed the relationship between acoustic emission and porous characteristics of the GAC.

In the bubblemetry method, it was demonstrated that the total volume of released air by a GAC grain depends on: 1) the pore accessibility of the liquid (related with the molecular size, surface tension and viscosity of the liquid), 2) the liquid temperature, 3) the immersion depth and 4) the liquid density.

The use of other immersing liquids like water or ethanol to obtain the bubbles was also explored, but the results were not satisfactory. The bubbling process using these liquids is so fast that it was not possible to capture the bubbles in a picture. Due to their low viscosity, coalescence phenomena occur making the measurement of the sizes of produced bubbles impossible.

Other liquids such as: phosphoric acid, lactic acid and paraffin were also researched (they're also transparent and their viscosity is higher than water), but again no satisfactory results were obtained: the counting process was quite difficult and not accurate because of the enormous number of produced bubbles, bubbles coalescence and attached on the GAC surface. Further on, only one side of the particle was visible under the microscope; more bubbles remained hidden at the other side of the GAC being thus non-detected. Therefore, using these liquids, around 30-50% of the information about the number of produced bubbles and its volume is unknown/lost, introducing a significant error in the measurement process. **Glycerol was the best immersing liquid to detect the bubble process.** However, the chemical and physical property of the liquids and the relationship with the GAC bubbling feature must be further studied.

The correlation between the liquid properties and the GAC bubbling pattern is not simple; liquids with similar physical properties (surface tension, density and viscosity) produced different bubbling patterns.

The bubbling pattern of a GAC depends not only on the chemical-physical properties (or one individual property) of the used liquid but also on the chemical-physical characteristics of the GAC surface and its interaction with the immersing liquid.

Relaxometry is a tool to determine the pore size distribution of a porous material using NMR based on the fact that the ^{1}H NMR spin-lattice and spin–spin relaxation time of water confined in a porous material changes according to the pore environment. NMR provides a convenient way of quantifying the pore size distributions and can give information on the nature of interaction of a fluid with the porous material confining it. **Measurements of the ^{1}H NMR transverse (T_2) relaxation was used for the characterization of the exhaustion level of the GAC samples in the rum filter.**

According to the T_2 values, all the pores were associated with tightly bound surface water in small pores (micropores) having short relaxation times. The pore size with a relaxation time of 18-19 μs was present in all the samples but its fractional contribution decreased from the Top to the Bottom of the filter.

The second relaxation time, corresponding to a second pore size type was more variable and separated in two groups: 22-24 μs and 26-28 μs which corresponded to more free water in the pore. A systematic increase of second type of pores (wider) was found from the top to the bottom with an abrupt and clustered change for GAC-1, GAC-1.3 and GAC-bottom. **The fractional contribution of the wider pores clearly increased from the Top to the Bottom of the filter.**

According to the relaxometry results, a long relaxation time (22-24 μs and 26-28 μs), represents "wider" pores than those represented by 18-19 μs which can be considered as "narrow" pores. The term: "wider" pores is related with unblocked, clean or "available" pores, while "narrow" pores can be associated with blocked or "occupied" pores.

The profile of the GAC exhaustion degree at different layers position into the rum filter based on NMR relaxometry showed that the value found **for GAC-1.3** is lower than the value observed in the sample GAC-1 creating **the inflection point in the systematic growing plot trajectory**.

This pattern was in line with the results from colorimetry, TGA/DTG, TD-GC/MS, CHNS-O elemental analysis, acoustic emission, bubblemetry, iodine number and contact pH.

Three novel methods for the characterization of granular activated carbon used in rum production were presented and compared with other analytical techniques.

Based on the obtained results, it can be stated that the **acoustic emission, immersion "bubblemetry" and colorimetric methods demonstrated to be suitable and sensitive tools to determine the exhaustion degree of GAC used in rum production**.

The results can be satisfactory correlated with iodine number, contact pH, CNHS-O elemental analysis, TGA, TD-GC/MS and NMR results. The facilities and advantages of all proposed methods for analyzing the exhausted level of GAC form very interesting complementary analytical techniques to characterize GAC beyond the sensorial judgement traditionally performed by rum specialists.

In contrast with the colorimetric method, which is just specifically applied for exhausted GAC used in rum production (or others which have been in contact with aged spirits), the acoustic emission and immersion "bubblemetry" methods can be applied for the characterization of GAC in general as they are intrinsically linked by the same physical phenomenon: the bubbling process. The simplicity and advantages of these proposed methodologies are very interesting as complementary analytical methods to characterize high-porosity materials in order to explore the GAC pores characteristic.

The above mentioned new GAC characterization methods offer in this particular case several advantages in comparison with well-known conventional techniques such as gas adsorption (BET). They are sensitive and non-destructive methods which can be performed quickly and thus are less time consuming. It does not need special experimental conditions or special reactants. Additionally, it was found that for detecting the exhaustion degree in used GAC the BET analysis could not be performed. Before BET analysis could be executed, the sample must be dried overnight at 300°C in vacuum.

In this case, the pre-treatment of the sample induced modifications in the studied GAC, desorption of a part of the absorbed organic compounds took place. It was even found that this required pre-treatment even did not satisfy and could damage the equipment. Therefore, the measured BET results are not presented among the applied methods for determining the exhaustion level of the GAC in rum production. The other proposed techniques are more reliable to determine the real exhaustion level, being an interesting tool for the control and management of GAC in the rum production process and analogue applications.

According to the results derived from all the applied methods, the exhaustion degree of the GAC at different layer positions in the rum filter revealed the following order:

GAC-Top > GAC-0.2> GAC-0.4> GAC-0.6> GAC-0.8> GAC-1.3≥GAC-1.0≥GAC-Bottom

An inflection point in the exhaustion level at GAC-1.3 in the rum filter was detected by all the performed methods. The possibility to detect this behavior in the GAC layers using the novel techniques (colorimetry, acoustic emission and bubblemetry) confirms the sensitivity and accuracy of the

measurements to study the GAC exhaustion process in rum production. According to the lower exhaustion degree observed in GAC-1, GAC-1.3 and GAC-Bottom, a possible reuse of these GAC layers to the rum filtration can be proposed. **Around 30% of the GAC as the length of the unused bed fraction in the rum filter can be efficiently reapplied in a complete new contactor/filter, mixed with virgin GAC.** In that case, the filling of a new rum filter should be started at the bottom using 70% of virgin GAC and then completed with partially exhausted GAC at the top. **This possibility is more cost-effective than removing all the GAC and replacing by expensive virgin GAC.**

Answering the first sub-question presented in this work, we concluded that an activated carbon is exhausted in rum production when it is featured by the following characteristics:

Method	**Main characteristics of an exhausted GAC in rum production**
Contact pH	Low contact pH: acidic: about 4.
Iodine number	Low iodine number: about 500.
CHNS-O	High hydrogen content: 2.5 times higher than the virgin GAC.
TGA	High weight loss after drying: about 18-20%, maximum desorption rate at high temperature: 0.08 %/°C featured by a desorption peak near to 500°C.
Colorimetry	Intense amber color after ammonia reaction: about 1.2 absorbance units at 634 nm.
TD-GC/MS	High relative abundance of fatty esters, phenolic compounds and pyrolyzed carbohydrates.
Acoustic emission (in water)	Low acoustic signal intensity at 1.3 kHz: Signal envelope maximal peak amplitude about 0.1 V and sound surface about 4 V·s.
Bubblemetry (in glycerol)	Low immersion total volume of pores: about 0.13 cm^3/g , averaged diameter of formed bubbles: about 0.15 mm.
NMR relaxometry (in water)	Low fractional contribution rate: about 20%, the amount of the "occupied" pores is bigger than the "available" pores per mass of sample.

As all the applied methods satisfactorily correlated, just one of them is an enough criteria to quantify the exhaustion level of the GAC sample. In contrast, considering that TD-GC/MS is a semi-quantitative method, it has to be supported by a quantitative counterpart using any of the other methods listed above. However, the iodine number must be carefully interpreted when an exhausted GAC in rum production is tested applying this method. Firstly, the iodine number method is originally used on fresh carbons. Also it was found that iodine can react with some adsorbed organic compounds which were detected in exhausted GAC used in rum production applying TD-GC/MS. Such reactions between iodine, alcohols and phenolics compounds have been reported by different authors. Therefore, testing exhausted carbon by iodine number method has to be analyzed just as a relative parameter in order to compare GAC samples.

In this study, thermal regeneration of exhausted GAC applied in rum production is analyzed. As it is the most exhausted activated carbon found in rum production, GAC-Top was used for the regeneration experiments**. Different temperatures (450-850°C) and residence times (5-100 min.)** (covering 20 natural experiments (performed five times each)) **were explored at lab scale** based on reported experiences in activated carbon regeneration loaded with different organic adsorbates. Among the performed experiments, **three specific regenerated GAC samples (RAC) were characterized using the gas sorption (BET) analysis. Two probe gases (argon at 87 K and nitrogen at 77 K) were applied** in order to compare the results between them and to correlate with acoustic emission measurements. The samples selected for the gas sorption study were regenerated at **the following combinations of regeneration temperature and residence time in the reactor: 450°C/100 min, 600°C/80 min and 800°C/40 min.** Additionally, **the virgin GAC was also evaluated**. The selection was made in order to cover low, medium and high regeneration temperature ranges at maximum residence time for each temperature. Two main objectives were addressed with this selection; firstly, to make an initial exploration about the more suitable regeneration temperature range and secondly, to provide representative data as diverse as possible in terms of porous characteristics to correlate with acoustic measurement in a wide range, covering different regeneration degrees.

Firstly, the exploratory regeneration was conducted at lab scale in a quartz reactor of 20 g of loading capacity.

The N_2 and Ar isotherms for all regenerated (RAC) and virgin carbons were type I with a hysteresis loop type H4 according to IUPAC classification, indicating a microporous nature of adsorbents. The hysteresis loops for the RAC samples were similar and broader than the GAC-virgin loop. This behavior can be more associated with the filling of micropores than with capillary condensation in mesopores according to the high values found for the "C*" BET constant related to the energy of monolayer adsorption. **For GAC-virgin, the highest apparent surface area was measured and was around 1570 and 1640 m^2/g for nitrogen and argon respectively**. **The apparent BET area of the regenerated carbons follows a growing trend according to the regeneration temperature applied.**

Although significant differences between the regenerated and the virgin GAC in terms of specific surface area and volume of pores was noticeable, **results were more descriptive using Ar as probe gas**. In this case, **a systematic increment in the specific surface area, volume of pores and pore width was observed in correspondence with the regeneration temperature**. Based on BET results using both probe gases, **the pore width ranged between super-micro and micropores respectively**. In general, the pores of the regenerated carbons had comparable sizes. **GAC virgin presented larger pores than the other samples and more porosity**. BET analyses confirmed narrow micro-porosity in RAC samples and lack presence of pores in the range of 2-3 nm. Comparing the pore size distribution between the GAC virgin and regenerated samples, it was found that **the pore sizes between 1.2 and 3 nm are clearly lesser present for RAC with different regeneration levels. This points to a preferential adsorption of organic compounds in the pores with a size within this range and subsequently pyrolyzed and depositing of carbonaceous residue during regeneration.**

The gas sorption results confirmed the significant effect of the applied temperature on the restoration of the porous characteristics in the regenerated GAC. **Based on Ar, at 450°C the recovering of apparent S_{BET} area and V_{DR} represented about 40 and 46% respectively from the original parameters in the virgin GAC.**

In contrast, at 800°C the restoration of the porous characteristics was around 53% for apparent S_{BET} area and 66% for V_{DR}. Similar values were obtained using N_2.

The BET results on these exploratory regeneration experiments demonstrated that in the case of the GAC regeneration in rum production, the process must be performed at temperatures higher than 800°C to obtain larger apparent surface area and volume of pores closer to the virgin material. Reported results for the regeneration of GAC loaded with organic compounds were confirmed in the case of regenerating GAC in rum production: a more effective removal of pyrolytic residues could be possible if regeneration were conducted over 800°C. **The adsorbed compounds in the exhausted GAC in rum production can be classified as Type III (high carbonaceous residue deposition)** according to the response to thermal treatment during regeneration which was in line with the TD-GC/MS results.

Among the predominant compounds detected by TD-GC/MS and the colorimetric method, phenolic compounds did have the highest contribution. In addition, the presence of tannins and lignin derivate from the oak wood during ageing process can produce a high carbonaceous residual fraction at 800°C. All detected phenolics compounds and tannins as polyphenols are mainly responsible of the residue deposition. The presence of dianhydro-glucopyranose in the exhausted GAC as pyrolyzed fraction of carbohydrates suggested the deposition of carbonaceous residues by non-volatile compounds like lignin derivates.**The acoustic emission results showed noticeable differences in the shape and signal amplitude between regenerated samples at lab scale**. **Regenerated carbons presented a main peak sharper than GAC-virgin** which was broader (still bubbling longer) and displaced in time. A relationship between the regeneration temperature and the main peak amplitude was observed. **The higher the regeneration temperature is, the higher the main peak**.

During thermal regeneration the porous structure and pore size distribution of the GAC change, opening new and wider pores and cracks giving to water an easier access to the more internal porosity (micro and mesopores).

The pore widening process enhances the fast removal of the air in form of bubbles from the internal pores which in turn creates a sound signal of higher amplitude.

The fast filling process of the small pores (via wider pores) produces fast increasing and decreasing of signal amplitude with high slope.

Although with apparently different phenomenological nature, **acoustic emission and the volumetric sorption analysis are linked and can not only be correlated but are also complementary**. **The volumetric sorption analysis indicated a narrowing process at micro-pore scale, in contrast, the acoustic signal pointed out a pores widening process occurring at the same time.**

The volume of air displaced by the flooding water which produces the GAC sound in the acoustic emission method is mainly coming from the micro and mesoporous structure of the carbon.

As the macropores do not significantly contribute to the total volume of pores in the GAC, their direct contribution to the acoustic signal amplitude in terms of the produced volume of air escaping in form of bubbles can be neglected. Nevertheless, the GAC **macroporosity plays an important role in defining the pattern of the acoustic signal envelope**.

The relationship between the acoustic signal envelope feature and the porous characteristics of the GAC **can be summarized in the following types of patterns**:

Type I- GAC with high microporosity and macroporosity: A broad main peak of high amplitude followed by a systematic decreasing trend featured by secondary peaks of comparable amplitude. The larger the volume of micropores, the broader is the signal peak.

Type II- GAC with high microporosity and low macroporosity: A broad main peak of moderate amplitude and delayed in time scale followed by a smooth decreasing trend slope featured by secondary peaks of comparable signal intensity which are gradually attenuated.

Type III-GAC with low microporosity and high macroporosity: A sudden and sharp main peak of very high amplitude followed by an abrupt decreasing trend featured by fewer secondary peaks of low amplitude. The lower the volume of micropores, the shorter is the initial main peak.

Type IV-GAC with low microporosity and macroporosity: A broad main peak of very low amplitude and delayed in time scale followed by a monotonic smooth decreasing trend slope without significant secondary peaks.

Based on gas adsorption and acoustic emission analyses the regenerated GAC samples are structurally different from the virgin GAC and exhausted GAC samples. The regeneration process produces changes in the GAC grain and in its porous structure. **From one side; carbonaceous residues of adsorbed organic compounds found in exhausted GAC (e.g. aromatics, phenolics and carbohydrates) lead to narrowing micropores; while the thermal treatment under steam-oxidizing environment produces structural damages in the GAC particles, opening wider pores (at meso and macro scale), slits and cracks in the regenerated carbons.**

The area under the envelope curve "integral" (sound surface (SS) expressed in V·s) was used as parameter to correlate with the gas sorption characterization. Satisfactory non-linear correlation between SS and the porous structure parameters of GAC were found. In both cases (Ar and N_2), a decreasing polynomial or exponential decay model can be fitted in order to estimate the apparent S_{BET} surface and V_{DR} based on acoustic measurements. However, a **better correlation was found for argon**. Additionally, by a comparative inspection on the plots, based on the sequential trajectory and the distribution of the data points, a more sensitive correlation for Ar was observed, especially in the case of V_{DR}. Thus, **argon was more suitable than N_2 to predict porous characteristics by correlating with the acoustic emission method**.

According to the BET analysis and acoustic emission method, the regeneration of the GAC used in rum production must be conducted at temperatures higher than 800°C in order to remove the carbonaceous residues damaging as less as possible the carbon structure and its mechanical properties. **The kinetic behavior of the regeneration performance at different temperatures based on SS as parameter demonstrated significant statistic differences in the SS values at different regeneration temperatures between RAC samples**.

Acoustic emission measurements suggested that at 600°C a thermal desorption of the majority of adsorbed volatile and semi-volatile compounds occurs. Between 600 and 800 °C pyrolysis of non-volatile compounds takes place but leaving a carbonaceous residue. The removal of these pyrolytic residues, take place above 800°C increasing the RAC porosity; featured by larger SS values.

The carbon regenerated at 850°C under lab controlled conditions presented more similar envelope shape in comparison with GAC-virgin than the other RAC samples. However, in contrast to the increment of regeneration temperature, evident differences between virgin and regenerated GAC remained obvious. After 20 min at 850°C, no statistical differences between the regeneration degrees reached in terms of SS were found; therefore, **the regeneration of the exhausted GAC in rum production must be conducted at 850°C, optimum/minimum residence time: 20 min, feeding to the reactor about 1kg of steam/kg of exhausted GAC.** Based on acoustic estimation, **at 850°C better restore of the porous characteristics were obtained in comparison with the other regeneration conditions explored**. In that case, considering the found correlation between SS and the porous characteristics determined by gas sorption; **an estimated restore of about 77% of the apparent surface area and around 86% of the volume of pores in terms of Ar at 87K was found.**

Based on the experimental results at lab scale, the off-site regeneration process at industrial scale in the industrial plant for producing activated carbon using a rotatory kiln located in the municipality of Baracoa (Eastern of Cuba) **was performed**. The industrial rotatory kiln in the plant was prepared to reproduce as close as possible the optimal regenerating conditions. **The reactor was loaded with 432 kg of exhausted GAC**. The exhaustion level of the material was confirmed based on the proposed methods (colorimetry, acoustic emission and bubblemetry). After regenerating the exhausted GAC in the industrial reactor**, a yield of 234 kg of RAC was obtained**. **The apparent density of the material before and after regeneration was quite different**. As it is expected, **the regenerated carbon had less apparent density (about 30% less) than the exhausted GAC**.

This result was in line with the TGA analysis. **At industrial scale, a yield of 54.2 and 75.4% in terms of mass and volume of regenerated GAC was obtained respectively.** The **main losses which influence the relative low yield in this first regeneration at industrial scale were identified: (1) High amount of adsorbed organic compounds** in the exhausted GAC (about 20%), **(2) Operating conditions in the industrial reactor** (mechanical stress/attrition and dust production), **(3) Insufficient amount of material to be processed** (about 50% of the loading capacity of the reactor). However, considering the TGA results, **the mass loss in the regeneration of exhausted GAC in rum production will never reach a value less than 20 wt. %, thus the maximum expected yield will be 80%.**

The **regenerated GAC at industrial scale** (234 kg) **was stored** in paper bags of 10 kg **and sent back to the rum factory in order to prepare the experimental industrial rum filter for refining aged aguardiente.**

The regenerated GAC at industrial scale was characterized using the acoustic emission method. The multi-peak pattern in the signal envelope of the regenerated GAC was again observed. **The signal envelope pattern of the industrially regenerated GAC was different in comparison with the regenerated GAC under controlled conditions in the laboratory**. **The regenerated GAC at industrial scale presented the sharpest main peak followed by an abrupt decay trend.** Although the signal envelope pattern of the industrially regenerated GAC showed a recovering of porous characteristics, **the found pattern was closer to type III than type I pattern as in the case of GAC lab-scale regenerated at the same conditions which trends to the virgin GAC pattern.**

The bubbling process for the industrially regenerated carbon starts almost immediately in a very sudden process after water-GAC contact. This initial behavior can be associated not only with the process of formation of new and wider pores but also with an **extra structural change of the GAC particles because of the mechanical damage during the rotation movement of the reactor** thus creating a colliding and attrition effect between the GAC particles.

The mechanical damage during industrial regeneration enhances the formation of slits and cracks in the external surface of the carbon particle creating easier access to the water, therefore producing an initial intense bubbling process which is translated in a high and sharp main peak.

The found signal envelope behavior of the industrially regenerated GAC pointed to adsorbed compounds and carbonaceous residues not appropriately removed from the pores in comparison with the regeneration performed in the lab at the same temperature and residence time. The controlled environment created at lab scale improves the results concerning to the regeneration efficiency and the GAC porous restore.

The SS of the signal envelope for the industrially regenerated carbon was also calculated. Based on the estimated porous characteristics using the acoustic method, **the restore of textural properties at industrial scale was lower than the regeneration results found in the lab experiments at the same conditions** of temperature and residence time.

The industrially regenerated carbon showed a restore of about 60% of the apparent surface area and around 70% of the volume of pores estimated in acoustic terms for Ar at 87K.

An adjustment of the operational parameters in the regeneration process at industrial scale must be considered in order to improve the results in terms of restore of porosity in the regenerated carbon. Parameters such as: residence time, rotating velocity and loading capacity in the reactor have to be further studied to minimize the structural damage of the GAC particle.

The industrially regenerated GAC was placed in an industrial rum contactor (filter) at the same target rum factory and connected to the aged aguardiente refining process. The filtered aguardiente using RAC was compared against a standard product using the Triangle sensorial test method. **According to the results for a board of 11 rum taste experts, the RAC can be successfully re-applied in the rum production process.**

An economic model was created based on a material balance for the new GAC management proposal. The proposed economic model focused on calculating the cost rates before and after the new GAC management strategy in order to obtain comparative economic cost indices**.**

Based on the economic model, a simulation was performed according to the increment of the number of cycles "n" and its influence on the economic performance of the GAC management proposal. Data simulation was performed under the following assumptions: (1) The GAC particle is deteriorated by attrition/abrasion due to the mechanical damage during the rotatory movement in the kiln during regeneration increasing the loss of material, (2) After each regeneration cycle, a destruction of pores occurs due to the severity of the treatment; also pyrolyzed residues of non-volatile adsorbed organic compounds can block pores reducing the time-of-exploitation of the regenerated GAC, (3) In each regeneration cycle, the regenerated carbon will have less time-of-exploitation because the accumulative loss of GAC adsorption capacity after regeneration.

The economic indices were calculated applying the economic model under the above mentioned assumptions which represent the more likely expected variation of the presented parameters influencing the rum filter performance using the new GAC management proposal.

A simulation of the changes on the GAC parameters performance in the rum production process **as function of number or regenerations pointed to a maximal economic benefit by applying the new management (regeneration and saving) expected in the first regeneration**, also for the rum production process without considering the regeneration. **The GAC regeneration process combined with a partially exhausted saving strategy produces a projected cost reduction of approximately 50% in the first cycle.** It was estimated that **an increment of the number of cycles will produce a reduction in the economic advantages derived from the new proposal**. Conforming the regeneration cycles increase, the damage to the GAC particle and loss of material will increase, and at the same time, the degree of regeneration reached will be lower. Therefore, the time-of-exploitation of the material will be less, thus diminishing the economic benefits derived from the regeneration practice.

Nevertheless, several years have to pass using regenerated and saved activated carbon in rum industry under the new GAC management proposal in order to know the changes in these parameters with the number of regenerations, thus validating the proposed economic model.

The presented economic model is an efficient , suitable and fast-predicting tool which offers significant advantages to rum producers in order to take important economic decisions concerning to the economic assessment and profitability of the new proposal of GAC management facing changes in the economic and/or industrial scenarios.

According to the presented results**, the sub-questions II and III which were formulated at the beginning of this research can be answered**: **the thermal regeneration can be successfully applied for the exhausted GAC in rum production. Additionally, it was demonstrated that it is possible to improve the management of GAC in rum production at the current conditions by introducing the regeneration and GAC saving strategy complemented with new, innovative, robust and more suitable quantitative analytical methods to characterize and monitor the GAC.**

The proposed GAC management strategy for Cuban rum production consists in the following steps:

(a) The GAC virgin is applied in the filtration process of aged aguardiente.

(b) The rum masters determine when the rum filter is "out of service" by exhaustion based on the sensorial judgement.

(c) The exhausted GAC (previously evaluated its exhaustion condition using the new methods: Acoustic emission, colorimetry or immersion bubblemetry) is send to the regeneration process. A regeneration temperature of 850°C and about 30 min of residence time in the reactor are required in advance for a proper GAC regeneration. The operational parameters in the reactor must be adjusted in order to optimize the regeneration process at industrial scale. Then, the regenerated carbon is send back to the rum production process to refill a new contactor.

(d) A fraction of the GAC volume of the rum filter "out of service" is recovered to be reused in the rum production process in order to complete the carbon bed in a new filter. The less exhaustion degree of the GAC layers located in the filter's bottom is determined using the new quantitative methods: Colorimetry, Acoustic Emission or Bubblemetry.

In that case, **the filling of a new rum filter using the saved volume of partially exhausted GAC must be started at the bottom refilling the first volumetric fraction of the filter of virgin and regenerated GAC and then, completed with the partially exhausted GAC at the top.** This possibility is more cost-effective than removing all the GAC and replacing by expensive virgin or only regenerated GAC.

(e) **The proposed GAC management strategy must be economically evaluated using the obtained economic assessment model**. Based on simulated results, **the new GAC management proposal produces a maximum projected cost reduction of about 50% in the first cycle**. It was estimated that **an increment of the number of cycles will produce a reduction in the economic advantages derived from the new proposal**.

(f) Based on the proposed new quantitative methods, sensorial judgement and economic criteria, after a limited number of cycles (GAC saving and regenerating) the regenerated GAC would not be reused in rum production any more. In this case, the GAC must be completely removed from the filter and replaced by fresh GAC starting the cycles again. **The removed GAC can be regenerated once more time and potential applications in adsorption systems in other industrial scenarios can be explored**, gaining an extra added value with the correspondently derived economic advantages.

Based on the original pursued objectives in this work, the following **general conclusions** can be stated:

1- **A new and improved proposal of GAC management in rum production based on the thermal regeneration of the exhausted GAC complemented with novel, robust, accurate and suitable quantitative methods to determine GAC porous characteristics was presented.**

2- **New quantitative methods to determine porous characteristics of granular activated carbons used in rum production were developed. The proposed methods are trustable, fast, robust and suitable techniques considering the rum producer facilities.**

3- **The proper conditions for the thermal regeneration of the exhausted GAC in order to restore its porous characteristics to be efficiently reused in the rum production process were determined.**

4- **The thermal regeneration at industrial scale of exhausted GAC used in rum production was performed. However, the adjustment of the operational parameters in the regeneration process at industrial scale must be further studied in order to improve the results in terms of porous restore of the regenerated carbon. The sensorial judgment of the filtered aged aguardiente using the regenerated GAC validated the reuse of regenerated carbon in rum industry. The economic viability of the new management proposal was demonstrated. Nevertheless, several years have to pass applying the new proposal in order to properly evaluate the effect of the number of regeneration and saving cycles on the cost-effectiveness of the new GAC management proposal.**

References

[1] Ferhan C., Aktas O., *Activated Carbon for Water and Wastewater Treatment,* WILEY-VCH Verlag GmbH & Co. KGaA , Istambul, Turkey.(**2011)**,46-321.

[2] Worch E*., Adsorption Technology in Water Treatment,* Walter de Gruyter GmbH & Co., ISBN 978-3-11-024022-1.(**2012**), 25-268.

[3] Françoise Rouquerol, Jean Rouquerol and Kenneth Sing, *Adsorption by Powders and Porous Solids: Principles, Methodology and Applications,* Academic Press, ISBN 0-12-598920-2, San Diego, C.A., USA. (**1999**),20-460.

[4] W. J. Thomas, Barry C., *Adsorption Technology and Design,* Elsevier Science & Technology Books, ISBN: 0750619597. (**1998**),28-212.

[5] Ferdi Schiith, Kenneth S. W. Sing, Jens Weitkamp , *Handbook of Porous Solids,* WILEY-VCH Verlag GmbH, Weinheim , Germany, ISBN 3-527-3024-8,(**2002**),156-293.

[6] Matthias T. Katsumi K., A.V. Neimark, J. P. Olivier, F. Rodriguez-Reinoso, J. Rouquerol and K. S.W. Sing., *Physisorption of gases, with special reference to the evaluation of surface area and pore size distribution (IUPAC Technical Report)*, IUPAC & De Gruyter, Pure Appl. Chem.(**2015**).

[7] K.V. Kumar, C.V. Calahorro, J.M. Juarez, M.M. Sabio, J.S. Albero, F.R. Reinoso, *Hybrid isotherms for adsorption and capillary condensation of N_2 at 77 K on porous and non-porous materials*, Chem. Eng. J. (162), (**2010**), 424–429.

[8] Roop C.B., Meenakshi G., *Activated Carbon Adsorption*, Taylor & Francis Group., Boca Raton, FL 33487-2742.(**2005**),44-415.

[9] P. Klobes and K. Meyer, *Porosity and Specific Surface Area Measurements for Solid Materials,* NIST Spec. Publ. 960-17, Washington, DC.(**2006**), 10-82.

[10] Marsh H., Rodriguez-Reynoso F., *Activated Carbon,* Elsevier Science & Technology Books, ISBN: 0080444636, (**2006**),13-317.

[11] G. Yanga , Honglin C.,H. Qina, Y. Feng, *Amination of activated carbon for enhancing phenol adsorption: Effect of nitrogen-containing functional groups*, Applied Surface Science. (**2014**) 299–305.

[12] P.Serp, Figueiredo J. L., *Carbon materials for catalysis*, john wiley & sons inc. publication.(**1998**),5-20.

[13] J. Rouquerol, F. Rouquerol, K. S. W. Sing, P. Llewellyn, G. Maurin. *Adsorption by Powders and Porous Solids: Principles, Methodology and Applications*, Academic Press (**2014**).

[14] E. R. Cohen, T. Cvitas, J. G. Frey, B. Holmström, K. Kuchitsu, R. Marquardt, I. Mills, F. Pavese, M. Quack, J. Stohner, H. L. Strauss, M. Takami, A. J. Thor. *Quantities, Units and Symbols in Physical Chemistry*, 3rd ed., RSC Publishing, Cambridge, UK (**2007**).

[15] S. Lowell, J. Shields, M. A. Thomas, M. Thommes, *Characterization of Porous Solids and Powders: Surface Area. Porosity and Density*, Springer, (**2004**).

[16] J. Rouquerol, P. Llewellyn, F. Rouquerol. *Study of Surfaces*, Sci. Catal. 49, (**2007**),160.

[17] Juan M. D. Tascón, E. J. Bottani, *Adsorption by Carbons*, Elsevier Ltd, ISBN: 978-0-08-044464-2, (**2008**), 79-685
[18] S. Brunauer, P. Emmett, E. Teller, Adsorption of gases in multimolecular layers J. Am. Chem. Soc. (60), (**1938**) 309–315.
[19] ASTM 4641-94 e1, Standard Practice of Pore Size Distributions of Catalysts from Nitrogen Desorption Isotherms, American Society for Testing and Materials, West Conshohocken, PA (**1999**).
[20] ISO 9277, Determination of the Specific Surface Area of Solids by Gas Adsorption Using the BET Method, International Organization for Standardization, Geneva (**1995**).
[21] Conner, W. C. and C. O. J. Bennett, "Are Real Catalyst Pore Morphologies and Surfaces Fractal?," J. Chem. Soc. Faraday Trans. 89 , (**1993**) 4109-4114.
[22] DIN 66131, Bestimmung der spezifischen Oberfläche von Feststoffen durch Gasadsorption nach Brunauer, Emmett und Teller (BET), DIN Deutsches Institut fuer Normung, Berlin (**1993**).
[23] M.M. Dubinin, L.V. Radushkevich, The equation of the characteristic curve of the activated charcoal, Proc. Acad. Sci. USSR Phys. Chem. Sec. 55, (**1947**), 331–337.
[24] M.M. Dubinin, *Adsorption in micropores*, J. Colloid & Interface. Sci. (23), (**1967**), 487–492.
[25] Stoeckli F., Daguerre E., Guillot A., *The development of micropore volumes and widths during physical activation of various precursors.* Carbon, Chemical Society, Washington D.C. 37 (**1999**); 2075-7
[26] Neimark AV., Lin Y., Ravikovitch PI., Thommes M., *Quenched solid density functional theory and pore size analysis of micro-mesoporous carbons*. Carbon; 47, (**2009**), 1617-28
[27] I. Langmuir, *The adsorption of gases on plane surfaces of glass, mica and platinum*, J. Am. Chem. (57), (**1918**), 1361–1403.
[28] *R.H.Perry, D.W. Green, Perry's Chemical Engineers"Handbook,* McGRAW-HILL, ISBN 0-07-049841-5, New York.(**1999**),Section 16.
[29] H. Freundlich, *Über die adsorption in lösungen* (adsorption in solution), Z. Phys. Chem. (57), (**1906**), 384–470.
[30] ISO/WD 14488, *Particle Size Analysis: Sample preparation-Sample splitting*, International Organization for Standardization, Geneva (**1999**).
[31] Van der Veen, A.M.H. and D. A. G. Nater, "Sample Preparation from Bulk Samples: An Overview," Fuel Processing Techn. 36, (**1993**), 1-7.
[32] *Zaid K., Chowdhury R., Scott S. G. P. Westerhoff B. J. Leto K. O., N. Christopher J. C., Activated Carbon: Solutions for Improving Water Quality,* American Water Works Association, Denver, CO, USA. (**2013),** 21-28.
[33] L.G. Hassan, B.N. Ajana, K.J. Umar, D.M. Sahabi, A.U. Itodo, and A. Uba, *Comparative Batch and Column Evaluation of Thermal and Wet Oxidative Regeneration of Commercial Activated Carbon Exhausted with Synthetic Dye*, Nigerian Journal of Basic and Applied Science, 20(2): 93-104, ISSN 0794-5698.(**2012**)

[34] Kang Sun, Jian-chun Jiang, Jun-ming Xu, *Chemical Regeneration of Exhausted Granular Activated Carbon Used in Citric Acid Fermentation Solution Decoloration*, Iran. J. Chem. Chem. Eng., (28),4.(**2009**)
[35] Kang Sun, *Study on Liquid-Phase Adsorption Behavior and Chemical Regeneration Mechanism of GAC [D]*, Nanjing: Institute of Chemical Industry of Forest Products, CAF, 39, (**2006**).
[36] United States Environmental Protection Agency (EPA) report, Wastewater Technology Fact Sheet: *Granular Activated Carbon Adsorption and Regeneration*, Washington, D.C.,USA, EPA 832-F-00-017.(**2000**).
[37] Bandosz T. J., *Activated Carbon Surfaces in Environmental Remediation, interface science and technology* , vol.7, Academic Press is an imprint of Elsevier. N. Y. ,USA.(**2006**),37-215.
[38] Shah I K, Pre P and Alappat B.J, *Regeneration of adsorbents spent with Volatile Organic Compounds (VOCs), In Proceedings of International Conference on Environment and Industrial Innovation,* Kualalumpur, (**2011**).
[39] McKay G, *Regeneration of adsorbents In Use of Adsorbents for the Removal of Pollutants from Wastewaters*, Boca Raton, FL, CRC Press, (**1996**).
[40] Alley R E, *Water Quality Control Handbook*, 2nd Ed., New York, NY: McGraw-Hill, Inc, (**2007**).
[41] I. K. Shah, P. Pre, B. J. Alappat, *Steam Regeneration of Adsorbents*: *An Experimental and Technical Review*, Chem Sci Trans., 2(4). (**2013**), 1078-1088.
[42] F. Salvador, C. Sanchez Jimenez, *A new method for regenerating activated carbon by thermal desorption with liquid water under subcritical conditions*, Carbon.(4), (**1996**),511-516.
[43] B.M. van Vliet, *The regeneration of activated carbon*, J. S. Afr. Inst. Min. Metal. vol. 91, (5).(**1991**),59-67.
[44] B. C. Moore , F. S. Cannon , J. A. Westrick , D. H. Metz , C. A. Shrive , J. DeMarco , D. J. Hartman, *Changes in GAC pore structure during full-scale water treatment at Cincinnati: a comparison between virgin and thermally reactivated GAC*, Carbon, (39). (**2001**),789–807.
[45] Xue Han, Hongfei Lin, Ying Zheng , *Regeneration methods to restore carbon adsorptive capacity of dibenzothiophene and neutral nitrogen heteroaromatic compounds*, Chemical Engineering Journal, (243). (**2014**), 315–325.
[46] Shenteng Chang, Chungsying Lu, Kun-Yi, Andrew Lin, *Comparisons of kinetics, thermodynamics and regeneration of tetramethyl ammonium hydroxide adsorption in aqueous solution with graphene oxide, zeolite and activated carbon*, Applied Surface Science, (326). (**2015**), 187–194.
[47] Haiyan Mao, Dingguo Zhou, Zaher Hashisho, Sunguo Wang, Heng Chen, Haiyan Wang, *Constant power and constant temperature microwave regeneration of toluene and acetone loaded on microporous activated carbon from agricultural residue*, Journal of Industrial and Engineering Chemistry, (21). (**2015**), 516–525.

[48] Yan-Juan Zhang, Zhen-Jiao Xing, Zheng-Kang Duan, Meng Li,Yin Wang, *Effects of steam activation on the pore structure and surface chemistry of activated carbon derived from bamboo waste*, Applied Surface Science, (315). (**2014**), 279–286.
[49] P.G. González, Y.B. Pliego-Cuervo, *Physicochemical and microtextural characterization of activated carbons produced from water steam activation of three bamboo species*, J. Anal. Appl. Pyrol. (99), (**2013**), 32–39.
[50] P. González-García, T.A. Centeno, E. Urones-Garrote, D. Ávila-Brande, L.C. Otero-Díaz, *Microstructure and surface properties of lignocellulosic-based activated carbons*, Appl. Surf. Sci. (265), (**2013**), 731–737.
[51] N. Mohamad Nor, L.C. Lau, K.T. Lee, A.R. Mohamed, *Synthesis of activated carbon from lignocellulosic biomass and its applications in air pollution control: a review*, J. Environ. Chem. Eng. (1) , (**2013**) ,658–666.
[52] F.A. López, T.A. Centeno, I. García-Díaz, F.J. Alguacil, *Textural and fuel characteristics of the chars produced by the pyrolysis of waste wood, and the properties of activated carbons prepared from them*, J. Anal. Appl. Pyrol. (104),(**2013**), 551–558.
[53] C. Bouchelta, M.S. Medjram, M. Zoubida, F.A. Chekkat, N. Ramdane, J.-P. Bellat,*Effects of pyrolysis conditions on the porous structure development of date pits activated carbon*, J. Anal. Appl. Pyrol.(94), (**2012**), 215–222.
[54] H. Demiral, I. Demiral, B. Karabacakoˇ glu, F. Tümsek, *Production of activated carbon from olive bagasse by physical activation*, Chem. Eng. Res. Des. (89), (**2011**),206–213.
[55] K. Fu, Q. Yue, B. Gao, Y. Sun, L. Zhu, *Preparation, characterization and application of lignin-based activated carbon from black liquor lignin by steam activation*, Chem. Eng. J. (228), (**2013**) , 1074–1082.
[56] J.E. Vargas, L.G. Gutierrez, J.C. Moreno-Piraján, *Preparation of activated carbons from seeds of Mucuna mutisiana by physical activation with steam*, J. Anal. Appl. Pyrol. (89), (**2010**) 307–312.
[57] R. Berenguer, J.P. Marco-Lozar, C. Quijada , D. Cazorla-Amoro , E. Morallo, *Electrochemical regeneration and porosity recovery of phenol-saturated granular activated carbon in an alkaline medium*, Carbon, (48), (**2010**), 2734 – 2745.
[58] Ava Heidari, Habibollah Younesi, Alimorad Rashidi, Ali Asghar Ghoreyshi, *Evaluation of CO_2 adsorption with eucalyptus wood based activated carbon modified by ammonia solution through heat treatment*, Chemical Engineering Journal, (254), (**2014**), 503–513.
[59] J.K. Jeon, H. Kim, Y.K. Park, C.H.F. Peden, D.H. Kim*, Regeneration of field-spent activated carbon catalysts for low-temperature selective catalytic reduction of NOx with NH3*, Chem. Eng. J. (174), (**2011**), 242–248.
[60] Seung Won Nahm, Wang Geun Shim, Young-Kwon Park, Sang Chai Kim, *Thermal and chemical regeneration of spent activated carbon and its adsorption property for toluene, Chemical Engineering Journal*. (210), (**2012**), 500–509.

[61] I. Guo, E. Du, *The effects of thermal regeneration conditions and inorganic compounds on the characteristics of activated carbon used in power plant*, Energy Proc. (17), (**2012**) 444–449.
[62] S.W. Nahm, W.G. Shim, Y. Park, S. Chai Kim, *Thermal and chemical regeneration of spent activated carbon and its adsorption property for toluene*, Chem. Eng. J. (210), (**2012**) 500–509.
[63] J. Carratala, M.A. Lillo-Rodenas, A. Linares-Solano, D. Cazorla-Amoro, *Regeneration of activated carbons saturated with benzene or toluene using an oxygen-containing atmosphere,* Chemical Engineering Science. (65), (**2010**), 2190–2198.
[64] K.Y. Foo, B.H. Hameed, *Microwave-assisted regeneration of activated carbon*, Bioresource Technology. (119), (**2012**), 234–240.
[65] K.Y. Foo, B.H. Hameed, *Coconut husk derived activated carbon via microwave induced activation: effects of activation agents, preparation parameters and adsorption performance,* Chemical Engineering Journal. (184), (**2012**) , 57–65.
[66] J.M. Valente Nabaisa, C. Laginhasa, M.M.L. Ribeiro Carrott, P.J.M. Carrott, J.E. Crespo Amorós, A.V. Nadal Gisbert, *Surface and porous characterisation of activated carbons made from a novel biomass precursor, the esparto grass*, Applied Surface Science. (265) (**2013**), 919– 924.
[67] J.K. Jeon, H. Kim, Y.K. Park, C.H.F. Pedenc, D.H. Kim*, Regeneration of field-spent activated carbon catalysts for low-temperature selective catalytic reduction of NOx with NH3*, Chem. Eng. J. (174), (**2011**), 242–248.
[68] W.G. Shim, S.C. Jung, S.G. Seo, S.C. Kim, *Evaluation of regeneration of spent three-way catalysts for catalytic oxidation of aromatic hydrocarbons*, Catal. Today. (164), (**2011**), 500–506.
[69] W.G. Shim, S.C. Kim, *Heterogeneous adsorption and catalytic oxidation of benzene, toluene and xylene over spent and chemically regenerated platinum catalyst supported on activated carbon*, Appl. Surf. Sci. (256), (**2010**), 5566–5571.
[70] Ljubisa R. Radovic ,*Chemistry and Physics of Carbon*,Vol.30, Taylor & Francis Group, Boca Raton, FL 33487-2742.(**2008**),16-38.
[71] Shah I K, Pre P and Alappat B.J, *Regeneration of adsorbents spent with Volatile Organic Compounds (VOCs), In Proceedings of International Conference on Environment and Industrial Innovation*, Kualalumpur, (**2011**).
[72] McKay G., *Regeneration of adsorbents In Use of Adsorbents for the Removal of Pollutants from Wastewaters*, Boca Raton, FL, CRC Press, (**1996**).
[73] Alley R E, *Water Quality Control Handbook*, 2nd Ed., New York, NY: McGraw-Hill, Inc, (**2007**).
[74] I. K. Shah, P. Pre, B. J. Alappat, *Steam Regeneration of Adsorbents*: *An Experimental and Technical Review*, Chem Sci Trans., 2(4). (**2013**), 1078-1088.
[75] B. Ledesma, S. Román, A. Álvarez-Murillo, E. Sabio, J.F. González, *Cyclic adsorption/thermal regeneration of activated carbons, Journal of Analytical and Applied Pyrolysis.* (106), (**2014**), 112–117.

[76] San Miguel, G., S. Lambert, and N. J. . Graham, *The regeneration of field-spent granular-activated carbons.* Water Research. (35), (**2001**), 2740-2748.
[77] Katherine He, *Environmental Footprint of Regenerating GAC: A Calculation of the Environmental Footprint of a Granular Activated Carbon Regeneration Facility*, Environmental Protection Agency (EPA) Ed. (**2012**),14-23.
[78] Hernández, O.Q. Science and technologies of distillates beverages. Res. Inst. Food Ind. Cuba (**2007**), 11, 19.
[79] Pino Jorge A., *Characterization of rum using solid-phase micro extraction with gas chromatography–mass spectrometry*, Food Chemistry. 104, (**2007**), 421–428.
[80] Pino Jorge A., Sebastian Tolle, Recep Gök , Peter Winterhalter, *Characterisation of odour-active compounds in aged rum*, Food Chemistry.132, (**2012**) ,1436–1441.
[81] H. Maarse, *Volatile compounds in foods and beverages*. TNO-CIVO Food Anal. Inst., Zeist, The Netherlands, Printed in New York, ISBN: 0-8247-8390-5.(**2010**),261-387.
[82] Reazin, G. *Chemical mechanism of whisky maturation*. Am. J. Enol. Vitic. (**1981**), 32, 283.
[83] Nabeta, K.; Onishi, M.; Masuda, M.; Koda, M.; Matsuyama, R. *Reaction of Wood Components during Maturation in Flavour of Distilled Beverages: Origin and Development*; Pigott J.R., Ed.; Horwood: Chichester, UK. (**1983**),241–255.
[84] Otzuka, K.; Morinaga, M. *Study of the mechanism of ageing of distilled liquors Part II. Distribution of phenolic compounds in aged distilled liquors*. Agric. Biol. Chem. (**1965**), 29, 27–31.
[85] Sponholz,*Volatile fatty acids in Caribbean rums and rum blends*. Deutsch. Lebensm. Rundsch.86,(**1990)**, 80–81.
[86] Suomalainenen, M.; Nykanen, L. *Investigation on the aroma of alcoholic beverages*. Naeringsmiddelindustren.85, (**1970**), 149–156.
[87] Parfait, A.; Jouret, C. *Formation of higher alcohols in rum*. Ann. Technol. Agricole.3, (**1975**),421–436.
[88] Nykanen, L.; Nykanen, I. *Flavour Components in Distilled Beverages*; Alko Ltd.: Helsinski, Finland, (**1991**).
[89] De Souza, M.; Vázquez, P.; del Mastro, N.; Acree, T.; Lavin, J.; Characterization of Cachaça and Rum Aroma. J. Agric. Food Chem. 54, (**2006**), 485−488.
[90] Nykanen, L.; Moring, I. *Aroma compounds dissolved from oak chips by alcohol*. Dev. Food Sci. 10, (**1984**), 339–346.
[91] Sarni, F.; Moutonet, M.; Puech, J.L.; Rabier, P. Effects of heat treatment of oak wood extractable compound. Holzforchung .44, (**1990**), 461–466.
[92] Queris, O.; Sánchez, M. *Efecto del Tostado de la Viruta de Roble Sobre la Composición de los Extractos*; IIIA.TI-126-1998, Publisher: Food Res. Inst. of Cuba, La Habana, Cuba, (**1998**).(in Spanish).
[93] Maga, J.A. *The contribution of wood to the flavour of alcoholic beverages*. Food Rev.5, (**1989**), 39–99.

[94] Serrano, J.A*. Characterisation of oak wood according to its origin and burning degree by GC and HPLC*. Viticul. Enol. Prof. 14, (**1991**), 61–72.
[95] Chen, C.; Chang, M., *Chemistry of lignin biodegradation. In biosynthesis and Biodegradation of Wood Components*; Ed. Academy Press Pub. (**1985**), 535–556.
[96] Skurihjin, I.; Nazarova, M.; Lichev, N.V. *Use of oak wood for maturing wine distillates*. Lozarsvo I Vinartsvo Moscow. 19, (**1970**), 40–44.
[97] Timmer, R.; Valois, J.P. *Phenolic compounds in rum*. J. Food Sci. 36, (**1971**), 462–463.
[98] Salo, P.; Lethonen, M.; Suomalainen, H. *The Development of Flavor during Ageing of Alcoholic Beverages*; The Swedish Food Institute SSIK: Goteborg, Sweden. (**1976**),87–108.
[99] Puech, J.L. *Phenolic compounds in oak wood extracts used in the ageing of brandies*. J. Sci. Food Agric. 42, (**1988**), 165–238.
[100] Puech, J.L.; Moutounet, M*. Phenolics compounds in ethanol-water extracts of oak wood in brandy*. Lebensm. Wiss. Technol. 25, (**1992**), 350–352.
[101] Maga, J.A. *The contribution of wood to the flavour of alcoholic beverages*. Food Rev. 5, (**1989**), 39–99.
[102] Abbott, N.; Puech, J.L.; Bayonove, C.; Baumes, R. *Determination of the aroma threshold of the cis and trans racemic forms of β-methyl-γ-octalactone by gas chromatography-sniffing analysis*. Am. J. Enol. Vinicult. 46, (**1995**), 292–294.
[103] Lehtonen, M.; Gref, B.; Puputti, E.; Suomalainen, *H. 2-Ethyl-3-methylbutyric acid, a new volatile fatty acid found in rum*. J. Agric. Food Chem. 25, (**1977**), 953–955.
[104] Ferrer, M.; Queris, O. *Efectodel ajuste del pH sobre las características de los rones cubanos,* IIIA. TI-123-1982, Pub:Food Research Institute of Cuba, La Habana, Cuba,(**1982**).(in Spanish)
[105] Queris, O.; Pino, A.; Villavicencio, M. *Efecto de la concentración alcohólica sobre la adsorción por el carbón activado de compuestos volátiles presentes en los aguardientes de caña*. In Proceedings of the 6th International Symposium of Food Production SIPAL, Bogotá, Colombia, 14/04/ (**2007**).
[106] Oshmian, L.; Isnatova, A. *Chemical activity of activated carbons on distilled beverages*, Lozarsvo I Vinartsvo Moscow. TsNIIPe, (XI): (**1961**), 242–250.
[107] ASTM. Standard Test Methods for Moisture in Activated Carbon, D 2867-04; ASTM International: West Conshohocken, PA, USA, (**2011**).
[108] Bertazzo, S.; Gentleman, E.; Cloyd, K. L.; Chester, A. H.; Yacoub, M. H.; Stevens, M. M..*Nano-analytical electron microscopy reveals fundamental insights into human cardiovascular tissue calcification.* Nature Materials*.* 12 (6) (**2013**), 576–583*.*
[109] Tahmasebi, Pejman; Javadpour, Farzam; Sahimi, Muhammad*. Three-Dimensional Stochastic Characterization of Shale SEM Images,*Transport in Porous Media. 110 (3) (**2015**), 521–531.

[110] Tahmasebi, Pejman; Javadpour, Farzam; Sahimi, Muhammad. *Multiscale and multiresolution modeling of shales and their flow and morphological properties.* Scientific Reports. 5(**2015**), 163-73.
[111] ASTM. Standard Test Method for Determination of Iodine Number of Activated Carbons, D4607-94; ASTM International: West Conshohocken, PA, USA, (**2011**).
[112] ASTM. Standard Test Method for Determination of Contact pH with Activated Carbon, D6851-02; ASTM International: West Conshohocken, PA, USA, (**2011**).
[113] Azizian, S.; *Kinetic models of sorption: A theoretical analysis*. *J. Colloid Interface Sci.* (**2004)**, *276*,47−52.
[114] Azizian, S.; Fallah, R.N. *A New empirical rate equation for adsorption kinetics at solid/solution interface. Appl. Surf. Sci.*(**2010)**, *256*, 5153−5156.
[115] Marczewski, A.W. *Application of mixed order rate equations to adsorption of methylene blue on mesoporous carbons*. *Appl. Surf. Sci.* (**2010)**, *256*, 5145−5152.
[116] J. B. Fernández, A. S. Roca, H. C. Fals, E. J. Macías and M. P. de la Parte: '*Application of vibroacoustic signals to evaluate tools profile changes in friction stir welding on AA 1050 H24 alloy'*. Sci. Technol. Weld. Join. 17(6) (**2012**) 501–510.
[117] E. J. Macías, A. S. Roca, H. C. Fals, J. C. S. Muro and J. B. Fernández, *Characterisation of friction stir spot welding process based on envelope analysis of vibro-acoustical signals*. Sci. Technol. Weld. Join. 20(2) (**2015**) 172–180.
[118] P.V.C. Hough, *Method and means for recognizing complex patterns*. U.S. Patent 3,069,654, Dec. 18, (**1962**).
[119] R.O. Duda, P. E. Hart, *Use of the Hough Transformation to Detect Lines and Curves in Pictures.* Comm. ACM 15 (1972) 11–15
[120] J. Jensen, *Hough Transform for Straight Lines*. Retrieved (Dec. **2011**).
[121] L. Fernandez, M. Oliveira, *Real-time line detection through an improved Hough transform voting scheme*. Pattern Recognition 41(1) (**2008**) 299–314
[122] F. Limberger, M. Oliveira, *Real-Time Detection of Planar Regions in Unorganized Point Clouds*. Pattern Recognition 48(6) (2015) 2043–2053
[123] L. Fernandes, M. Oliveira, *A general framework for subspace detection in unordered multidimensional data*. Pattern Recognition 45(9) (**2012**) 3566–3579
[124] R. Tahir, F. van den Heuvel, *Efficient Hough transform for automatic detection of cylinders in point clouds*, Proceedings of the 11th Annual Conference of the Advanced School for Computing and Imaging (ASCI '05), The Netherlands, (**2005**).
[125] Brownstein K.R., Tarr C.E., *Importance of classical diffusion in NMR studies of water in biological cells*, Phys. Rev. A .,19, (**1979**) 2446–2453.
[126] Aksnes D.W., Kimtys L.,*1H and 2H NMR studies of benzene confined in porous solids: melting point depression and pore size distribution*, Solid State Nuclear Magnetic Resonance.,25, (**2004**) 146–152

[127] Valckenborg R., Kopinga L., *Cryoporometry and relaxometry of water in silica-gels*, Magnetic Resonance Imaging. 19, (**2001**), 489–491.
[128] Valori A., McDonald P., Scrivener K., *The morphology of C–S–H: Lessons from 1H nuclear magnetic resonance relaxometry*, Cement and Concrete Research. 49, (**2013**), 65–81.
[129] Stingaciu L., Pohlmeier A., *Characterization of unsaturated porous media by high-field and low-field NMR relaxometry*, Water Resources Research. (**2009**), vol. 45.
[130] Stingaciu L. Weihermüller L., *Determination of pore size distribution and hydraulic properties using nuclear magnetic resonance relaxometry: A comparative study of laboratory methods*, Water Resources Research, vol. 46, (**2010**) 110-15.
[131] Rijniers L.A., Magusin P., *Sodium NMR relaxation in porous materials,* Journal of Magnetic Resonance. 167, (**2004**),25–30.
[132] Washburn K., Birdwell J., *Updated methodology for nuclear magnetic resonance characterization of shales*, Journal of Magnetic Resonance. 233 , (**2013**), 17–28.
[133] Nakashima Y., *Nuclear Magnetic Resonance Properties of Water-Rich Gels of Kunigel-V1 Bentonite*, Journal of Nuclear Science and Technology. Vol. 41, No. 10, (**2004**), 981–992.
[134] Hansen E.W., Fonnum G., *Pore Morphology of Porous Polymer Particles Probed by NMR Relaxometry and NMR Cryoporometry*, J. Phys. Chem. B. 109, (**2005**) , 295-303.
[135] Yi-Qiao Song, *Determining Pore Sizes Using an Internal Magnetic Field*, Journal of Magnetic Resonance. 143, (**2000**), 397–401.
[136] Conte P., Berns E., *Applications and New Developments of Magnetic Resonance Techniques in Soil Science*, The Open Magnetic Resonance Journal, Volume 3. (**2010**), 874-98.
[137] IOP science, *Probing surface interactions by combining NMR cryoporometry and NMR relaxometry*, J. Phys. D: Appl. Phys. 38, (**2005**), 1950-51.
[138] Yi-Qiao Song, *Magnetic Resonance of Porous Media (MRPM): A perspective*, Journal of Magnetic Resonance. 229, (**2013**), 12–24.
[139] Jorand R., Fehr A., *Study of the variation of thermal conductivity with water saturation using nuclear magnetic resonance*, Journal of Geophysical Research, vol. 116. (**2011)**.482-93
[140] S. Schreurs, J.-P. François, P. Adriaensens and J. Gelan , *Qualitative and quantitative analysis of solid state free induction decay (1H NMR) curves using a combination of the methods of Gardner and Prony*: *Isotactic Polypropylene as a case study.*, J. Phys. Chem. B. 103, (**1999**),1393-1401.
[141] H. Berghmans, P. Adriaensens, L. Storme, D. Vanderzande, J. Gelan, and S. Paoletti, B. Ruytinx, *1H-NMR relaxation study of the gelation of syndiotactic poly(methyl methacrylate) in toluene*, Macromolecules. 34, (**2001**), 522-528.

[142] S. D'hollander, C. Joseph Gommes, R. Mens, P. Adriaensens, B. Goderis, F. Du Prez, *Modeling the Morphology and Mechanical Behavior of Shape Memory Polyurethanes based on solid-state NMR and Synchrotron SAXS/WAXD*, Journal of Materials Chemistry. 20(17), (**2010**), 3475-3486.
[143] Josip M., Andreja K.,*Colour changes of modified oak wood in indoor environment*, Eur. J. Wood Prod. Springer-Verlag,(**2012**), 287-95.
[144] Josip M., Nikola S., *Wood color changes by ammonia fuming*, BioResources.7, (**2012**), 3767-3778.
[145] Piotr B., Marek J., *Mechanical properties of glue bonds in black locust wood treated with ammonia*, Forestry and Wood Tech. 73, (**2011**), 162-166.
[146] Petr Č., Aleš D., *The effect of heat and ammonia treatment on colour response of oak wood (quercus robur) and comparison of some physical and mechanical properties*, Maderas Ciencia y Tecnología. 2013, 15, 375-389.
[147] Weigl M., Pockl J., Selected properties of gas phase ammonia treated wood, Eur. J. Wood Prod. , Springer-Verlag. 67, (**2009**),103–109.
[148] Qun-Li Luo, Wen-Hui Nan, Yu Li, Xiang Chen, *Oxidation of alcohols to carbonyl compounds with molecular iodine in the presence of potassium tert-butoxide*, General Papers, ARKIVOC, (**2014**),350-361
[149] R. M. Moriarty, O. Prakash, *Oxidation of Phenolic Compounds with Organo-hypervalent Iodine Reagents*, Organic Reactions, Wiley Online Library, Published Online; DOI: 10.1002/0471264180.(**2004**).
[150] R. Ohmura , M Takahata, H.Togo, *Metal-free one-pot oxidative conversion of benzylic alcohols and benzylic halides into aromatic amides with molecular iodine in aq. ammonia and hydrogen peroxide,* Tetrahedrom letters. 51 (2010) 4378-81.
[151] Wallas, S.M. *Reaction Kinetics for Chemical Engineers*; John Wiley & Sons Inc.: New York, NY, USA, (**1972**).
[152] Levenspiel, O. *Chemical Reaction Engineering*; John Wiley & Sons Inc.: New York, NY, USA, (**1989**).
[153] Froment, G.F.; Bischoff, K.B. *Chemical Reactor Analysis and Design*; John Wiley & Sons Inc.: Somerest, NJ, USA, (**1990**).
[154] A.I.Fedorchenko, A.A.Chernov, *Exact solution of the problem of gas segregation in the process of crystallization*. International Journal of Heat and Mass Transfer. 46, (**2003**), 915–919.
[155] E.J. Terrill, K.W. Melville, *A broadband acoustic technique for measuring bubble size distributions: laboratory and shallow water measurements*, Journal of Atmospheric and Oceanic Technology. 17, (**2000**), 220–239.
[156] J.B. Gilbert, M.S.Howea,, R.M.Koch*, On sound generated by gas-jet impingement on a bubbly gas–water interface, with application to supercavity self-noise* .Journal of Sound and Vibration. 331, (**2012**), 4438–4447
[157] K.W. Commander, A. Prosperetti*, Linear pressure waves in bubbly liquids: comparison between theory and experiments*, Journal of the Acoustical Society of America. 85 (2), (**1989**) 732–746.

[158] M.M.Havlickova, *The Cocoa Sound Effect—Audible Rising of the Tone Pitch*, Prague, Private Communications. (**1997**),784-99.
[159] M.Tabacchi, C.Asensio, I.Pavón, M.Recuero, J.Mir, M.C.Artal, *A statistical pattern recognition approach for the classification of cooking stages. The boiling water .* Applied Acoustics. 74, (**2013**) 1022–1032
[160] R. Manasseh, S. Yoshida, M. Rudman, *Bubble formation processes and bubble acoustic signals*, Third International Conference on Multiphase Flow, Lyon, France. (**1998**)
[161] A. Nikolovska, R. Manasseh, A. Ooi, *Visualizing the acoustic field around bubbles using a hydrophone—scanning method*, The Seventh Asian Symposium on Visualization, Singapore, (**2003**).
[162] A. Vazquez, R.M. Sanchez, E. Salinas-Rodrıíguez, A. Soria, R. Manasseh, *A glance at three measurement techniques for bubble size determination*, Experimental Thermal and Fluid Science. 30 (1), (**2005**) 49–57.
[163] Doney GD. *Acoustic Boiling Detection*. Dept. of Nuclear, Engineering, Massachusetts Institute of Technology Edition, US. (**1994**).
[164] G.K.Batchelor, *Compression waves in a suspension of gas bubbles in liquid*, Fluid Dynamics Transactions. 4, (**1969**), 425–445.
[165] A.W.Foley, M.S.Howe, T.A.Brungart, *Spectrum of the sound produced by a jet-impinging on the gas–water interface of a supercavity*, Journal of Sound and Vibration. 329 (**2010**) 415–424.
[166] Mirko C˘udina, Jurij Prezelj, *Detection of cavitation in operation of kinetic pumps. Use of discrete frequency tone in audible spectra.* Applied Acoustics. 70, (**2009**), 540–546
[167] Z. Travnıcek, A.I.Fedorchenko, M.Pavelka,J.Hruby. *Visualization of the hot chocolate sound effect by spectrograms*, Institute of Thermomechanics, v.v.i., Academy of Sciences of the Czech Republic, Prague 8, Czech Republic. Journal of Sound and Vibration. 331, (**2012**) 5387–5392.
[168] W. Kracht a, J.A. Finch b, *Using sound to study bubble coalescence.*
Journal of Colloid and Interface Science, 332 (**2009**), 237–245.
[169] C.E.Brennen, *Cavitation and Bubble Dynamics*, Oxford University Press. (**1995**).

Journal Contribution

1) Crespo Sariol H.; Yperman, J.; Brito Sauvanell Á.; Carleer, R.; Navarro Campa J.; Gryglewicz G. "A novel acoustic approach for the characterization of granular activated carbons used in the rum production". *Ultrasonic* **(2016)**, *70*, 53–63.
2) Crespo Sariol H., Vanreppelen K., Yperman J., Brito Sauvanell, Á.; Carleer R., Navarro Campa J. "A colorimetric method for the determination of the exhaustion level of granular activated carbons used in the rum production". *Beverages* (**2016)**, *2*, 24.
3) Crespo Sariol H., Yperman J., Brito Sauvanell, Á.; Carleer R., Navarro Campa J., "Characterization of granular activated carbons used in the rum production by immersion bubble-metric technique in a pure liquid". J. Food Process & Beverages **(2016)**, 4, 1–10.
4) Crespo Sariol H., Mariño Peacok T., Yperman J., Sánchez Roca Á., Carvajal Fals H., Brito Sauvanell Á., Carleer R., Czech J., Ledea Vargas J. and Navarro Campa J. ; "Comparative study between acoustic emission analysis and immersion bubble-metric technique, TGA and TD-GC/MS in view of the characterization of granular activated carbons used in the rum production". *Beverages* (**2017)**, *3*, 12.
5) Crespo Sariol H., Maggen J., Czech J., Reekmans G., Reggers G., Adriaensens P., Yperman J., Brito Sauvanell Á., Carleer R. and Navarro Campa, J.;"Characterization of the exhaustion profile of activated carbon in industrial rum "filters" based on TGA, TD-GC/MS, colorimetry and NMR relaxometry". *Materials Today Communications* **(2017)**,*11*, 1-10.
6) Crespo Sariol H., Mariño Peacok T., Yperman J., Leyssens K., Meynen V., Sánchez Roca Á., Carvajal Fals H., Brito Sauvanell Á., Carleer R. and Navarro Campa, J.; "Characterization of thermally regenerated activated carbons used in rum production by acoustic emission analysis, N_2 and Ar gas adsorption". *J Adv Chem Eng* (**2017)**, *7: 176,*1-10.

Conference Material

1) Poster: Crespo Sariol H., Rivera Soto M.; "Estudio del agotamiento de carbón activado utilizado en la fabricación de rones cubanos". Simposio Internacional de Química (SIQ-2013), Cayo Santamaría, Cuba. June 4-7 (**2013)**.
2) Oral presentation: Crespo Sariol H.C, Prieto Ametller Y.; "Regeneración del carbón activado utilizado en la fabricación de rones cubanos". II Taller nacional: Cátedra Azucarera Álvaro Reynoso, Santiago de Cuba, Cuba. May 31 (**2014)**.
3) Oral presentation: Crespo Sariol H.; "Regeneration possibilities of exhausted carbon in Cuban rum industries". 3rd Light rum scientific-technical international forum, Santiago de Cuba, Cuba. June 24-26 (**2015)**.
4) Poster: Peacok M. T., Rivera Soto M., Crespo Sariol H.., Rivera Y.; "Aplicación del carbón activado agotado y regenerado del proceso de rones en la adsorción de Ni y Co ". Simposio Internacional de Química (SIQ-2016), Cayo Santamaría, Cuba. June 7-10 (**2016)**.

Supplementary Materials

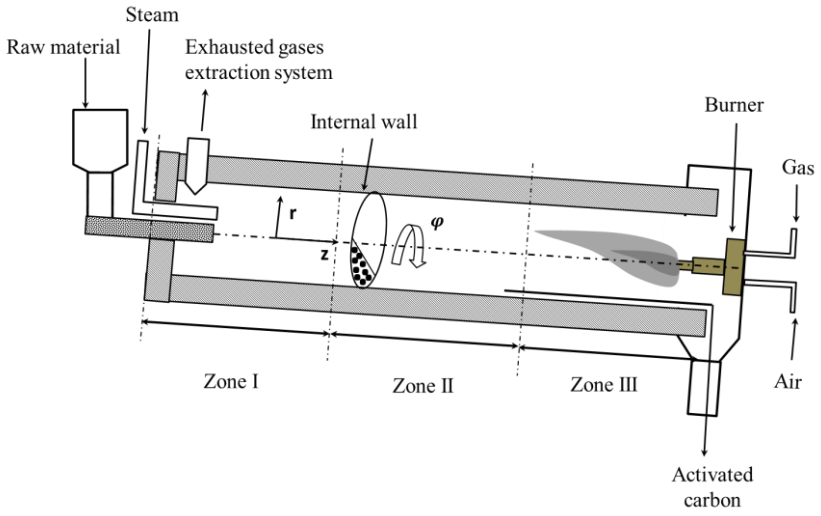

S1 (a): Schematic operational diagram of a typical rotatory kiln for activated carbon production using counter current direct flame heating system according to the mechanical 3D diagram (a).

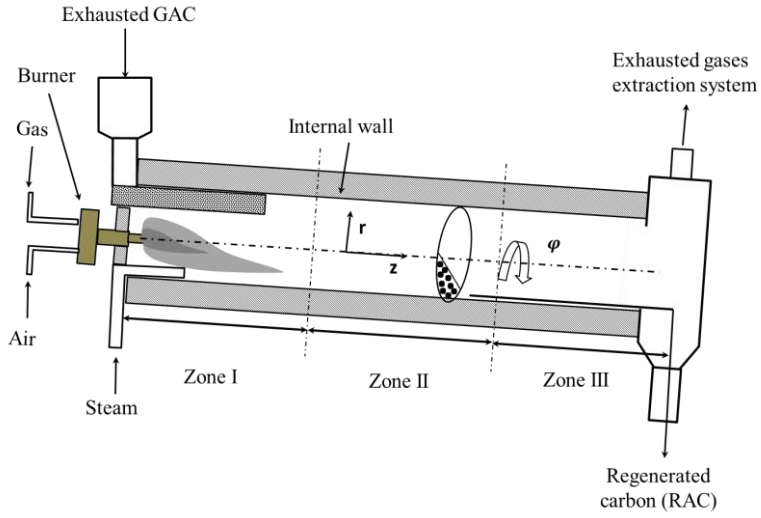

S1 (b): Schematic operational diagram of the industrial rotatory kiln for regenerating at industrial scale the exhausted GAC used in rum production. In that case, the direct flame heating system is used but in a concurrent flow process.

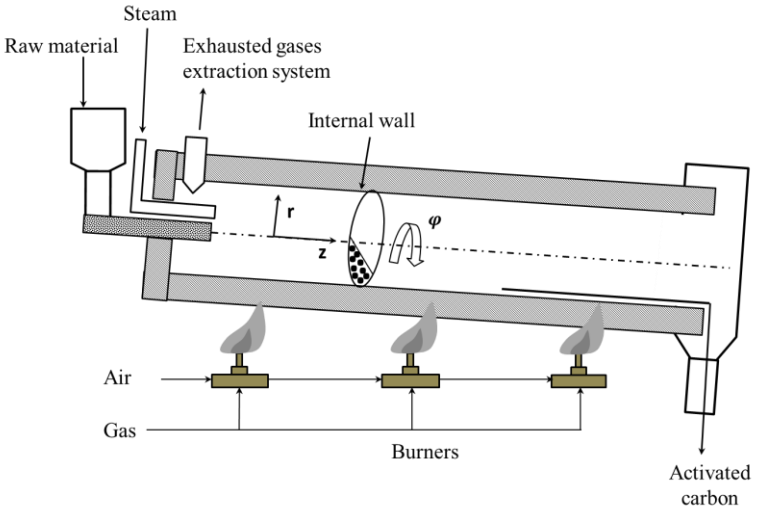

S1(c): Schematic operational diagram of a typical rotatory kiln for activated carbon production using indirect flame heating.

Figure S1 (a), (b) and (c): Schematic diagram of the main types of industrial rotatory kiln for AC manufacturing.

In the rotatory kiln reactors, the temperature and residence time can be modified by regulating the air/gas rate in the burner and the rotation speed (φ) respectively. The saturated steam to create the oxidizing atmosphere in the reactor can also be controlled from the boiler. The boiler just produces a saturated steam which once inside of the reactor (high temperature) suddenly flashes as superheated steam. In the case of counter and concurrent processes with direct flame heating systems (Figure S1 (a) and (b)), three main distinctive zones can be distinguished. These zones are demarking the change in the temperature profile within the reactor which in turn, describes the thermic changes in the material during the regeneration process.

In the counter current system, (Figure S1 (a)) the temperature of the GAC increases from Zone I to Zone III. On the contrary, in the concurrent process (Figure S1 (b)), the temperature decreases from Zone I to Zone III. Counter current process offers advantages for the GAC regeneration in comparison with the concurrent system.

In the counter current process, the systematic increment of the temperature permits the removal of the adsorbed compounds according to its volatility. In that way, the stages involved in the regeneration process (drying, thermal desorption, pyrolysis and activation) occurs in an ordered/sequential way.

On the other hand, in the concurrent process (Figure S1 (b)) (Implemented in the Cuban AC factory which was considered for the regeneration process at industrial scale) several disadvantages can be realized/deduced. For instance, the exhausted GAC is feed to the reactor in front of the fame: the hottest zone (about 850 °C), thus receiving a sort of "thermic shock" that abruptly desorb all the compounds at the same time occurring an overlapping of the regeneration steps, thus producing more structural damage in the regenerated carbon. This concurrent system, presents as advantage the possibility of cooling down the material during the process after crossing zone I as zone II and III are colder. In that case, the energy consumption for cooling down the regenerated material to reach a proper storage temperature (about 50 °C) is lesser than the counter current and the indirect flame heating systems where the material has to be cooled down from a higher temperature, i.e. temperature of activation.

The indirect heating system (Figure S1 (d)) presents the better operational conditions for the regeneration process. With more homogeneous and sustained heating system, the indirect heating guaranties the correct temperature during the whole activation/regeneration process at different residence times by controlling the rotation speed in the reactor. Additionally, the exhausted combustion gases are not in direct contact with the material within the kiln; therefore, a cleaner product can be ensured. Unfortunately, a plant for activated carbon production applying indirect heating technology is not available in Cuba so far.

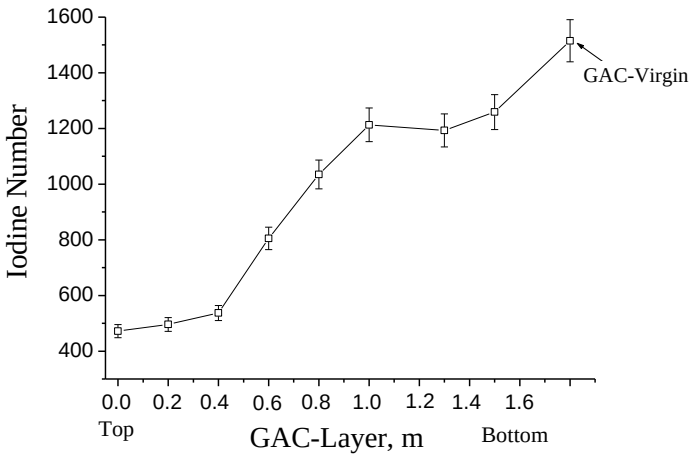

(a)

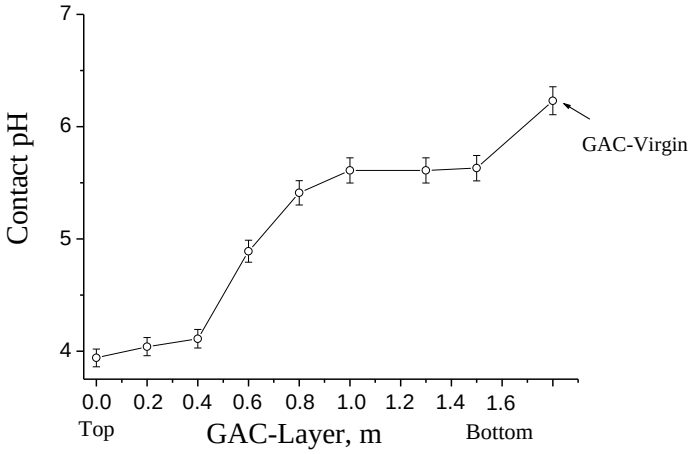

(b)

Fig. S2: Trends of Iodine Number (a) and Contact pH (b) as functions of the GAC layer position in the rum filter. The GAC virgin has been plotted in order for comparing with the GAC samples from the rum filter.

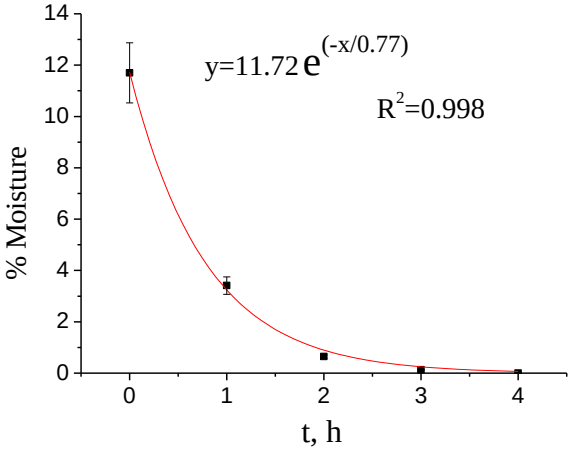

Fig.S3: Drying curve for GAC-Top (most exhausted).

Fig.S4: Preparing the industrial rum filter with regenerated GAC.

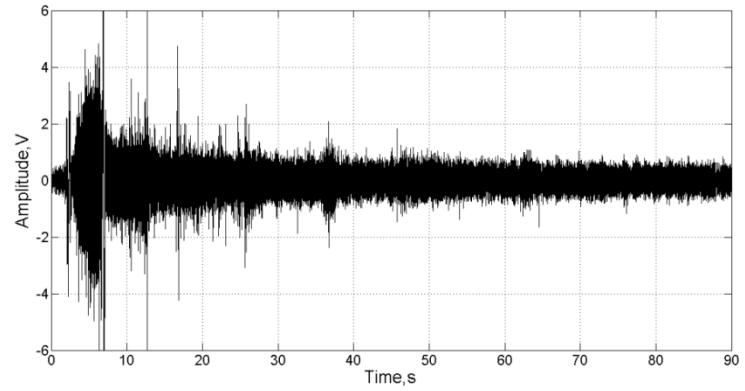

(a)

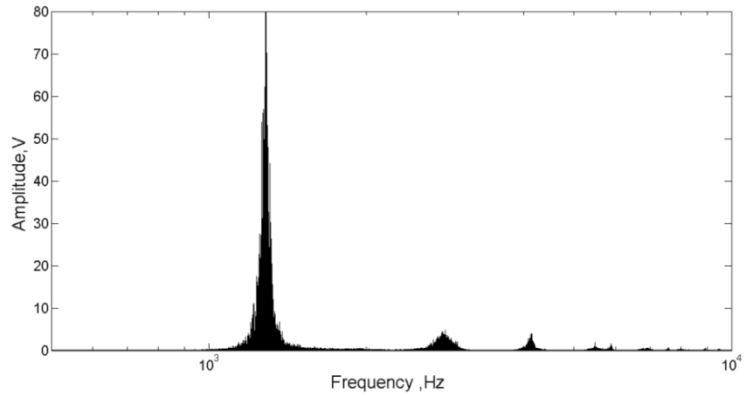

(b)

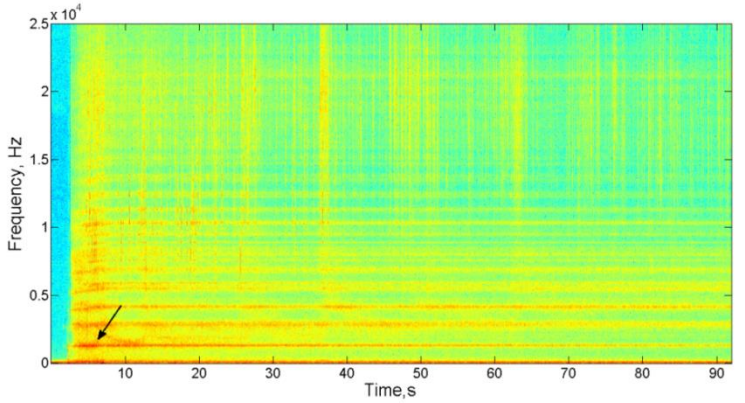

(c)

Fig.S5: RMS (a), frequency component distribution (b) and spectrogram (c) of the acoustic signal produced by the regenerated GAC at industrial scale